APPENDIX C.3

Surface Wave Data

TABLE C-2
Summary of Multichannel Analyses of Surface Waves and ReMi Testing

Number	MASW Line	Approximate Location	City
1	Z1-S1	Silver Ridge Avenue (N/O Silver Ridge Way)	Los Angeles
2	Z1-S2	Allesandro Street at Crystal Street	Los Angeles
3	Z1-S3	Echo Park Avenue at Donaldson Street	Los Angeles
4	Z1-S4	Pirtle Street (NE/O Lowe Street)	Los Angeles
5	Z1-S5	Stadium Way (SW/O I-5), Along Seismic Line Z1-G3	Los Angeles
6	Z1-S6	Stadium Way (SW/O I-5), Along Seismic Line Z1-G3	Los Angeles
7	Z1-S7	Shoredale Avenue (N/O Blake Avenue)	Los Angeles
8	Z1-S8	Thorpe Avenue (SW/O Cypress Avenue)	Los Angeles
9	Z1-S9	Granada Street (N/O Cypress Avenue)	Los Angeles
10	Z1-S10	Loosmore Street at Pleasant View Avenue	Los Angeles
11	Z1-S11	E. Avenue 31 at Sichel Street	Los Angeles
12	Z1-S12	Arroyo Seco Avenue (N/O Amabel Street)	Los Angeles
13	Z1-S13	Midland Street at E. Avenue 39	Los Angeles
14	Z1-S14	Huntington Drive S., Along Seismic Line Z1-G4	Los Angeles
15	Z1-S15	Huntington Drive S., Along Seismic Line Z1-G4	Los Angeles
16	Z1-S16	N. Eastern Avenue, Along Seismic Line Z1-G5	Los Angeles
17	Z1-S17	N. Eastern Avenue, Along Seismic Line Z1-G5	Los Angeles
18	Z1-S18	Sierra Street at Rolle Street	Los Angeles
19	Z1-S19	Budau Avenue (E/O Phelps Avenue)	Los Angeles
20	Z1-S20	Highbury Avenue (S/O Valley Boulevard)	Los Angeles
21	Z2-S1	York Boulevard (W/O Verdugo Road)	Los Angeles
22	Z2-S2	N. Avenue 46, Along Seismic Line Z2-G1	Los Angeles
23	Z2-S3	N. Avenue 46, Along Seismic Line Z2-G1	Los Angeles
24	Z2-S4	Cleland Avenue at Terrace 49	Los Angeles
25	Z2-S5	N. Avenue 56 (SE/O Aldama Street)	Los Angeles
26	Z2-S6	E/O N. Avenue 52 and Granada Street	Los Angeles
27	Z2-S7	Figueroa Street, Along Seismic Line Z2-G2	Los Angeles
28	Z2-S8	Figueroa Street, Along Seismic Line Z2-G2	Los Angeles
29	Z2-S9	Redfield Avenue (E/O Monterey Road)	Los Angeles
30	Z2-S10	Pueblo Avenue, Along Seismic Line Z2-G3	Los Angeles
31	Z2-S11	Pueblo Avenue, Along Seismic Line Z2-G3	Los Angeles
32	Z2-S12	Allan Street (E/O Farnsworth Avenue)	Los Angeles
33	Z3-S1	San Miguel Road (N/O Sierra View Road)	Pasadena
34	Z3-S2	Palmetto Drive (E/O S. Pasadena Avenue)	Pasadena
35	Z3-S3	S. Raymond Avenue, Along Seismic Line Z3-G1	Pasadena
36	Z3-S4	S. Raymond Avenue, Along Seismic Line Z3-G1	Pasadena
37	Z3-S5	Arlington Drive (W/O S. Pasadena Avenue)	Pasadena
38	Z3-S6	S. Grand Avenue, Along Seismic Line Z3-G2	Pasadena
39	Z3-S7	S. Grand Avenue, Along Seismic Line Z3-G2	South Pasadena
40	Z3-S8	Repton Street at N. Avenue 65	Los Angeles

TABLE C-2
Summary of Multichannel Analyses of Surface Waves and ReMi Testing

Number	MASW Line	Approximate Location	City
41	Z3-S9	San Pascual Avenue, Along Seismic Line Z3-G3	Los Angeles
42	Z3-S10	San Pascual Avenue, Along Seismic Line Z3-G3	Los Angeles
43	Z3-S11	Meridian Avenue at Buena Vista Street	South Pasadena
44	Z3-S12	Brent Avenue at Hope Street	South Pasadena
45	Z3-S13	Pasadena Avenue, Along Seismic Line Z3-G4	South Pasadena
46	Z3-S14	Pasadena Avenue, Along Seismic Line Z3-G4	South Pasadena
47	Z3-S15	Meridian Avenue (N/O Monterey Road)	South Pasadena
48	Z3-S16	Marengo Avenue at Spruce Street	South Pasadena
49	Z3-S17	Via del Rey, Along Seismic Line Z3-G5	South Pasadena
50	Z3-S18	Via del Rey, Along Seismic Line Z3-G5	South Pasadena
51	Z3-S19	Berkshire Avenue (N/O Kendall Avenue)	South Pasadena
52	Z3-S20	Westmont Drive at Keats Street	Alhambra
53	Z3-S21	Winchester Avenue, Along Seismic Line Z3-G6	Alhambra
54	Z3-S22	Winchester Avenue, Along Seismic Line Z3-G6	Alhambra
55	Z3-S23	Westmont Drive, Along Seismic Line Z3-G7	Alhambra
56	Z3-S24	Westmont Drive, Along Seismic Line Z3-G7	Alhambra
57	Z4-S1	Vinedo Avenue at Oneida Street	Pasadena
58	Z4-S2	Oxford Road (S/O Orlando Road)	San Marino
59	Z4-S3	Oxford Road, Along Seismic Line Z4-G1	San Marino
60	Z4-S4	Oxford Road, Along Seismic Line Z4-G1	San Marino
61	Z4-S5	Virginia Road (S/O Monterey Road)	San Marino
62	Z4-S6	E. Huntington Drive, Along Seismic Line Z4-G2	Alhambra
63	Z4-S7	E. Huntington Drive, Along Seismic Line Z4-G2	Alhambra
64	Z4-S8	W. McLean Street (NE/O N. Garfield Avenue)	Alhambra
65	Z4-S9	N. Bushnell Avenue (N/O Larch Street)	Alhambra
66	Z4-S10	S. Date Avenue (S/O W. Commonwealth Avenue)	Alhambra
67	Z5-S1	Hammill Road (S/O Rio Hondo Parkway)	El Monte
68	Z5-S2	Farago Avenue (N/O Grand Avenue)	Temple City
69	Z5-S3	La Rosa Drive at Ryland Avenue	Temple City
70	Z5-S4	Cloverly Avenue (N/O Blackley Street)	Temple City
71	Z5-S6	S. Gladys Avenue (S/O E. Fairview Avenue)	San Gabriel
72	Z5-S7	Abbot Avenue at Hazell Way	San Gabriel
73	Z5-S8	E. Shorb Street, Along Seismic Line Z5-G2	Alhambra
74	Z5-S9	E. Shorb Street, Along Seismic Line Z5-G2	Alhambra
75	Z5-S10	W. Adams Avenue at S. 2nd Street	Alhambra
76	Z5-S11	Benito Avenue (N/O W. Shorb Street)	Alhambra
77	Z5-S12	Edgewood Drive, Along Seismic Line Z5-G3	Alhambra
78	Z5-S13	Edgewood Drive, Along Seismic Line Z5-G3	Alhambra

REPORT

SURFACE WAVE MEASUREMENTS

SR-710 Tunnel Technical Study
Los Angeles County, California

Prepared for

CH2M HILL
6 Hutton Centre Drive, # 700
Santa Ana, CA 92707

Prepared by

GEOVision Geophysical Services
1124 Olympic Drive
Corona, California 92881
(951) 549-1234

Report 9001-01

October 5, 2009

TABLE OF CONTENTS

LIST OF TABLES

LIST OF FIGURES

1 INTRODUCTION

In-situ seismic measurements using active and passive surface wave techniques were performed at various sites within the SR-710 Tunnel Study Areas, located in Los Angeles County, California. The measurements were conducted from February 24, 2009 through May 19, 2009. The purpose of this investigation was to provide shear (S) wave velocity profiles to a depth of 60 meters (200 ft) to support site characterization and screening of the five tunnel study zones. Some of the surface wave soundings were acquired near the ends of the 17 seismic reflection profiles acquired during the investigation to provide additional data for seismic interpretation.

The active surface wave technique utilized during this investigation consisted of the multi-channel analysis of surface waves (MASW) method. The passive surface wave techniques utilized consisted of the refraction microtremor and the array microtremor methods. At many sites active surface wave techniques (SASW and MASW) with the utilization of portable energy sources, such as hammers and weight drops, are sufficient to obtain a 30 m S-wave velocity sounding. Larger energy sources, such as a bulldozer, may be used to image to depths of up to 100 m, but are not typically applicable in developed urban environments. Passive surface wave techniques, such as the refraction microtremor method of Louie, 2001 or the array microtremor technique, can be used to extend depth of investigation at sites that have adequate noise levels.

S-wave velocity models developed from surface wave soundings have many potential applications related to site characterization including correlation of seismic properties between boreholes; estimating depth to bedrock (providing there is sufficient contrast in velocity between bedrock and overlying sediments), estimating N-value using emperical correlations between S-wave velocity and N-value, estimation of excavatability or rippability of rock. The S-wave velocity models can also be used to determine average S-wave velocity over depth intervals. For example, the average shear wave velocity of the upper 30 m or 100 ft (V_S30) is used in the Uniform Building Code (UBC) and International Building Code (IBC) to separate sites into classes for seismic design.

MASW and refraction microtremor data were collected at 78 locations within the five tunnel study zones, labeled Zones 1 to 5 (Figure 1). Array microtremor data, using an “L” shaped array, were collected at 69 of the locations. The 78 surface wave soundings included 20 soundings in Zone 1, 12 soundings in Zone 2, 24 soundings in Zone 3, 10 soundings in Zone 4 and 12 soundings in Zone 5 as shown on Figure 1. A total of 35 surface wave soundings were conducted on seismic reflection profiles acquired as part of this investigation and reported separately. The remaining 43 surface wave soundings were distributed throughout the tunnel study zones.

This report contains the results of the active and passive surface wave measurements conducted at 78 locations at the site. An overview of the surface wave methods is given in Section 2. Field and data reduction and modeling procedures are discussed in Sections 3 and 4, respectively. Interpretation and results are presented in Section 5. Section 6 presents our conclusions. References and our professional certification are presented in Sections 7 and 8, respectively.

2 OVERVIEW OF THE SURFACE WAVE METHODS

A discussion of active and passive surface wave methods is provided in the technical note included as Appendix A. Active surface wave techniques include the spectral analysis of surface waves (SASW) and multi-channel array surface wave (MASW) methods. Passive surface wave techniques include the refraction and array microtremor methods.

The basis of surface wave methods is the dispersive characteristic of Rayleigh waves when propagating in a layered medium. The phase velocity, V_R, depends primarily on the material properties (V_S, mass density, and Poisson's ratio or compression wave velocity) over a depth of approximately one wavelength. Waves of different wavelengths, λ, (or frequencies, f) sample different depths. As a result of the variance in the shear stiffness of the layers, waves with different wavelengths travel at different phase velocities; hence, dispersion. A surface wave dispersion curve, or dispersion curve for short, is the variation of V_R with λ or f.

The MASW method is an in-situ seismic method for determining shear wave velocity (V_S) profiles [Park et al., 1999a and 1999b, Foti, 2000]. Surface wave techniques are non-invasive and non-destructive, with all testing performed on the ground surface at strain levels in the soil in the elastic range (< 0.001%). MASW testing consists of collecting multi-channel seismic data in the field and applying a wavefield transform to obtain the dispersion curve and data modeling.

A detailed description of the MASW method is given by Park, 1999a and 1999b. Ground motions are recorded by 24 or more geophones spaced 1 to 2 m apart and aligned in a linear array and connected to a seismograph. A wavefield transform, such as the f-k or τ-p transform, is applied to the time history data to isolate the surface wave dispersion curve. PICKWIN95, software developed by Oyo Corporation is typically used to process the MASW data and obtain the dispersion curve.

The refraction microtremor technique is a passive surface wave technique developed by Dr. John Louie at University of Nevada, Reno. A detailed description of this technique can be found in Louie, 2001. The refraction microtremor method differs from the more established array microtremor technique in that it uses a linear receiver array rather than a triangular or circular array. Unlike the MASW method, which uses an active energy source (i.e. hammer), the microtremor technique records background noise emanating from ocean wave activity, wind noise, traffic, industrial activity, construction, etc. Refraction microtremor field procedures consist of laying out a linear array of 24, 4.5 to 8 Hz geophones and recording 10, or more, 15 to 60 second noise records. These noise records are reduced using the software package SeisOpt® ReMi™ v2.0 by Optim™ Software and Data Services. This package is used to generate and combine the slowness (p) – frequency (f) transform of the noise records. The surface wave dispersion curve is picked at the lower envelope of the surface wave energy identified in the p-f spectrum.

A detailed discussion of the array microtremor method can be found in Okada, 2003. This technique uses 4 to 24 receivers aligned in a 2-dimensional array. Triangle, circle, semi-circle and "L" shaped arrays are commonly used, although any 2-dimensional arrangement of receivers can be used. Receivers typically consist of 1 to 4.5 Hz geophones. The triangle array, which consists of several embedded equilateral triangles, is often used as it provides good results with a relatively small number of geophones. With this array the outer side of the triangle should be at least equal to the desired depth of investigation. The “L” array is useful at sites located at the corner of perpendicular intersecting streets. Typically 10 to 20, 30-second noise records are acquired for analysis. The surface wave dispersion curve is estimated by calculating the spatial autocorrelation (SPAC) function for the time-history data. A first-order Bessel function is fit to the SPAC function to obtain the dispersion curve (phase velocity at each frequency). PICKWIN95, software developed by Oyo Corporation is typically used to process the array microtremor data and obtain the dispersion curve.

The active and passive surface wave techniques compliment one another as outlined below:

- SASW/MASW techniques image the shallow velocity structure which cannot be imaged by the microtremor technique and is needed for an accurate V_S30/V_S100' estimate.
- Microtremor techniques work best in noisy environments where SASW/MASW depth investigation may be limited.
- In a noisy environment the microtremor technique will usually extend the depth of an SASW/MASW sounding.
- The degree of fit in the overlapping portion of the dispersion curves from the two techniques provides a level of confidence in the results.

The dispersion curves generated from the active and passive surface wave soundings are generally combined and modeled. Typically WinSASW V1, developed at the University of Texas at Austin, or WINSASW V2 (Joh, 2002) is used to model the data, whereby through iterative forward and/or inverse modeling, a V_S profile is found whose theoretical dispersion curve is a close fit to the field data.

The final model profile is assumed to represent actual site conditions. Several options exist for forward modeling: a formulation that takes into account only fundamental-mode Rayleigh wave motion (called the 2-D solution) and one that includes all stress waves and incorporates receiver geometry (3-D solution) [Roesset et al., 1991].

The theoretical model used to interpret the dispersion assumes horizontally layered, laterally invariant, homogeneous-isotropic material. Although these conditions are seldom strictly met at a site, the results of active and/or passive surface wave testing provide a good “global” estimate of the material properties along the array. The results may be more representative of the site than a borehole “point” estimate.

Based on our experience at other sites, the shear wave velocity models determined by surface wave testing are within 20% of the velocities that would be determined by other seismic methods [Brown, 1998]. The average velocity of the upper 30 m or 100 ft, however, is much more accurate than this, often to better than 5%, because it is less sensitive to the layering in the model.

3 FIELD PROCEDURES

MASW and refraction microtremor data were collected at 78 locations within the five SR-710 tunnel study zones (Figure 1). The approximate locations of the surface wave soundings are presented in Table 1. Array microtremor data were collected at 69 of the 78 surface wave locations as shown in Table 2.

A typical MASW field layout is shown in Appendix A and Figure 2. MASW equipment used during this investigation consisted of a Geometrics Geode signal enhancement seismograph, 4.5 Hz vertical geophones, seismic cable with 1 to 3 m (3.3 to 9.8 ft) takeouts, a 3 lb hammer, a 16 lb sledge hammer, a truck-mounted accelerated weight drop (AWD) and an aluminum plate. MASW data were acquired along a linear array with 1 to 2 m (3.3 to 6.6 ft) geophone spacing as outlined in Table 2. Shot points were typically located 1, 3 and 5 m (3.3, 9.8 and 16.4 ft) from the end geophone locations. Typically, the 3 lb hammer was used for the 1 m (3.3 ft) offset source locations, a 16 lb sledge hammer was used for the 3 m (9.8 ft) offset source locations, and the 16 lb sledge hammer and/or AWD were used for the 5 m (16.4 ft) offset source locations. Only the hammer energy sources could be used for the MASW survey at some locations because of space or permitting limitations. Data from the transient impacts (hammers) were averaged 5 times to improve the signal-to-noise ratio. Surface waves were monitored by 24 Oyo Geospace 4.5 Hz geophones and recorded by a Geometrics Geode signal enhancement seismograph. Photographs of typical MASW equipment are presented in Appendix A. All field data was saved to hard disk and documented in a field notebook.

Refraction microtremor measurements were made along a linear array of 24, 4.5 Hz geophones with a 6 m (19.7 ft) geophone spacing, as possible. When a 6 m geophone spacing was not possible due to space limitations, it was adjusted to a 4 or 5.5 m (13.1 or 18 ft) spacing as outlined in Table 2. The refraction microtremor arrays were typically located along sidewalks. A typical field layout is shown in Appendix A. A Geometrics Geode, 24 bit, 24-channel seismic recording system was used to record thirty 30 second noise records using a 2 ms sample rate. Data were stored on a laptop computer for later processing and field geometry and associated files names were documented in a field notebook.

Array microtremor measurements were made along a 24-channel "L"-shaped array using 4.5Hz geophones with a geophone spacing of 6 m (19.7 ft) when possible. When a geophone spacing of 6 m was not possible because of space limitations, a 5 or 5.5 m (16.4 or 18 ft) geophone spacing was used as outlined in Table 2. The array microtremor measurements were typically made along sidewalks of intersecting streets. Occasionally, the geometry of the streets required that the intersecting legs of the array were at an angle other than 90 degrees (i.e. "V" shaped rather than "L" shaped array). A Geometrics Geode, 24 bit, 24-channel seismic recording system was used to record thirty 30 second noise records using a 2ms sample rate. Data were stored on a laptop computer for later processing and field geometry and associated files names were documented in a field notebook.

Surface wave sounding locations or seismic lines to which they were tied were surveyed with a Trimble Pro XRS GPS system with OmniStar submeter differential corrections. Estimated accuracy of the locations and elevations are nominally about 1 m (3.3 ft) and 2 m (6.6 ft), respectively.

4 DATA REDUCTION AND MODELING

The MASW data were reduced using the software PICKWIN95 developed by Oyo Corporation and the following steps:

- Input seismic record into software.
- Enter receiver spacing, geometry and wavelength restrictions, as necessary.
- Apply wavefield transform to seismic record to convert the data to phase velocity – frequency space.
- Identify and pick dispersion curve.
- Repeat for all shot records and merge dispersion curves.
- Convert dispersion curves to WinSASW format for modeling.

The refraction microtremor data were reduced using the Optim™ Software and Data Services SeisOpt® ReMi™ v4.0 data analysis package. Data reduction steps included the following:

- Conversion of SEG-2 format field files to SEG-Y format.
- Data preprocessing which includes trace-equalization gaining and DC offset removal.
- Erasing receiver geometry present in the file header.
- Computing the velocity spectrum of each record by p-f transformation.
- Combining the individual p-f transforms into one image.
- Picking and saving the velocity spectrum image.
- Conversion of the dispersion curve to WinSASW format for modeling.

The array microtremor and refraction microtremor data were reduced using the software PICKWIN95 developed by Oyo Corporation and the following steps:

- Input all seismic records into software.
- Enter receiver spacing, geometry and wavelength restrictions, as necessary.
- Calculate the SPAC function for each seismic record and average.
- For each frequency calculate the degree of fit of a first-order Bessel function to the SPAC function for a multitude of phase velocities.
- Identify and pick dispersion curve as the best fit of the Bessel function for each frequency.
- Convert dispersion curves to WinSASW format for modeling

Example wavefield transforms of the MASW and microtremor data are presented in Figure 3. The surface wave dispersion curves from the active and passive surface wave data were combined to obtain a composite surface wave dispersion curve. Due to lateral velocity variation at many of the surface wave sounding locations, most likely related to subsurface bedrock topography or the often steeply dipping bedrock units, it was not always possible to combine all of the passive surface wave data sets with the MASW data. The datasets with the best agreement were used to create the composite dispersion curve.

The location of surface wave sounding Z1-S17 was such that reliable active and passive surface wave data were not obtained. An S-wave velocity model was not generated for this sounding.

Once a composite surface wave dispersion curve was developed an iterative forward modeling process was used to generate an S-wave velocity model for the sounding. During this process an initial velocity model was generated based on general characteristics of the dispersion curve. The theoretical dispersion curve was then generated using the 2-D modeling algorithm (fundamental mode Rayleigh wave dispersion module) and compared to the field dispersion curve. Adjustments were then made to the thickness and velocities of each layer and the process repeated until an acceptable fit to the field data was obtained.

Data inputs into the modeling software included layer thickness, S-wave velocity, P-wave velocity and mass density. P-wave velocity and mass density only have a very small influence (i.e. less than 10%) on the S-wave velocity model generated from a surface wave dispersion curve. However, realistic assumptions for P-wave velocity, which is impacted significantly by the location of the water table, and mass density will slightly improve the accuracy of the S-wave velocity model.

Constant mass density values of 1.9 to 2.3 g/cc were used in the velocity profiles for subsurface soils and rock. Within the normal range encountered in geotechnical engineering, variation in mass density has a negligible effect on surface wave dispersion. During data modeling, the compression wave velocity, V_P, of unsaturated soils was estimated using a Poisson's ratio, ν, of 0.33 and the relationship:

$$V_P = V_S \, [(2(1-\nu))/(1-2\nu)]^{0.5}.$$

Several approaches were used to estimate groundwater depth in the vicinity of the surface wave soundings. These included a simple, interactive, 2 to 3 layer seismic refraction analysis of MASW shot records and/or selected seismic reflection shot records; review of borehole velocity logs, and interpolation between boreholes or seismic reflection lines. Groundwater depth was assumed for modeling purposes when reasonable estimates could not be made from available surface and borehole geophysical data.

Borehole velocity logs within each of the five tunnel study zones (Zones 1 to 5) were reviewed to correlate P-wave velocity of saturated sediments with S-wave velocity. Borehole velocity and geologic logs were also reviewed to determine if S-wave velocity could be used to differentiate bedrock from overlying sediments. Borehole velocity logs (reported separately) for 6 boreholes (Z1-B3, Z1-B4, Z1-B5, Z1-B6, Z1-B7 and Z1-B8) were available in Zone 1. Borehole velocity logs for 4 boreholes (Z2-B1, Z2-B3, Z2-B4 and Z2-B5) were available in Zone 2. Borehole velocity logs for 12 boreholes (Z3-B1 to Z3-B12) were available in Zone 3. A borehole velocity log for one borehole (Z4-B4) was available in Zone 4. Borehole velocity logs were not available for Zone 5.

5 INTERPRETATION AND RESULTS

5.1 Zone 1

Twenty (20) surface wave soundings were conducted within Zone 1 (Z1-S1 to Z1-S20) as shown in Figure 1. Six of these surface wave soundings were located near the ends of seismic reflection lines and the remaining 14 soundings were distributed throughout the zone.

The fit of the theoretical dispersion curve to the experimental data collected at each site and the modeled V_S profiles for Z1-S1 to Z1-S16 and Z1-S18 to Z1-S20 are presented in Figures 4 to 22, respectively. The resolution decreases gradually with depth because of the loss of sensitivity of the dispersion curve to changes in V_S at greater depth. The V_S depth profiles used to match the field data are provided in tabular form as Tables 3 to 21. The location of surface wave sounding Z1-S17 was such that reliable active and passive surface wave data were not obtained and, therefore, an S-wave velocity model was not generated.

The surface wave phase velocities from the microtremor measurements are generally in good agreement with those from the MASW data in the region of overlapping wavelength. Differences in the surface wave dispersion curves between the two techniques result from the passive surface wave data being averaged over much longer arrays with lateral velocity variation having differing affects on the various data sets. The estimated depths of investigation for the combined active and passive surface wave soundings are between 60 and 70 m (197 and 230 ft), as shown on Tables 3 to 21.

For the purpose of data modeling, groundwater depths for 16 of the soundings (Z1-S2, Z1-S4 and Z1-S7 to Z1-S20) were estimated from simple seismic refraction analysis of MASW shot records with groundwater modeled in the 3 to 10 m (10 to 33 ft) depth range. The other 4 soundings (Z1-S1, Z1-S3, Z1-S5 and Z1-S6) were located at higher elevations in areas with outcropping bedrock. The MASW arrays were not long enough to map approximate groundwater depth at these locations. For the purpose of data modeling, groundwater was assumed to be at a depth of 50 m (164 ft) for Z1-S1 and Z1-S3, 45 m (148 ft) for Z1-S5 and 30 m (98 ft) for Z1-S6. Seismic reflection shot records along seismic line Z1-G3 (Figure 1) indicate that groundwater may be shallower along surface wave soundings Z1-S5 and Z1-S6; however, groundwater depth is not expected to have much impact on the S-wave velocity models in this area. Based on review of six (6) Zone 1 borehole velocity logs, the inferred P-wave velocity of saturated sediments was assumed to range from 1,650 to 2,150 m/s (5,413 to 7,054 ft/s) depending upon S-wave velocity. The modeled/assumed saturated sediments can be identified in Tables 3 to 21 based on inferred P-wave velocity of 1,650 m/s (5,413 ft/s), or greater.

Review of 6 available borehole velocity logs in Zone 1 (Z1-B3, Z1-B4, Z1-B5, Z1-B6, Z1-B7 and Z1-B8), geologic maps and borehole geologic logs indicate that bedrock in Zone 1 primarily consists of siltstone, shale and sandstone units of the Puente Formation. Overlying sediments were typically observed to have S-wave velocity below 350 m/s (1,148 ft/s), although sediment velocities up to 450 m/s (1,476 ft/s) were observed. Decomposed and intensely fractured sedimentary rock was found to often have S-wave velocity in the sediment range. Highly to moderately weathered bedrock often had S-wave velocity in the 350 to 600 m/s range (1,148 to

1,969 ft/s) and slightly weathered and fresh rock were found to often have S-wave velocity greater than 700 m/s (2,297 ft/s). Therefore, S-wave velocity above 350 m/s (1,148 ft/s) in the surface wave velocity models (Figures 4 to 22 and Tables 3 to 21) are generally associated with bedrock. Lower velocities will typically be associated with sediments and occasionally decomposed rock.

The average S-wave velocity of the upper 30 and 60 m (V_S30 and V_S60) and the modeled S-wave velocity at a depth of 60 m (197 ft) for the Zone 1 surface wave soundings are summarized in Table 22. V_S30 and V_S60 range from 181 to 500 m/s (594 to 1641 ft/s) and 269 to 580 m/s (884 to 1,903 ft/s), respectively. Fifteen (15) of the surface wave soundings have V_S30 less than 360 m/s (1,181 ft/s). S-wave velocity at a depth of 60 m (197 ft) ranges from 675 to 850 m/s (2,215 to 2,789 ft/s).

S-wave velocity models were generated for surface wave soundings near each end of two of the three seismic reflection profiles acquired in Zone 1 (Z1-G3 and Z1-G4). Surface wave soundings Z1-S5 and Z1-S6 were conducted in the southwestern and northeastern portions of seismic line Z1-G3, respectively. The S-wave velocity models for these soundings are very similar indicating that there may not be significant lateral velocity variation in the immediate vicinity of the seismic line. Surface wave soundings Z1-S14 and Z1-S15 were conducted in the southwestern and northeastern portions of seismic line Z1-G4, respectively. The S-wave velocity models for these soundings are different with moderately weathered bedrock about 11 m (36 ft) shallower in the vicinity of Z1-S15 located near the northeast end of the line. It should be noted that the surface wave data acquired along Z1-S14 and Z1-S15 were difficult to model due to significant lateral velocity variation of the sediments and highly variable bedrock depths, which cannot adequately be represented by a 1-D model. MASW data and passive “L” array data were in good agreement for Z1-S14 yielding an S-wave velocity model with very low sediment velocity and the lowest Zone 1 V_S30 (181 m/s). The low V_S30 was primarily the result of the very low sediment velocities in the upper 10 m (33 ft), which were in the 125 to 160 m/s (410 to 525 ft/s) range. The passive linear array data acquired along a 138 m profile at this site were in very poor agreement with the MASW data acquired along a 34.5 m profile and “L” array data and were, therefore, not used for modeling. Explanations for the difference between the different data sets include significant variation of near surface sediment velocity and bedrock depth over the longer passive linear array or negative impact of a directional noise bias on passive linear array data. Models of the passive linear array data (not included) indicate that near surface sediment velocities may be higher and bedrock as much as 6 m (20 ft) shallower adjacent to the MASW array. Only passive “L” array data were used to model Z1-S15, which was similar to Z1-S14, because the MASW data could not be accurately reduced, possibly due to complicated shallow velocity structure, and passive linear array data were noisy, possibly due to limited azimuth of noise sources (i.e. unidirectional rather than omnidirectional noise sources).

Three boreholes are located within about 175 m (574 ft) of surface wave soundings: Z1-B3 about 172 m (565 ft) from Z1-S8, Z1-B4 about 25 m (82 ft) of Z1-S13, and Z1-B6 about 148 m (486 ft) from Z1-S15. Borehole locations are shown on Figure 1. Borehole S-wave velocity data for Z1-B3 are plotted with the surface wave S-wave velocity model for Z1-S8 in Figure 11. This plot illustrates the resolution differences between the two methods with the surface wave velocity models providing more averaged (i.e. thicker layer) velocity models. The two velocity models are in reasonable agreement given the distance between the surface wave sounding and the borehole and resolution limitations of the surface wave methods relative to borehole PS Suspension velocity log. Borehole S-wave velocity data for Z1-B6 are plotted with the surface wave S-wave velocity model for Z1-S14, located about 330 m (1,083 ft) and the closer Z1-S15 in Figures 17 and 18, respectively. The sediment velocities are much higher in the PS Suspension velocity log, likely due to significant lateral sediment velocity variation discussed previously for these surface wave soundings. The bedrock velocities between the two methods are in good agreement considering likely variation of bedrock depth and weathering. Borehole S-wave velocity data for Z1-B4 are plotted with the surface wave S-wave velocity model for Z1-S13 in Figure 16. The two velocity models are in good agreement considering the resolution capabilities of the two methods and potential lateral velocity variation in this geologic environment. Assuming that the subsurface velocity structure is the same beneath the surface wave sounding as at the borehole location, the surface wave method does not detect a possible 5 m (16 ft) thick low velocity layer at a depth of 19 m (62.3 ft) and as a result overestimates the depth to the higher velocity underlying sedimentary rock. It is not possible to resolve a low velocity layer of this thickness and depth due to the presence of underlying high velocity rock.

5.2 Zone 2

Twelve (12) surface wave soundings were conducted within Zone 2 (Z2-S1 to Z2-S12) as shown in Figure 1. Six of these surface wave soundings were located near the ends of seismic reflection lines and the remaining 6 soundings were distributed throughout the zone.

The fit of the theoretical dispersion curve to the experimental data collected at each site and the modeled V_S profiles for Z2-S1 to Z2-S12 are presented in Figures 23 to 34, respectively. The resolution decreases gradually with depth because of the loss of sensitivity of the dispersion curve to changes in V_S at greater depth. The V_S depth profiles used to match the field data are provided in tabular form as Tables 23 to 34.

The surface wave phase velocities from the microtremor measurements are generally in good agreement with those from the MASW data in the region of overlapping wavelength. Differences in the surface wave dispersion curves between the two techniques result from the passive surface wave data being averaged over much longer arrays with lateral velocity variation having differing affects on the various data sets. The estimated depths of investigation for the combined active and passive surface wave soundings are between 60 and 70 m (197 and 230 ft), as shown on Tables 23 to 34.

For the purpose of data modeling, groundwater depths for 11 of the 12 soundings (Z2-S1 to Z2-S4 and Z2-S6 to Z2-S12) were estimated from simple seismic refraction analysis of MASW shot records with groundwater modeled in the 2 to 9 m (7 to 30 ft) depth range. The MASW array was not long enough at Z2-S5 to map approximate groundwater depth, which was estimated to be greater than 14 m (46 ft) deep. For the purpose of data modeling, groundwater was assumed to be at a depth of 15 m (49 ft) at Z2-S5. Based on review of four (4) Zone 2 borehole velocity logs, the inferred P-wave velocity of saturated sediments was assumed to range from 1,650 to 2,750 m/s (5,413 to 9,022 ft/s) depending upon S-wave velocity. The modeled/assumed saturated sediments can be identified in Tables 23 to 34 based on inferred P-wave velocity of 1,650 m/s (5,413 ft/s), or greater.

Review of 4 available borehole velocity logs in Zone 2 (Z2-B1, Z2-B3, Z2-B4 and Z2-B5) and geologic maps indicates that bedrock in Zone 1 primarily consists of siltstone, claystone, sandstone and conglomerate units of the Fernando, Puente and Topanga Formations. Overlying sediments were typically observed to have S-wave velocity below 350 m/s (1,148 ft/s). Decomposed and intensely fractured sedimentary rock was found to often have S-wave velocity in the sediment range. S-wave velocity of the sedimentary bedrock ranged from about 350 m/s (1,148 ft/s) to over 1,500 m/s (4,921 ft/s). The variable S-wave velocity in the sedimentary rock is a function of degree of weathering, fracturing and lithology. S-wave velocity above 350 m/s (1,148 ft/s) in the surface wave velocity models (Figures 23 to 34 and Tables 23 to 34) is most likely associated with bedrock. Lower velocities will typically be associated with sediments and/or decomposed/highly weathered and fractured rock.

V_S30, V_S60 and the modeled S-wave velocity at a depth of 60 m (197 ft) for the Zone 2 surface wave soundings are summarized in Table 35. V_S30 and V_S60 range from 256 to 423 m/s (838 to 1,389 ft/s) and 330 to 552 m/s (1,081 to 1,811 ft/s), respectively. Eight (8) of the 12 surface wave soundings have V_S30 less than 360 m/s (1,181 ft/s). S-wave velocity at a depth of 60 m (197 ft) ranges from 420 to 825 m/s (1,378 to 2,707 ft/s).

S-wave velocity models were generated for surface wave soundings near each end of the three seismic reflection profiles acquired in Zone 2 (Z2-G1 to Z2-G3). Surface wave soundings Z2-S3 and Z2-S2 were conducted in the southern and northern portions of seismic line Z2-G1, respectively. The S-wave velocity models for these soundings are very similar, with less than 10% velocity variation in bedrock, indicating that there may not be significant lateral velocity variation in the immediate vicinity of the seismic line. Surface wave soundings Z2-S7 and Z2-S8 were conducted in the southwestern and northeastern portions of seismic line Z2-G2, respectively. The S-wave velocity models for these soundings are similar in the upper 40 m (131 ft) and different at greater depths. The significant lateral velocity variation at depth may be related to changes in bedrock weathering, fracturing or lithology associated with dipping sedimentary units. Surface wave soundings Z2-S10 and Z2-S11 were conducted in the northwestern and southeastern portions of seismic line Z2-G3, respectively. The S-wave velocity models for these soundings are very similar, with less than 10% velocity variation in bedrock, indicating that there may not be significant lateral velocity variation in the immediate vicinity of the seismic line.

No boreholes were drilled in close proximity to any of the surface wave soundings conducted in Zone 2.

5.3 Zone 3

Twenty four (24) surface wave soundings were conducted within Zone 3 (Z3-S1 to Z3-S24) as shown in Figure 1. Fourteen (14) of these surface wave soundings were located near the ends of 7 seismic reflection lines and the remaining 10 soundings were distributed throughout the zone.

The fit of the theoretical dispersion curve to the experimental data collected at each site and the modeled V_S profiles for Z3-S1 to Z3-S24 are presented in Figures 35 to 58, respectively. The resolution decreases gradually with depth because of the loss of sensitivity of the dispersion curve to changes in V_S at greater depth. The V_S depth profiles used to match the field data are provided in tabular form as Tables 36 to 59.

The surface wave phase velocities from the microtremor measurements are generally in good agreement with those from the MASW data in the region of overlapping wavelength. Differences in the surface wave dispersion curves between the two techniques result from the passive surface wave data being averaged over much longer arrays with lateral velocity variation having differing affects on the various data sets. The estimated depths of investigation for the combined active and passive surface wave soundings are between 60 and 75 m (197 and 246 ft), as shown on Tables 36 to 59.

For the purpose of data modeling, groundwater depths for 16 of the 24 soundings (Z3-S1, Z3-S6, Z3-S7, Z3-S9 to Z3-S11, Z3-S13, Z3-S14, Z3-S16 to Z3-S18 and Z3-S20 to Z3-S24) were estimated from simple seismic refraction analysis of MASW or seismic reflection shot records with groundwater modeled in the 3 to 17 m (10 to 56 ft) depth range. Groundwater depths for 4 soundings (Z3-S2 to Z3-S5) were interpreted from nearby borehole velocity logs and interpolated as necessary. Groundwater in the vicinity of these surface wave soundings was modeled in the 30 to 45 m (98 to 148 ft) depth range. The MASW profiles were not long enough to image depth to groundwater at four of the sounding locations (Z3-S8, Z3-S12, Z3-S15 and Z3-S19). Simple seismic refraction analysis of the MASW shot records indicated that groundwater was deeper than 14 m (46 ft) at these locations and for the purpose of modeling groundwater was assumed to be at a depth of 15 m (49 ft). Based on review of 12 Zone 3 borehole velocity logs, the inferred P-wave velocity of saturated sediments was assumed to range from 1,500 to 3,500 m/s (4,921 to 11,483 ft/s) depending upon S-wave velocity. The modeled/assumed saturated sediments can be identified in Tables 36 to 59 based on inferred P-wave velocity of 1,500 m/s (4,921 ft/s), or greater.

Review of 12 available borehole velocity logs in Zone 3 (Z3-B1 to Z3-B12), geologic maps, geologic cross sections and borehole geologic logs indicates that bedrock in Zone 3 consists of siltstone, claystone, sandstone and conglomerate units of the Fernando, Puente and Topanga Formations and crystalline basement rock. Overlying sediments are typically observed to have S-wave velocity in the 175 to 600 m/s (574 to 1,969 ft/s) range. The higher sediment velocities are typically associated with older alluvial deposits encountered in boreholes Z3-B2 to Z3-B4 located north of the Eagle Rock Fault. Typically, a thinner sequence of sediments overlie bedrock south of the Eagle Rock Fault and sediment S-wave velocity rarely exceeded 400 m/s (1,312 ft/s). S-wave velocity of sedimentary rock encountered in the boreholes is in the 325 to 1,850 m/s (1,066 to 6,070 ft/s) range. S-wave velocity of 375 to 450 m/s (1,230 to 1,476 ft/s) is more typical of the lowest velocity for sedimentary rock in many of the boreholes. The variable S-wave velocity in the sedimentary rock is a function of degree of weathering, fracturing and lithology. S-wave velocity of decomposed to weathered crystalline basement rock encountered in boreholes is typically in the 650 to 1,400 m/s (2,133 to 4,593 ft/s) range, but is expected to get much higher as weathering decreases. In areas with crystalline basement north of the Eagle Rock Fault, S-wave velocity over 650 m/s (2,133 ft/s) is probably associated with bedrock with lower velocities associated with overlying sediments. South of the Eagle Rock Fault, S-wave velocity over 400 m/s (1,312 ft/s) will commonly be associated with sedimentary bedrock. Lower velocities will often be associated with sediments; however, there is quite a bit of overlap in sediment and highly weathered sedimentary rock S-wave velocity within Zone 3.

The average S-wave velocity of the upper 30 and 60 m (V_S30 and V_S60) and the modeled S-wave velocity at a depth of 60 m (197 ft) for the Zone 3 surface wave soundings are summarized in Table 60. V_S30 and V_S60 range from 313 to 496 m/s (1,027 to 1627 ft/s) and 361 to 662 m/s (1,184 to 2,172 ft/s), respectively. Twelve (12) of the 24 surface wave soundings have V_S30 less than 360 m/s (1,181 ft/s). S-wave velocity at a depth of 60 m (197 ft) in highly variable in Zone 3, ranging from 435 to 1,250 m/s (1,427 to 4,101 ft/s).

S-wave velocity models were generated for surface wave soundings near each end of the 7 seismic reflection profiles acquired in Zone 3 (Z3-G1 to Z3-G7). Surface wave soundings Z3-S3 and Z3-S4 were conducted at the northern and southern ends of seismic line Z3-G1, respectively. The S-wave velocity models for these soundings are very similar and V_S30 is almost identical indicating that there is no significant lateral velocity variation along the seismic line. Surface wave soundings Z3-S6 and Z3-S7 were conducted at the northern and southern ends of seismic line Z3-G2, respectively. There is more than a 10% difference in the S-wave velocity models and V_S30 for these soundings indicating that there is significant lateral velocity variation along the seismic line, possibly resulting from a geologic structure bisecting the line or steeply dipping geologic units. Surface wave soundings Z3-S9 and Z3-S10 were conducted at the southwestern and northeastern ends of seismic line Z3-G3, respectively. There is a large difference in the S-wave velocity models and V_S30 for these soundings indicating that there is significant lateral velocity variation along the seismic line, possibly resulting from a geologic structure bisecting the line or steeply dipping geologic units. Surface wave soundings Z3-S13 and Z3-S14 were conducted in the northeastern and southwestern portions of seismic line Z3-G4, respectively. The S-wave velocity models for these soundings are very similar and V_S30 is almost identical indicating that there is no significant lateral velocity variation along the seismic line. Surface wave soundings Z3-S17 and Z3-S18 were conducted in the north central and south central portions of seismic line Z3-G5, respectively. The S-wave velocity models for these soundings are very similar, except for small variation in the depth of high velocity bedrock. There is about an 11% difference in V_S30 and V_S60 between the two soundings, therefore some lateral velocity variation associated with deepening bedrock or variation of the weathering profile is present. Surface wave soundings Z3-S21 and Z3-S22 were conducted in the northern and southern portions of seismic line Z3-G6, respectively. There is some variation of near surface and deep velocity structure in the S-wave velocity models for these soundings. Additionally, there is about a 6 to 8% difference in V_S30 and V_S60 between the two soundings and, therefore, some lateral velocity variation occurs along the seismic line. Surface wave soundings Z3-S23 and Z3-S24 were conducted near the northern and southern ends of seismic line Z3-G7, respectively. There is a large difference in the S-wave velocity models and V_S30 for these soundings indicating that there is significant lateral velocity variation along the seismic line, possibly resulting from a geologic structure bisecting the line, steeply dipping geologic units or variable bedrock weathering.

Four (4) boreholes are located within about 155 m (509 ft) of surface wave soundings: Z3-B2 about 114 m (375 ft) from Z3-S2, Z3-B4 about 34 m (110 ft) from Z3-S3, Z3-B9 about 110 m (360 ft) from Z3-S13 and Z3-B12 about 155 m (509 ft) from Z3-S20. Additionally, borehole Z3-B7 is located on seismic reflection line Z3-G3 between surface wave soundings Z3-S9 and Z3-S10. Borehole locations are shown on Figure 1.

Borehole S-wave velocity data for Z3-B2 are plotted with the surface wave S-wave velocity model for Z3-S2 in Figure 36. This plot illustrates the resolution differences between the two methods with the surface wave velocity models providing more averaged (i.e. thicker layer) velocity models. The surface wave velocity model generally has much lower S-wave velocity than the velocity log, which may be the result of lateral velocity variation in the sediments overlying weathered crystalline basement rocks and variable depth to and weathering profile of the basement rock. Borehole S-wave velocity data for Z3-B4 are plotted with the surface wave S-wave velocity model for Z3-S3 in Figure 37. The two velocity models are in good agreement considering the differing resolution capabilities of the two methods. Borehole S-wave velocity data for Z3-B9 are plotted with the surface wave S-wave velocity model for Z3-S13 in Figure 47. The surface wave velocity model generally has slightly lower S-wave velocity than the velocity log, which may be the result of lateral velocity variation between the borehole and surface wave sounding locations. Borehole S-wave velocity data for Z3-B12 are plotted with the surface wave S-wave velocity model for Z3-S20 in Figure 54. The two velocity models are in good agreement considering the differing resolution capabilities of the two methods and distance between the test locations. Borehole S-wave velocity data for Z3-B7 are plotted along the surface wave S-wave velocity models for Z3-S9 and Z3-S10 on Figure 43 and 44, respectively. Both the borehole and surface wave soundings are located on seismic reflection line Z3-G3. As previously discussed, there is significant difference between the two surface wave models. As would be expected, the borehole S-wave velocities lie between the two surface wave models although they are more similar to Z3-S10 below a depth of 30 m (98 ft).

5.4 Zone 4

Ten (10) surface wave soundings were conducted within Zone 4 (Z4-S1 to Z2-S10) as shown in Figure 1. Five of these surface wave soundings were located on seismic reflection lines and the remaining 5 soundings were distributed throughout the zone.

The fit of the theoretical dispersion curve to the experimental data collected at each site and the modeled V_S profiles for Z4-S1 to Z4-S10 are presented in Figures 59 to 68, respectively. The resolution decreases gradually with depth because of the loss of sensitivity of the dispersion curve to changes in V_S at greater depth. The V_S depth profiles used to match the field data are provided in tabular form as Tables 61 to 70.

The surface wave phase velocities from the microtremor measurements are generally in good agreement with those from the MASW data in the region of overlapping wavelength. Differences in the surface wave dispersion curves between the two techniques result from the passive surface wave data being averaged over much longer arrays with lateral velocity variation having differing affects on the various data sets. The estimated depths of investigation for the combined active and passive surface wave soundings are between 60 and 70 m (197 and 230 ft), as shown on Tables 61 to 70.

For the purpose of data modeling, attempts were made to estimate groundwater depth from simple seismic refraction analysis of MASW shot records and seismic records at the ends of two seismic reflection profiles. MASW profiles were not long enough to determine approximate groundwater depth. Groundwater depth was estimated to be on the order of 65 m (213 ft) in the vicinity of seismic reflection profiles Z4-G1 and Z4-G2. Therefore, for data modeling, groundwater was assumed to be 65 m (213 ft) deep in the vicinity of surface wave soundings Z4-S1 to Z4-S7 and then, based on borehole and geophysical control in the adjacent zones, shallow to the southwest between Z4-S8 and Z4-S10. Based on review of a single Zone 4 borehole velocity log, the inferred P-wave velocity of saturated sediments was assumed to range from

1,600 to 1,750 m/s (5,249 to 5,741 ft/s) depending upon S-wave velocity. The modeled/assumed saturated sediments can be identified in Tables 61 to 70 based on inferred P-wave velocity of 1,600 m/s (5,249 ft/s), or greater.

Review of the borehole velocity log for Z4-B4, located in the southwestern corner of Zone 4 (Figure 1), geologic maps and cross sections indicates that bedrock in Zone 4 primarily consists of siltstone, claystone and sandstone units of the Puente Formation and crystalline basement rock. Bedrock is expected to deepen to the northeast and with the exception of the southwestern portion of Zone 4 may exceed 120 m (400 ft) in depth. The borehole velocity log for Z4-B4 indicates that seismic velocity alone may not be useful to distinguish sedimentary rock from overlying sediments. Sediments encountered in the upper 26 m (85 ft) in this borehole have S-wave velocity in the 275 to 550 m/s (902 to 1,804 ft/s) range, whereas decomposed rock immediately beneath the sediments has an S-wave velocity as low as 300 m/s (984 ft/s). Thick sequences of old alluvial sediments in the northeastern portion of Zone 4 may have S-wave velocity increasing with depth to over 600 m/s (1,969 ft/s), similar to the velocities observed in some units of the Puente Formation.

V_S30, V_S60 and the modeled S-wave velocity at a depth of 60 m (197 ft) for the Zone 4 surface wave soundings are summarized in Table 71. V_S30 and V_S60 range from 288 to 373 m/s (944 to 1,225 ft/s) and 349 to 484 m/s (1,144 to 1,589 ft/s), respectively. Seven (7) of the 10 surface wave soundings have V_S30 less than 360 m/s (1,181 ft/s). S-wave velocity at a depth of 60 m (197 ft) ranges from 475 to 600 m/s (1,558 to 1,969 ft/s) with the exception of Z4-S1, which has a modeled S-wave velocity of 850 m/s (2,789 ft/s) at this depth.

S-wave velocity models were generated for surface wave soundings near each end of the two seismic reflection profiles acquired in Zone 4 (Z4-G1 and Z4-G2). Surface wave soundings Z4-S2 to Z4-S4 were conducted in the northern, central and southern portions of seismic line Z4-G1, respectively. The S-wave velocity models for these soundings are quite variable, as may be expected because the Raymond Fault Zone bisects the seismic line. Surface wave soundings Z4-S6 and Z4-S7 were conducted in the northeastern and southwestern portions of seismic line Z4-G2, respectively. The S-wave velocity models for these soundings are almost identical indicating that there is not significant lateral velocity variation in the immediate vicinity of the seismic line.

No boreholes were drilled in close proximity to any of the surface wave soundings conducted in Zone 4.

5.5 Zone 5

Twelve (12) surface wave soundings were conducted within Zone 5 (Z5-S1 to Z5-S4 and Z5-S6 to S5-S13) as shown in Figure 1. Four of these surface wave soundings were located on seismic reflection lines and the remaining 8 soundings were distributed throughout the zone.

The fit of the theoretical dispersion curve to the experimental data collected at each site and the modeled V_S profiles for Z5-S1 to Z5-S4 and Z5-S6 to Z5-S13 are presented in Figures 69 to 80, respectively. The resolution decreases gradually with depth because of the loss of sensitivity of the dispersion curve to changes in V_S at greater depth. The V_S depth profiles used to match the field data are provided in tabular form as Tables 72 to 83.

The surface wave phase velocities from the microtremor measurements are generally in good agreement with those from the MASW data in the region of overlapping wavelength. Differences in the surface wave dispersion curves between the two techniques result from the passive surface wave data being averaged over much longer arrays with lateral velocity variation having differing affects on the various data sets. The estimated depths of investigation for the combined active and passive surface wave soundings are between 60 and 70 m (197 and 230 ft), as shown on Tables 72 to 83.

For the purpose of data modeling, attempts were made to estimate groundwater depth from simple seismic refraction analysis of MASW shot records and seismic records at the ends of two seismic reflection profiles. MASW profiles were not long enough to determine approximate groundwater depth. Groundwater depth was estimated to be on the order of 56 m (184 ft) and 16 m (52 ft) in the vicinity of seismic reflection profiles Z5-G2 and Z5-G3, respectively. Therefore, for data modeling, groundwater was assumed to be 50 to 56 m (164 to 184 ft) deep in the vicinity of surface wave soundings Z5-S1 to Z5-S9, 40 m (131 ft) at Z5-S10, 25 m (82 ft) at Z5-S11 and 16 m (52 ft) at Z5-S12 and Z5-S13. Subsurface geologic conditions in Zone 5 are expected to be similar to those in Zone 4 and, therefore, the inferred P-wave velocity of saturated sediments was assumed to range from 1,600 to 1,750 m/s (5,249 to 5,741 ft/s) depending upon S-wave velocity. The modeled/assumed saturated sediments can be identified in Tables 72 to 83 based on inferred P-wave velocity of 1,600 m/s (5,249 ft/s), or greater.

Boreholes were not drilled in Zone 5. Review of geologic maps and cross sections indicates that bedrock in Zone 5 primarily consists of siltstone, claystone and sandstone units of the Puente Formation and siltstone and claystone of the Fernando Formation. Bedrock is expected to deepen to the east and, with the exception of the western corner of Zone 5, may significantly exceed 120 m (400 ft) in depth. Because the geology in Zone 5 is expected to be similar to that in Zone 4, it is unlikely that S-wave velocity if useful for distinguishing bedrock from overlying sediments. Additionally, bedrock over most of Zone 5 is much deeper than the surface wave soundings can image.

V_S30, V_S60 and the modeled S-wave velocity at a depth of 60 m (197 ft) for the Zone 5 surface wave soundings are summarized in Table 84. V_S30 and V_S60 range from 303 to 392 m/s (994 to 1,287 ft/s) and 362 to 435 m/s (1,187 to 1,429 ft/s), respectively. Eight (8) of the 12 surface wave soundings have V_S30 less than 360 m/s (1,181 ft/s). S-wave velocity at a depth of 60 m (197 ft) ranges from 475 to 625 m/s (1,558 to 2,051 ft/s) and in nominally in the 500 to 550 m/s (1,640 to 1,804 ft/s) range.

S-wave velocity models were generated for surface wave soundings near each end of the two seismic reflection profiles acquired in Zone 5 (Z5-G2 and Z5-G3). Surface wave soundings Z5-S8 and Z5-S9 were conducted in the eastern and western portions of seismic line Z5-G2, respectively. The S-wave velocity models for these soundings are typically within 10% of seismic velocity and V_S30 and V_S60 are within 5% indicating that there is not significant lateral velocity variation in the immediate vicinity of the seismic line. Surface wave soundings Z5-S12 and Z5-S13 were conducted in the northern and southern portions of seismic line Z5-G3, respectively. The S-wave velocity models, V_S30 and V_S60 for these soundings are typically within 11% of seismic velocity indicating that there is not significant lateral velocity variation in the immediate vicinity of the seismic line.

6 CONCLUSIONS

Active and passive surface wave data were collected at 78 locations within the five SR-710 Tunnel Study Zones, located in Los Angeles County, California. The measurements were conducted from February 24, 2009 through May 19, 2009. The purpose of the investigation was to support site characterization and screening efforts and a seismic reflection survey conducted as part of the investigation and reported separately. Surface wave sounding locations are shown on Figure 1 along with the five tunnel study zones, borehole locations and seismic reflection lines. A total of 35 of the surface wave soundings were conducted on seismic reflection lines and the remaining 43 soundings were distributed throughout the tunnel study zones.

The S-wave velocity models derived from the surface wave soundings and summaries are presented as Figures 4 to 80 and Tables 3 to 84. The average S-wave velocity of the upper 30 and 60 m (V_S30 and V_S60) and the modeled S-wave velocity at a depth of 60 m (197 ft) for the surface wave soundings conducted in Zones 1 to 5 are summarized in Tables 22, 35, 60, 71 and 84, respectively. V_S30 and V_S60 range from 181 to 500 m/s (594 to 1641 ft/s) and 269 to 662 m/s (884 to 2,172 ft/s), respectively. Fifty (50) of the surface wave soundings have V_S30 less than 360 m/s (1,181 ft/s). Modeled S-wave velocity at a depth of 60 m (197 ft) is highly variable ranging from about 420 to 1,250 m/s (1,378 to 4,101 ft/s).

Surface wave data were acquired and modeled at least two locations on each of the 17 seismic reflection lines except for Z1-G5, where one of the surface wave soundings did not yield data that could be modeled. The surface wave soundings indicated than 9 of the seismic lines (Z1-G3, Z2-G1, Z2-G2, Z2-G3, Z3-G1, Z3-G4, Z4-G2, Z5-G2 and Z5-G3) have only minor lateral velocity variation. Therefore, potential geologic structures bisecting these lines do not have a significant impact on subsurface velocity structure. There is significant lateral velocity variation along the other 7 seismic reflection lines (Z1-G4, Z3-G2, Z3-G3, Z3-G5, Z3-G6, Z3-G7 and Z4-G1). The lateral velocity variation along these seismic lines may be the result of a geologic structure, such as a fault, bisecting the line or, alternatively, may be the result of dipping geologic units, variable bedrock depths or variable bedrock weathering profiles.

Review of borehole velocity logs from boreholes primarily located in Zones 1 to 3 indicated that S-wave velocity may be applicable for differentiating sediments from shallow sedimentary rock in Zones 1 and 2. In these zones, S-wave velocity below 350 m/s (1,148 ft/s) was typically found to be associated with sediments, whereas higher velocities were associated with sedimentary rock. However, decomposed rock was occasionally found to have S-wave velocity in the sediment range. The application of S-wave velocity to differentiate sediments from bedrock was more difficult in Zone 3 due to thick accumulations of high velocity, old alluvial sediments in the northern portion of the zone. In areas with crystalline basement north of the Eagle Rock Fault, S-wave velocity over 650 m/s (2,133 ft/s) was found to be typically associated with bedrock and lower velocities associated with overlying sediments. South of the Eagle Rock Fault, S-wave velocity over 400 m/s (1,312 ft/s) was often found to be associated with sedimentary bedrock. However, there was some overlap in S-wave velocity between sediments and weathered sedimentary rock in Zone 3. There was limited borehole control in Zones 4 and 5, and with the exception of the southwestern corner of these zones, bedrock was expected to be much deeper than the exploration limits of the surface wave method.

7 REFERENCES

Brown, L.T., 1998, "Comparison of V_S profiles from SASW and borehole measurements at strong motion sites in Southern California", Master's thesis, University of Texas at Austin.

Foti, S., 2000, "Multistation Methods for Geotechnical Characterization using Surface Waves", Ph.D. Dissertation, Politecnico di Torino, Italy.

Joh, S.H., 2002, "WinSASW Version 2.0, Data Interpretation and Analysis for SASW Measurements", Department of Civil Engineering, Chung-Ang University, Anseong, Korea.

Louie, J.N., 2001, "Faster, Better: Shear-Wave Velocity to 100 Meters Depth from Refraction Microtremor Arrays", Bulletin of the Seismological Society of America, vol. 91, no. 2, p. 347-364.

Okada, H, 2003, "The Microtremor Survey Method," Society of Exploration Geophysics Geophysical Monograph Series, Number 12, 135p.

Park, C.B., Miller, R.D. and Xia, J., 1999a, "Multimodal analysis of high frequency surface waves", *Proceedings of the Symposium on the Application of Geophysics to Engineering and Environmental Problems '99*, 115-121.

Park, C.B., Miller, R.D. and Xia, J., 1999b, "Multichannel analysis of surface waves", Geophysics, Vol 64, No. 3, 800-808.

Roesset, J.M., Chang, D.W. and Stokoe, K.H., II, 1991, "Comparison of 2-D and 3-D Models for Analysis of Surface Wave Tests," *Proceedings,* 5th *International Conference on Soil Dynamics and Earthquake Engineering*, Karlsruhe, Germany.

8 CERTIFICATION

All geophysical data, analysis, interpretations, conclusions, and recommendations in this document have been prepared under the supervision of and reviewed by a **GEO*Vision*** California Professional Geophysicist.

10/05/09

Antony J. Martin — Date

California Professional Geophysicist GP989

GEO*Vision* Geophysical Services

* This geophysical investigation was conducted under the supervision of a California Professional Geophysicist using industry standard methods and equipment. A high degree of professionalism was maintained during all aspects of the project from the field investigation and data acquisition, through data processing interpretation and reporting. All original field data files, field notes and observations, and other pertinent information are maintained in the project files and are available for the client to review for a period of at least one year.

A professional geophysicist's certification of interpreted geophysical conditions comprises a declaration of his/her professional judgment. It does not constitute a warranty or guarantee, expressed or implied, nor does it relieve any other party of its responsibility to abide by contract documents, applicable codes, standards, regulations or ordinances.

APPENDIX A

TECHNICAL NOTE

ACTIVE AND PASSIVE SURFACE WAVE TECHNIQUES

ACTIVE AND PASSIVE SURFACE WAVE TECHNIQUES

GEOVision geophysical services

Overview

Active and passive surface wave techniques are relatively new in-situ seismic methods for determining shear wave velocity (V_S) profiles. Testing is performed on the ground surface, allowing for less costly measurements than with traditional borehole methods. The basis of surface wave techniques is the dispersive characteristic of Rayleigh waves when traveling through a layered medium. Rayleigh wave velocity is determined by the material properties (primarily shear wave velocity, but also to a lesser degree compression wave velocity and material density) of the subsurface to a depth of approximately 1 to 2 wavelengths. As shown in the adjacent diagram, longer wavelengths penetrate deeper and their velocity is affected by the material properties at greater depth. Surface wave testing consists of measuring the surface wave dispersion curve at a site and modeling it to obtain the corresponding shear wave velocity profile.

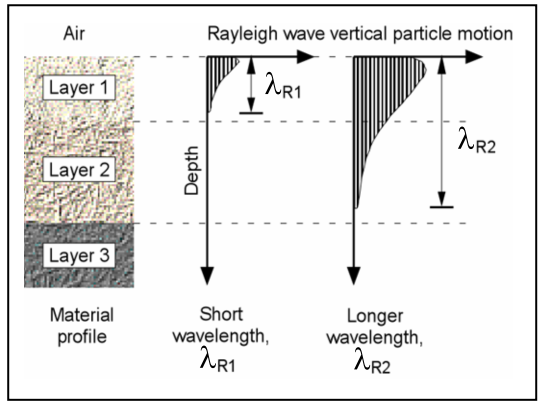

Active Surface Wave Techniques

Active surface wave techniques measure surface waves generated by dynamic sources such as hammers, weight drops, electromechanical shakers, vibroseis and bulldozers. These techniques include the spectral analysis of surface waves (SASW) and multi-channel array surface wave (MASW) methods.

Hammer Energy Sources

Accelerated Weight Drop

Electromechanical Shaker

Bulldozer Energy Source

1124 Olympic Drive, Corona, California 92881 ph. 951-549-1234 fx 951-549-1236 www.geovision.com

The SASW method is optimized for conducting V_S depth soundings. A dynamic source is used to generate surface waves of different wavelengths (or frequencies) which are monitored by two or more receivers at known offsets. An expanding receiver spread and optimized source-receiver geometry are used to minimize near field effects, body wave signal and attenuation. A dynamic signal analyzer is typically used to calculate the phase and coherence of the cross spectrum of the time history data collected at a pair of receivers. During data analysis, an interactive masking process is used to discard low quality data and to unwrap the phase spectrum, as shown in the figure below. The dispersion curve (Rayleigh wave phase velocity versus frequency or alternatively wavelength) is calculated from the unwrapped phase spectrum.

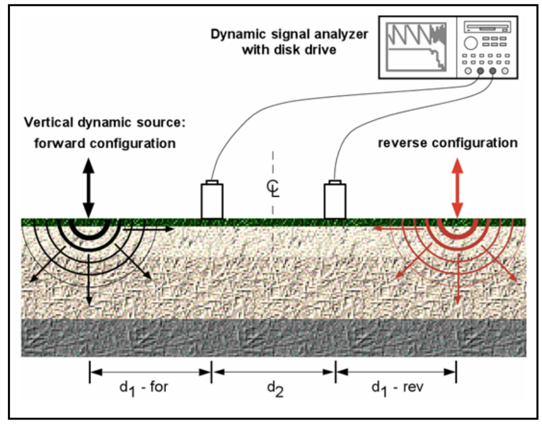

SASW Setup

HP Dynamic Signal Analyzer

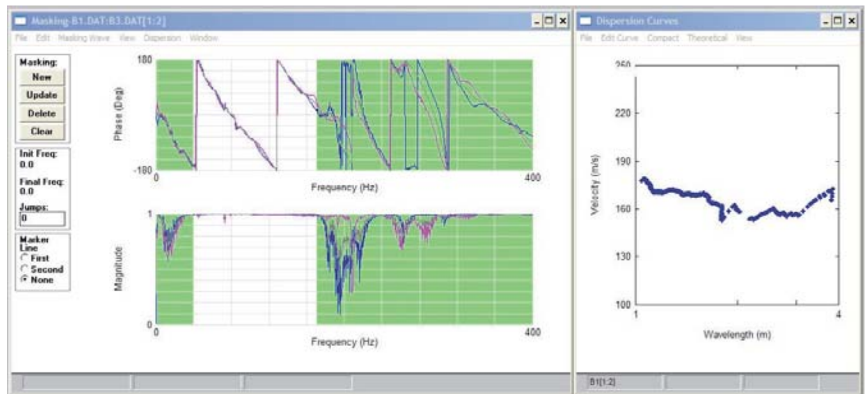

Masking of Wrapped Phase Spectrum and Resulting Dispersion Curve

The MASW field layout is similar to that of the seismic refraction technique. Twenty four, or more, geophones are laid out in a linear array with 1 to 2m spacing and connected to a multi-channel seismograph as shown below. This technique is ideally suited to 2D V_S imaging, with data collected in a roll-along manner similar to that of the seismic reflection technique. The source is offset at a predetermined distance from the near geophone usually determined by field testing. The Rayleigh wave dispersion curve is obtained by a wavefield transformation of the seismic record such as the f-k or τ-p transforms. These transforms are very effective at isolating surface wave energy from that of body waves. The dispersion curve is picked as the peak of the surface wave energy in slowness (or velocity) – frequency space as shown. One advantage of the MASW technique is that the wavefield transformation may not only identify the fundamental mode but also higher modes of surface waves. At some sites, particularly those with large velocity inversions, higher surface wave modes may contain more energy than the fundamental mode.

MASW Field Setup

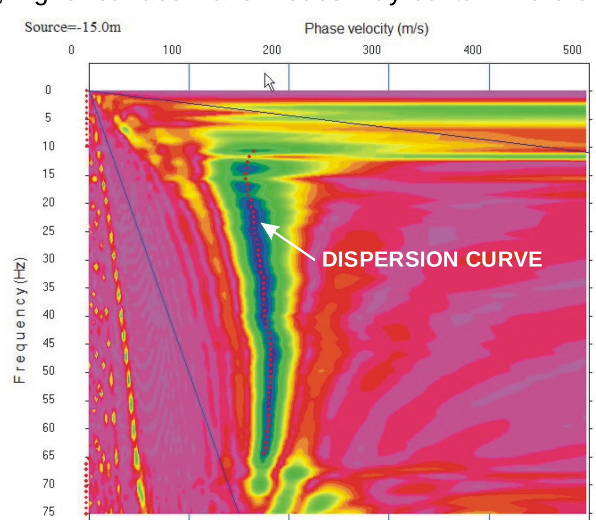

Wavefield Transform of MASW data

Passive Surface Wave Techniques
Passive surface wave techniques measure noise; surface waves from ocean wave activity, traffic, factories, etc. These techniques include the array microtremor and refraction microtremor (REMI) techniques.

The array microtremor technique typically uses 7 or more 4.5- or 1-Hz geophones arranged in a two-dimensional array. The most common arrays are the triangle, circle, semi-circle and "L" arrays. The triangle array, which consists of several embedded equilateral triangles, is often used as it provides good results with a relatively small number of geophones. With this array the outer side of the triangle should be at least as long as the desired depth of investigation. Typically, fifteen to twenty 30-second noise records are acquired for analysis. The spatial autocorrelation (SPAC) technique is one of several methods that can be used to estimate the Rayleigh wave dispersion curve. A first order Bessel function is fit to the SPAC function to determine the phase velocity for particular frequency. The image shown below shows the degree of fitness of the Bessel function to the SPAC function for a wide range of phase velocity and frequency. The dispersion curve, is the peak (best fit), as shown in the figure below.

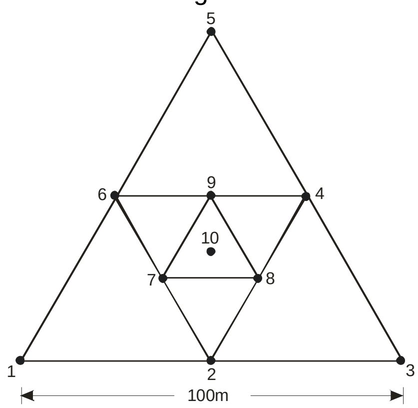

Triangle Array Geometry

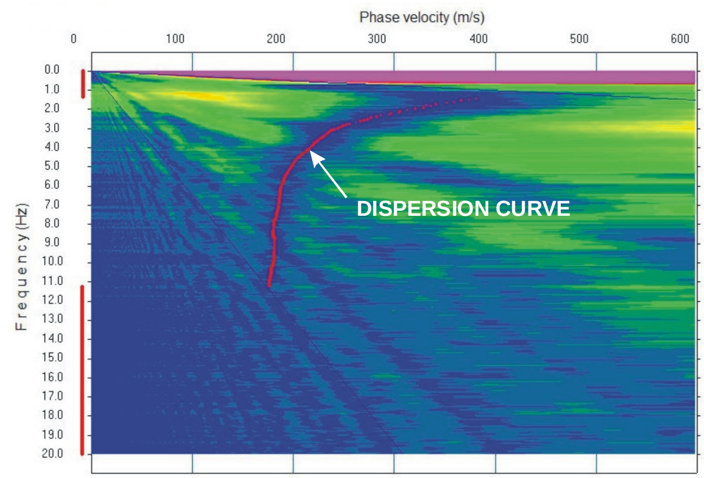

Dispersion Curve from Array Microtremor Measurements

The refraction microtremor (REMI) technique uses a field layout similar to the seismic refraction method (hence its name). Twenty-four, 4.5 Hz geophones are laid out in a linear array with a spacing of 6 to 8m and fifteen to twenty 30-second noise records are acquired. A slowness-frequency (p-f) wavefield transform is used to separate Rayleigh wave energy from that of other waves. Because the noise field can originate from any direction, the wavefield transform is conducted for multiple vectors through the geophone array, all of which are summed. The dispersion curve is defined as the lower envelope of the Rayleigh wave energy in p-f space. Because the lower envelope is picked rather than the energy peak (energy traveling along the profile is slower than that approaching from an angle), this technique may be somewhat more subjective than the others, particularly at low frequencies. The SPAC technique can also be used to extract the surface wave dispersion curve from linear array microtremor data providing there are omni-directional noise sources.

Refraction Microtremor Array Layout

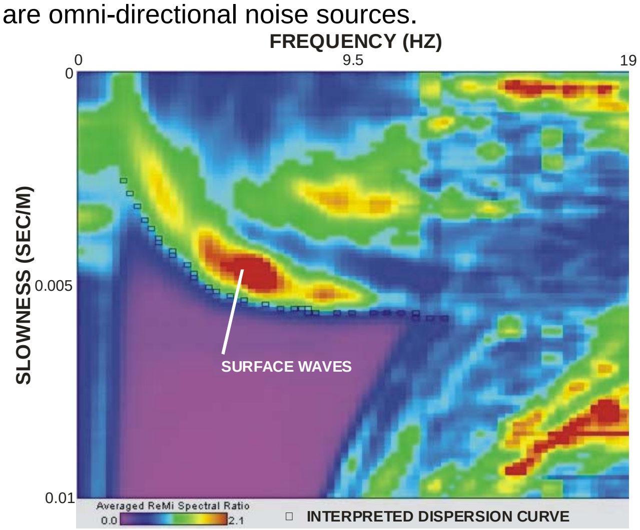

Wavefield Transform of REMI Data

Depth of Investigation

Active surface wave investigations typically use various sized sledge hammers to image the shear wave velocity structure to depths of up to 15m. Weight drops and electromechanical shakers can often be used to image to depths of 30m. Bulldozers and vibroseis trucks can be used to image to depths as great as 100m. Passive surface wave techniques can often image shear wave velocity structure to depths of over 100m, given sufficient noise sources and space for the receiver array. Large passive arrays, utilizing long-period seismometers with GPS clocks have been used to image shear wave velocity structure to depths of several kilometers.

Combined Active and Passive Surface Wave Testing

The combined use of active and passive techniques may offer significant advantages on many investigations. It can be very costly to mobilize large energy sources for 30m/100ft active surface wave soundings. In urban environments, the combined use of active and passive surface wave techniques can image to these depths without the need for large energy sources. We have found that dispersion curves from active and passive surface wave techniques are generally in good agreement, making the combined use of the two techniques viable. It is not recommended that passive surface wave techniques be applied alone for UBC/IBC site classification investigations. Microtremor techniques do not generally characterize near surface velocity, which may have a significant impact of the average shear wave velocity of the upper 30m or 100ft and so should always be used in conjunction with SASW or MASW. An SASW sounding to a depth of 30m requires at least a 60m linear array. If sufficient space is not available for this, it may be possible to use a 45m triangle array on the site or place a 100-200m long REMI array along an adjacent sidewalk or an “L” array at an adjacent street intersection.

Microtremor Measurements along Sidewalk

Modeling

There are several options for interpreting surface wave dispersion curves, depending on the accuracy required in the shear wave velocity profile. A simple empirical analysis can be done to estimate the average shear wave velocity profile. For greater accuracy, forward modeling of fundamental-mode Rayleigh wave dispersion as well as full stress wave propagation can be performed using several software packages. A formal inversion scheme may also be used. With many of the analytical approaches, background information on the site can be incorporated into the model and the resolution of the final profile may be quantified.

Applications

Active and passive surface wave testing can be used to obtain V_S profiles for:

- UBC/IBC site classification for seismic design
- Earthquake site response
- Seismic microzonation
- Liquefaction analysis
- Soil compaction control
- Mapping subsurface stratigraphy
- Locating potentially weak zones in earthen embankments and levees

Case History

The figures below show the surface wave dispersion curves and alternative shear wave velocity models for a site in Los Angeles, California. All of the previous figures illustrating SASW, MASW, array and refraction microtremor techniques were from this site. The dispersion curves from all four methods are shown on the left along with the theoretical dispersion curves for alternative S-wave velocity versus depth models on the right. Conditions at this site were very poor for active surface wave techniques because of the presence of very low velocity hydraulic fill. In fact, with active surface wave techniques it was only possible to image to a depth of about 12.5m with energy sources typically capable of imaging to 30m. There is excellent agreement in the dispersion curves generated from all of the methods over the overlapping wavelength ranges. The minor differences probably result from variable velocity of the hydraulic fill within the sampling volume of the specific methods. Two Vs versus depth models were generated to illustrate the difficulty modeling the highly variable, near surface velocity structure evident in the PS log. The two surface wave models yielded similar values for the average shear-wave velocity of the upper 30m (V_S30), 201 and 202 m/s, illustrating that Vs30 is much more tightly constrained than the actual layer thicknesses and velocities in the models. V_S30 estimated from the PS log (194 m/s) is within 4% of that estimated from the two surface wave models (201 and 202 m/s). The small differences in V_S30 between the two methods may easily result from the different sampling regimes (borehole versus large area) rather than errors in either of the methods.

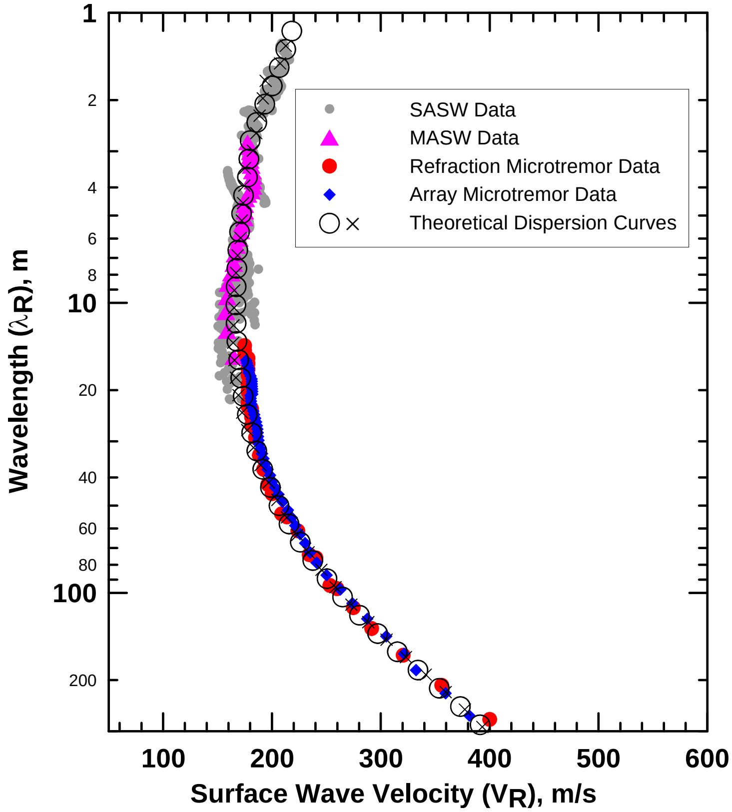

Field Data and Theoretical Dispersion Curve

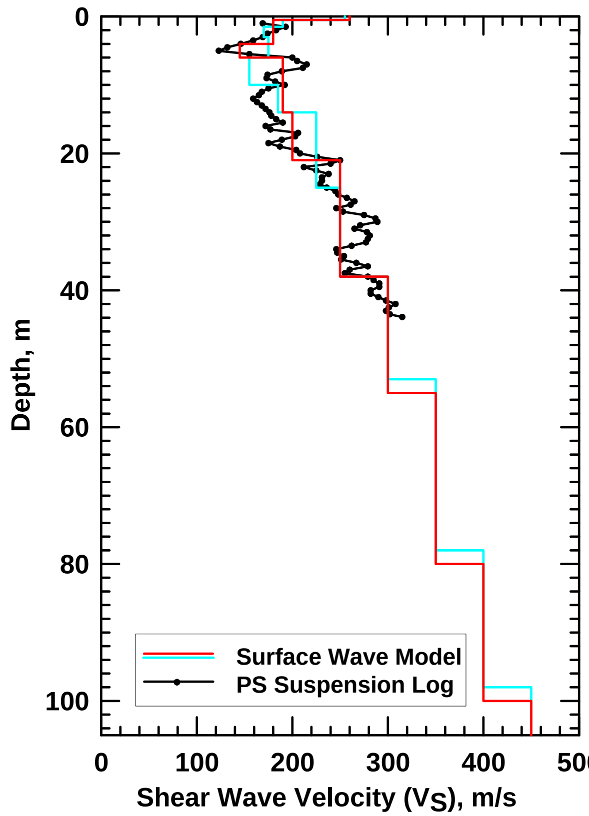

V_S Model

In contrast to borehole measurements which are point estimates, surface wave testing is a global measurement, that is, a much larger volume of the subsurface is sampled. The resulting profile is representative of the subsurface properties averaged over distances of up to several hundred feet. Although surface wave techniques do not have the layer sensitivity or accuracy (velocity and layer thickness) of borehole techniques; the average velocity over a large depth interval (i.e. the average shear wave velocity of the upper 30m or 100ft) is very well constrained. Because surface wave methods are non-invasive and non-destructive, it is relatively easy to obtain the necessary permits for testing. At sites that are favorable for surface wave propagation, active and passive surface wave techniques allow appreciable cost and time savings.

TABLES

Table 1 Surface Wave Sounding Locations

Surface Wave Sounding	Northing (ft)	Easting (ft)	Elevation (ft)	Elevation (m)
Z1-S1	1858859	6484375	602	184
Z1-S2	1860241	6486978	365	111
Z1-S3	1855713	6486181	572	174
Z1-S4	1858034	6487619	354	108
Z1-S5	1854017	6488212	558	170
Z1-S6	1854836	6488769	495	151
Z1-S7	1855081	6490960	339	103
Z1-S8	1855912	6493275	343	105
Z1-S9	1857467	6492596	373	114
Z1-S10	1857156	6493973	405	124
Z1-S11	1851776	6497134	388	118
Z1-S12	1854510	6496669	375	114
Z1-S13	1855365	6498202	387	118
Z1-S14	1851778	6503719	430	131
Z1-S15	1852614	6504404	443	135
Z1-S16	1853425	6507732	458	140
Z1-S17	1851189	6507746	451	137
Z1-S18	1852828	6501056	519	158
Z1-S19	1850601	6508208	460	140
Z1-S20	1849226	6512497	410	125
Z2-S1	1867725	6491385	495	151
Z2-S2	1867940	6496459	512	156
Z2-S3	1866836	6496205	498	152
Z2-S4	1864067	6497693	589	179
Z2-S5	1863749	6501923	562	171
Z2-S6	1862660	6500632	560	171
Z2-S7	1860704	6500564	504	154
Z2-S8	1861511	6501933	518	158
Z2-S9	1859442	6505698	565	172
Z2-S10	1855524	6508114	529	161
Z2-S11	1854560	6508588	489	149
Z2-S12	1851917	6511435	435	133
Z3-S1	1873355	6508880	856	261
Z3-S2	1872437	6515241	803	245
Z3-S3	1870876	6516649	760	232
Z3-S4	1868917	6516666	740	226
Z3-S5	1869134	6514649	792	241
Z3-S6	1868529	6512309	685	209
Z3-S7	1867430	6512291	685	209

California State Plane coordinate system, North American Datum 1983, Zone V (0405), US Survey Feet
Horizontal accuracy is approximately 1m, vertical accuracy is approximately 2m.

Table 1 (continued)   Surface Wave Sounding Locations

Surface Wave Sounding	Northing (ft)	Easting (ft)	Elevation (ft)	Elevation (m)
Z3-S8	1865577	6507915	629	192
Z3-S9	1865625	6509614	581	177
Z3-S10	1866852	6511062	606	185
Z3-S11	1866385	6514149	752	229
Z3-S12	1864933	6516620	662	202
Z3-S13	1864229	6511117	628	191
Z3-S14	1863395	6510579	624	190
Z3-S15	1863362	6514035	653	199
Z3-S16	1860840	6517236	576	176
Z3-S17	1859471	6510276	626	191
Z3-S18	1859110	6510324	616	188
Z3-S19	1858453	6513474	563	171
Z3-S20	1855555	6513374	527	161
Z3-S21	1853042	6513102	455	139
Z3-S22	1852143	6513121	430	131
Z3-S23	1849598	6513201	418	127
Z3-S24	1848525	6513200	430	131
Z4-S1	1873443	6532600	689	210
Z4-S2	1870461	6528291	675	206
Z4-S3	1868812	6528564	608	185
Z4-S4	1867261	6528903	572	174
Z4-S5	1865714	6525732	558	170
Z4-S6	1862787	6522740	551	168
Z4-S7	1861952	6521747	553	168
Z4-S8	1859713	6521908	536	164
Z4-S9	1857271	6519012	525	160
Z4-S10	1854206	6516832	494	150
Z5-S1	1858186	6559083	338	103
Z5-S2	1857834	6552545	319	97
Z5-S3	1857071	6547330	328	100
Z5-S4	1857431	6542974	349	106
Z5-S6	1854909	6534525	361	110
Z5-S7	1853910	6530313	371	113
Z5-S8	1851881	6527893	375	114
Z5-S9	1851805	6526574	400	122
Z5-S10	1852828	6523633	440	134
Z5-S11	1851500	6519232	458	139
Z5-S12	1849766	6516622	436	133
Z5-S13	1848767	6516641	422	129

California State Plane coordinate system, North American Datum 1983, Zone V (0405), US Survey Feet
Horizontal accuracy is approximately 1m, vertical accuracy is approximately 2m.

Table 2 Active and Passive Surface Wave Sounding Geometry

Surface Wave Sounding	MASW Receiver Spacing (m)	Passive Linear Array Receiver Spacing (m)	Passive "L" Array Receiver Spacing (m)
Z1-S1	1.5	4	NC
Z1-S2	1.5	6	6
Z1-S3	1.5	6	6
Z1-S4	1.5	6	6
Z1-S5	1.5	6	6
Z1-S6	1.5	6	NC
Z1-S7	1.5	6	6
Z1-S8	1.5	6	NC
Z1-S9	1.5	6	6
Z1-S10	1.5	6	6
Z1-S11	1.5	6	6
Z1-S12	1.5	6	6
Z1-S13	1.5	6	6
Z1-S14	1.5	6	6
Z1-S15	1.5	6	6
Z1-S16	1.5	6	6
Z1-S17	1.5	6	6
Z1-S18	1.5	6	6
Z1-S19	1.5	6	6
Z1-S20	1.5	6	6
Z2-S1	1.5	6	6
Z2-S2	1.5	6	6
Z2-S3	1.5	6	6
Z2-S4	1.5	6	6
Z2-S5	1.5	6	6
Z2-S6	1.5	6	6
Z2-S7	1.5	6	5
Z2-S8	1.5	5.5	5.5
Z2-S9	1.5	6	6
Z2-S10	1.5	6	6
Z2-S11	1.5	6	6
Z2-S12	1.5	6	6
Z3-S1	1.5	6	6
Z3-S2	1.5	6	6
Z3-S3	1.5	6	6
Z3-S4	1.5	6	6
Z3-S5	1.5	6	6
Z3-S6	1.5	6	6
Z3-S7	1.5	6	6
Z3-S8	1.5	6	6
Z3-S9	1.5	6	6
Z3-S10	1.5	6	NC
Z3-S11	1.5	6	6
Z3-S12	1.5	6	6
Z3-S13	1.5	6	NC
Z3-S14	1.5	6	6
Z3-S15	1.5	6	6
Z3-S16	1.5	6	6
Z3-S17	1.5	6	6
Z3-S18	1.5	6	6
Z3-S19	1.5	6	6
Z3-S20	1.5	6	6
Z3-S21	1 & 2	6	6
Z3-S22	1.5	6	6
Z3-S23	1 & 2	6	NC
Z3-S24	1.5	6	6
Z4-S1	1.5	6	6
Z4-S2	1.5	6	NC
Z4-S3	1.5	6	NC
Z4-S4	1.5	6	NC
Z4-S5	1.5	6	6
Z4-S6	1.5	6	6
Z4-S7	1.5	6	6
Z4-S8	1.5	6	6
Z4-S9	1.5	6	6
Z4-S10	1.5	6	6
Z5-S1	1.5	6	6
Z5-S2	1.5	6	6
Z5-S3	1.5	6	6
Z5-S4	1.5	6	6
Z5-S6	1.5	6	6
Z5-S7	1.5	6	6
Z5-S8	1.5	6	6
Z5-S9	1.5	6	6
Z5-S10	1.5	6	6
Z5-S11	1.5	6	6
Z5-S12	1.5	6	6
Z5-S13	1.5	6	6

Note: NC = Not Conducted

Table 3 Velocity Model for Surface Wave Array Z1-S1

Approx. Elevation of Top of Layer		Depth to Top of Layer		Layer Thickness		S-Wave Velocity		Inferred P-Wave Velocity	
m	ft	m	ft	m	ft	m/s	ft/s	m/s	ft/s
184	603.7	0	0.0	2	6.6	285	935	570	1870
182	597.1	2	6.6	2	6.6	315	1033	630	2067
180	590.6	4	13.1	3	9.8	325	1066	650	2133
177	580.7	7	23.0	5	16.4	350	1148	700	2297
172	564	12	39	12	39	375	1230	750	2460
160	525	24	79	13	43	430	1411	860	2821
147	482	37	121	13	43	675	2215	1350	4429
134	440	50	164	7	23	675	2215	1850	6070
127	417	57	187	>13	>43	725	2379	2150	7054

Approximate depth of investigation is 70m.

Table 4 Velocity Model for Surface Wave Array Z1-S2

Approx. Elevation of Top of Layer		Depth to Top of Layer		Layer Thickness		S-Wave Velocity		Inferred P-Wave Velocity	
m	ft	m	ft	m	ft	m/s	ft/s	m/s	ft/s
111	364.2	0	0.0	1.5	4.9	210	689	420	1378
109.5	359.3	1.5	4.9	2.5	8.2	145	476	290	951
107	351.0	4	13.1	6	19.7	310	1017	620	2034
101	331.4	10	32.8	9	29.5	310	1017	1650	5413
92	301.8	19	62.3	15	49.2	400	1312	1850	6070
77	252.6	34	111.5	20	65.6	525	1722	1850	6070
57	187.0	54	177.2	>16	>52.5	700	2297	2150	7054

Approximate depth of investigation is 70m.

Table 5 Velocity Model for Surface Wave Array Z1-S3

Approx. Elevation of Top of Layer		Depth to Top of Layer		Layer Thickness		S-Wave Velocity		Inferred P-Wave Velocity	
m	ft	m	ft	m	ft	m/s	ft/s	m/s	ft/s
174	570.9	0	0.0	1.5	4.9	140	459	280	919
172.5	565.9	1.5	4.9	2	6.6	265	869	530	1739
170.5	559.4	3.5	11.5	5.5	18.0	375	1230	750	2460
165	541.3	9	29.5	12	39.4	425	1394	850	2788
153	502	21	69	12	39	600	1969	1200	3937
141	463	33	108	17	56	750	2461	1500	4921
124	407	50	164	18	59	750	2461	2150	7054
106	348	68	223	>2	>7	850	2789	2150	7054

Approximate depth of investigation is 70m.

Table 6 Velocity Model for Surface Wave Array Z1-S4

Approx. Elevation of Top of Layer		Depth to Top of Layer		Layer Thickness		S-Wave Velocity		Inferred P-Wave Velocity	
m	ft	m	ft	m	ft	m/s	ft/s	m/s	ft/s
108	354.3	0	0.0	1.5	4.9	135	443	270	886
106.5	349.4	1.5	4.9	2	6.6	175	574	350	1148
104.5	342.8	3.5	11.5	5.5	18.0	265	869	530	1739
99	324.8	9	29.5	4	13.1	265	869	1650	5413
95	312	13	43	10	33	425	1394	1850	6070
85	279	23	75	15	49	525	1722	1850	6070
70	230	38	125	>22	>72	700	2297	2150	7054

Approximate depth of investigation is 60m.

Table 7 Velocity Model for Surface Wave Array Z1-S5

Approx. Elevation of Top of Layer		Depth to Top of Layer		Layer Thickness		S-Wave Velocity		Inferred P-Wave Velocity	
m	ft	m	ft	m	ft	m/s	ft/s	m/s	ft/s
170	557.7	0	0.0	1.5	4.9	270	886	540	1772
168.5	552.8	1.5	4.9	4.5	14.8	200	656	400	1312
164	538.1	6	19.7	12	39.4	300	984	600	1969
152	498.7	18	59.1	13	42.7	450	1476	900	2952
139	456.0	31	101.7	15	49.2	600	1969	1200	3937
124	406.8	46	150.9	>24	>78.7	800	2625	2150	7054

Approximate depth of investigation is 70m.

Table 8 Velocity Model for Surface Wave Array Z1-S6

Approx. Elevation of Top of Layer		Depth to Top of Layer		Layer Thickness		S-Wave Velocity		Inferred P-Wave Velocity	
m	ft	m	ft	m	ft	m/s	ft/s	m/s	ft/s
151	495.4	0	0.0	2	6.6	220	722	440	1444
149	488.8	2	6.6	3	9.8	200	656	400	1312
146	479.0	5	16.4	12	39.4	300	984	600	1969
134	439.6	17	55.8	13	42.7	450	1476	900	2953
121	397.0	30	98.4	15	49.2	600	1969	1850	6070
106	347.8	45	147.6	>25	>82.0	800	2625	2150	7054

Approximate depth of investigation is 70m.

Table 9 Velocity Model for Surface Wave Array Z1-S7

Approx. Elevation of Top of Layer		Depth to Top of Layer		Layer Thickness		S-Wave Velocity		Inferred P-Wave Velocity	
m	ft	m	ft	m	ft	m/s	ft/s	m/s	ft/s
103	337.9	0	0.0	1.5	4.9	210	689	420	1378
101.5	333.0	1.5	4.9	2.5	8.2	200	656	400	1312
99	324.8	4	13.1	5	16.4	220	722	440	1444
94	308.4	9	29.5	9	29.5	275	902	1650	5413
85	278.9	18	59.1	17	55.8	450	1476	1850	6070
68	223.1	35	114.8	20	65.6	550	1804	1850	6070
48	157.5	55	180.4	>15	>49.2	700	2297	2150	7054

Approximate depth of investigation is 70m.

Table 10 Velocity Model for Surface Wave Array Z1-S8

Approx. Elevation of Top of Layer		Depth to Top of Layer		Layer Thickness		S-Wave Velocity		Inferred P-Wave Velocity	
m	ft	m	ft	m	ft	m/s	ft/s	m/s	ft/s
105	344.5	0	0.0	1.5	4.9	135	443	270	886
103.5	339.6	1.5	4.9	2.5	8.2	230	755	460	1509
101	331.4	4	13.1	5	16.4	200	656	400	1312
96	315.0	9	29.5	13	42.7	300	984	1650	5413
83	272.3	22	72.2	26	85.3	475	1558	1850	6070
57	187.0	48	157.5	15	49.2	675	2215	1850	6070
42	137.8	63	206.7	>7	>23.0	800	2625	2150	7054

Approximate depth of investigation is 70m.

Table 11 Velocity Model for Surface Wave Array Z1-S9

Approx. Elevation of Top of Layer		Depth to Top of Layer		Layer Thickness		S-Wave Velocity		Inferred P-Wave Velocity	
m	ft	m	ft	m	ft	m/s	ft/s	m/s	ft/s
114	374.0	0	0.0	1.5	4.9	150	492	300	984
112.5	369.1	1.5	4.9	2.5	8.2	175	574	350	1148
110	360.9	4	13.1	4	13.1	275	902	550	1804
106	347.8	8	26.2	14	45.9	320	1050	1650	5413
92	301.8	22	72.2	20	65.6	475	1558	1850	6070
72	236.2	42	137.8	15	49.2	675	2215	1850	6070
57	187.0	57	187.0	>13	>42.7	800	2625	2150	7054

Approximate depth of investigation is 70m.

Table 12 Velocity Model for Surface Wave Array Z1-S10

Approx. Elevation of Top of Layer		Depth to Top of Layer		Layer Thickness		S-Wave Velocity		Inferred P-Wave Velocity	
m	ft	m	ft	m	ft	m/s	ft/s	m/s	ft/s
124.0	406.8	0.0	0.0	1.5	4.9	180	591	360	1181
122.5	401.9	1.5	4.9	2.0	6.6	220	722	440	1444
120.5	395.3	3.5	11.5	3.3	10.7	195	640	390	1280
117.3	384.7	6.8	22.1	0.3	0.8	325	1066	650	2133
117.0	383.9	7.0	23.0	9.8	32.0	325	1066	1650	5413
107.3	351.9	16.8	55.0	20.0	65.6	500	1640	1850	6070
87.3	286.3	36.8	120.6	15.0	49.2	675	2215	1850	6070
72.3	237.0	51.8	169.8	>8.3	>27.1	800	2625	2150	7054

Approximate depth of investigation is 60m.

Table 13 Velocity Model for Surface Wave Array Z1-S11

Approx. Elevation of Top of Layer		Depth to Top of Layer		Layer Thickness		S-Wave Velocity		Inferred P-Wave Velocity	
m	ft	m	ft	m	ft	m/s	ft/s	m/s	ft/s
118.0	387.1	0.0	0.0	1.8	5.7	205	673	410	1345
116.3	381.4	1.8	5.7	3.0	9.8	425	1394	850	2788
113.3	371.6	4.8	15.6	1.3	4.1	265	869	530	1739
112.0	367.5	6.0	19.7	2.5	8.2	265	869	1650	5413
109.5	359.3	8.5	27.9	11.0	36.1	325	1066	1650	5413
98.5	323.2	19.5	64.0	20.0	65.6	525	1722	1850	6070
78.5	257.5	39.5	129.6	>25.5	>83.7	850	2789	2150	7054

Approximate depth of investigation is 65m.

Table 14 Velocity Model for Surface Wave Array Z1-S12

Approx. Elevation of Top of Layer		Depth to Top of Layer		Layer Thickness		S-Wave Velocity		Inferred P-Wave Velocity	
m	ft	m	ft	m	ft	m/s	ft/s	m/s	ft/s
114	374.0	0	0.0	1.5	4.9	190	623	380	1247
112.5	369.1	1.5	4.9	2.5	8.2	315	1033	630	2067
110	360.9	4	13.1	4	13.1	335	1099	670	2198
106	347.8	8	26.2	1	3.3	350	1148	700	2297
105	344.5	9	29.5	6	19.7	350	1148	1650	5413
99	324.8	15	49.2	19	62.3	475	1558	1850	6070
80	262.5	34	111.5	20	65.6	725	2379	1850	6070
60	196.9	54	177.2	>16	>52.5	775	2543	2150	7054

Approximate depth of investigation is 70m.

Table 15 Velocity Model for Surface Wave Array Z1-S13

Approx. Elevation of Top of Layer		Depth to Top of Layer		Layer Thickness		S-Wave Velocity		Inferred P-Wave Velocity	
m	ft	m	ft	m	ft	m/s	ft/s	m/s	ft/s
118	387.1	0	0.0	1.5	4.9	205	673	410	1345
116.5	382.2	1.5	4.9	2.5	8.2	300	984	600	1969
114	374.0	4	13.1	4	13.1	335	1099	670	2198
110	360.9	8	26.2	1	3.3	365	1198	730	2395
109	357.6	9	29.5	8	26.2	365	1198	1650	5413
101	331.4	17	55.8	15	49.2	400	1312	1850	6070
86	282.2	32	105.0	25	82.0	650	2133	1850	6070
61	200.1	57	187.0	>3	>9.8	800	2625	2150	7054

Approximate depth of investigation is 60m.

Table 16 Velocity Model for Surface Wave Array Z1-S14

Approx. Elevation of Top of Layer		Depth to Top of Layer		Layer Thickness		S-Wave Velocity		Inferred P-Wave Velocity	
m	ft	m	ft	m	ft	m/s	ft/s	m/s	ft/s
131	429.8	0	0.0	1.5	4.9	125	410	250	820
129.5	424.9	1.5	4.9	1.5	4.9	160	525	320	1050
128	419.9	3	9.8	7	23.0	130	427	1650	5413
121	397.0	10	32.8	6	19.7	195	640	1650	5413
115	377.3	16	52.5	15	49.2	235	771	1650	5413
100	328.1	31	101.7	20	65.6	500	1640	1850	6070
80	262.5	51	167.3	>9	>29.5	700	2297	1850	6070

Approximate depth of investigation is 60m.

Table 17 Velocity Model for Surface Wave Array Z1-S15

Approx. Elevation of Top of Layer		Depth to Top of Layer		Layer Thickness		S-Wave Velocity		Inferred P-Wave Velocity	
m	ft	m	ft	m	ft	m/s	ft/s	m/s	ft/s
135	442.9	0	0.0	2	6.6	125	410	250	820
133	436.4	2	6.6	1	3.3	150	492	300	984
132	433.1	3	9.8	7	23.0	150	492	1650	5413
125	410.1	10	32.8	5	16.4	195	640	1650	5413
120	393.7	15	49.2	5	16.4	275	902	1650	5413
115	377.3	20	65.6	20	65.6	575	1886	1850	6070
95	311.7	40	131.2	20	65.6	650	2133	1850	6070
75	246.1	60	196.9	>5	>16.4	850	2789	2150	7054

Approximate depth of investigation is 65m.

Table 18 Velocity Model for Surface Wave Array Z1-S16

Approx. Elevation of Top of Layer		Depth to Top of Layer		Layer Thickness		S-Wave Velocity		Inferred P-Wave Velocity	
m	ft	m	ft	m	ft	m/s	ft/s	m/s	ft/s
140	459.3	0	0.0	2.5	8.2	230	755	460	1509
137.5	451.1	2.5	8.2	0.5	1.6	190	623	380	1247
137	449.5	3	9.8	4	13.1	190	623	1650	5413
133	436.4	7	23.0	6	19.7	225	738	1650	5413
127	416.7	13	42.7	13	42.7	265	869	1650	5413
114	374.0	26	85.3	25	82.0	400	1312	1850	6070
89	292.0	51	167.3	>19	>62.3	550	1804	1850	6070

Approximate depth of investigation is 70m.

Table 19 Velocity Model for Surface Wave Array Z1-S18

Approx. Elevation of Top of Layer		Depth to Top of Layer		Layer Thickness		S-Wave Velocity		Inferred P-Wave Velocity	
m	ft	m	ft	m	ft	m/s	ft/s	m/s	ft/s
158	518.4	0	0.0	2	6.6	150	492	300	984
156	511.8	2	6.6	2	6.6	220	722	440	1444
154	505.2	4	13.1	4	13.1	230	755	460	1509
150	492.1	8	26.2	8	26.2	220	722	1650	5413
142	465.9	16	52.5	10	32.8	400	1312	1650	5413
132	433.1	26	85.3	20	65.6	450	1476	1850	6070
112	367.5	46	150.9	20	65.6	725	2379	2150	7054
92	301.8	66	216.5	>4	>13.1	825	2707	2150	7054

Approximate depth of investigation is 70m.

Table 20 Velocity Model for Surface Wave Array Z1-S19

Approx. Elevation of Top of Layer		Depth to Top of Layer		Layer Thickness		S-Wave Velocity		Inferred P-Wave Velocity	
m	ft	m	ft	m	ft	m/s	ft/s	m/s	ft/s
140	518.4	0	0.0	1.5	4.9	265	869	530	1739
138.5	513.5	1.5	4.9	1.5	4.9	400	1312	799.9	2624
137	508.5	3	9.8	2	6.6	550	1804	1149.9	3773
135	502.0	5	16.4	2	6.6	550	1804	1850	6070
133	495.4	7	23.0	9	29.5	475	1558	1850	6070
124	465.9	16	52.5	15	49.2	575	1886	1850	6070
109	416.7	31	101.7	15	49.2	650	2133	1850	6070
94	367.5	46	150.9	>14	>45.9	750	2461	2150	7054

Approximate depth of investigation is 60m.

Table 21 Velocity Model for Surface Wave Array Z1-S20

Approx. Elevation of Top of Layer		Depth to Top of Layer		Layer Thickness		S-Wave Velocity		Inferred P-Wave Velocity	
m	ft	m	ft	m	ft	m/s	ft/s	m/s	ft/s
125	459.3	0	0.0	1.5	4.9	195	640	390	1280
123.5	454.4	1.5	4.9	1.5	4.9	285	935	570	1870
122	449.5	3	9.8	3	9.8	285	935	1650	5413
119	439.6	6	19.7	8	26.2	300	984	1650	5413
111	413.4	14	45.9	11.5	37.7	375	1230	1850	6070
99.5	375.7	25.5	83.7	26	85.3	515	1690	1850	6070
73.5	290.4	51.5	169.0	>18.5	>60.7	775	2543	2150	7054

Approximate depth of investigation is 70m.

Table 22 Summary of Zone 1 Surface Wave Investigation

Surface Wave Array	Vs30 (m/s)	Vs30 (ft/s)	Vs60 (m/s)	Vs60 (ft/s)	Vs @ 60m (m/s)	Vs @ 60m (ft/s)
Z1-S1	362	1188	452	1481	725	2379
Z1-S2	299	982	382	1254	700	2297
Z1-S3	394	1292	512	1680	750	2461
Z1-S4	315	1033	423	1387	700	2297
Z1-S5	317	1039	430	1412	800	2625
Z1-S6	323	1059	439	1440	800	2625
Z1-S7	295	967	384	1259	700	2297
Z1-S8	280	919	368	1209	675	2215
Z1-S9	302	990	398	1307	800	2625
Z1-S10	328	1077	437	1433	800	2625
Z1-S11	359	1177	477	1565	850	2789
Z1-S12	378	1240	487	1599	775	2543
Z1-S13	354	1161	455	1492	800	2625
Z1-S14	181	594	269	884	700	2297
Z1-S15	230	754	336	1102	850	2789
Z1-S16	249	818	317	1041	550	1804
Z1-S18	273	894	364	1194	725	2379
Z1-S19	500	1641	580	1903	750	2461
Z1-S20	335	1099	422	1384	775	2543

Note: Vs30 = average S-wave velocity of upper 30 m. Vs60 = average S-wave velocity of upper 60 m.

Table 23 Velocity Model for Surface Wave Array Z2-S1

Approx. Elevation of Top of Layer		Depth to Top of Layer		Layer Thickness		S-Wave Velocity		Inferred P-Wave Velocity	
m	ft	m	ft	m	ft	m/s	ft/s	m/s	ft/s
151	495.4	0	0.0	1.5	4.9	160	525	320	1050
149.5	490.5	1.5	4.9	0.5	1.6	235	771	470	1542
149	488.8	2	6.6	2	6.6	235	771	1650	5413
147	482.3	4	13.1	4	13.1	300	984	1650	5413
143	469.2	8	26.2	9	29.5	475	1558	1825	5988
134	439.6	17	55.8	15	49.2	700	2297	2200	7218
119	390.4	32	105.0	>28	>91.9	800	2625	2200	7218

Approximate depth of investigation is 60m.

Table 24 Velocity Model for Surface Wave Array Z2-S2

Approx. Elevation of Top of Layer		Depth to Top of Layer		Layer Thickness		S-Wave Velocity		Inferred P-Wave Velocity	
m	ft	m	ft	m	ft	m/s	ft/s	m/s	ft/s
156	511.8	0	0.0	1.5	4.9	325	1066	650	2133
154.5	506.9	1.5	4.9	1.5	4.9	295	968	590	1936
153	502.0	3	9.8	3	9.8	295	968	1650	5413
150	492.1	6	19.7	13	42.7	290	951	1650	5413
137	449.5	19	62.3	15	49.2	400	1312	1825	5988
122	400.3	34	111.5	35	114.8	600	1969	1825	5988
87	285.4	69	226.4	>1	>3.3	800	2625	2200	7218

Approximate depth of investigation is 70m.

Table 25 Velocity Model for Surface Wave Array Z2-S3

Approx. Elevation of Top of Layer		Depth to Top of Layer		Layer Thickness		S-Wave Velocity		Inferred P-Wave Velocity	
m	ft	m	ft	m	ft	m/s	ft/s	m/s	ft/s
152	498.7	0	0.0	1.5	4.9	175	574	350	1148
150.5	493.8	1.5	4.9	1.5	4.9	180	591	360	1181
149	488.8	3	9.8	4.5	14.8	180	591	1650	5413
144.5	474.1	7.5	24.6	14	45.9	265	869	1650	5413
131	428.1	22	70.5	15	49.2	375	1230	1825	5988
116	378.9	37	119.8	32	105.0	550	1804	1825	5988
84	274.0	69	224.7	>1	>3.3	650	2133	2200	7218

Approximate depth of investigation is 70m.

Table 26 Velocity Model for Surface Wave Array Z2-S4

Approx. Elevation of Top of Layer		Depth to Top of Layer		Layer Thickness		S-Wave Velocity		Inferred P-Wave Velocity	
m	ft	m	ft	m	ft	m/s	ft/s	m/s	ft/s
179	587.3	0	0.0	2.75	9.0	200	656	400	1312
176.25	578.2	2.75	9.0	1.25	4.1	360	1181	720	2362
175	574.1	4	13.1	3.5	11.5	360	1181	1650	5413
171.5	562.7	7.5	24.6	6.5	21.3	300	984	1650	5413
165	541.3	14	45.9	29	95.1	375	1230	1825	5988
136	446.2	43	141.1	22	72.2	420	1378	1825	5988
114	374.0	65	213.3	>5	>16.4	750	2461	2200	7218

Approximate depth of investigation is 70m.

Table 27 Velocity Model for Surface Wave Array Z2-S5

Approx. Elevation of Top of Layer		Depth to Top of Layer		Layer Thickness		S-Wave Velocity		Inferred P-Wave Velocity	
m	ft	m	ft	m	ft	m/s	ft/s	m/s	ft/s
171	561.0	0	0.0	1.75	5.7	245	804	490	1608
169.25	555.3	1.75	5.7	4.75	15.6	320	1050	630	2067
164.5	539.7	6.5	21.3	10	32.8	265	869	520	1706
154.5	506.9	16.5	54.1	8.5	27.9	310	1017	1650	5413
146	479.0	25	82.0	22	72.2	400	1312	1825	5988
124	406.8	47	154.2	>23	>75.5	525	1722	1825	5988

Approximate depth of investigation is 70m.

Table 28 Velocity Model for Surface Wave Array Z2-S6

Approx. Elevation of Top of Layer		Depth to Top of Layer		Layer Thickness		S-Wave Velocity		Inferred P-Wave Velocity	
m	ft	m	ft	m	ft	m/s	ft/s	m/s	ft/s
171	561.0	0	0.0	4	13.1	190	623	380	1247
167	547.9	4	13.1	3	9.8	250	820	500	1640
164	538.1	7	23.0	4.5	14.8	325	1066	1650	5413
159.5	523.3	11.5	37.7	9.5	31.2	425	1394	1825	5988
150	492.1	21	68.9	18	59.1	550	1804	1825	5988
132	433.1	39	128.0	>21	>68.9	700	2297	2200	7218

Approximate depth of investigation is 60m.

Table 29 Velocity Model for Surface Wave Array Z2-S7

Approx. Elevation of Top of Layer		Depth to Top of Layer		Layer Thickness		S-Wave Velocity		Inferred P-Wave Velocity	
m	ft	m	ft	m	ft	m/s	ft/s	m/s	ft/s
154	505.2	0	0.0	1.5	4.9	300	984	600	1969
152.5	500.3	1.5	4.9	1.25	4.1	260	853	520	1706
151.25	496.2	2.75	9.0	5.25	17.2	395	1296	790	2592
146	479.0	8	26.2	10	32.8	395	1296	1825	5988
136	446.2	18	59.1	10	32.8	370	1214	1825	5988
126	413.4	28	91.9	13	42.7	420	1378	1825	5988
113	370.7	41	134.5	>29	>95.1	575	1886	1825	5988

Approximate depth of investigation is 70m.

Table 30 Velocity Model for Surface Wave Array Z2-S8

Approx. Elevation of Top of Layer		Depth to Top of Layer		Layer Thickness		S-Wave Velocity		Inferred P-Wave Velocity	
m	ft	m	ft	m	ft	m/s	ft/s	m/s	ft/s
158	518.4	0	0.0	3.75	12.3	330	1083	660	2165
154.25	506.1	3.75	12.3	3.25	10.7	395	1296	790	2592
151	495.4	7	23.0	2	6.6	395	1296	1825	5988
149	488.8	9	29.5	37	121.4	360	1181	1825	5988
112	367.5	46	150.9	10	32.8	450	1476	1825	5988
102	334.6	56	183.7	>4	>13.1	650	2133	1825	5988

Approximate depth of investigation is 60m.

Table 31 Velocity Model for Surface Wave Array Z2-S9

Approx. Elevation of Top of Layer		Depth to Top of Layer		Layer Thickness		S-Wave Velocity		Inferred P-Wave Velocity	
m	ft	m	ft	m	ft	m/s	ft/s	m/s	ft/s
172	564.3	0	0.0	2	6.6	165	541	330	1083
170	557.7	2	6.6	3	9.8	310	1017	620	2034
167	547.9	5	16.4	1.5	4.9	310	1017	1650	5413
165.5	543.0	6.5	21.3	7	23.0	350	1148	1825	5988
158.5	520.0	13.5	44.3	10	32.8	450	1476	1825	5988
148.5	487.2	23.5	77.1	13	42.7	675	2215	2200	7218
135.5	444.6	36.5	119.8	>23.5	>77.1	825	2707	2200	7218

Approximate depth of investigation is 60m.

Table 32 Velocity Model for Surface Wave Array Z2-S10

Approx. Elevation of Top of Layer		Depth to Top of Layer		Layer Thickness		S-Wave Velocity		Inferred P-Wave Velocity	
m	ft	m	ft	m	ft	m/s	ft/s	m/s	ft/s
161.0	528.2	0.0	0.0	2.0	6.6	170	558	330	1083
159.0	521.7	2.0	6.6	3.0	9.8	250	820	620	2034
156.0	511.8	5.0	16.4	3.0	9.8	295	968	590	1936
153.0	502.0	8.0	26.2	1.0	3.3	300	984	600	1969
152.0	498.7	9.0	29.5	9.0	29.5	300	984	1825	5988
143.0	469.2	18.0	59.1	20.0	65.6	425	1394	1825	5988
123.0	403.5	38.0	124.7	>32.0	>105.0	550	1804	1825	5988

Approximate depth of investigation is 70m.

Table 33 Velocity Model for Surface Wave Array Z2-S11

Approx. Elevation of Top of Layer		Depth to Top of Layer		Layer Thickness		S-Wave Velocity		Inferred P-Wave Velocity	
m	ft	m	ft	m	ft	m/s	ft/s	m/s	ft/s
149.0	488.8	0.0	0.0	2.0	6.6	170	558	340	1115
147.0	482.3	2.0	6.6	2.0	6.6	275	902	550	1804
145.0	475.7	4.0	13.1	2.0	6.6	275	902	1650	5413
143.0	469.2	6.0	19.7	8.0	26.2	245	804	1650	5413
135.0	442.9	14.0	45.9	8.0	26.2	275	902	1825	5988
127.0	416.7	22.0	72.2	20.0	65.6	400	1312	1825	5988
107.0	351.0	42.0	137.8	>28.0	>91.9	550	1804	1825	5988

Approximate depth of investigation is 70m.

Table 34 Velocity Model for Surface Wave Array Z2-S12

Approx. Elevation of Top of Layer		Depth to Top of Layer		Layer Thickness		S-Wave Velocity		Inferred P-Wave Velocity	
m	ft	m	ft	m	ft	m/s	ft/s	m/s	ft/s
133	436.4	0	0.0	2	6.6	170	558	340	1115
131	429.8	2	6.6	2	6.6	190	623	380	1247
129	423.2	4	13.1	2	6.6	215	705	430	1411
127	416.7	6	19.7	3	9.8	325	1066	650	2133
124	406.8	9	29.5	10	32.8	325	1066	1650	5413
114	374.0	19	62.3	20	65.6	300	984	1650	5413
94	308.4	39	128.0	15	49.2	450	1476	1825	5988
79	259.2	54	177.2	>16	>52.5	575	1886	1825	5988

Approximate depth of investigation is 70m.

Table 35 Summary of Zone 2 Surface Wave Investigation

Surface Wave Array	Vs30 (m/s)	Vs30 (ft/s)	Vs60 (m/s)	Vs60 (ft/s)	Vs @ 60m (m/s)	Vs @ 60m (ft/s)
Z2-S1	423	1389	552	1811	800	2625
Z2-S2	325	1068	412	1353	600	1969
Z2-S3	256	838	338	1109	550	1804
Z2-S4	329	1078	361	1183	420	1378
Z2-S5	301	988	359	1179	525	1722
Z2-S6	350	1150	455	1492	700	2297
Z2-S7	374	1227	430	1412	575	1886
Z2-S8	361	1186	385	1263	650	2133
Z2-S9	382	1254	515	1688	825	2707
Z2-S10	314	1031	389	1276	550	1804
Z2-S11	278	911	351	1153	550	1804
Z2-S12	277	909	330	1081	575	1886

Note: Vs30 = average S-wave velocity of upper 30 m. Vs60 = average S-wave velocity of upper 60 m.

Table 36 Velocity Model for Surface Wave Array Z3-S1

Approx. Elevation of Top of Layer		Depth to Top of Layer		Layer Thickness		S-Wave Velocity		Inferred P-Wave Velocity	
m	ft	m	ft	m	ft	m/s	ft/s	m/s	ft/s
261	856.3	0	0.0	1.5	4.9	240	787	480	1575
259.5	851.4	1.5	4.9	3.5	11.5	360	1181	720	2362
256	839.9	5	16.4	12	39.4	360	1181	1750	5741
244	800.5	17	55.8	21	68.9	525	1722	2100	6890
223	731.6	38	124.7	30	98.4	725	2379	2100	6890
193	633.2	68	223.1	>2	>6.6	900	2953	2400	7874

Approximate depth of investigation is 70m.

Table 37 Velocity Model for Surface Wave Array Z3-S2

Approx. Elevation of Top of Layer		Depth to Top of Layer		Layer Thickness		S-Wave Velocity		Inferred P-Wave Velocity	
m	ft	m	ft	m	ft	m/s	ft/s	m/s	ft/s
245	803.8	0	0.0	1.75	5.7	150	492	300	984
243.25	798.1	1.75	5.7	3.75	12.3	310	1017	620	2034
239.5	785.8	5.5	18.0	10	32.8	375	1230	750	2460
229.5	753.0	15.5	50.9	17	55.8	425	1394	850	2788
212.5	697.2	32.5	106.6	20	65.6	500	1640	1925	6316
192.5	631.6	52.5	172.2	20	65.6	650	2133	2100	6890
172.5	565.9	72.5	237.9	>2.5	>8.2	1000	3281	2800	9186

Approximate depth of investigation is 75m.

Table 38 Velocity Model for Surface Wave Array Z3-S3

Approx. Elevation of Top of Layer		Depth to Top of Layer		Layer Thickness		S-Wave Velocity		Inferred P-Wave Velocity	
m	ft	m	ft	m	ft	m/s	ft/s	m/s	ft/s
232	761.2	0	0.0	2	6.6	235	771	470	1542
230	754.6	2	6.6	3.5	11.5	260	853	520	1706
226.5	743.1	5.5	18.0	16.5	54.1	405	1329	810	2657
210	689.0	22	72.2	15	49.2	450	1476	900	2953
195	639.8	37	121.4	8	26.2	600	1969	1200	3937
187	613.5	45	147.6	12	39.4	600	1969	2100	6890
175	574.1	57	187.0	>13	>42.7	800	2625	2800	9186

Approximate depth of investigation is 70m.

Table 39 Velocity Model for Surface Wave Array Z3-S4

Approx. Elevation of Top of Layer		Depth to Top of Layer		Layer Thickness		S-Wave Velocity		Inferred P-Wave Velocity	
m	ft	m	ft	m	ft	m/s	ft/s	m/s	ft/s
226	741.5	0	0.0	7	23.0	275	902	550	1804
219	718.5	7	23.0	14	45.9	390	1280	780	2559
205	672.6	21	68.9	15	49.2	475	1558	950	3116
190	623.4	36	118.1	9	29.5	650	2133	1300	4265
181	593.8	45	147.6	11	36.1	650	2133	2100	6890
170	557.7	56	183.7	>14	>45.9	900	2953	2800	9186

Approximate depth of investigation is 70m.

Table 40 Velocity Model for Surface Wave Array Z3-S5

Approx. Elevation of Top of Layer		Depth to Top of Layer		Layer Thickness		S-Wave Velocity		Inferred P-Wave Velocity	
m	ft	m	ft	m	ft	m/s	ft/s	m/s	ft/s
241	790.7	0	0.0	1.75	5.7	245	804	490	1608
239.25	784.9	1.75	5.7	5.25	17.2	375	1230	750	2460
234	767.7	7	23.0	10	32.8	500	1640	1000	3281
224	734.9	17	55.8	10	32.8	650	2133	1300	4265
214	702.1	27	88.6	3	9.8	750	2461	1500	4921
211	692.3	30	98.4	7	23.0	750	2461	2400	7874
204	669.3	37	121.4	10	32.8	1000	3281	2800	9186
194	636.5	47	154.2	>23	>75.5	1200	3937	2800	9186

Approximate depth of investigation is 70m.

Table 41 Velocity Model for Surface Wave Array Z3-S6

Approx. Elevation of Top of Layer		Depth to Top of Layer		Layer Thickness		S-Wave Velocity		Inferred P-Wave Velocity	
m	ft	m	ft	m	ft	m/s	ft/s	m/s	ft/s
209	685.7	0	0.0	2	6.6	270	886	540	1772
207	679.1	2	6.6	3	9.8	325	1066	650	2133
204	669.3	5	16.4	2	6.6	325	1066	1750	5741
202	662.7	7	23.0	8	26.2	370	1214	1750	5741
194	636.5	15	49.2	8	26.2	465	1526	1925	6316
186	610.2	23	75.5	17	55.8	650	2133	2100	6890
169	554.5	40	131.2	20	65.6	775	2543	2400	7874
149	488.8	60	196.9	>10	>32.8	1000	3281	2800	9186

Approximate depth of investigation is 70m.

Table 42 Velocity Model for Surface Wave Array Z3-S7

Approx. Elevation of Top of Layer		Depth to Top of Layer		Layer Thickness		S-Wave Velocity		Inferred P-Wave Velocity	
m	ft	m	ft	m	ft	m/s	ft/s	m/s	ft/s
209	685.7	0	0.0	3	9.8	290	951	580	1903
206	675.9	3	9.8	3	9.8	300	984	600	1969
203	666.0	6	19.7	1	3.3	300	984	1750	5741
202	662.7	7	23.0	7	23.0	475	1558	1925	6316
195	639.8	14	45.9	15	49.2	650	2133	2100	6890
180	590.6	29	95.1	17	55.8	750	2461	2400	7874
163	534.8	46	150.9	>14	>45.9	975	3199	2800	9186

Approximate depth of investigation is 60m.

Table 43 Velocity Model for Surface Wave Array Z3-S8

Approx. Elevation of Top of Layer		Depth to Top of Layer		Layer Thickness		S-Wave Velocity		Inferred P-Wave Velocity	
m	ft	m	ft	m	ft	m/s	ft/s	m/s	ft/s
192	629.9	0	0.0	1.5	4.9	260	853	520	1706
190.5	625.0	1.5	4.9	6	19.7	395	1296	790	2592
184.5	605.3	7.5	24.6	7.5	24.6	360	1181	710	2329
177	580.7	15	49.2	2.5	8.2	360	1181	1750	5741
174.5	572.5	17.5	57.4	9	29.5	375	1230	1750	5741
165.5	543.0	26.5	86.9	15	49.2	425	1394	1925	6316
150.5	493.8	41.5	136.2	>18.5	>60.7	550	1804	2100	6890

Approximate depth of investigation is 60m.

Table 44 Velocity Model for Surface Wave Array Z3-S9

Approx. Elevation of Top of Layer		Depth to Top of Layer		Layer Thickness		S-Wave Velocity		Inferred P-Wave Velocity	
m	ft	m	ft	m	ft	m/s	ft/s	m/s	ft/s
177	580.7	0	0.0	2	6.6	285	935	570	1870
175	574.1	2	6.6	4	13.1	260	853	520	1706
171	561.0	6	19.7	5	16.4	260	853	1750	5741
166	544.6	11	36.1	21	68.9	350	1148	1925	6316
145	475.7	32	105.0	34	111.5	435	1427	2100	6890
111	364.2	66	216.5	>4	>13.1	625	2051	2100	6890

Approximate depth of investigation is 70m.

Table 45 Velocity Model for Surface Wave Array Z3-S10

Approx. Elevation of Top of Layer		Depth to Top of Layer		Layer Thickness		S-Wave Velocity		Inferred P-Wave Velocity	
m	ft	m	ft	m	ft	m/s	ft/s	m/s	ft/s
185.0	607.0	0	0.0	2.5	8.2	175	574	350	1148
182.5	598.8	2.5	8.2	0.5	1.6	310	1017	620	2034
182.0	597.1	3	9.8	2.5	8.2	310	1017	1750	5741
179.5	588.9	5.5	18.0	5	16.4	440	1444	1925	6316
174.5	572.5	10.5	34.4	20	65.6	520	1706	2100	6890
154.5	506.9	30.5	100.1	>39.5	>129.6	740	2428	2400	7874

Approximate depth of investigation is 70m.

Table 46 Velocity Model for Surface Wave Array Z3-S11

Approx. Elevation of Top of Layer		Depth to Top of Layer		Layer Thickness		S-Wave Velocity		Inferred P-Wave Velocity	
m	ft	m	ft	m	ft	m/s	ft/s	m/s	ft/s
229.0	751.3	0	0.0	2	6.6	215	705	430	1411
227.0	744.8	2	6.6	3	9.8	260	853	520	1706
224.0	734.9	5	16.4	4	13.1	280	919	560	1837
220.0	721.8	9	29.5	1.5	4.9	325	1066	650	2133
218.5	716.9	10.5	34.4	12.5	41.0	325	1066	1750	5741
206.0	675.9	23	75.5	20	65.6	415	1362	1925	6316
186.0	610.2	43	141.1	>27	>88.6	625	2051	2100	6890

Approximate depth of investigation is 70m.

Table 47 Velocity Model for Surface Wave Array Z3-S12

Approx. Elevation of Top of Layer		Depth to Top of Layer		Layer Thickness		S-Wave Velocity		Inferred P-Wave Velocity	
m	ft	m	ft	m	ft	m/s	ft/s	m/s	ft/s
202	662.7	0	0.0	1.5	4.9	200	656	400	1312
200.5	657.8	1.5	4.9	2	6.6	260	853	520	1706
198.5	651.2	3.5	11.5	3.5	11.5	235	771	470	1542
195	639.8	7	23.0	8.5	27.9	340	1115	680	2231
186.5	611.9	15.5	50.9	11.5	37.7	350	1148	1750	5741
175	574.1	27	88.6	22	72.2	400	1312	1925	6316
153	502.0	49	160.8	>35	>114.8	675	2215	2100	6890

Approximate depth of investigation is 70m.

Table 48 Velocity Model for Surface Wave Array Z3-S13

Approx. Elevation of Top of Layer		Depth to Top of Layer		Layer Thickness		S-Wave Velocity		Inferred P-Wave Velocity	
m	ft	m	ft	m	ft	m/s	ft/s	m/s	ft/s
191	626.6	0	0.0	1.5	4.9	240	787	480	1575
189.5	621.7	1.5	4.9	2	6.6	275	902	550	1804
187.5	615.2	3.5	11.5	3.5	11.5	340	1115	680	2231
184	603.7	7	23.0	8	26.2	400	1312	800	2624
176	577.4	15	49.2	2	6.6	470	1542	940	3084
174	570.9	17	55.8	15	49.2	470	1542	1925	6316
159	521.7	32	105.0	15	49.2	550	1804	2100	6890
144	472.4	47	154.2	25	82.0	725	2379	2100	6890
119	390.4	72	236.2	>3	>9.8	1000	3281	2800	9186

Approximate depth of investigation is 75m.

Table 49 Velocity Model for Surface Wave Array Z3-S14

Approx. Elevation of Top of Layer		Depth to Top of Layer		Layer Thickness		S-Wave Velocity		Inferred P-Wave Velocity	
m	ft	m	ft	m	ft	m/s	ft/s	m/s	ft/s
190	623.4	0	0.0	1.5	4.9	170	558	340	1115
188.5	618.4	1.5	4.9	2.5	8.2	265	869	530	1739
186	610.2	4	13.1	3	9.8	390	1280	780	2559
183	600.4	7	23.0	8	26.2	425	1394	850	2788
175	574.1	15	49.2	2	6.6	475	1558	950	3116
173	567.6	17	55.8	15	49.2	475	1558	1925	6316
158	518.4	32	105.0	15	49.2	575	1886	2100	6890
143	469.2	47	154.2	>23	>75.5	725	2379	2100	6890

Approximate depth of investigation is 70m.

Table 50 Velocity Model for Surface Wave Array Z3-S15

Approx. Elevation of Top of Layer		Depth to Top of Layer		Layer Thickness		S-Wave Velocity		Inferred P-Wave Velocity	
m	ft	m	ft	m	ft	m/s	ft/s	m/s	ft/s
199	652.9	0	0.0	1.5	4.9	190	623	380	1247
197.5	648.0	1.5	4.9	2.5	8.2	260	853	520	1706
195	639.8	4	13.1	2.5	8.2	300	984	600	1969
192.5	631.6	6.5	21.3	8.5	27.9	350	1148	700	2297
184	603.7	15	49.2	4	13.1	350	1148	1750	5741
180	590.6	19	62.3	16	52.5	400	1312	1925	6316
164	538.1	35	114.8	16	52.5	500	1640	2100	6890
148	485.6	51	167.3	>19	>62.3	750	2461	2100	6890

Approximate depth of investigation is 70m.

Table 51 Velocity Model for Surface Wave Array Z3-S16

Approx. Elevation of Top of Layer		Depth to Top of Layer		Layer Thickness		S-Wave Velocity		Inferred P-Wave Velocity	
m	ft	m	ft	m	ft	m/s	ft/s	m/s	ft/s
176	577.4	0	0.0	2.5	8.2	225	738	450	1476
173.5	569.2	2.5	8.2	5	16.4	380	1247	760	2493
168.5	552.8	7.5	24.6	2.5	8.2	370	1214	740	2427
166	544.6	10	32.8	12	39.4	370	1214	1750	5741
154	505.2	22	72.2	20	65.6	425	1394	1925	6316
134	439.6	42	137.8	>28	>91.9	500	1640	1925	6316

Approximate depth of investigation is 70m.

Table 52 Velocity Model for Surface Wave Array Z3-S17

Approx. Elevation of Top of Layer		Depth to Top of Layer		Layer Thickness		S-Wave Velocity		Inferred P-Wave Velocity	
m	ft	m	ft	m	ft	m/s	ft/s	m/s	ft/s
191	626.6	0	0.0	2	6.6	215	705	430	1411
189	620.1	2	6.6	6	19.7	290	951	580	1903
183	600.4	8	26.2	8	26.2	290	951	1750	5741
175	574.1	16	52.5	5.5	18.0	350	1148	1750	5741
169.5	556.1	21.5	70.5	10	32.8	700	2297	2100	6890
159.5	523.3	31.5	103.3	10	32.8	800	2625	2400	7874
149.5	490.5	41.5	136.2	>28.5	>93.5	1250	4101	2800	9186

Approximate depth of investigation is 70m.

Table 53 Velocity Model for Surface Wave Array Z3-S18

Approx. Elevation of Top of Layer		Depth to Top of Layer		Layer Thickness		S-Wave Velocity		Inferred P-Wave Velocity	
m	ft	m	ft	m	ft	m/s	ft/s	m/s	ft/s
188	616.8	0	0.0	1.5	4.9	195	640	390	1280
186.5	611.9	1.5	4.9	6.5	21.3	285	935	570	1870
180	590.6	8	26.2	11	36.1	285	935	1750	5741
169	554.5	19	62.3	7	23.0	350	1148	1750	5741
162	531.5	26	85.3	10	32.8	650	2133	2100	6890
152	498.7	36	118.1	10	32.8	800	2625	2400	7874
142	465.9	46	150.9	>24	>78.7	1250	4101	2800	9186

Approximate depth of investigation is 70m.

Table 54 Velocity Model for Surface Wave Array Z3-S19

Approx. Elevation of Top of Layer		Depth to Top of Layer		Layer Thickness		S-Wave Velocity		Inferred P-Wave Velocity	
m	ft	m	ft	m	ft	m/s	ft/s	m/s	ft/s
171	561.0	0	0.0	1.5	4.9	260	853	520	1706
169.5	556.1	1.5	4.9	2.5	8.2	400	1312	799.9	2624
167	547.9	4	13.1	5	16.4	320	1050	640	2100
162	531.5	9	29.5	6	19.7	350	1148	700	2297
156	511.8	15	49.2	4	13.1	350	1148	1750	5741
152	498.7	19	62.3	11	36.1	375	1230	1750	5741
141	462.6	30	98.4	35	114.8	550	1804	2100	6890
106	347.8	65	213.3	>5	>16.4	705	2313	2100	6890

Approximate depth of investigation is 70m.

Table 55 Velocity Model for Surface Wave Array Z3-S20

Approx. Elevation of Top of Layer		Depth to Top of Layer		Layer Thickness		S-Wave Velocity		Inferred P-Wave Velocity	
m	ft	m	ft	m	ft	m/s	ft/s	m/s	ft/s
161	528.2	0	0.0	2	6.6	255	837	510	1673
159	521.7	2	6.6	5	16.4	315	1033	630	2067
154	505.2	7	23.0	3	9.8	315	1033	1750	5741
151	495.4	10	32.8	10	32.8	350	1148	1750	5741
141	462.6	20	65.6	15	49.2	375	1230	1750	5741
126	413.4	35	114.8	30	98.4	550	1804	2100	6890
96	315.0	65	213.3	>5	>16.4	700	2297	2100	6890

Approximate depth of investigation is 70m.

Table 56 Velocity Model for Surface Wave Array Z3-S21

Approx. Elevation of Top of Layer		Depth to Top of Layer		Layer Thickness		S-Wave Velocity		Inferred P-Wave Velocity	
m	ft	m	ft	m	ft	m/s	ft/s	m/s	ft/s
139	456.0	0	0.0	2	6.6	320	1050	640	2100
137	449.5	2	6.6	8	26.2	300	984	600	1969
129	423.2	10	32.8	6	19.7	350	1148	699.9	2296
123	403.5	16	52.5	15	49.2	350	1148	1750	5741
108	354.3	31	101.7	30	98.4	450	1476	1925	6316
78	255.9	61	200.1	>9	>29.5	650	2133	2100	6890

Approximate depth of investigation is 70m.

Table 57 Velocity Model for Surface Wave Array Z3-S22

Approx. Elevation of Top of Layer		Depth to Top of Layer		Layer Thickness		S-Wave Velocity		Inferred P-Wave Velocity	
m	ft	m	ft	m	ft	m/s	ft/s	m/s	ft/s
131	429.8	0	0.0	3	9.8	275	902	550	1804
128	419.9	3	9.8	8	26.2	385	1263	769.9	2526
120	393.7	11	36.1	5	16.4	350	1148	700	2297
115	377.3	16	52.5	12	39.4	350	1148	1750	5741
103	337.9	28	91.9	25	82.0	450	1476	1925	6316
78	255.9	53	173.9	>17	>55.8	700	2297	2100	6890

Approximate depth of investigation is 70m.

Table 58 Velocity Model for Surface Wave Array Z3-S23

Approx. Elevation of Top of Layer		Depth to Top of Layer		Layer Thickness		S-Wave Velocity		Inferred P-Wave Velocity	
m	ft	m	ft	m	ft	m/s	ft/s	m/s	ft/s
127	416.7	0	0.0	1.5	4.9	175	574	350	1148
125.5	411.7	1.5	4.9	2.5	8.2	285	935	570	1870
123	403.5	4	13.1	3	9.8	335	1099	670	2198
120	393.7	7	23.0	5	16.4	375	1230	749.9	2460
115	377.3	12	39.4	24	78.7	375	1230	1750	5741
91	298.6	36	118.1	26	85.3	450	1476	1925	6316
65	213.3	62	203.4	>8	>26.2	665	2182	2100	6890

Approximate depth of investigation is 70m.

Table 59 Velocity Model for Surface Wave Array Z3-S24

Approx. Elevation of Top of Layer		Depth to Top of Layer		Layer Thickness		S-Wave Velocity		Inferred P-Wave Velocity	
m	ft	m	ft	m	ft	m/s	ft/s	m/s	ft/s
131	429.8	0	0.0	1.5	4.9	240	787	480	1575
129.5	424.9	1.5	4.9	2.5	8.2	275	902	550	1804
127	416.7	4	13.1	5	16.4	325	1066	650	2133
122	400.3	9	29.5	3	9.8	450	1476	899.9	2952
119	390.4	12	39.4	13	42.7	450	1476	1925	6316
106	347.8	25	82.0	28	91.9	525	1722	1925	6316
78	255.9	53	173.9	>17	>55.8	700	2297	2100	6890

Approximate depth of investigation is 70m.

Table 60 Summary of Zone 3 Surface Wave Investigation

Surface Wave Array	Vs30 (m/s)	Vs30 (ft/s)	Vs60 (m/s)	Vs60 (ft/s)	Vs @ 60m (m/s)	Vs @ 60m (ft/s)
Z3-S1	405	1329	501	1644	725	2379
Z3-S2	355	1165	423	1388	650	2133
Z3-S3	373	1223	451	1479	800	2625
Z3-S4	374	1227	468	1535	900	2953
Z3-S5	496	1627	662	2172	1200	3937
Z3-S6	414	1358	528	1732	1000	3281
Z3-S7	478	1568	609	1998	975	3199
Z3-S8	370	1214	424	1391	550	1804
Z3-S9	313	1027	361	1184	435	1427
Z3-S10	412	1352	528	1732	740	2428
Z3-S11	316	1037	391	1283	625	2051
Z3-S12	314	1030	377	1237	675	2215
Z3-S13	396	1299	479	1572	725	2379
Z3-S14	393	1289	482	1581	725	2379
Z3-S15	337	1106	412	1352	750	2461
Z3-S16	365	1198	410	1345	500	1640
Z3-S17	351	1152	522	1713	1250	4101
Z3-S18	315	1033	468	1535	1250	4101
Z3-S19	351	1152	428	1404	550	1804
Z3-S20	339	1112	407	1335	700	2297
Z3-S21	333	1093	381	1250	650	2133
Z3-S22	354	1161	411	1348	700	2297
Z3-S23	342	1122	382	1253	450	1476
Z3-S24	396	1298	463	1519	700	2297

Note: Vs30 = average S-wave velocity of upper 30 m. Vs60 = average S-wave velocity of upper 60 m.

Table 61 Velocity Model for Surface Wave Array Z4-S1

Approx. Elevation of Top of Layer		Depth to Top of Layer		Layer Thickness		S-Wave Velocity		Inferred P-Wave Velocity	
m	ft	m	ft	m	ft	m/s	ft/s	m/s	ft/s
210	689.0	0	0.0	2	6.6	255	837	510	1673
208	682.4	2	6.6	3	9.8	275	902	550	1804
205	672.6	5	16.4	4	13.1	300	984	600	1969
201	659.4	9	29.5	8	26.2	350	1148	700	2297
193	633.2	17	55.8	8	26.2	425	1394	850	2789
185	607.0	25	82.0	10	32.8	550	1804	1100	3609
175	574.1	35	114.8	10	32.8	700	2297	1300	4265
165	541.3	45	147.6	>15	>49.2	850	2789	1700	5577

Approximate depth of investigation is 60m.

Table 62 Velocity Model for Surface Wave Array Z4-S2

Approx. Elevation of Top of Layer		Depth to Top of Layer		Layer Thickness		S-Wave Velocity		Inferred P-Wave Velocity	
m	ft	m	ft	m	ft	m/s	ft/s	m/s	ft/s
206	675.9	0	0.0	1.5	4.9	255	837	510	1673
204.5	670.9	1.5	4.9	2.5	8.2	300	984	600	1969
202	662.7	4	13.1	13	42.7	340	1115	680	2231
189	620.1	17	55.8	17	55.8	450	1476	900	2952
172	564.3	34	111.5	25	82.0	575	1886	1150	3773
147	482.3	59	193.6	5	16.4	600	1969	1200	3937
142	465.9	64	210.0	>6	>19.7	600	1969	1750	5741

Approximate depth of investigation is 70m.

Table 63 Velocity Model for Surface Wave Array Z4-S3

Approx. Elevation of Top of Layer		Depth to Top of Layer		Layer Thickness		S-Wave Velocity		Inferred P-Wave Velocity	
m	ft	m	ft	m	ft	m/s	ft/s	m/s	ft/s
185	607.0	0	0.0	3	9.8	265	869	530	1739
182	597.1	3	9.8	3	9.8	255	837	510	1673
179	587.3	6	19.7	12	39.4	240	787	480	1575
167	547.9	18	59.1	25	82.0	385	1263	770	2526
142	465.9	43	141.1	22	72.2	500	1640	1000	3281
120	393.7	65	213.3	>5	>16.4	500	1640	1700	5577

Approximate depth of investigation is 70m.

Table 64 Velocity Model for Surface Wave Array Z4-S4

Approx. Elevation of Top of Layer		Depth to Top of Layer		Layer Thickness		S-Wave Velocity		Inferred P-Wave Velocity	
m	ft	m	ft	m	ft	m/s	ft/s	m/s	ft/s
174	570.9	0	0.0	3	9.8	265	869	530	1739
171	561.0	3	9.8	3	9.8	275	902	550	1804
168	551.2	6	19.7	9	29.5	285	935	570	1870
159	521.7	15	49.2	25	82.0	440	1444	880	2887
134	439.6	40	131.2	20	65.6	500	1640	1000	3281
114	374.0	60	196.9	5	16.4	600	1969	1200	3937
109	357.6	65	213.3	>5	>16.4	600	1969	1750	5741

Approximate depth of investigation is 70m.

Table 65 Velocity Model for Surface Wave Array Z4-S5

Approx. Elevation of Top of Layer		Depth to Top of Layer		Layer Thickness		S-Wave Velocity		Inferred P-Wave Velocity	
m	ft	m	ft	m	ft	m/s	ft/s	m/s	ft/s
170	557.7	0	0.0	2	6.6	245	804	490	1608
168	551.2	2	6.6	3	9.8	275	902	550	1804
165	541.3	5	16.4	4	13.1	250	820	500	1640
161	528.2	9	29.5	11	36.1	350	1148	700	2297
150	492.1	20	65.6	13	42.7	400	1312	800	2624
137	449.5	33	108.3	17	55.8	500	1640	1000	3281
120	393.7	50	164.0	15	49.2	600	1969	1200	3937
105	344.5	65	213.3	>5	>16.4	600	1969	1750	5741

Approximate depth of investigation is 70m.

Table 66 Velocity Model for Surface Wave Array Z4-S6

Approx. Elevation of Top of Layer		Depth to Top of Layer		Layer Thickness		S-Wave Velocity		Inferred P-Wave Velocity	
m	ft	m	ft	m	ft	m/s	ft/s	m/s	ft/s
168	551.2	0	0.0	2	6.6	265	869	530	1739
166	544.6	2	6.6	3	9.8	255	837	510	1673
163	534.8	5	16.4	4	13.1	300	984	600	1969
159	521.7	9	29.5	11	36.1	350	1148	700	2297
148	485.6	20	65.6	13	42.7	400	1312	800	2624
135	442.9	33	108.3	20	65.6	500	1640	1000	3281
115	377.3	53	173.9	12	39.4	550	1804	1100	3609
103	337.9	65	213.3	>5	>16.4	550	1804	1750	5741

Approximate depth of investigation is 70m.

Table 67 Velocity Model for Surface Wave Array Z4-S7

Approx. Elevation of Top of Layer		Depth to Top of Layer		Layer Thickness		S-Wave Velocity		Inferred P-Wave Velocity	
m	ft	m	ft	m	ft	m/s	ft/s	m/s	ft/s
168	551.2	0	0.0	1.5	4.9	235	771	470	1542
166.5	546.3	1.5	4.9	2.5	8.2	265	869	530	1739
164	538.1	4	13.1	5	16.4	300	984	600	1969
159	521.7	9	29.5	11	36.1	350	1148	700	2297
148	485.6	20	65.6	15	49.2	400	1312	800	2624
133	436.4	35	114.8	20	65.6	500	1640	1000	3281
113	370.7	55	180.4	10	32.8	550	1804	1100	3609
103	337.9	65	213.3	>5	>16.4	550	1804	1750	5741

Approximate depth of investigation is 70m.

Table 68 Velocity Model for Surface Wave Array Z4-S8

Approx. Elevation of Top of Layer		Depth to Top of Layer		Layer Thickness		S-Wave Velocity		Inferred P-Wave Velocity	
m	ft	m	ft	m	ft	m/s	ft/s	m/s	ft/s
164	538.1	0	0.0	1.5	4.9	190	623	380	1247
162.5	533.1	1.5	4.9	2.5	8.2	250	820	500	1640
160	524.9	4	13.1	6	19.7	300	984	600	1969
154	505.2	10	32.8	6	19.7	350	1148	700	2297
148	485.6	16	52.5	15	49.2	400	1312	800	2624
133	436.4	31	101.7	14	45.9	500	1640	1000	3281
119	390.4	45	147.6	10	32.8	600	1969	1200	3937
109	357.6	55	180.4	>15	>49.2	600	1969	1750	5741

Approximate depth of investigation is 70m.

Table 69 Velocity Model for Surface Wave Array Z4-S9

Approx. Elevation of Top of Layer		Depth to Top of Layer		Layer Thickness		S-Wave Velocity		Inferred P-Wave Velocity	
m	ft	m	ft	m	ft	m/s	ft/s	m/s	ft/s
160	524.9	0	0.0	1	3.3	210	689	420	1378
159	521.7	1	3.3	2	6.6	290	951	580	1903
157	515.1	3	9.8	4.5	14.8	275	902	550	1804
152.5	500.3	7.5	24.6	6.5	21.3	350	1148	700	2297
146	479.0	14	45.9	12	39.4	400	1312	800	2624
134	439.6	26	85.3	24	78.7	500	1640	1000	3281
110	360.9	50	164.0	>20	>65.6	500	1640	1700	5577

Approximate depth of investigation is 70m.

Table 70 Velocity Model for Surface Wave Array Z4-S10

Approx. Elevation of Top of Layer		Depth to Top of Layer		Layer Thickness		S-Wave Velocity		Inferred P-Wave Velocity	
m	ft	m	ft	m	ft	m/s	ft/s	m/s	ft/s
150.0	492.1	0	0.0	1.5	4.9	245	804	490	1608
148.5	487.2	1.5	4.9	4.5	14.8	315	1033	630	2067
144.0	472.4	6	19.7	5	16.4	350	1148	700	2297
139.0	456.0	11	36.1	17	55.8	410	1345	820	2690
122.0	400.3	28	91.9	7	23.0	475	1558	950	3116
115.0	377.3	35	114.8	30	98.4	475	1558	1700	5577
85.0	278.9	65	213.3	>5	>16.4	525	1722	1700	5577

Approximate depth of investigation is 70m.

Table 71 Velocity Summary of Zone 4 Surface Wave Investigation

Surface Wave Array	Vs30 (m/s)	Vs30 (ft/s)	Vs60 (m/s)	Vs60 (ft/s)	Vs @ 60m (m/s)	Vs @ 60m (ft/s)
Z4-S1	362	1188	484	1589	850	2789
Z4-S2	369	1210	443	1454	600	1969
Z4-S3	288	944	349	1144	500	1640
Z4-S4	341	1120	398	1307	600	1969
Z4-S5	328	1076	401	1315	600	1969
Z4-S6	337	1105	402	1318	550	1804
Z4-S7	337	1107	399	1308	550	1804
Z4-S8	333	1093	412	1353	600	1969
Z4-S9	355	1164	415	1361	500	1640
Z4-S10	373	1225	418	1372	475	1558

Note: Vs30 = average S-wave velocity of upper 30 m. Vs60 = average S-wave velocity of upper 60 m.

Table 72 Velocity Model for Surface Wave Array Z5-S1

Approx. Elevation of Top of Layer		Depth to Top of Layer		Layer Thickness		S-Wave Velocity		Inferred P-Wave Velocity	
m	ft	m	ft	m	ft	m/s	ft/s	m/s	ft/s
103	337.9	0	0.0	5.25	17.2	190	623	380	1247
97.75	320.7	5.25	17.2	4.75	15.6	275	902	550	1804
93	305.1	10	32.8	8	26.2	375	1230	750	2460
85	278.9	18	59.1	8	26.2	450	1476	900	2952
77	252.6	26	85.3	24	78.7	475	1558	950	3116
53	173.9	50	164.0	>20	>65.6	475	1558	1700	5577

Approximate depth of investigation is 70m.

Table 73 Velocity Model for Surface Wave Array Z5-S2

Approx. Elevation of Top of Layer		Depth to Top of Layer		Layer Thickness		S-Wave Velocity		Inferred P-Wave Velocity	
m	ft	m	ft	m	ft	m/s	ft/s	m/s	ft/s
97	318.2	0	0.0	3	9.8	290	951	580	1903
94	308.4	3	9.8	8	26.2	255	837	510	1673
86	282.2	11	36.1	20	65.6	365	1198	730	2395
66	216.5	31	101.7	19	62.3	425	1394	850	2788
47	154.2	50	164.0	6	19.7	425	1394	1600	5249
41	134.5	56	183.7	>14	>45.9	500	1640	1700	5577

Approximate depth of investigation is 70m.

Table 74 Velocity Model for Surface Wave Array Z5-S3

Approx. Elevation of Top of Layer		Depth to Top of Layer		Layer Thickness		S-Wave Velocity		Inferred P-Wave Velocity	
m	ft	m	ft	m	ft	m/s	ft/s	m/s	ft/s
100	328.1	0	0.0	3.5	11.5	200	656	400	1312
96.5	316.6	3.5	11.5	5	16.4	250	820	500	1640
91.5	300.2	8.5	27.9	13.5	44.3	360	1181	720	2362
78	255.9	22	72.2	18	59.1	425	1394	850	2788
60	196.9	40	131.2	10	32.8	500	1640	1000	3281
50	164.0	50	164.0	>20	>65.6	500	1640	1700	5577

Approximate depth of investigation is 70m.

Table 75 Velocity Model for Surface Wave Array Z5-S4

Approx. Elevation of Top of Layer		Depth to Top of Layer		Layer Thickness		S-Wave Velocity		Inferred P-Wave Velocity	
m	ft	m	ft	m	ft	m/s	ft/s	m/s	ft/s
106	347.8	0	0.0	2	6.6	210	689	420	1378
104	341.2	2	6.6	9	29.5	250	820	500	1640
95	311.7	11	36.1	23	75.5	355	1165	710	2329
72	236.2	34	111.5	16	52.5	450	1476	900	2952
56	183.7	50	164.0	5	16.4	500	1640	1000	3281
51	167.3	55	180.4	>15	>49.2	500	1640	1700	5577

Approximate depth of investigation is 70m.

Table 76 Velocity Model for Surface Wave Array Z5-S6

Approx. Elevation of Top of Layer		Depth to Top of Layer		Layer Thickness		S-Wave Velocity		Inferred P-Wave Velocity	
m	ft	m	ft	m	ft	m/s	ft/s	m/s	ft/s
110	360.9	0	0.0	4	13.1	220	722	440	1444
106	347.8	4	13.1	7	23.0	320	1050	640	2100
99	324.8	11	36.1	14	45.9	350	1148	700	2296
85	278.9	25	82.0	15	49.2	450	1476	900	2952
70	229.7	40	131.2	15	49.2	525	1722	1050	3445
55	180.4	55	180.4	5	16.4	525	1722	1700	5577
50	164.0	60	196.9	>10	>32.8	625	2051	1750	5741

Approximate depth of investigation is 70m.

Table 77 Velocity Model for Surface Wave Array Z5-S7

Approx. Elevation of Top of Layer		Depth to Top of Layer		Layer Thickness		S-Wave Velocity		Inferred P-Wave Velocity	
m	ft	m	ft	m	ft	m/s	ft/s	m/s	ft/s
113	370.7	0	0.0	1.75	5.7	235	771	470	1542
111.25	365.0	1.75	5.7	6.25	20.5	325	1066	650	2133
105	344.5	8	26.2	10	32.8	350	1148	700	2297
95	311.7	18	59.1	18	59.1	450	1476	900	2952
77	252.6	36	118.1	20	65.6	525	1722	1050	3445
57	187.0	56	183.7	>14	>45.9	525	1722	1700	5577

Approximate depth of investigation is 70m.

Table 78 Velocity Model for Surface Wave Array Z5-S8

Approx. Elevation of Top of Layer		Depth to Top of Layer		Layer Thickness		S-Wave Velocity		Inferred P-Wave Velocity	
m	ft	m	ft	m	ft	m/s	ft/s	m/s	ft/s
114	374.0	0	0.0	2.5	8.2	305	1001	610	2001
111.5	365.8	2.5	8.2	3.5	11.5	335	1099	670	2198
108	354.3	6	19.7	6	19.7	275	902	550	1804
102	334.6	12	39.4	10	32.8	400	1312	800	2624
92	301.8	22	72.2	20	65.6	475	1558	950	3116
72	236.2	42	137.8	14	45.9	550	1804	1100	3609
58	190.3	56	183.7	>14	>45.9	550	1804	1700	5577

Approximate depth of investigation is 70m.

Table 79 Velocity Model for Surface Wave Array Z5-S9

Approx. Elevation of Top of Layer		Depth to Top of Layer		Layer Thickness		S-Wave Velocity		Inferred P-Wave Velocity	
m	ft	m	ft	m	ft	m/s	ft/s	m/s	ft/s
122	400.3	0	0.0	2	6.6	210	689	420	1378
120	393.7	2	6.6	6	19.7	315	1033	630	2067
114	374.0	8	26.2	10	32.8	320	1050	640	2100
104	341.2	18	59.1	35	114.8	475	1558	950	3116
69	226.4	53	173.9	3	9.8	500	1640	1000	3281
66	216.5	56	183.7	>14	>45.9	500	1640	1700	5577

Approximate depth of investigation is 70m.

Table 80 Velocity Model for Surface Wave Array Z5-S10

Approx. Elevation of Top of Layer		Depth to Top of Layer		Layer Thickness		S-Wave Velocity		Inferred P-Wave Velocity	
m	ft	m	ft	m	ft	m/s	ft/s	m/s	ft/s
134	439.6	0	0.0	2	6.6	300	984	600	1969
132	433.1	2	6.6	9	29.5	275	902	550	1804
123	403.5	11	36.1	14	45.9	375	1230	750	2460
109	357.6	25	82.0	8	26.2	525	1722	1050	3445
101	331.4	33	108.3	7	23.0	550	1804	1100	3609
94	308.4	40	131.2	27	88.6	550	1804	1700	5577
67	219.8	67	219.8	>3	>9.8	665	2182	1750	5741

Approximate depth of investigation is 70m.

Table 81 Velocity Model for Surface Wave Array Z5-S11

Approx. Elevation of Top of Layer		Depth to Top of Layer		Layer Thickness		S-Wave Velocity		Inferred P-Wave Velocity	
m	ft	m	ft	m	ft	m/s	ft/s	m/s	ft/s
139	456.0	0	0.0	1.5	4.9	190	623	380	1247
137.5	451.1	1.5	4.9	3.5	11.5	285	935	570	1870
134	439.6	5	16.4	7	23.0	350	1148	700	2297
127	416.7	12	39.4	8	26.2	400	1312	800	2625
119	390.4	20	65.6	5	16.4	465	1526	930	3051
114	374.0	25	82.0	30	98.4	465	1526	1700	5577
84	275.6	55	180.4	>15	>49.2	525	1722	1725	5659

Approximate depth of investigation is 70m.

Table 82 Velocity Model for Surface Wave Array Z5-S12

Approx. Elevation of Top of Layer		Depth to Top of Layer		Layer Thickness		S-Wave Velocity		Inferred P-Wave Velocity	
m	ft	m	ft	m	ft	m/s	ft/s	m/s	ft/s
133	436.4	0	0.0	2.5	8.2	275	902	550	1804
130.5	428.1	2.5	8.2	2	6.6	255	837	510	1673
128.5	421.6	4.5	14.8	4.5	14.8	350	1148	700	2297
124	406.8	9	29.5	7	23.0	450	1476	900	2953
117	383.9	16	52.5	20	65.6	450	1476	1600	5249
97	318.2	36	118.1	>34	>111.5	500	1640	1700	5577

Approximate depth of investigation is 70m.

Table 83 Velocity Model for Surface Wave Array Z5-S13

Approx. Elevation of Top of Layer		Depth to Top of Layer		Layer Thickness		S-Wave Velocity		Inferred P-Wave Velocity	
m	ft	m	ft	m	ft	m/s	ft/s	m/s	ft/s
129	423.2	0	0.0	2.5	8.2	205	673	410	1345
126.5	415.0	2.5	8.2	2.5	8.2	300	984	600	1969
124	406.8	5	16.4	7	23.0	350	1148	700	2297
117	383.9	12	39.4	4	13.1	400	1312	800	2624
113	370.7	16	52.5	14	45.9	400	1312	1600	5249
99	324.8	30	98.4	29	95.1	450	1476	1700	5577
70	229.7	59	193.6	>11	>36.1	550	1804	1725	5659

Approximate depth of investigation is 70m.

Table 84 Summary of Zone 5 Surface Wave Investigation

Surface Wave Array	Vs30 (m/s)	Vs30 (ft/s)	Vs60 (m/s)	Vs60 (ft/s)	Vs @ 60m (m/s)	Vs @ 60m (ft/s)
Z5-S1	325	1065	386	1265	475	1558
Z5-S2	320	1050	367	1205	500	1640
Z5-S3	320	1049	381	1251	500	1640
Z5-S4	303	994	362	1187	500	1640
Z5-S6	329	1080	396	1299	625	2051
Z5-S7	366	1202	426	1396	525	1722
Z5-S8	364	1196	428	1403	550	1804
Z5-S9	353	1157	407	1335	500	1640
Z5-S10	348	1141	425	1396	550	1804
Z5-S11	367	1205	414	1358	525	1722
Z5-S12	392	1287	435	1429	500	1640
Z5-S13	351	1151	395	1297	550	1804

Note: Vs30 = average S-wave velocity of upper 30 m. Vs60 = average S-wave velocity of upper 60 m.

FIGURES

FIGURE 1
SITE MAP

SR-710 TUNNEL
TECHNICAL STUDY
LOS ANGELES COUNTY, CALIFORNIA

PREPARED FOR
CH2M HILL

TYPICAL PASSIVE SURFACE WAVE SETUP

SEISMIC RECORDER SYSTEM

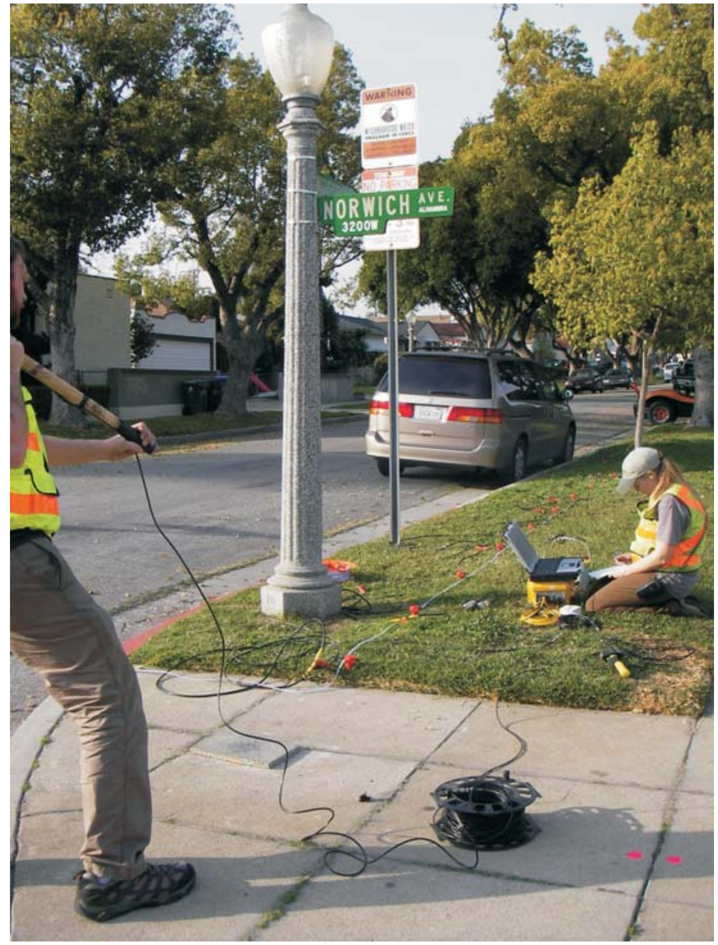

TYPICAL MASW SETUP

GEOVision geophysical services

Project # 9001
Date: JUL 17, 2009
Drawn By: A MARTIN
Approved By: [signature]
File R:\...Project Files\2009\9001ch2mhill\report\figures\Figure2.cdr

FIGURE 2
PHOTOGRAPHS OF PASSIVE AND
ACTIVE SURFACE ARRAY FIELD LAYOUT

SR-710 TUNNEL TECHNICAL STUDY
LOS ANGELES COUNTY, CALIFORNIA

PREPARED FOR
CH2M HILL

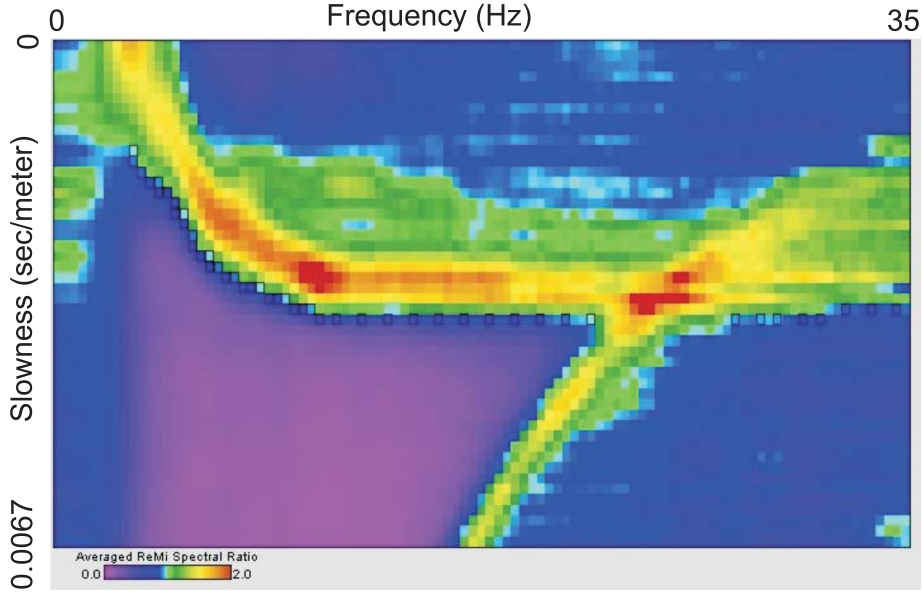

Wavefield Transform of Linear Array Passive Surface Wave Data using Optim SeisOpt ReMi Data Analysis Package (Z2-S2)

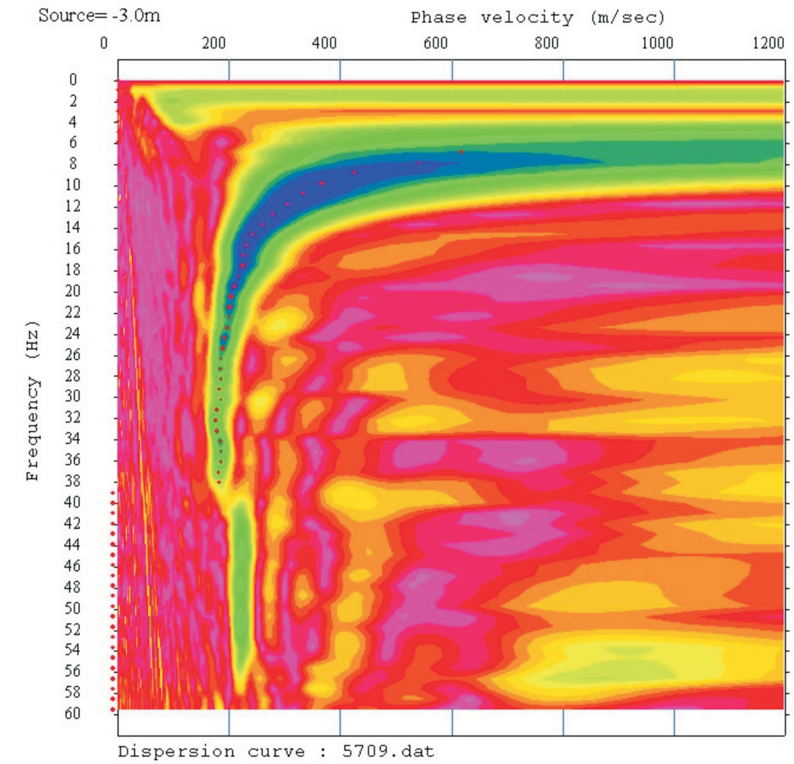

Wavefield Transform of MASW Data (Z2-S6)

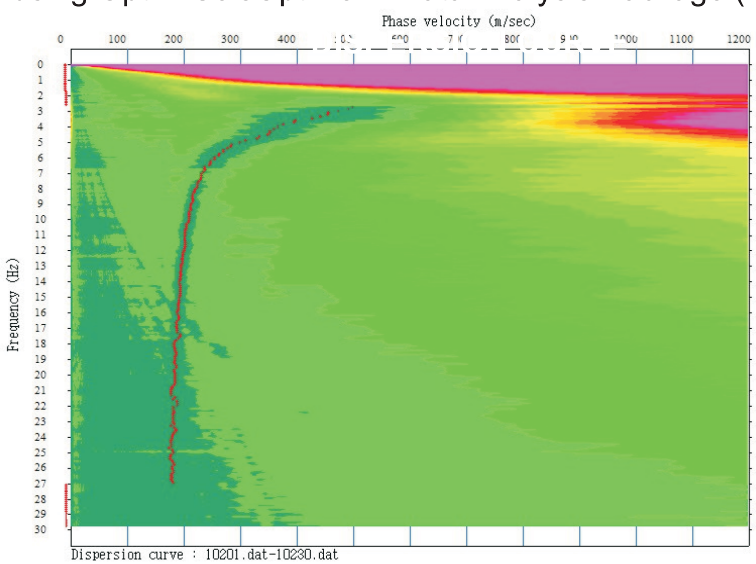

Wavefield Transform of "L" array Passive Surface Wave Data using Spatial Autocorrelation Method (Z1-S16)

GEOVision geophysical services	FIGURE 3 TYPICAL WAVEFIELD TRANSFORMS OF ACTIVE AND PASSIVE SURFACE WAVE DATA
Project # 9001 Date: JUL 20, 2009	SR-710 TUNNEL TECHNICAL STUDY LOS ANGELES COUNTY, CALIFORNIA
Drawn By: A MARTIN Approved By: Antony J Martin	PREPARED FOR CH2M HILL
File R:\...Project Files\2009\9001ch2mhill\report\figures\Figure 3.cdr	

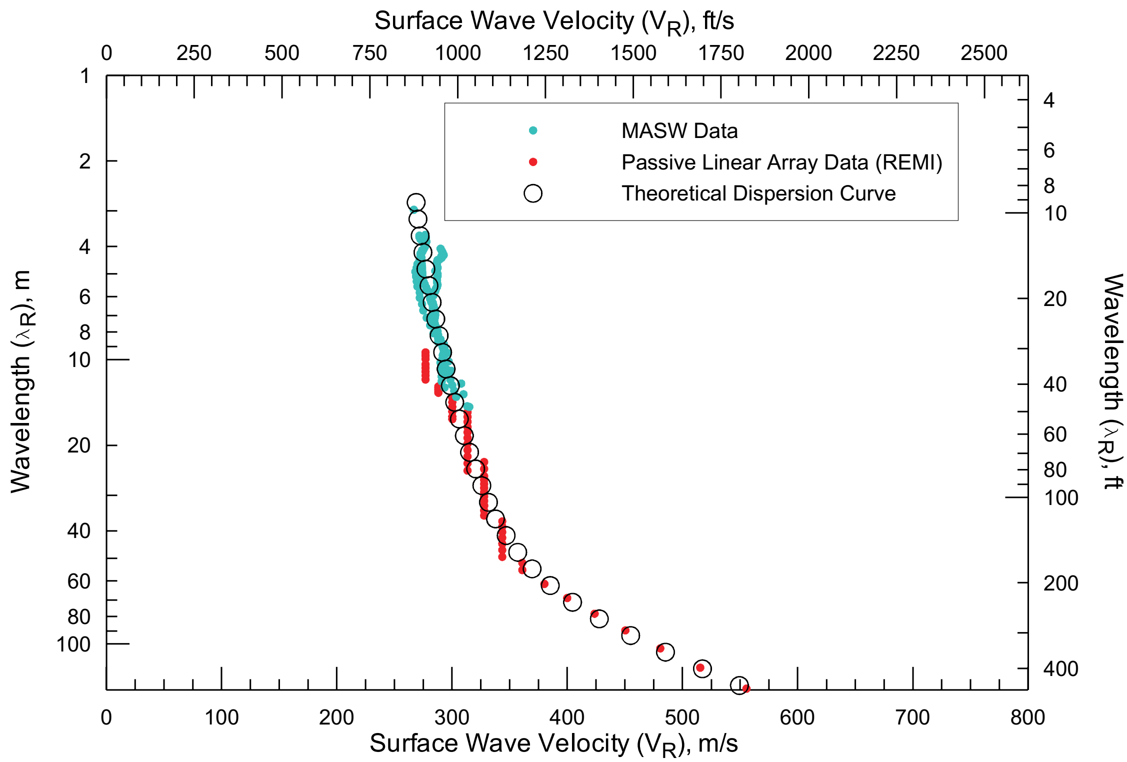

Comparison of Field Experimental Data and Theoretical Dispersion Curve from Active and Passive Surface Wave Array Z1-S1

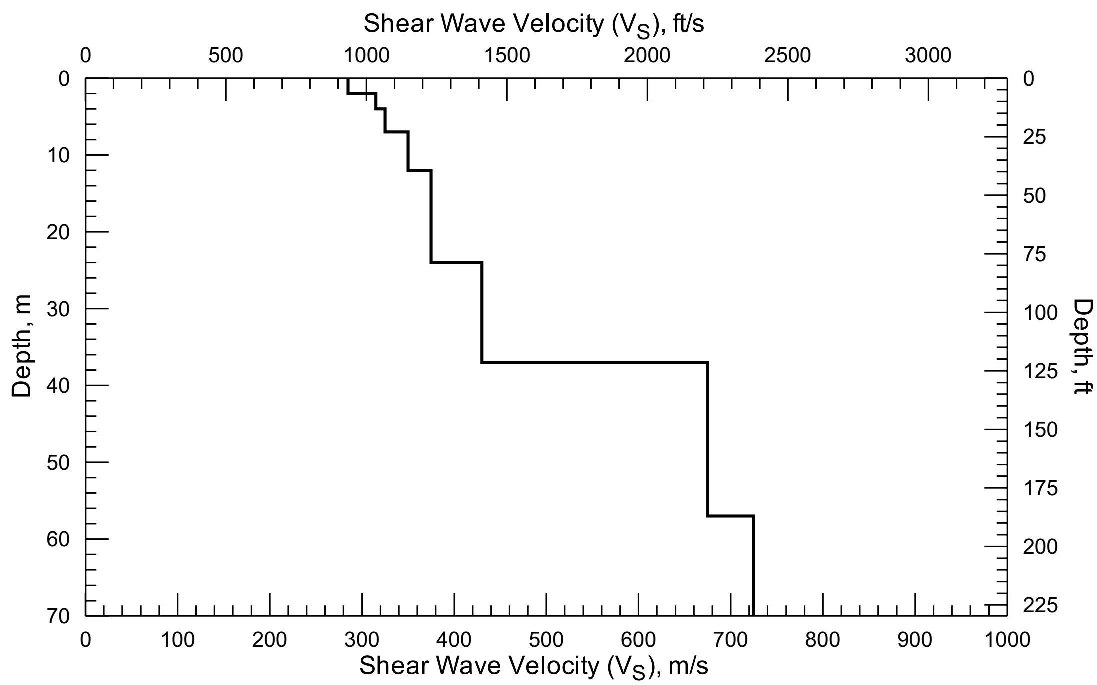

V_S Model from Active and Passive Surface Wave Array Z1-S1

GEOVision geophysical services	FIGURE 4 VELOCITY MODEL FOR ACTIVE AND PASSIVE SURFACE WAVE ARRAY Z1-S1
Project # 9001 Date: JUL 17, 2008 Drawn By: A MARTIN Approved By: Antony J Martin	SILVER RIDGE AVE LOS ANGELES, CALIFORNIA
File R:\...Project Files\2009\9001ch2mhill\report\figures\Figure4.cdr	PREPARED FOR CH2M HILL

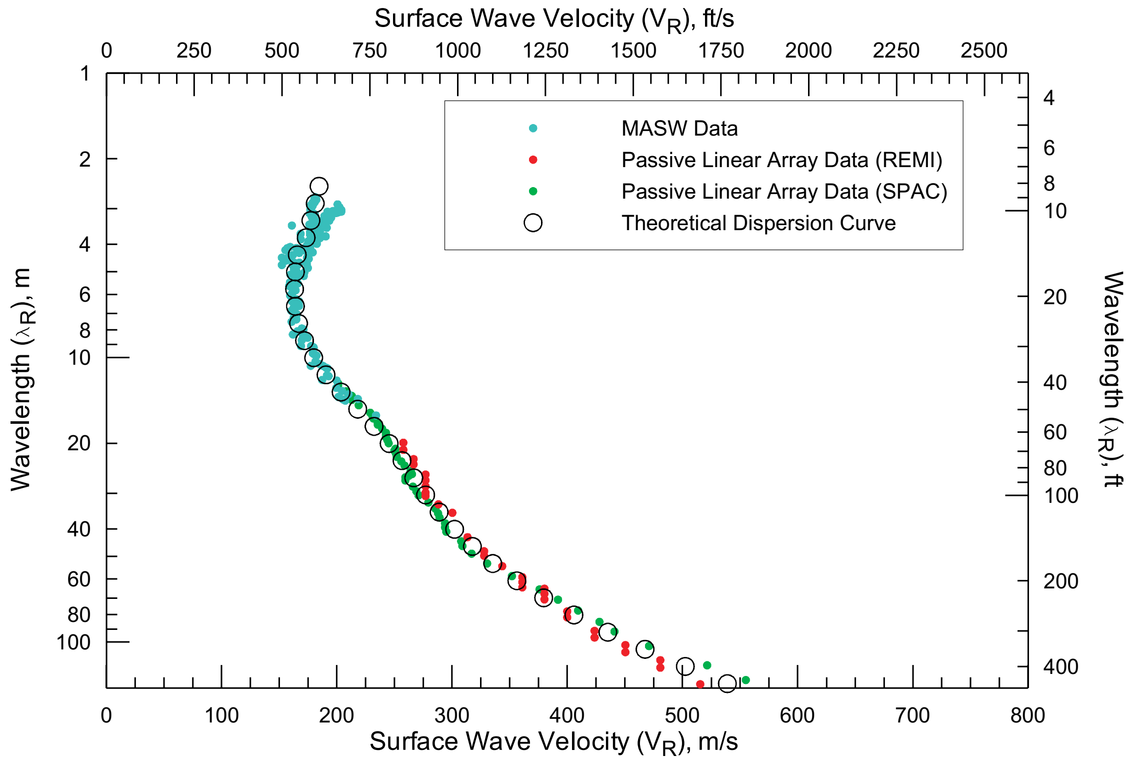

Comparison of Field Experimental Data and Theoretical Dispersion Curve from Active and Passive Surface Wave Array Z1-S2

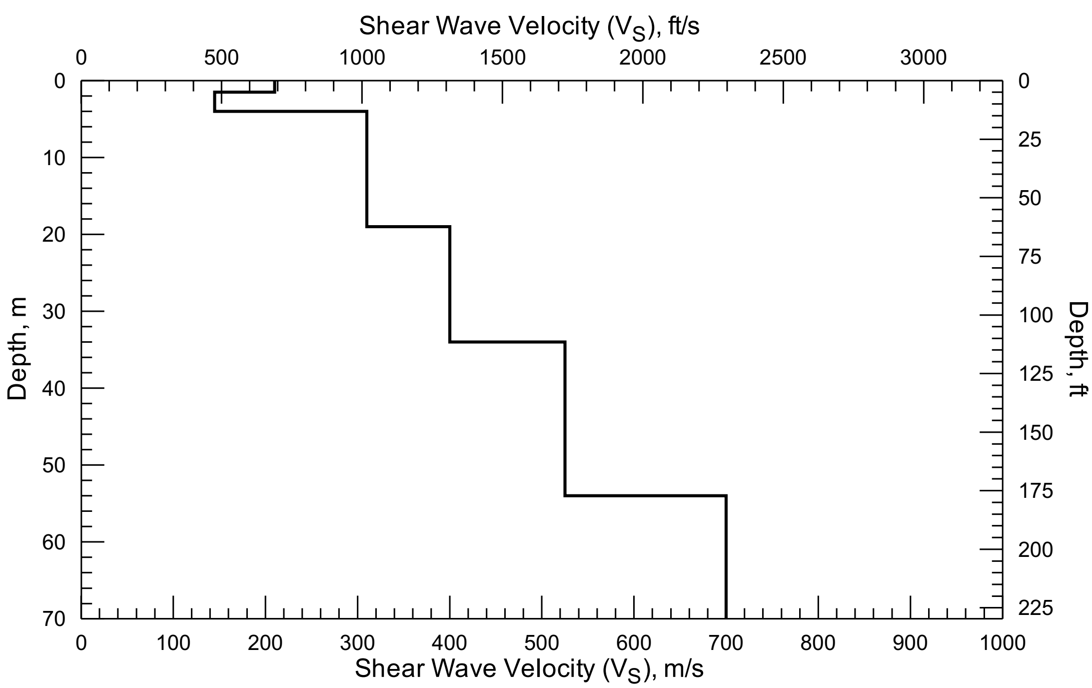

V_S Model from Active and Passive Surface Wave Array Z1-S2

GEOVision geophysical services	FIGURE 5 VELOCITY MODEL FOR ACTIVE AND PASSIVE SURFACE WAVE ARRAY Z1-S2
Project # 9001 Date: JUL 17, 2008 Drawn By: A MARTIN Approved By:	CRYSTAL ST AND ALLESANDRO ST LOS ANGELES, CALIFORNIA
File R:\...Project Files\2009\9001ch2mhill\report\figures\Figure5.cdr	PREPARED FOR CH2M HILL

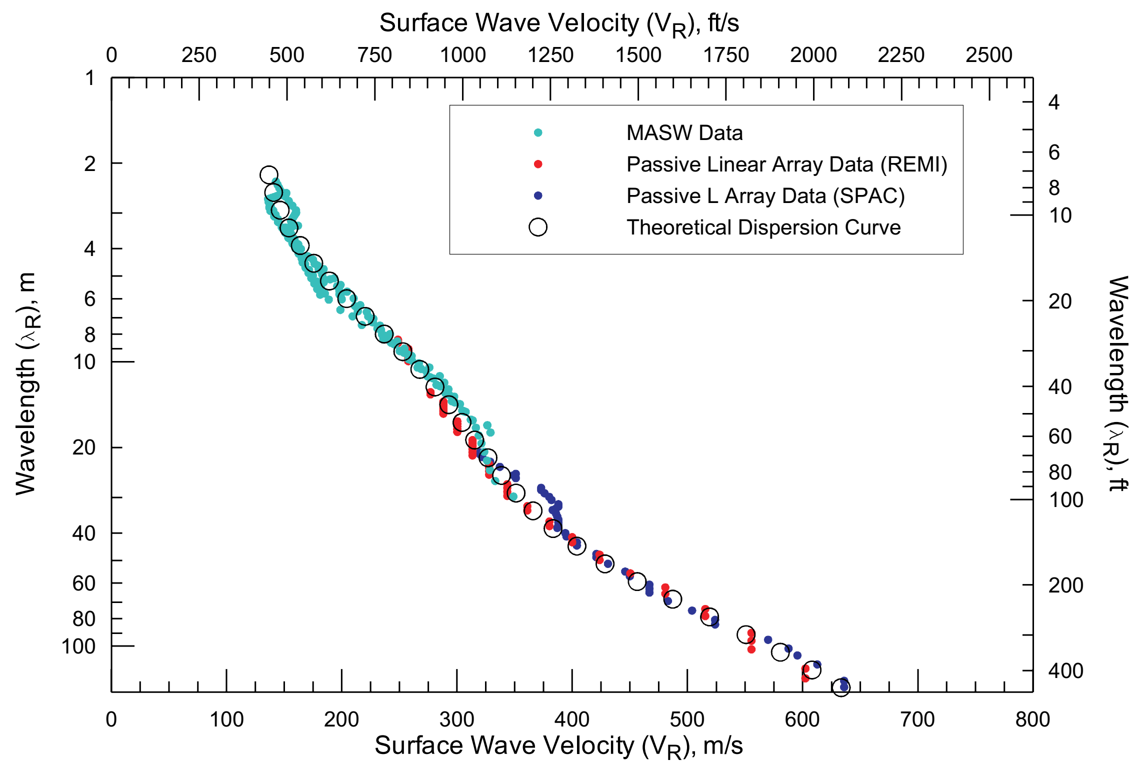

Comparison of Field Experimental Data and Theoretical Dispersion Curve from Active and Passive Surface Wave Array Z1-S3

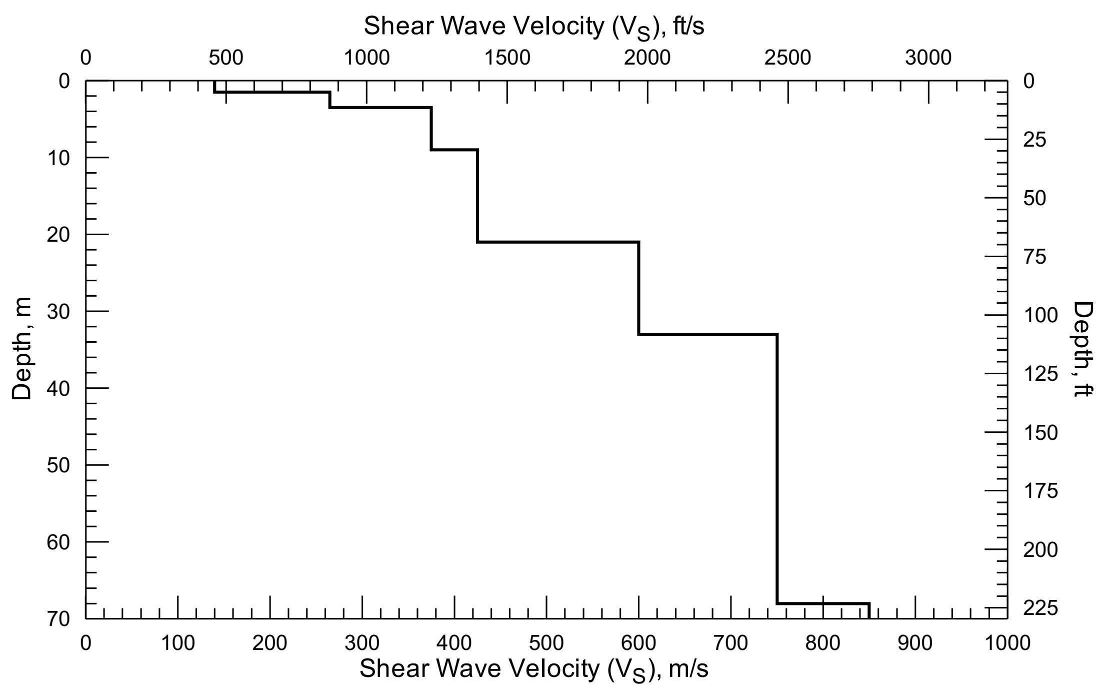

V_S Model from Active and Passive Surface Wave Array Z1-S3

GEOVision geophysical services	FIGURE 6 VELOCITY MODEL FOR ACTIVE AND PASSIVE SURFACE WAVE ARRAY Z1-S3
Project # 9001 Date: JUL 17, 2008 Drawn By: A MARTIN Approved By: [signature]	ECHO PARK AVE AND DONALDSON ST LOS ANGELES, CALIFORNIA
File R:\...Project Files\2009\9001ch2mhill\report\figures\Figure6.cdr	PREPARED FOR CH2M HILL

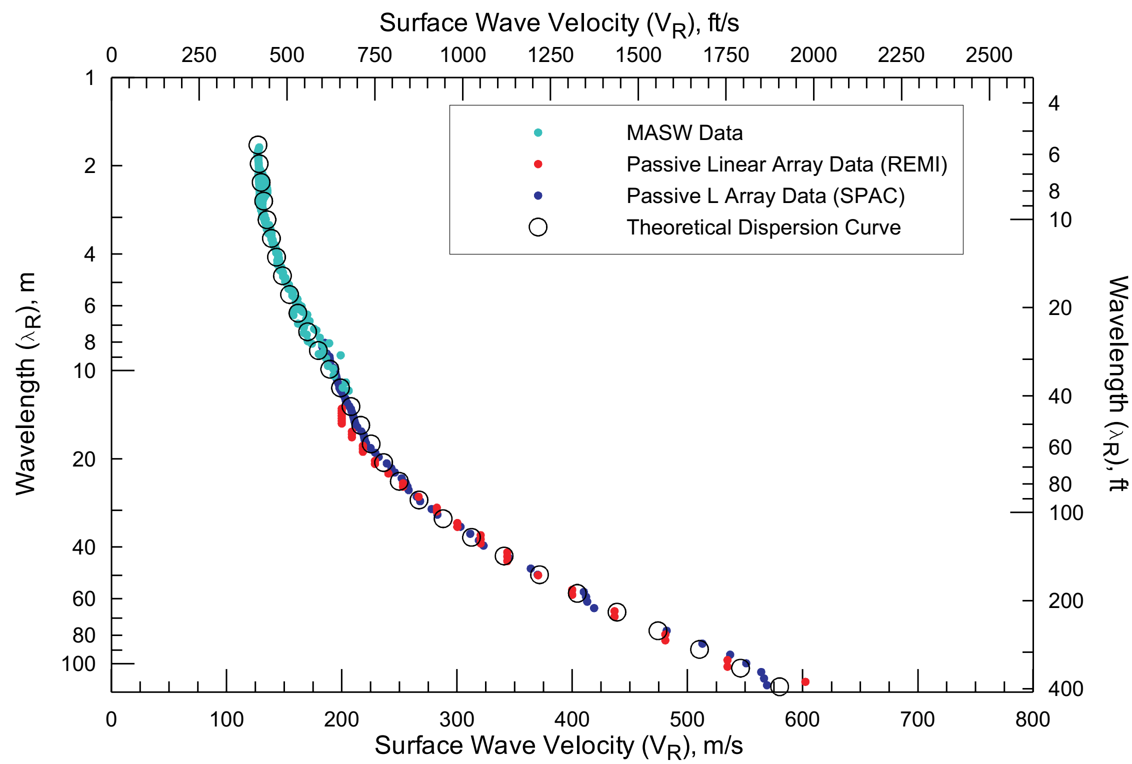

Comparison of Field Experimental Data and Theoretical Dispersion Curve from Active and Passive Surface Wave Array Z1-S4

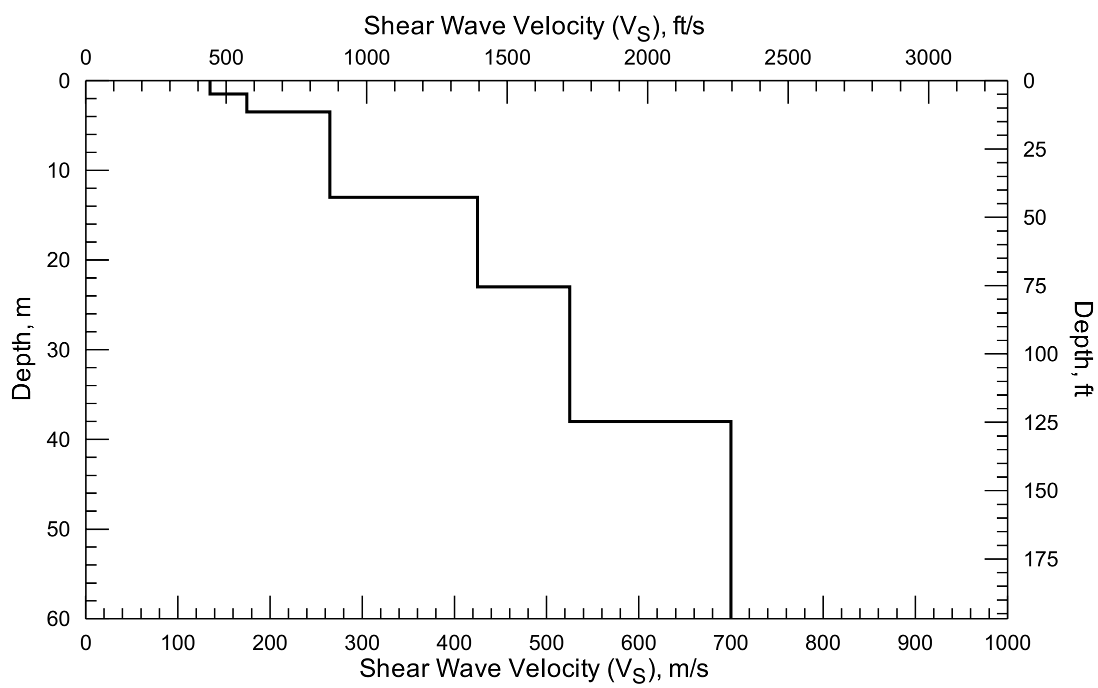

V_S Model from Active and Passive Surface Wave Array Z1-S4

GEOVision geophysical services

Project # 9001
Date: JUL 17, 2008
Drawn By: A MARTIN
Approved By: [signature]

FIGURE 7
VELOCITY MODEL FOR ACTIVE AND PASSIVE SURFACE WAVE ARRAY Z1-S4

PIRTLE ST AND LOWE ST
LOS ANGELES, CALIFORNIA

PREPARED FOR
CH2M HILL

File R:\...Project Files\2009\9001ch2mhill\report\figures\Figure7.cdr

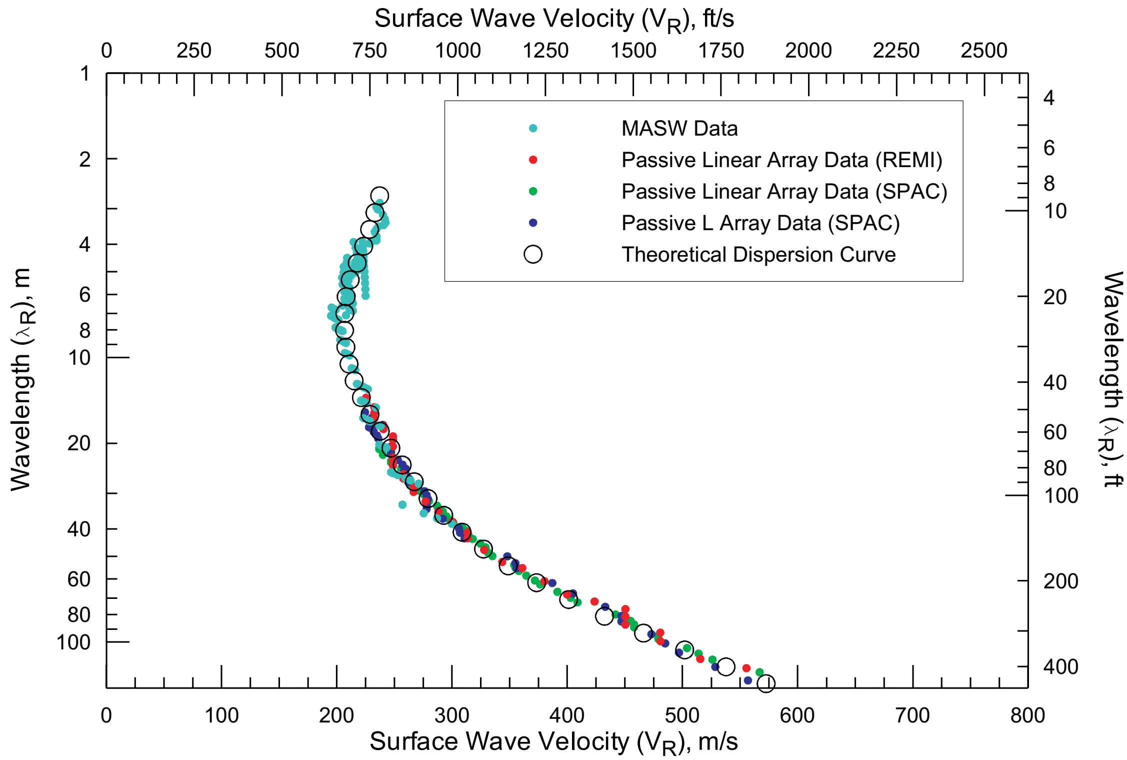

Comparison of Field Experimental Data and Theoretical Dispersion Curve from Active and Passive Surface Wave Array Z1-S5

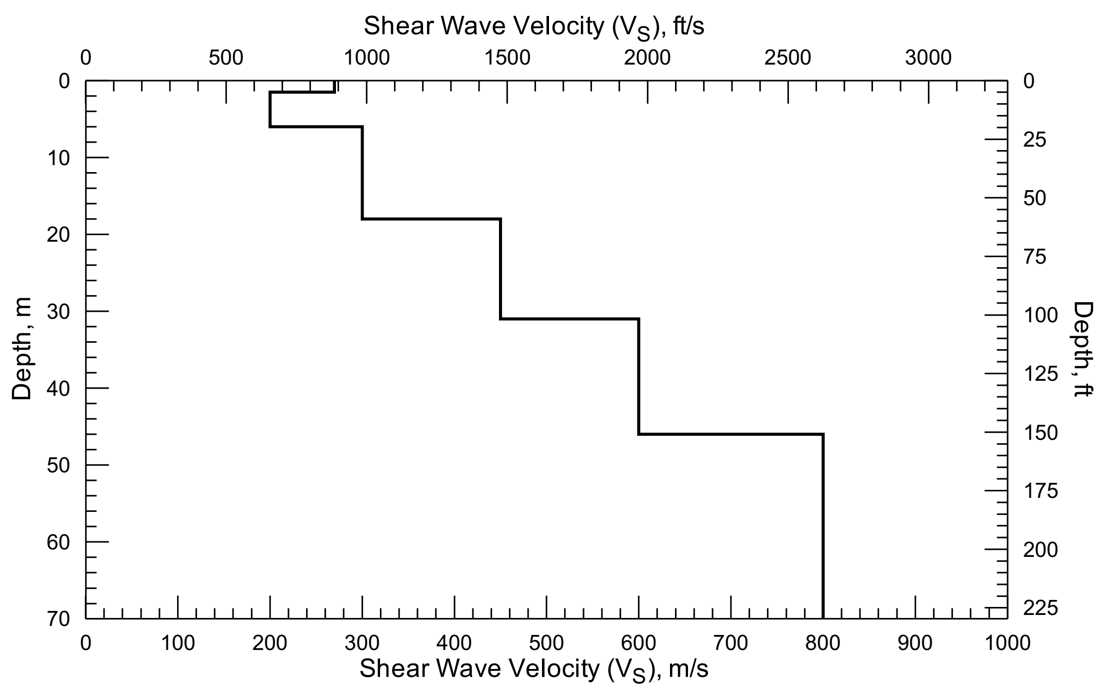

V_S Model from Active and Passive Surface Wave Array Z1-S5

GEOVision geophysical services

Project # 9001
Date: JUL 17, 2008
Drawn By: A MARTIN
Approved By: [signature]
File R:\...Project Files\2009\9001ch2mhill\report\figures\Figure8.cdr

FIGURE 8
VELOCITY MODEL FOR ACTIVE AND PASSIVE SURFACE WAVE ARRAY Z1-S5

STADIUM WAY
LOS ANGELES, CALIFORNIA

PREPARED FOR
CH2M HILL

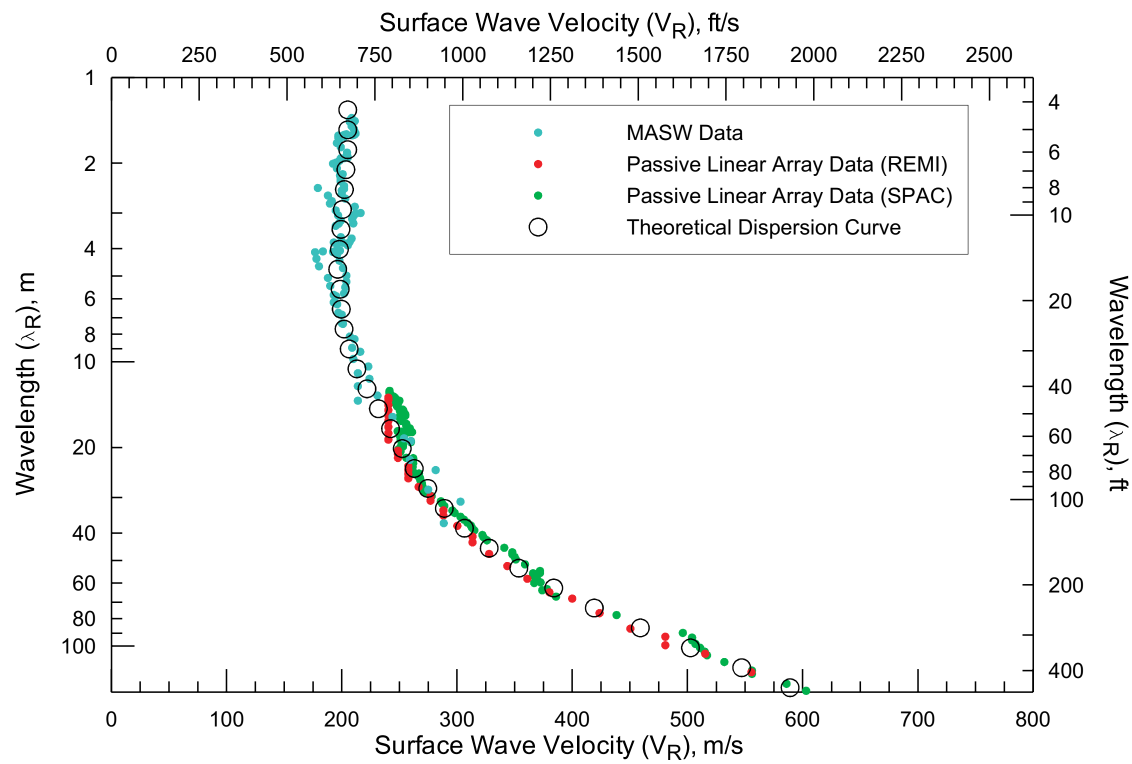

Comparison of Field Experimental Data and Theoretical Dispersion Curve from Active and Passive Surface Wave Array Z1-S6

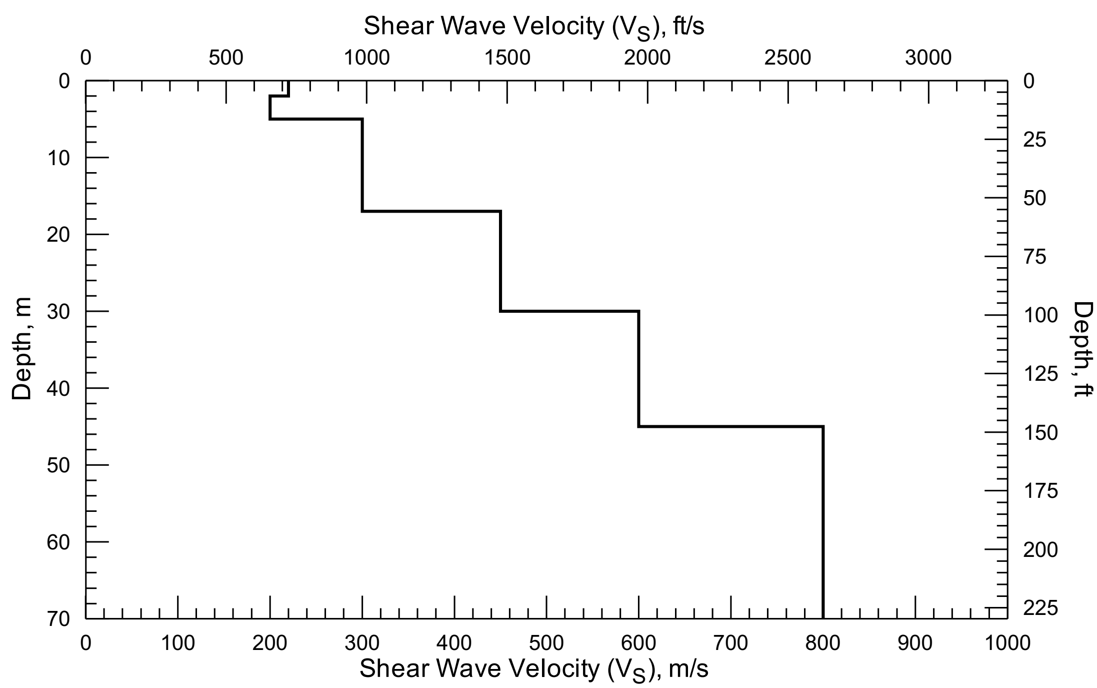

V_S Model from Active and Passive Surface Wave Array Z1-S6

GEOVision geophysical services	FIGURE 9 VELOCITY MODEL FOR ACTIVE AND PASSIVE SURFACE WAVE ARRAY Z1-S6
Project # 9001 Date: JUL 17, 2008 Drawn By: A MARTIN Approved By:	STADIUM WAY LOS ANGELES, CALIFORNIA
File R:\...Project Files\2009\9001ch2mhill\report\figures\Figure9.cdr	PREPARED FOR CH2M HILL

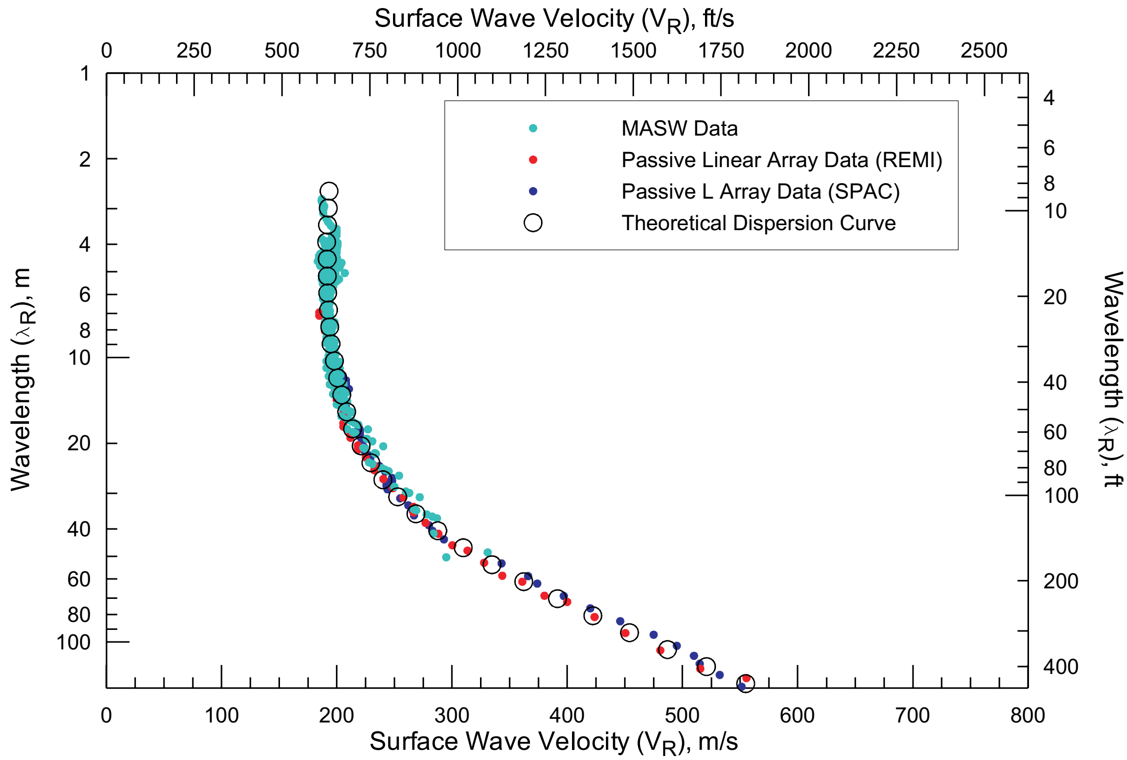

Comparison of Field Experimental Data and Theoretical Dispersion Curve from Active and Passive Surface Wave Array Z1-S7

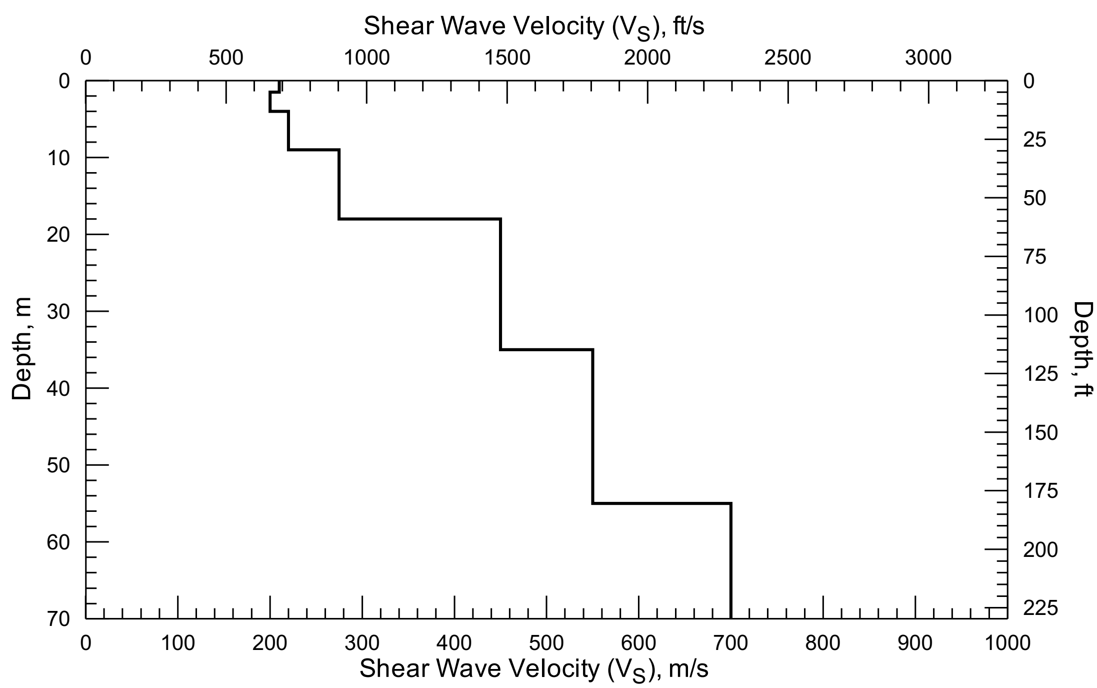

V_S Model from Active and Passive Surface Wave Array Z1-S7

GEOVision geophysical services

Project # 9001
Date: JUL 17, 2008
Drawn By: A MARTIN
Approved By: [signature]
File R:\...Project Files\2009\9001ch2mhill\report\figures\Figure10.cdr

FIGURE 10
VELOCITY MODEL FOR ACTIVE AND PASSIVE SURFACE WAVE ARRAY Z1-S7

SHOREDALE AVE AND BLAKE AVE, LOS ANGELES, CALIFORNIA

PREPARED FOR CH2M HILL

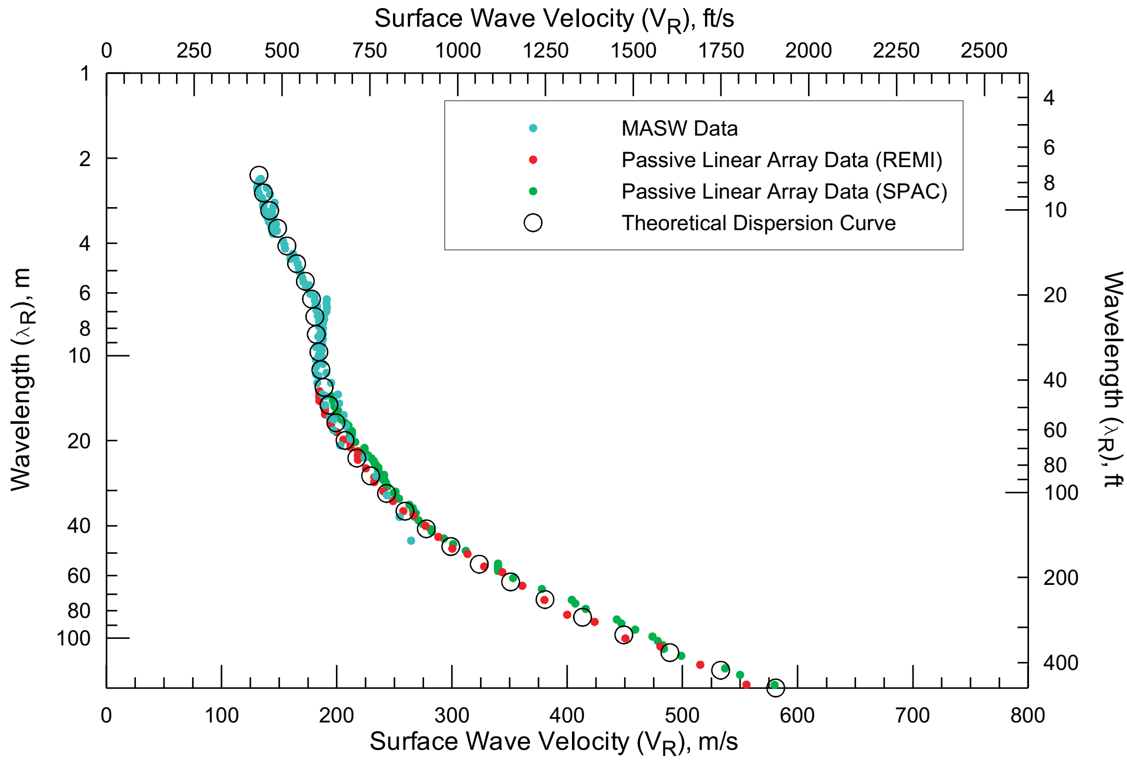

Comparison of Field Experimental Data and Theoretical Dispersion Curve from Active and Passive Surface Wave Array Z1-S8

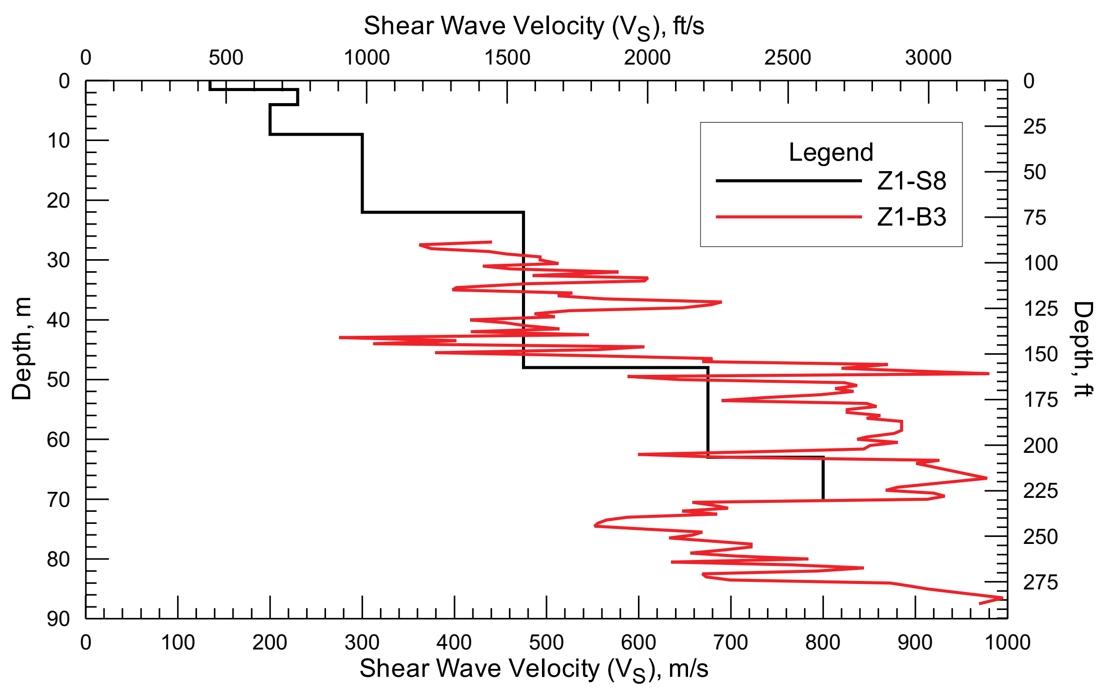

V_S Model from Active and Passive Surface Wave Array Z1-S8

GEOVision geophysical services	FIGURE 11 VELOCITY MODEL FOR ACTIVE AND PASSIVE SURFACE WAVE ARRAY Z1-S8
Project # 9001 Date: JUL 17, 2008 Drawn By: A MARTIN	THORPE AVE BETWEEN CYPRESS AVE AND NORTH SAN FERNANDO RD, LOS ANGELES, CALIFORNIA
Approved By: *[signature]* File R:\...Project Files\2009\9001ch2mhill\report\figures\Figure11.cdr	PREPARED FOR CH2M HILL

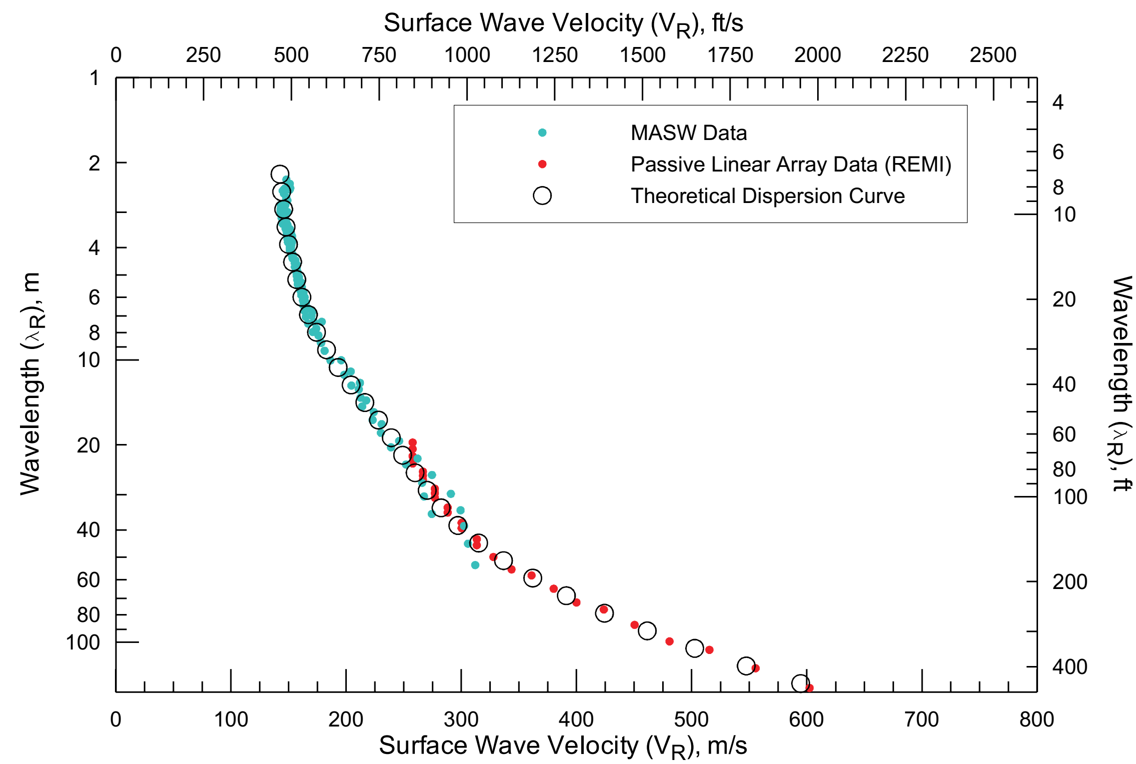

Comparison of Field Experimental Data and Theoretical Dispersion Curve from Active and Passive Surface Wave Array Z1-S9

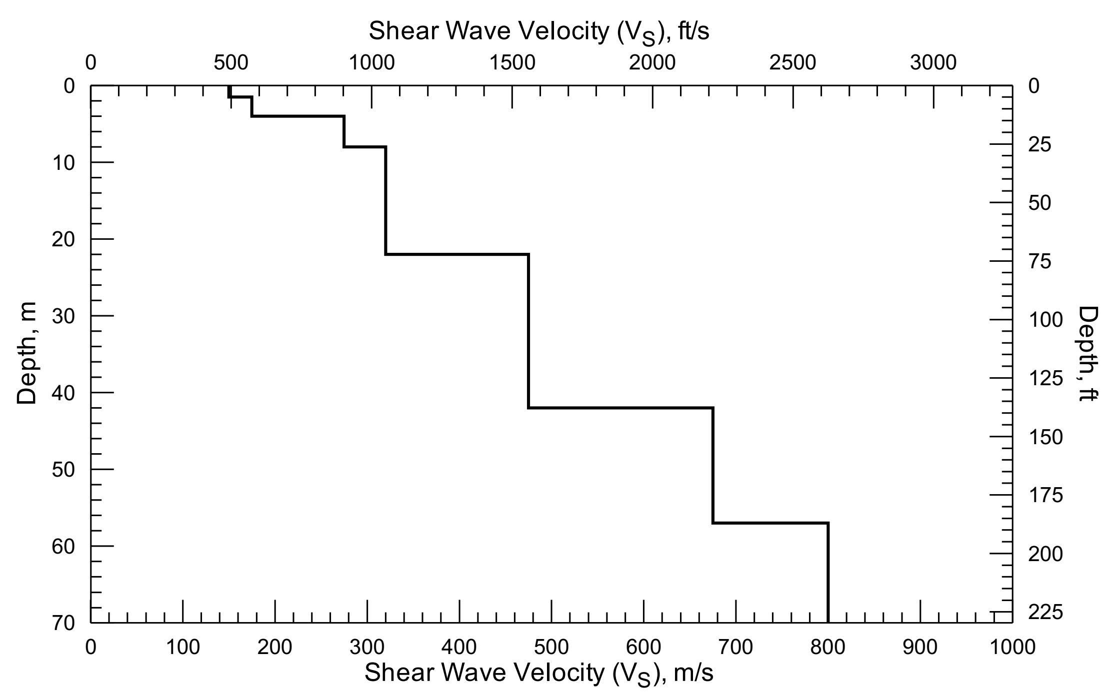

V_S Model from Active and Passive Surface Wave Array Z1-S9

GEOVision geophysical services

Project # 9001
Date: JUL 17, 2008
Drawn By: A MARTIN
Approved By:

File R:\...Project Files\2009\9001ch2mhill\report\figures\Figure12.cdr

FIGURE 12
VELOCITY MODEL FOR ACTIVE AND PASSIVE SURFACE WAVE ARRAY Z1-S9

CYPRESS AVE AND GRANADA ST, LOS ANGELES, CALIFORNIA

PREPARED FOR
CH2M HILL

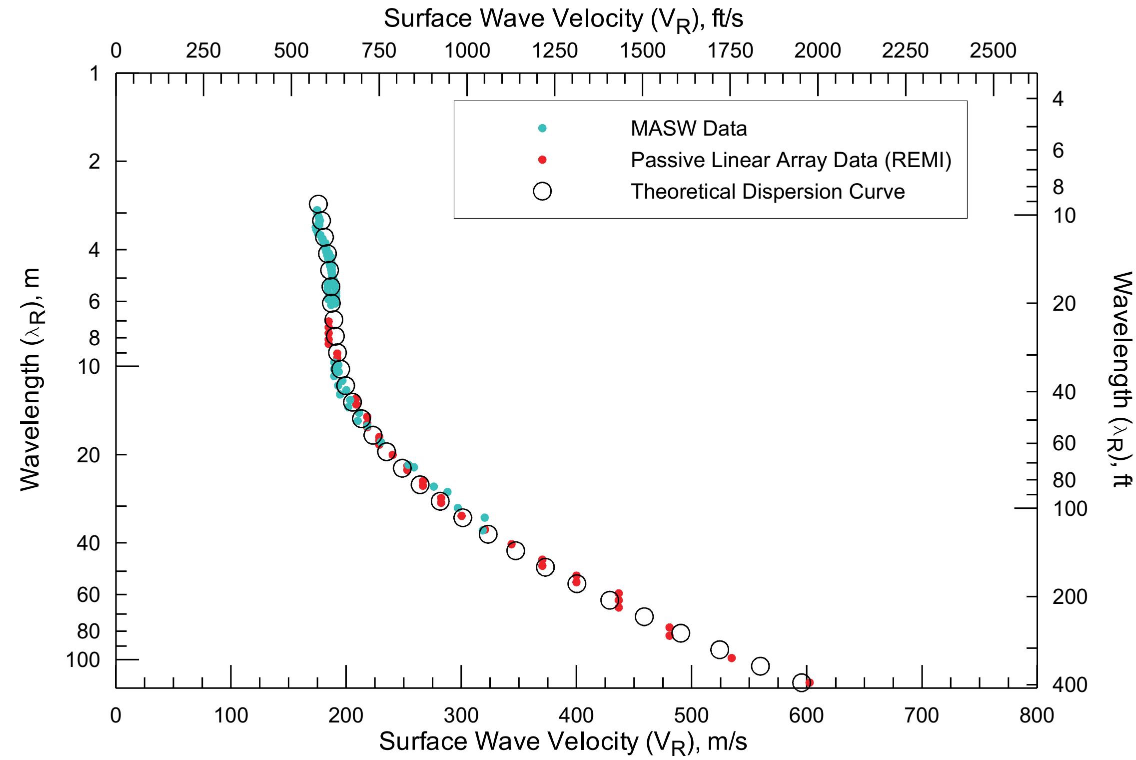

Comparison of Field Experimental Data and Theoretical Dispersion Curve from Active and Passive Surface Wave Array Z1-S10

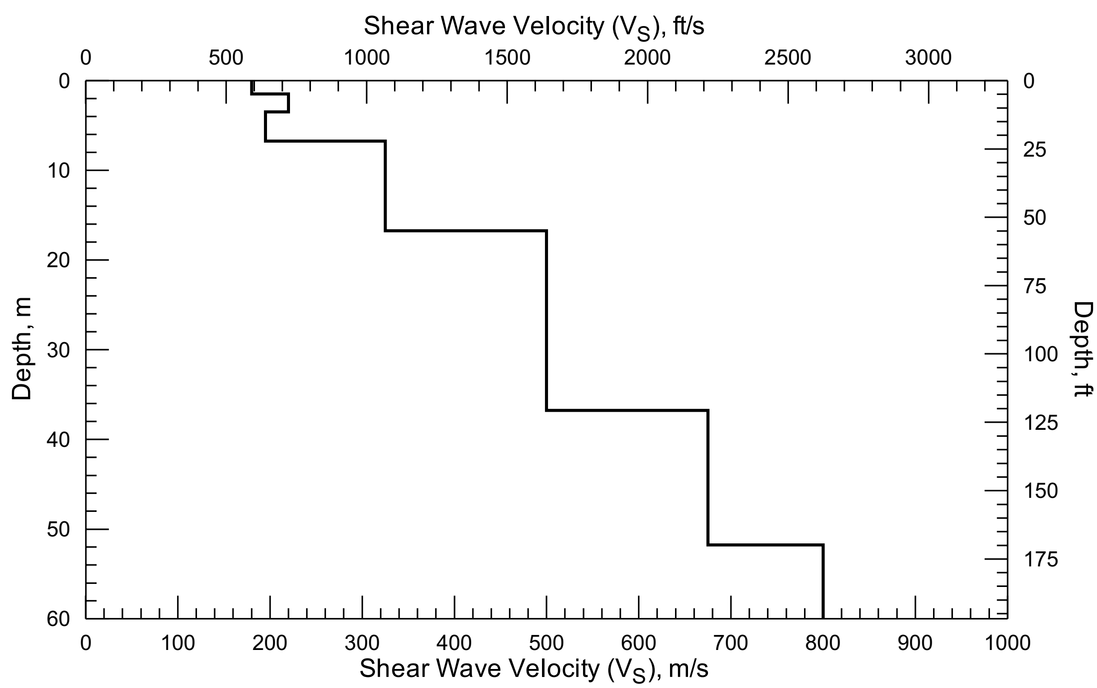

V_S Model from Active and Passive Surface Wave Array Z1-S10

GEOVision geophysical services	FIGURE 13 VELOCITY MODEL FOR ACTIVE AND PASSIVE SURFACE WAVE ARRAY Z1-S10
Project # 9001 Date: JUL 17, 2008 Drawn By: A MARTIN	PLEASANT VIEW AVE AND LOOSMORE ST, LOS ANGELES, CALIFORNIA
Approved By: Antony J Martin File R:\...Project Files\2009\9001ch2mhill\report\figures\Figure13.cdr	PREPARED FOR CH2M HILL

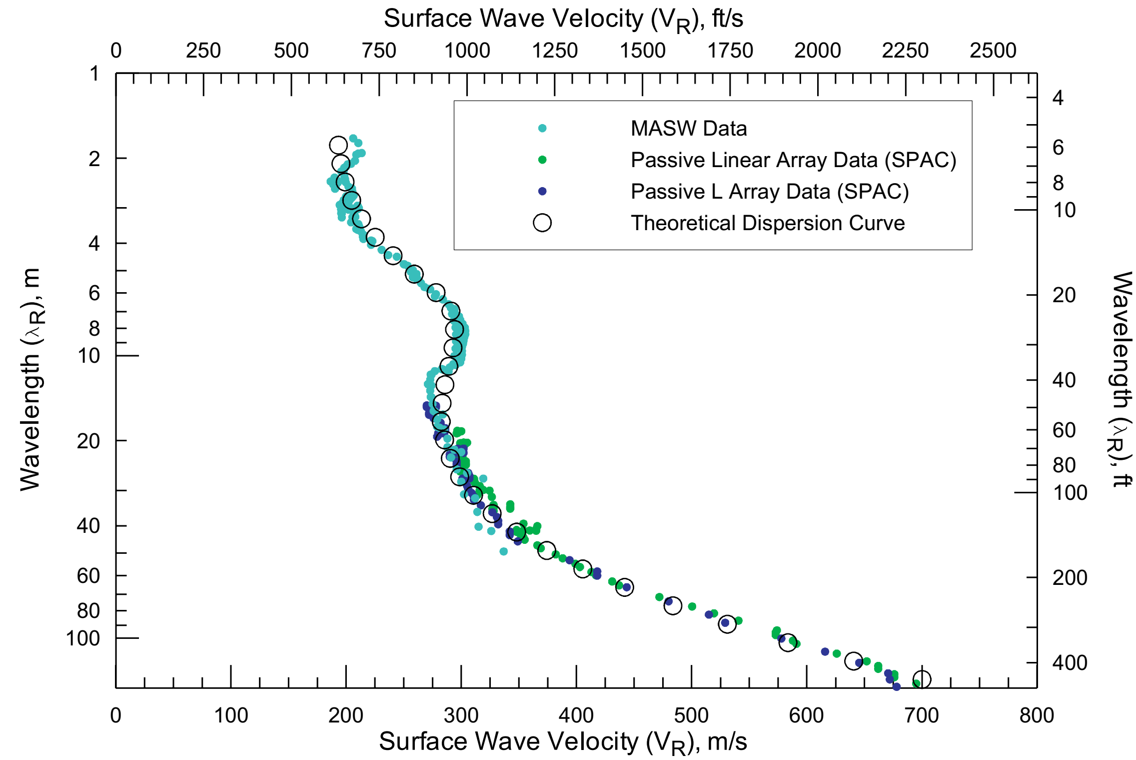

Comparison of Field Experimental Data and Theoretical Dispersion Curve from Active and Passive Surface Wave Array Z1-S11

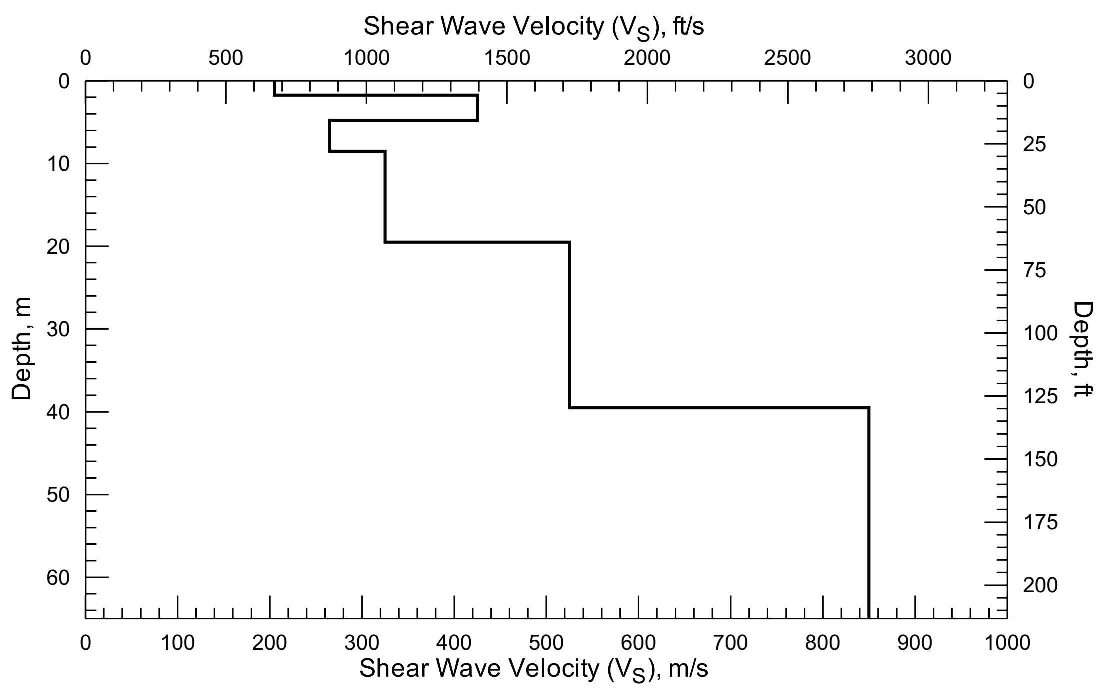

V_S Model from Active and Passive Surface Wave Array Z1-S11

GEOVision geophysical services	FIGURE 14 VELOCITY MODEL FOR ACTIVE AND PASSIVE SURFACE WAVE ARRAY Z1-S11
Project # 9001 Date: JUL 17, 2008 Drawn By: A MARTIN Approved By: [signature]	E. AVENUE 31 AND SICHELL ST, LOS ANGELES, CALIFORNIA
File R:\...Project Files\2009\9001ch2mhill\report\figures\Figure14.cdr	PREPARED FOR CH2M HILL

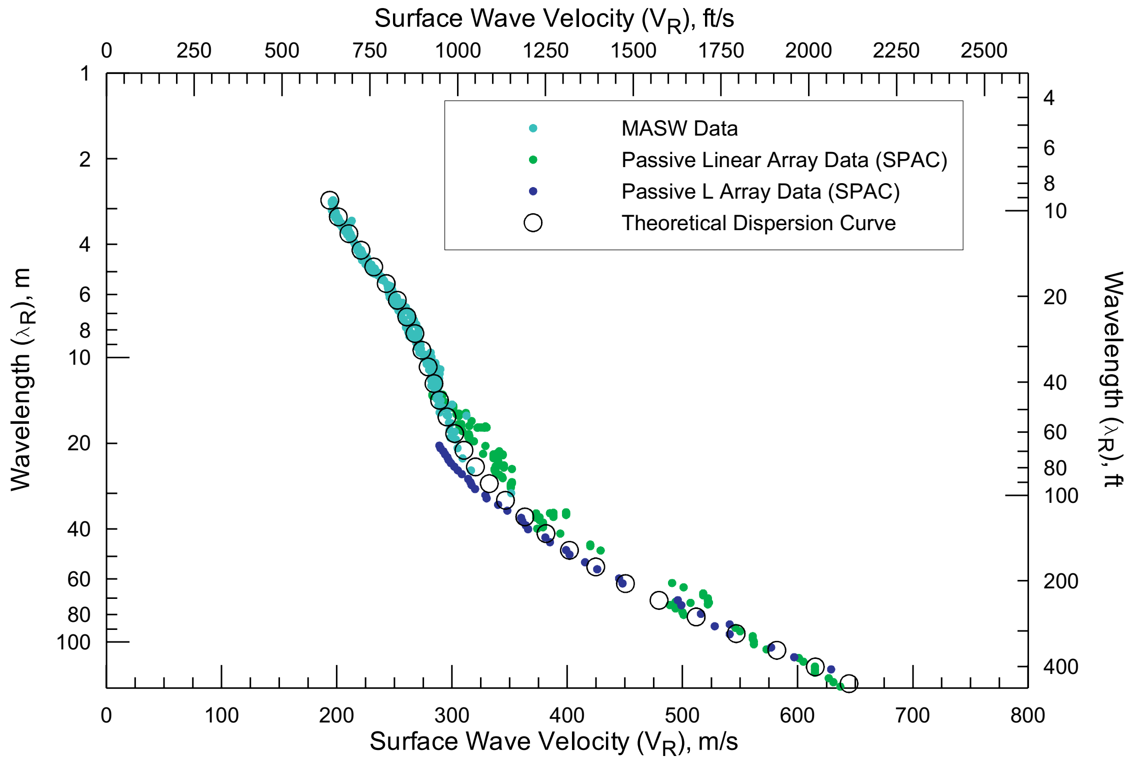

Comparison of Field Experimental Data and Theoretical Dispersion Curve from Active and Passive Surface Wave Array Z1-S12

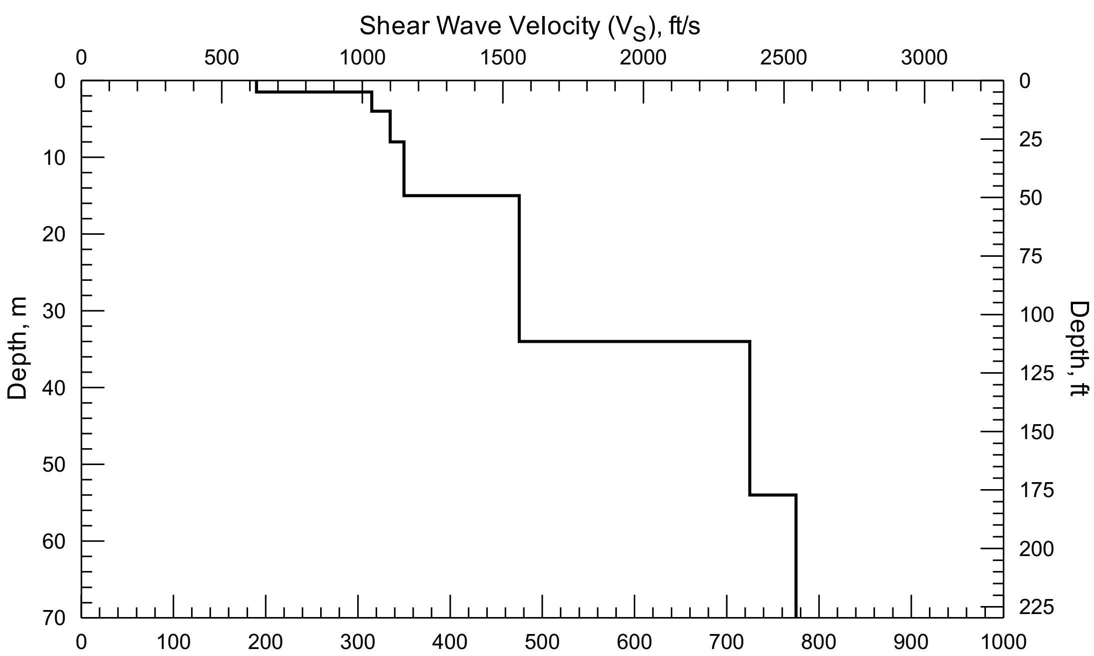

V_S Model from Active and Passive Surface Wave Array Z1-S12

GEOVision geophysical services	FIGURE 15 VELOCITY MODEL FOR ACTIVE AND PASSIVE SURFACE WAVE ARRAY Z1-S12
Project # 9001 Date: JUL 17, 2008 Drawn By: A MARTIN	ARROYO SECO AVE AND AMABEL ST, LOS ANGELES, CALIFORNIA
Approved By: [signature] File R:\...Project Files\2009\9001ch2mhill\report\figures\Figure15.cdr	PREPARED FOR CH2M HILL

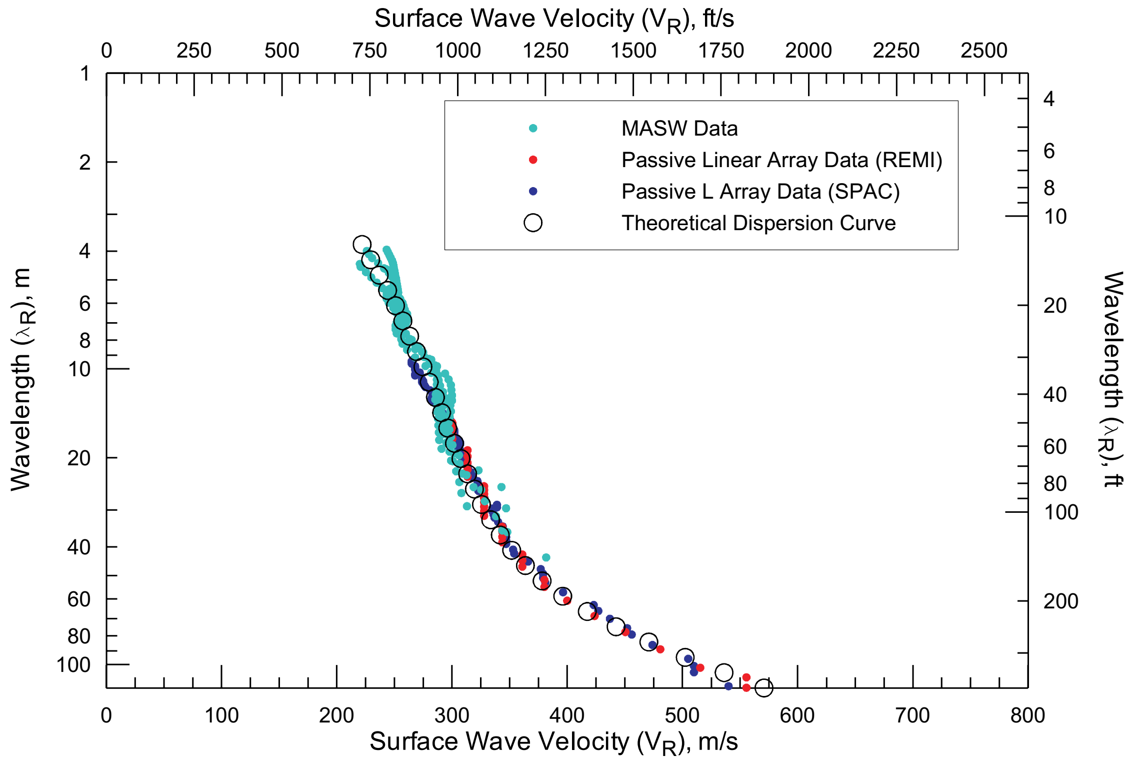

Comparison of Field Experimental Data and Theoretical Dispersion Curve from Active and Passive Surface Wave Array Z1-S13

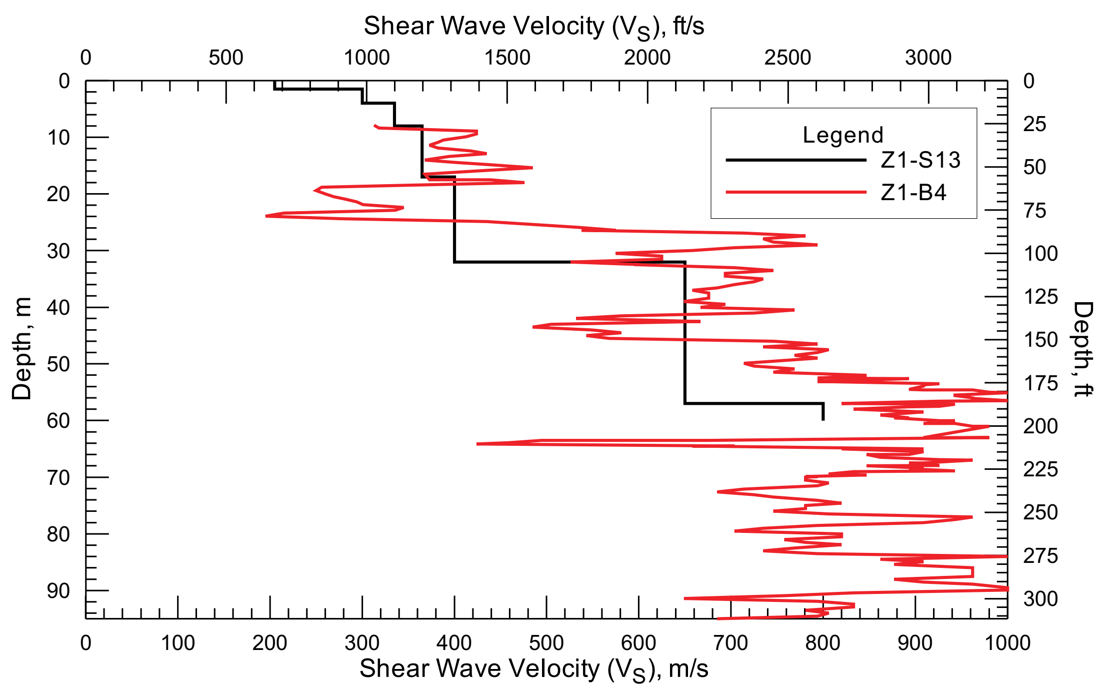

V_S Model from Active and Passive Surface Wave Array Z1-S13

GEOVision geophysical services	FIGURE 16 VELOCITY MODEL FOR ACTIVE AND PASSIVE SURFACE WAVE ARRAY Z1-S13
Project # 9001 Date: JUL 17, 2008	MIDLAND ST AND E. AVENUE 39, LOS ANGELES, CALIFORNIA
Drawn By: A MARTIN Approved By: [signature] File R:\...Project Files\2009\9001ch2mhill\report\figures\Figure16.cdr	PREPARED FOR CH2M HILL

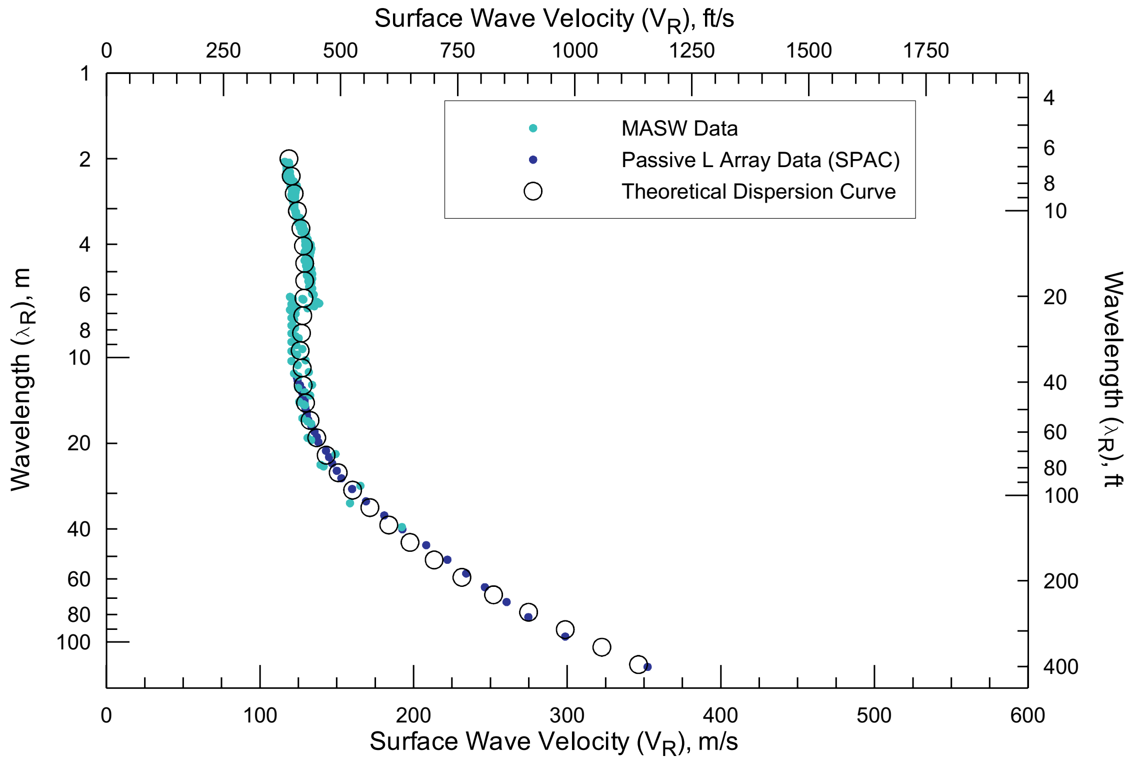

Comparison of Field Experimental Data and Theoretical Dispersion Curve from Active and Passive Surface Wave Array Z1-S14

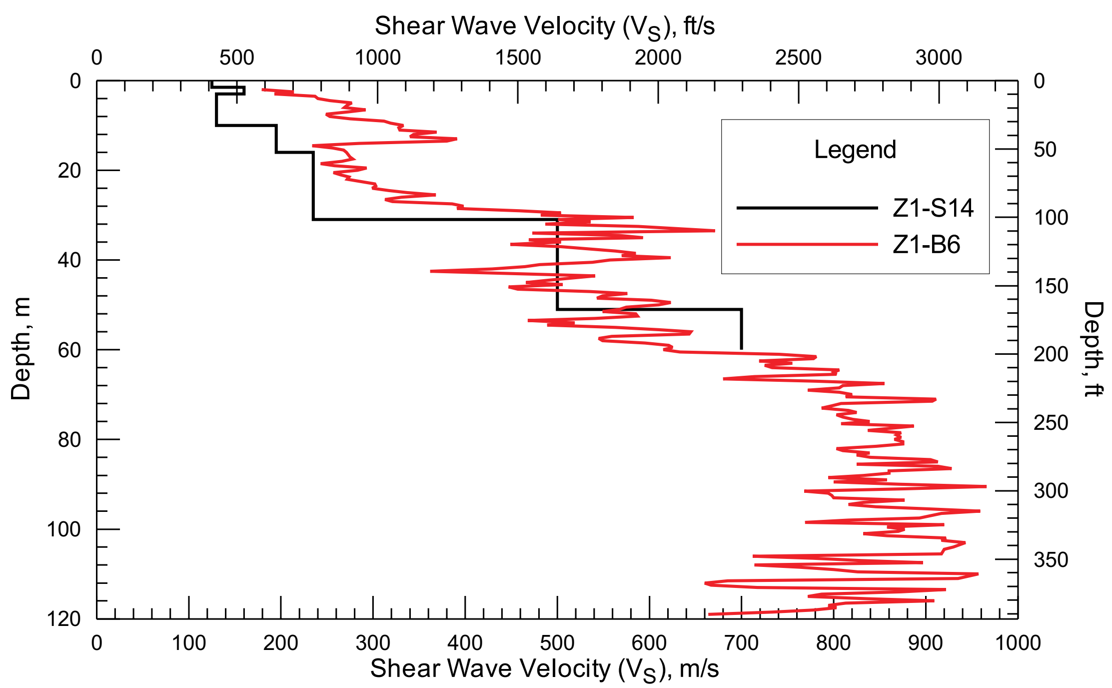

V_S Model from Active and Passive Surface Wave Array Z1-S14

GEOVision geophysical services	FIGURE 17 VELOCITY MODEL FOR ACTIVE AND PASSIVE SURFACE WAVE ARRAY Z1-S14
Project # 9001 Date: JUL 17, 2008 Drawn By: A MARTIN	HUNTINGTON DR SOUTH AND ESMERELDA ST, LOS ANGELES, CALIFORNIA
Approved By: Antony J Martin File R:\...Project Files\2009\9001ch2mhill\report\figures\Figure17.cdr	PREPARED FOR CH2M HILL

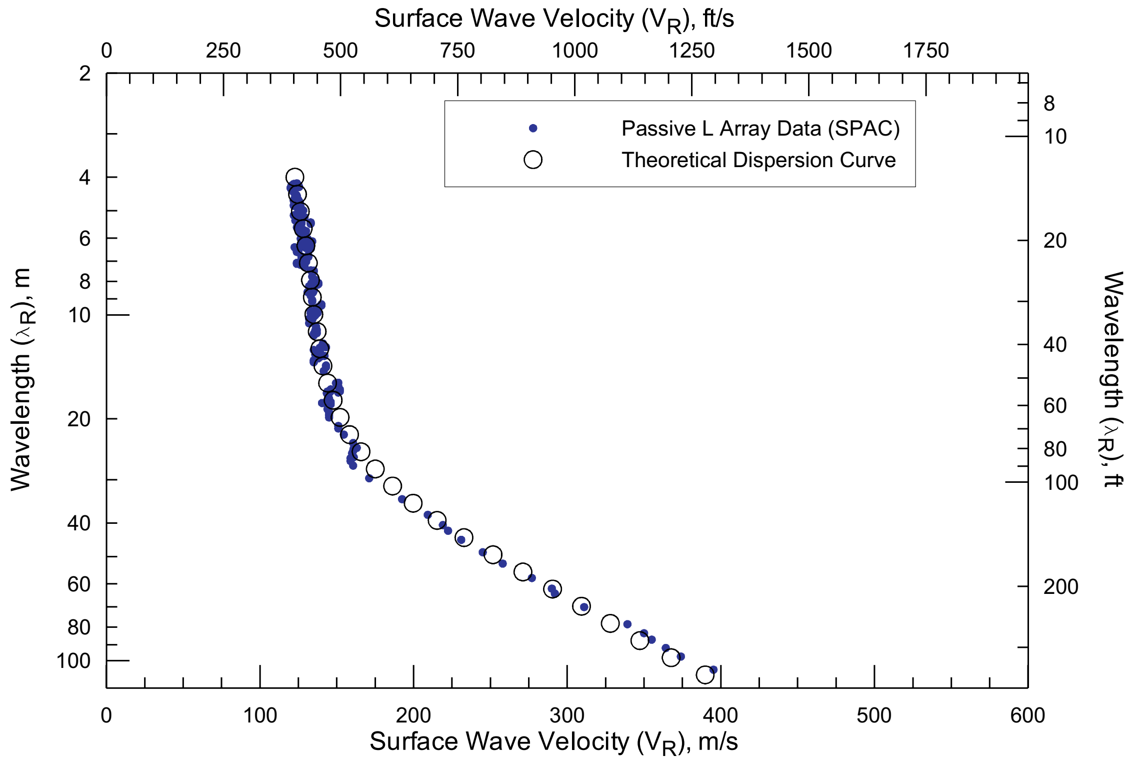

Comparison of Field Experimental Data and Theoretical Dispersion Curve from Active and Passive Surface Wave Array Z1-S15

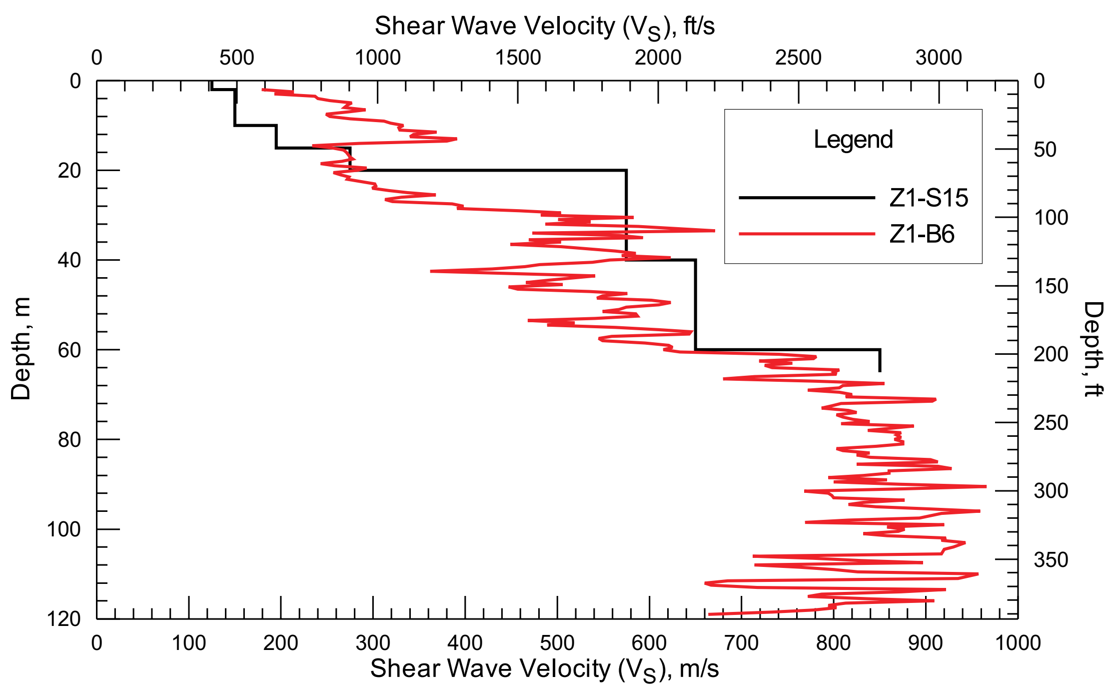

V_S Model from Active and Passive Surface Wave Array Z1-S15

GEOVision geophysical services	FIGURE 18 VELOCITY MODEL FOR ACTIVE AND PASSIVE SURFACE WAVE ARRAY Z1-S15
Project # 9001 Date: JUL 17, 2008 Drawn By: A MARTIN	HUNTINGTON DR SOUTH AND TOPAZ ST, LOS ANGELES, CALIFORNIA
Approved By: [signature] File R:\...Project Files\2009\9001ch2mhill\report\figures\Figure18.cdr	PREPARED FOR CH2M HILL

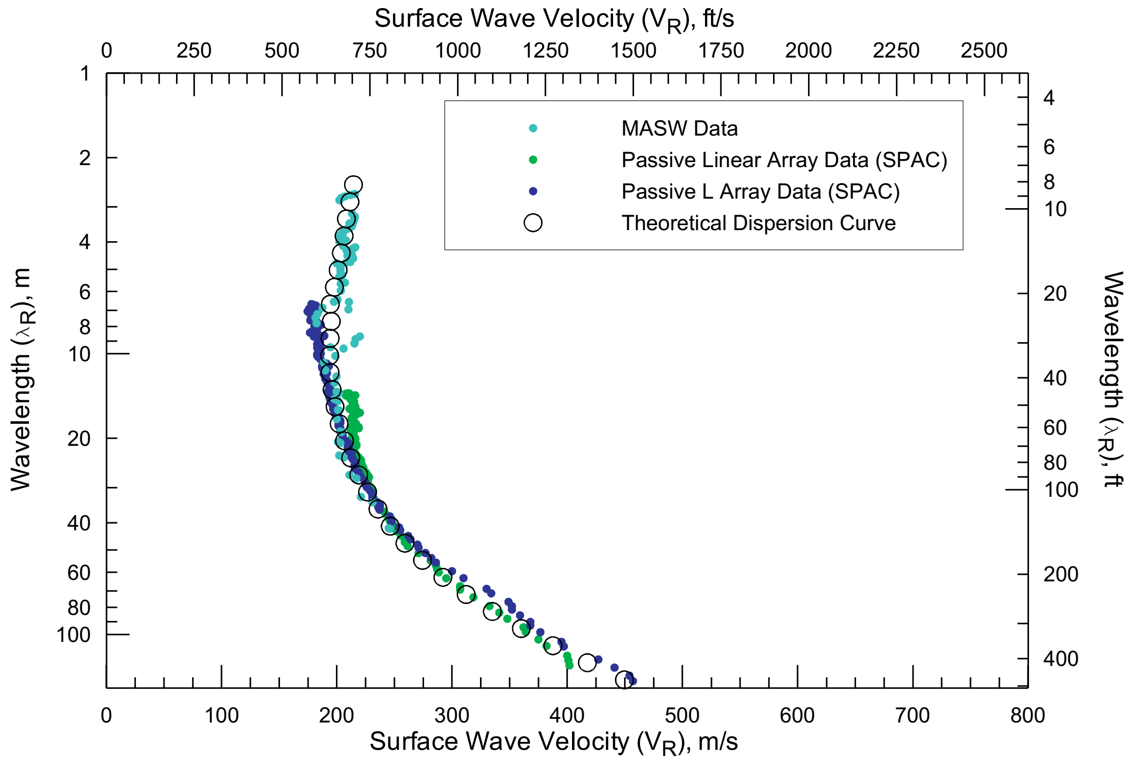

Comparison of Field Experimental Data and Theoretical Dispersion Curve from Active and Passive Surface Wave Array Z1-S16

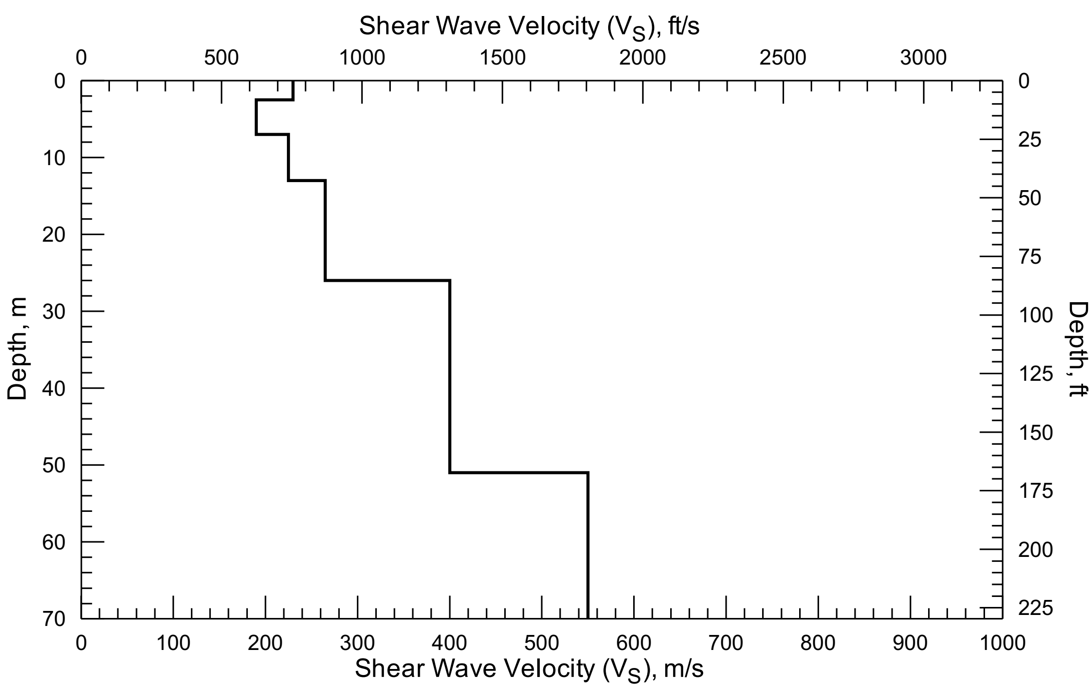

V_S Model from Active and Passive Surface Wave Array Z1-S16

GEOVision geophysical services	FIGURE 19 VELOCITY MODEL FOR ACTIVE AND PASSIVE SURFACE WAVE ARRAY Z1-S16
Project # 9001 Date: JUL 17, 2008 Drawn By: A MARTIN Approved By: Antony J Martin	EASTERN AVE AND TWINING ST, LOS ANGELES, CALIFORNIA
File R:\...Project Files\2009\9001ch2mhill\report\figures\Figure19.cdr	PREPARED FOR CH2M HILL

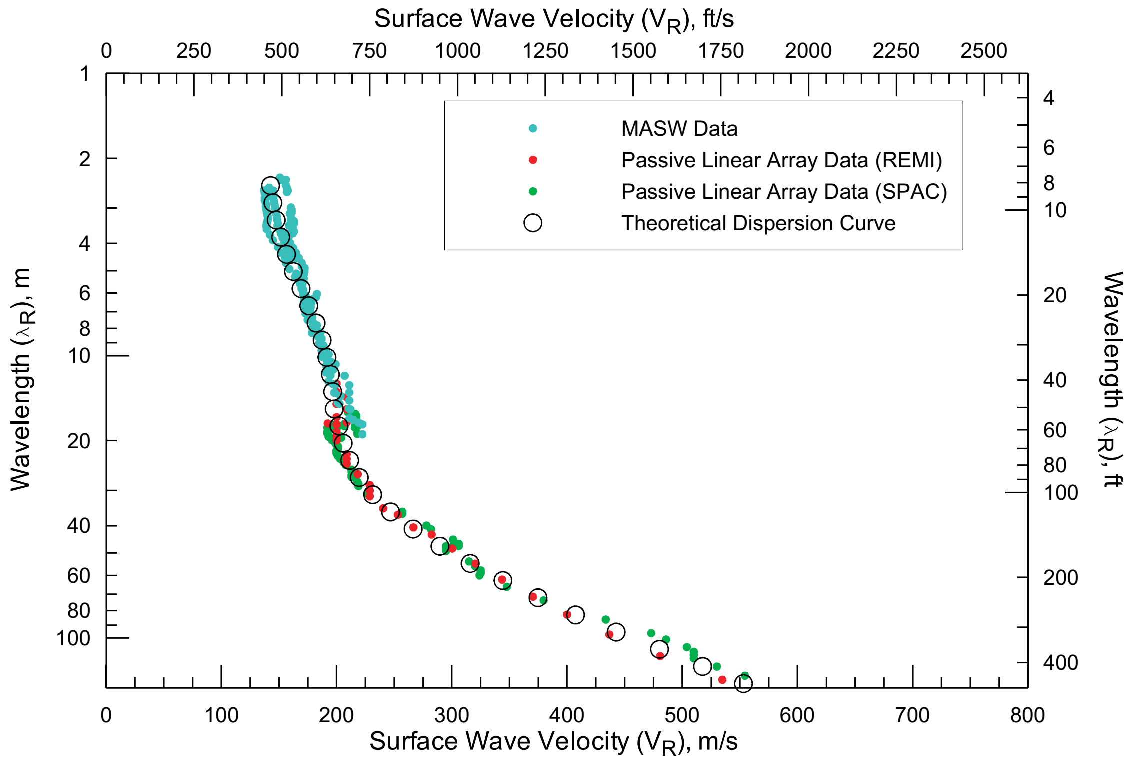

Comparison of Field Experimental Data and Theoretical Dispersion Curve from Active and Passive Surface Wave Array Z1-S18

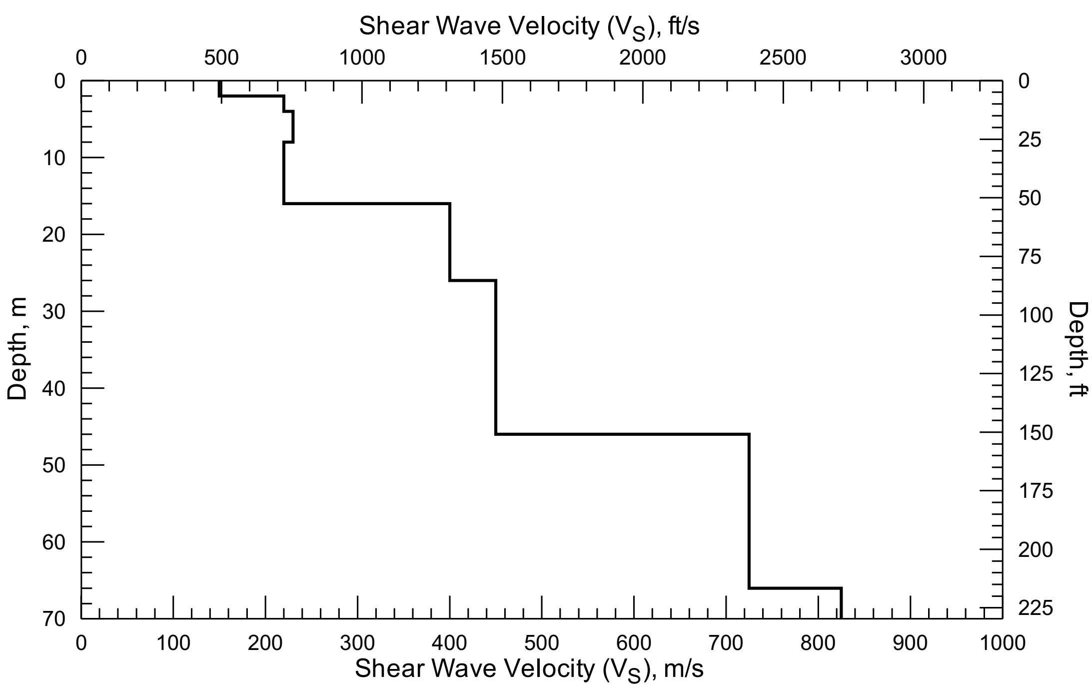

V_S Model from Active and Passive Surface Wave Array Z1-S18

GEOVision geophysical services	FIGURE 20 VELOCITY MODEL FOR ACTIVE AND PASSIVE SURFACE WAVE ARRAY Z1-S18
Project # 9001 Date: JUL 17, 2008	SIERRA ST AND ROLLE ST, LOS ANGELES, CALIFORNIA
Drawn By: A MARTIN Approved By: Antony J Martin	PREPARED FOR CH2M HILL
File R:\...Project Files\2009\9001ch2mhill\report\figures\Figure20.cdr	

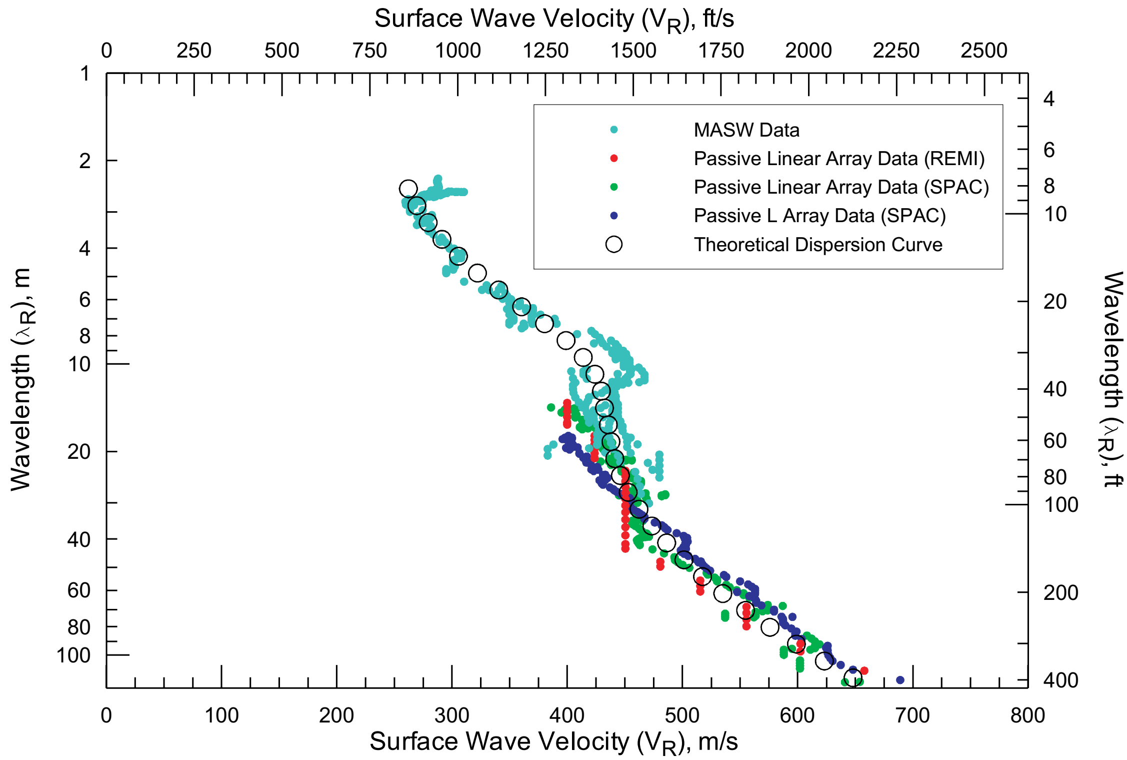

Comparison of Field Experimental Data and Theoretical Dispersion Curve from Active and Passive Surface Wave Array Z1-S19

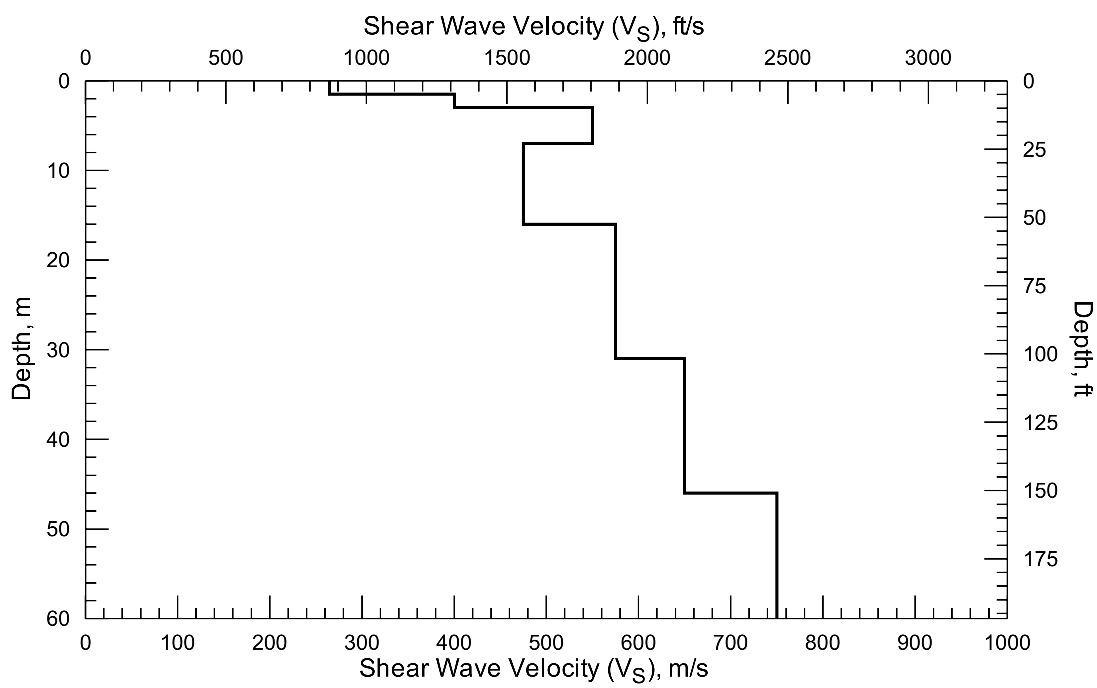

V_S Model from Active and Passive Surface Wave Array Z1-S19

GEOVision geophysical services	FIGURE 21 VELOCITY MODEL FOR ACTIVE AND PASSIVE SURFACE WAVE ARRAY Z1-S19
Project # 9001 Date: JUL 17, 2008 Drawn By: A MARTIN	PHELPS AVE AND BUDAU PL, LOS ANGELES, CALIFORNIA
Approved By: [signature] File R:\...Project Files\2009\9001ch2mhill\report\figures\Figure21.cdr	PREPARED FOR CH2M HILL

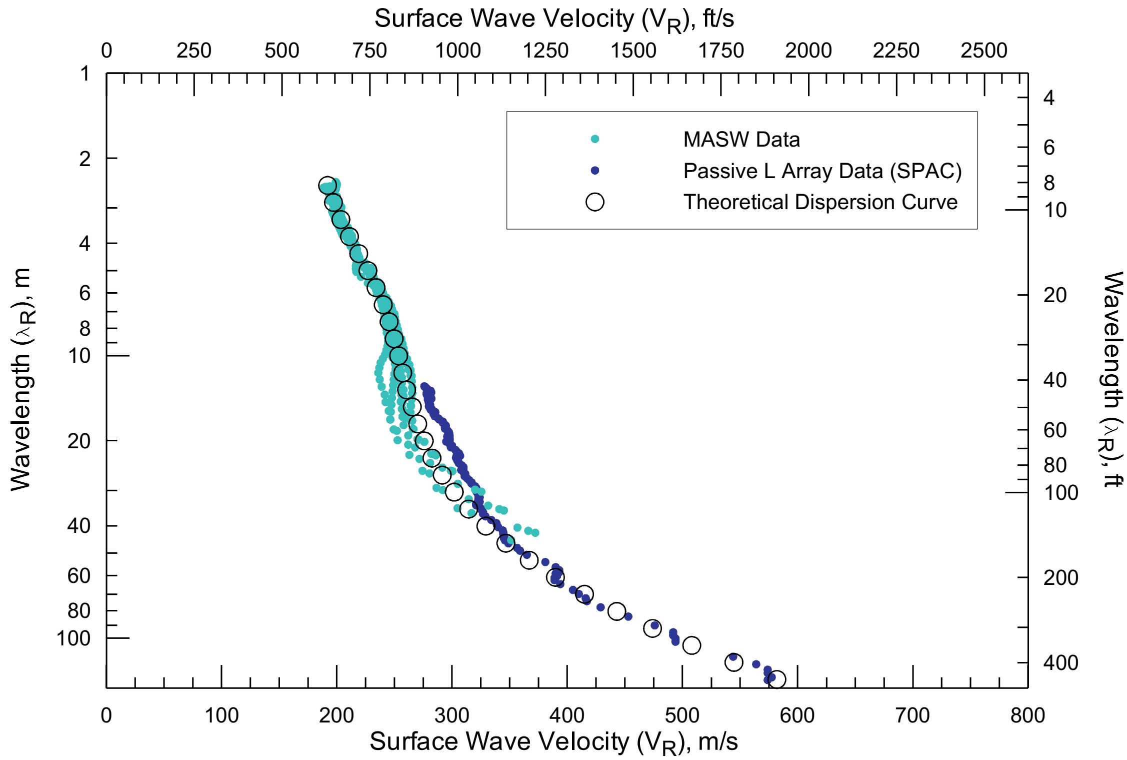

Comparison of Field Experimental Data and Theoretical Dispersion Curve from Active and Passive Surface Wave Array Z1-S20

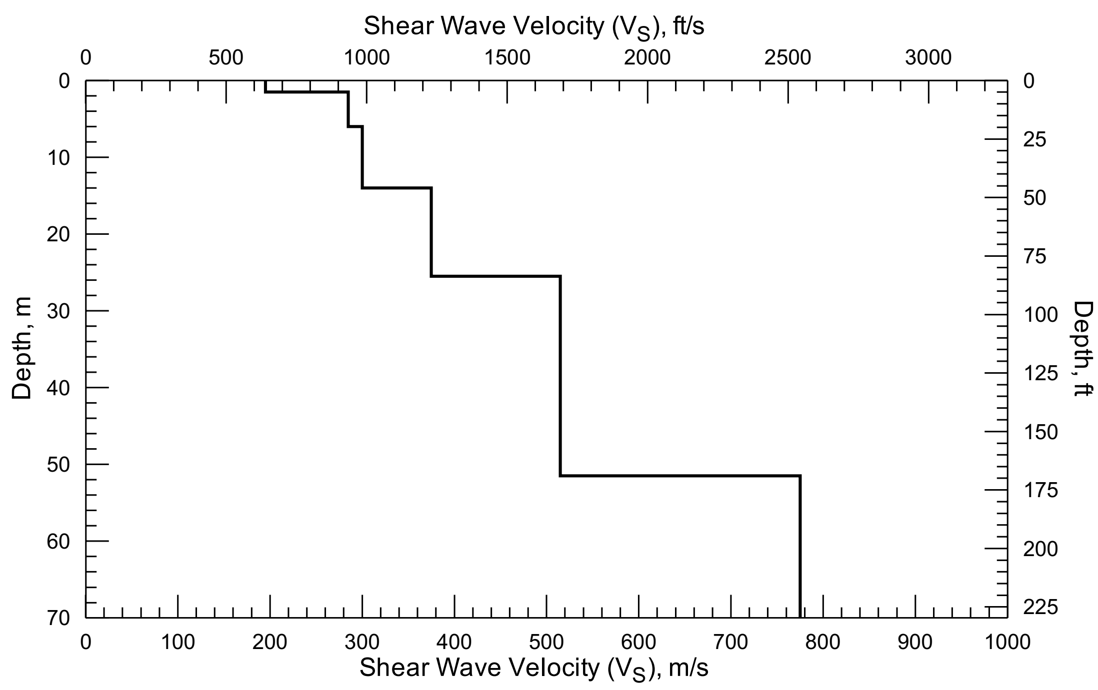

V_S Model from Active and Passive Surface Wave Array Z1-S20

GEOVision geophysical services	FIGURE 22 VELOCITY MODEL FOR ACTIVE AND PASSIVE SURFACE WAVE ARRAY Z1-S20
Project # 9001 Date: JUL 17, 2008 Drawn By: A MARTIN Approved By: [signature]	NEAR WEST VALLEY BLVD AND HIGHBURY AVE, LOS ANGELES, CALIFORNIA
File R:\...Project Files\2009\9001ch2mhill\report\figures\Figure22.cdr	PREPARED FOR CH2M HILL

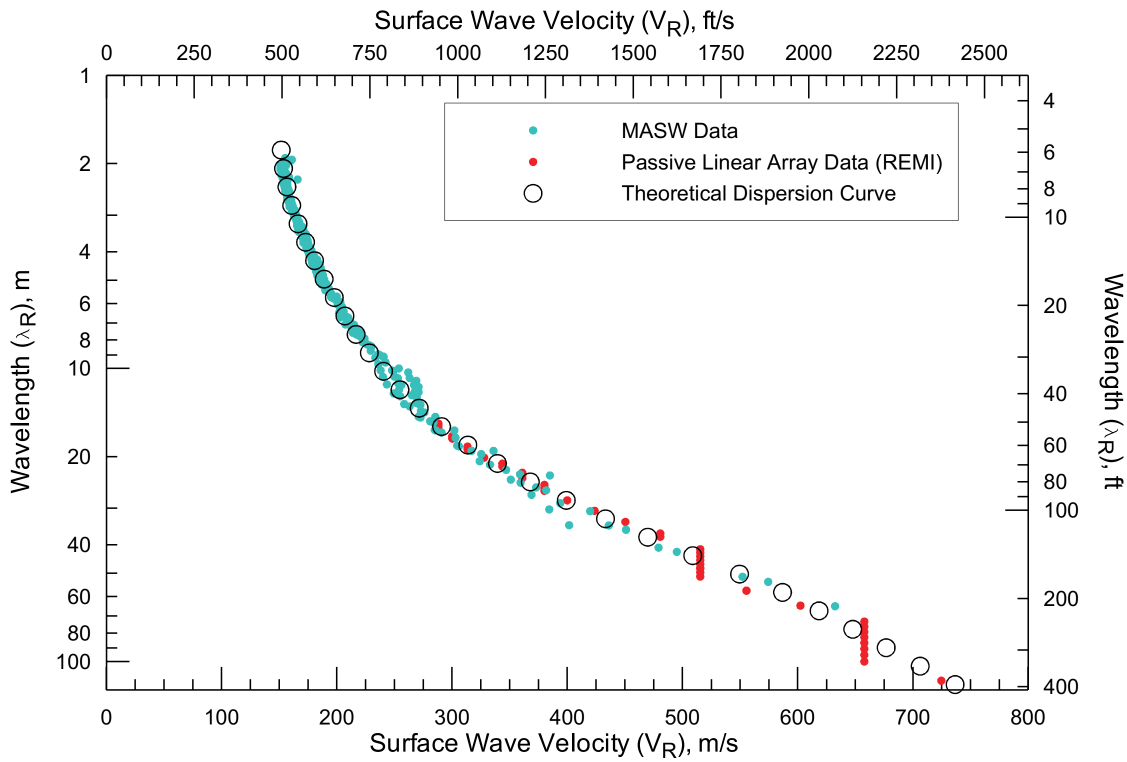

Comparison of Field Experimental Data and Theoretical Dispersion Curve from Active and Passive Surface Wave Array Z2-S1

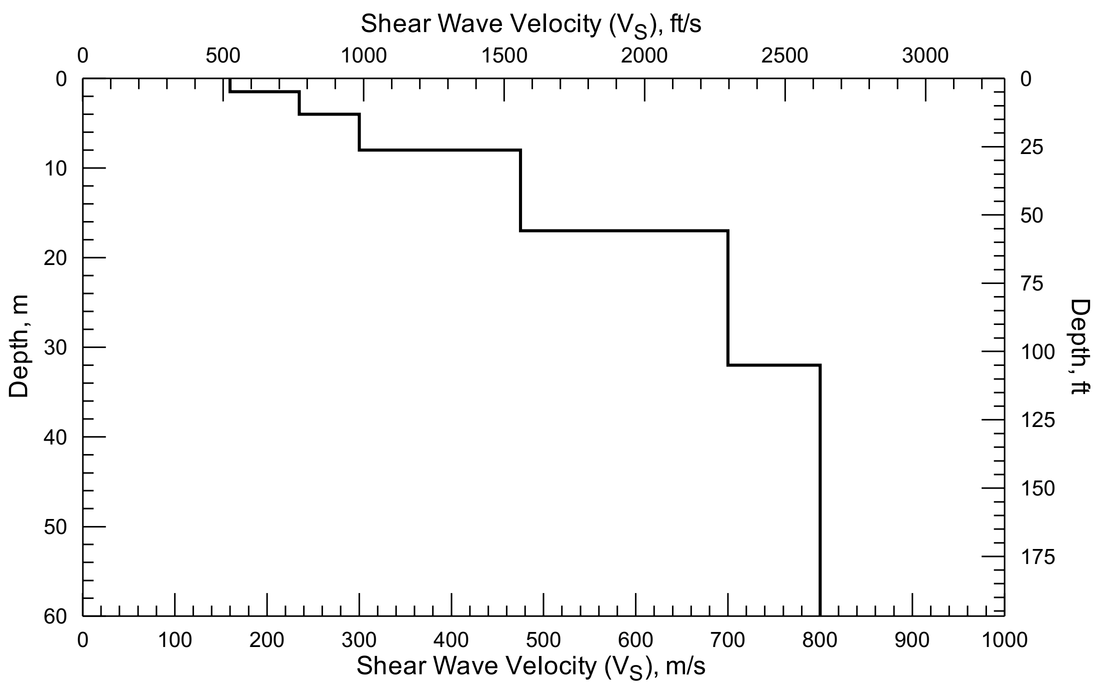

V_S Model from Active and Passive Surface Wave Array Z2-S1

GEOVision geophysical services

Project # 9001
Date: JUL 23, 2009
Drawn By: A MARTIN
Approved By:

File R:\...Project Files\2009\9001ch2mhill\report\figures\Figure23.cdr

FIGURE 23
VELOCITY MODEL FOR ACTIVE AND PASSIVE SURFACE WAVE ARRAY Z2-S1

NEAR VERDUGO RD AND YORK BLVD, LOS ANGELES, CALIFORNIA

PREPARED FOR
CH2M HILL

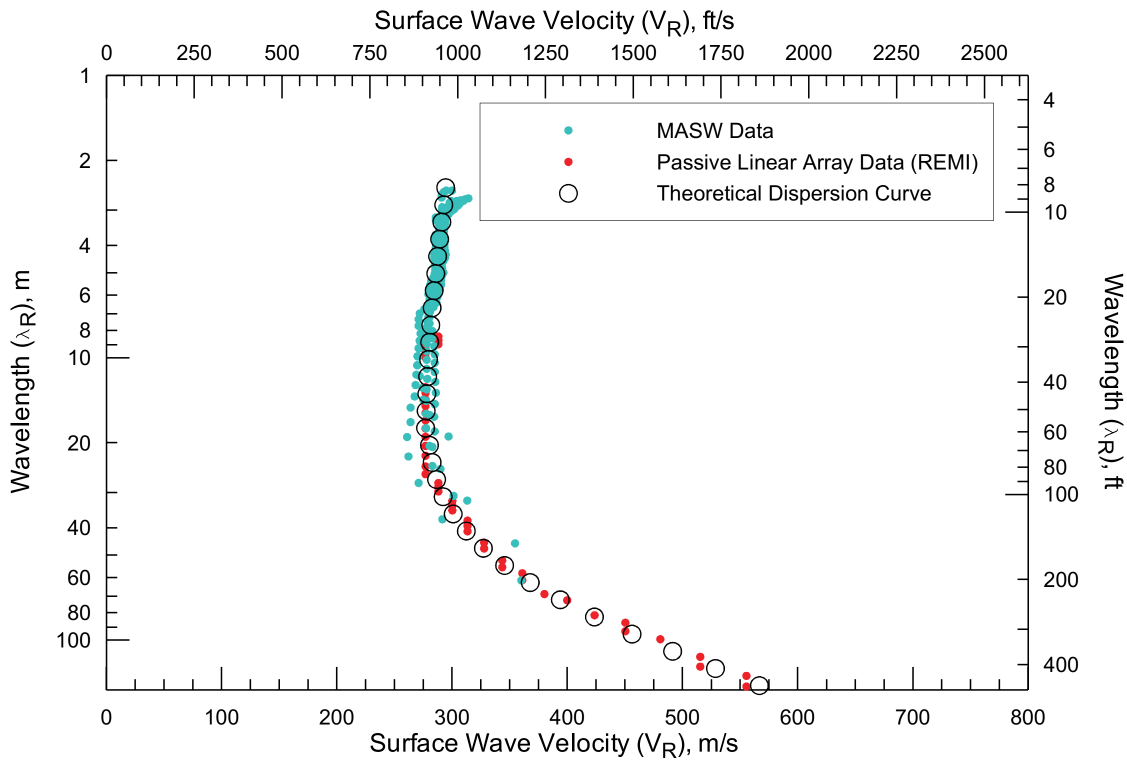

Comparison of Field Experimental Data and Theoretical Dispersion Curve from Active and Passive Surface Wave Array Z2-S2

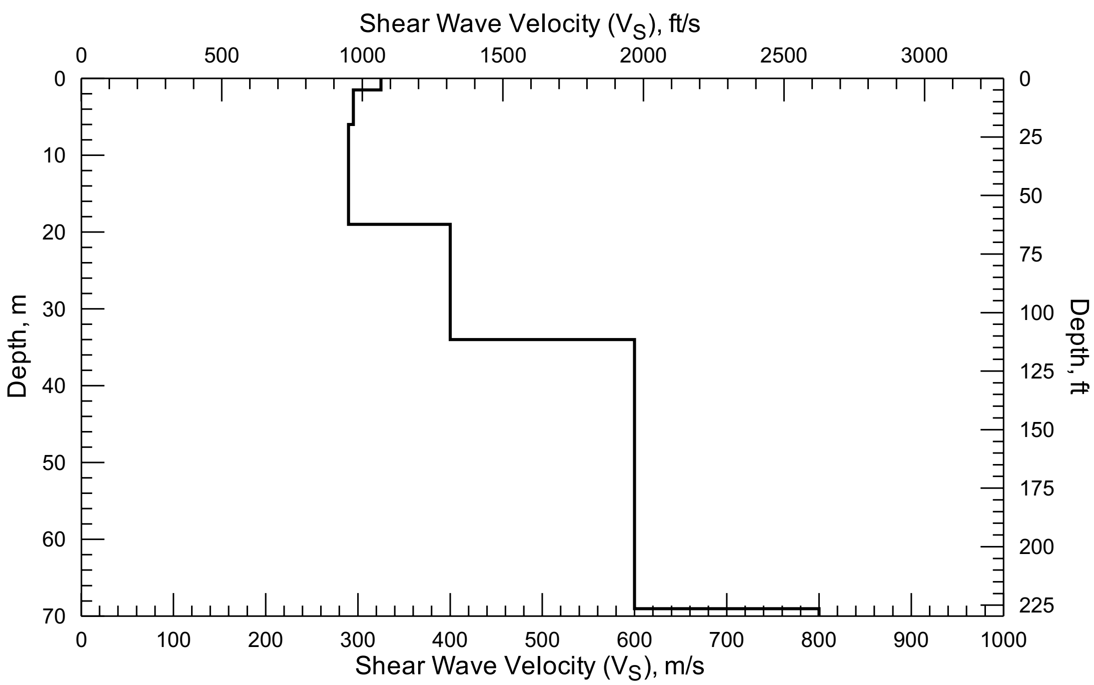

V_S Model from Active and Passive Surface Wave Array Z2-S2

GEOVision geophysical services	FIGURE 24 VELOCITY MODEL FOR ACTIVE AND PASSIVE SURFACE WAVE ARRAY Z2-S2
Project # 9001 Date: JUL 23, 2009 Drawn By: A MARTIN Approved By: [signature]	ALUMNI AVENUE AND AVENUE 46, LOS ANGELES, CALIFORNIA
File R:\...Project Files\2009\9001ch2mhill\report\figures\Figure24.cdr	PREPARED FOR CH2M HILL

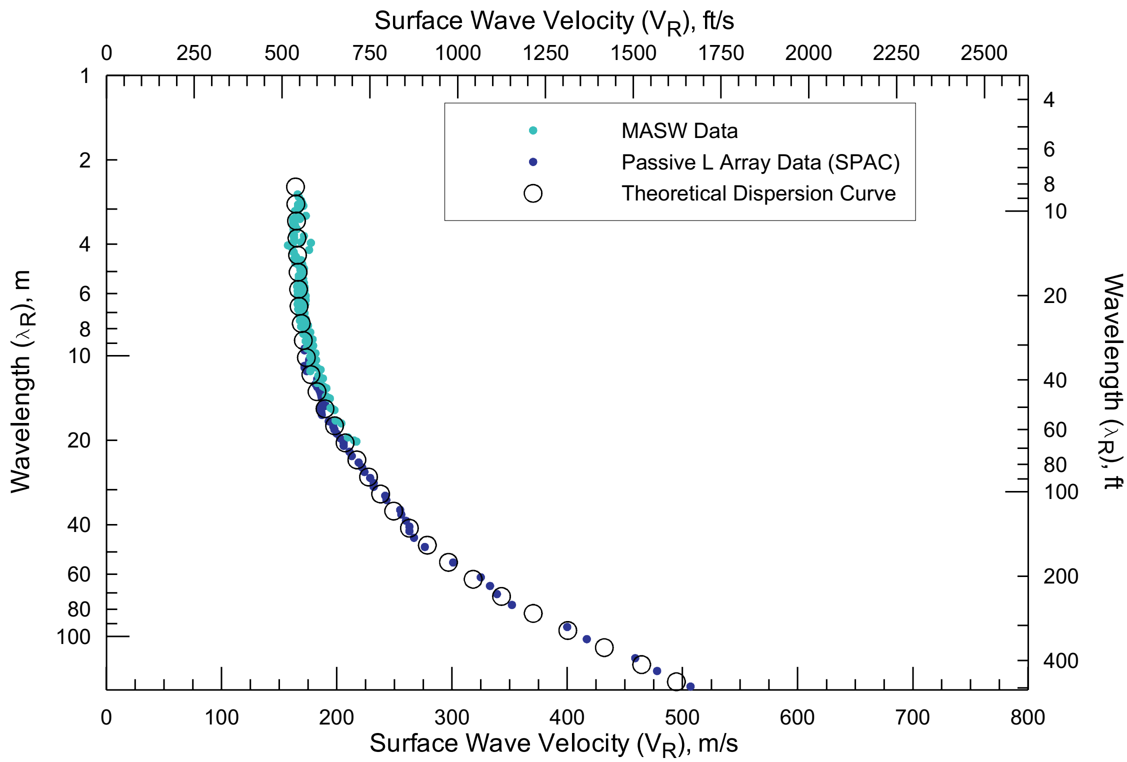

Comparison of Field Experimental Data and Theoretical Dispersion Curve from Active and Passive Surface Wave Array Z2-S3

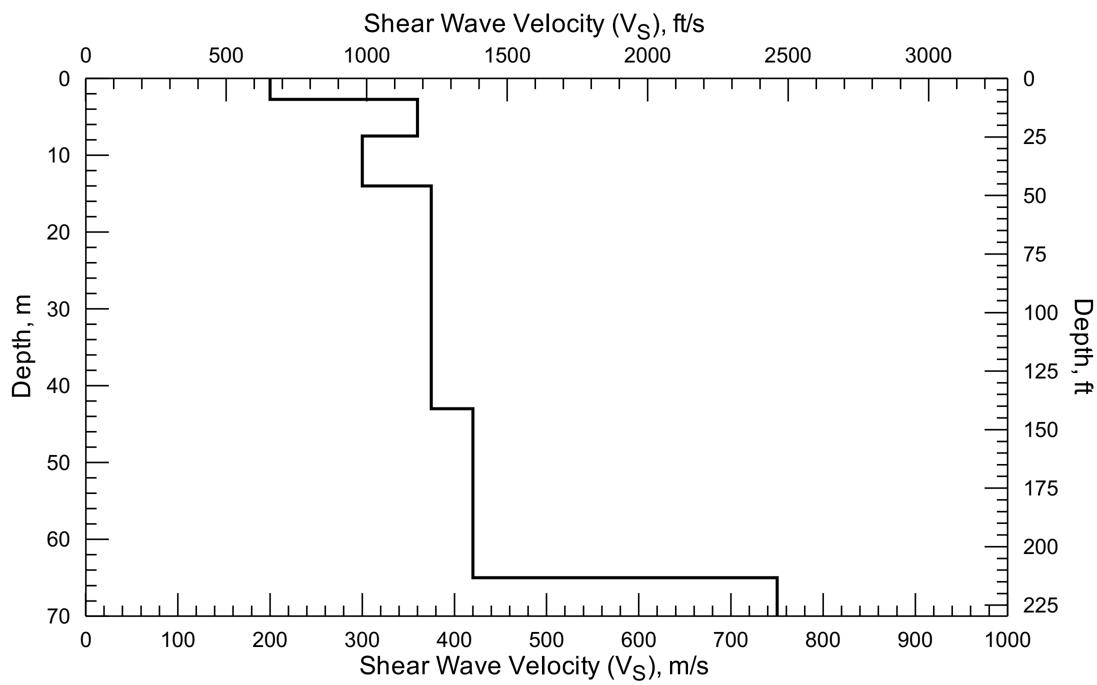

V_S Model from Active and Passive Surface Wave Array Z2-S3

GEOVision geophysical services	FIGURE 25 VELOCITY MODEL FOR ACTIVE AND PASSIVE SURFACE WAVE ARRAY Z2-S3
Project # 9001 Date: JUL 23, 2009	LINCOLN AVE AND AVENUE 46, LOS ANGELES, CALIFORNIA
Drawn By: A MARTIN Approved By: Antony J Martin	PREPARED FOR CH2M HILL
File R:\...Project Files\2009\9001ch2mhill\report\figures\Figure25.cdr	

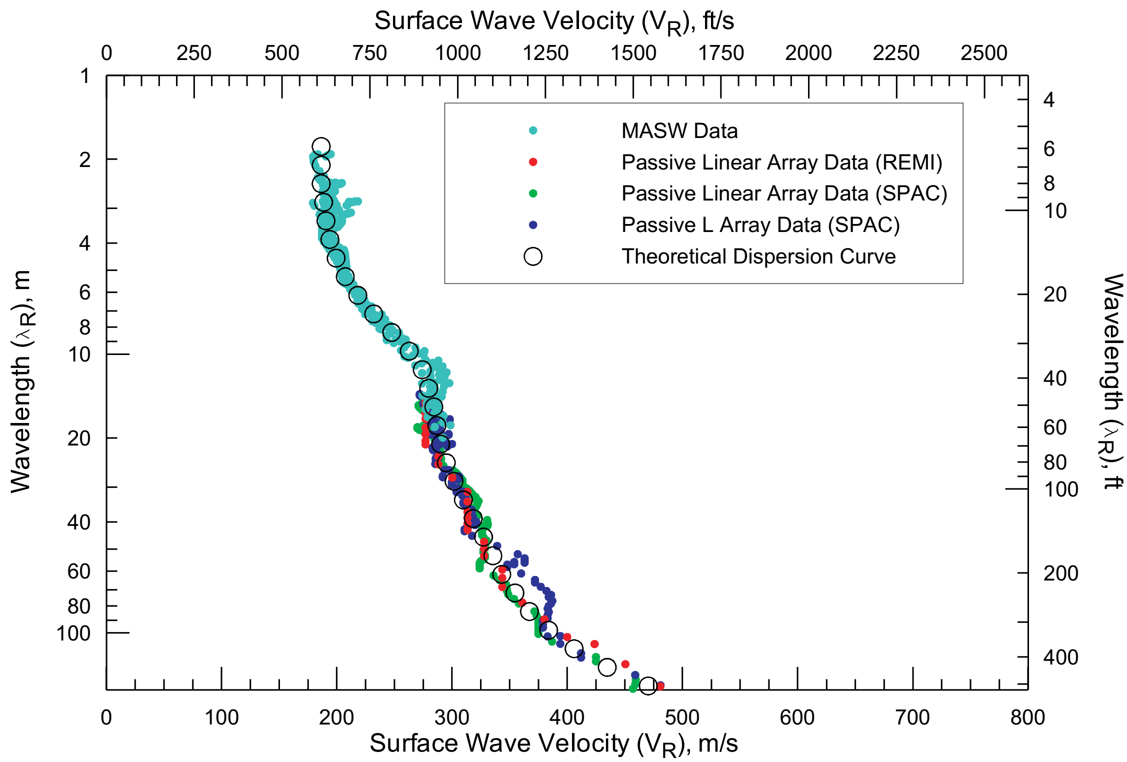

Comparison of Field Experimental Data and Theoretical Dispersion Curve from Active and Passive Surface Wave Array Z2-S4

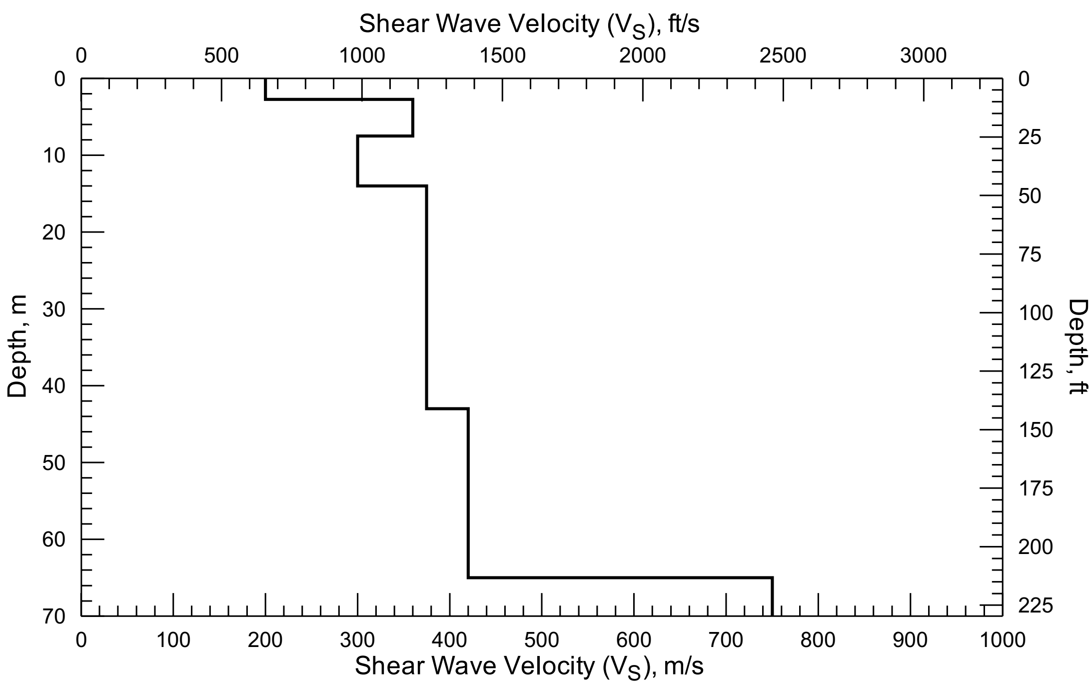

V_S Model from Active and Passive Surface Wave Array Z2-S4

GEOVision geophysical services	FIGURE 26 VELOCITY MODEL FOR ACTIVE AND PASSIVE SURFACE WAVE ARRAY Z2-S4
Project # 9001 Date: JUL 23, 2009 Drawn By: A MARTIN Approved By: [signature]	CLELAND AVE AND TERRACE 49, LOS ANGELES, CALIFORNIA
File R:\...Project Files\2009\9001ch2mhill\report\figures\Figure26.cdr	PREPARED FOR CH2M HILL

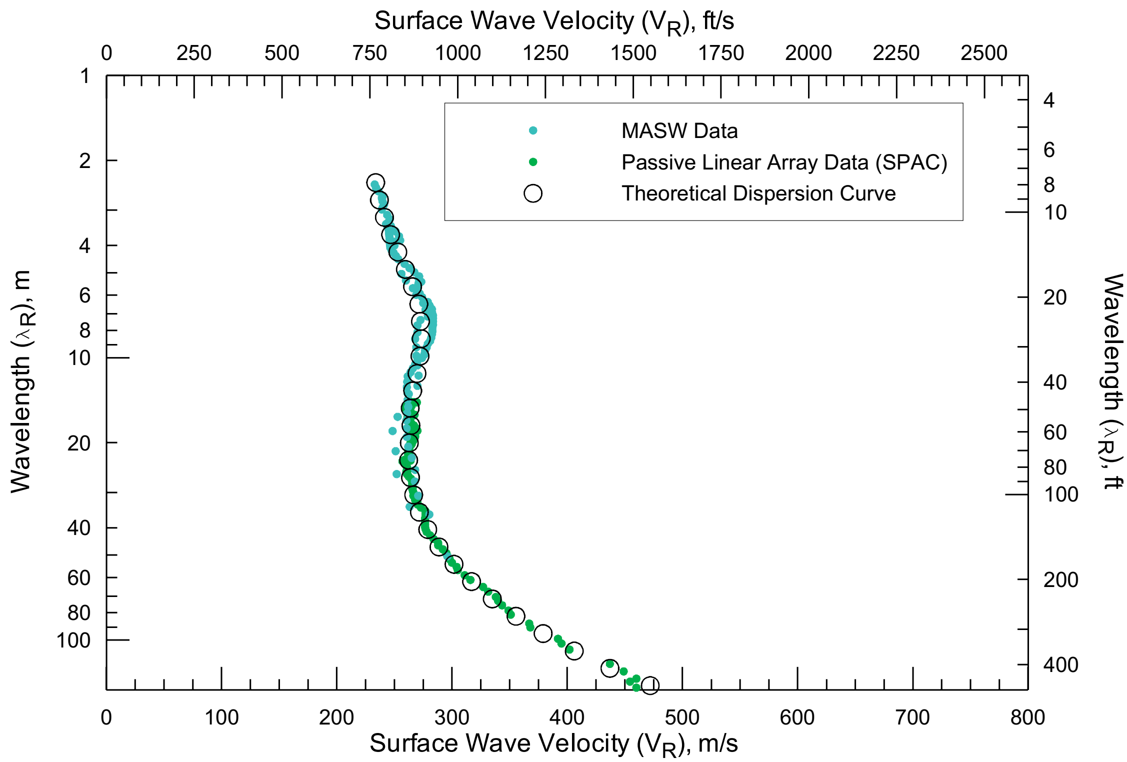

Comparison of Field Experimental Data and Theoretical Dispersion Curve from Active and Passive Surface Wave Array Z2-S5

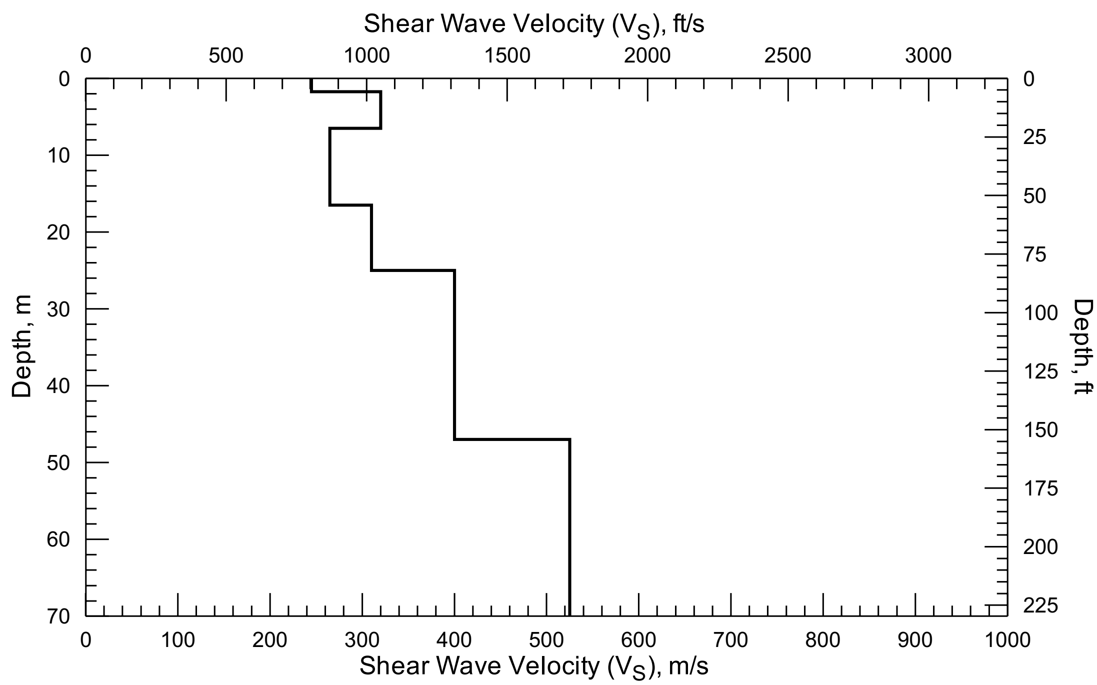

V_S Model from Active and Passive Surface Wave Array Z2-S5

GEOVision geophysical services	FIGURE 27 VELOCITY MODEL FOR ACTIVE AND PASSIVE SURFACE WAVE ARRAY Z2-S5
Project # 9001 Date: JUL 23, 2009 Drawn By: A MARTIN	ALDAMA ST AND NORTH AVENUE 56, LOS ANGELES, CALIFORNIA
Approved By: Antony J Martin File R:\...Project Files\2009\9001ch2mhill\report\figures\Figure27.cdr	PREPARED FOR CH2M HILL

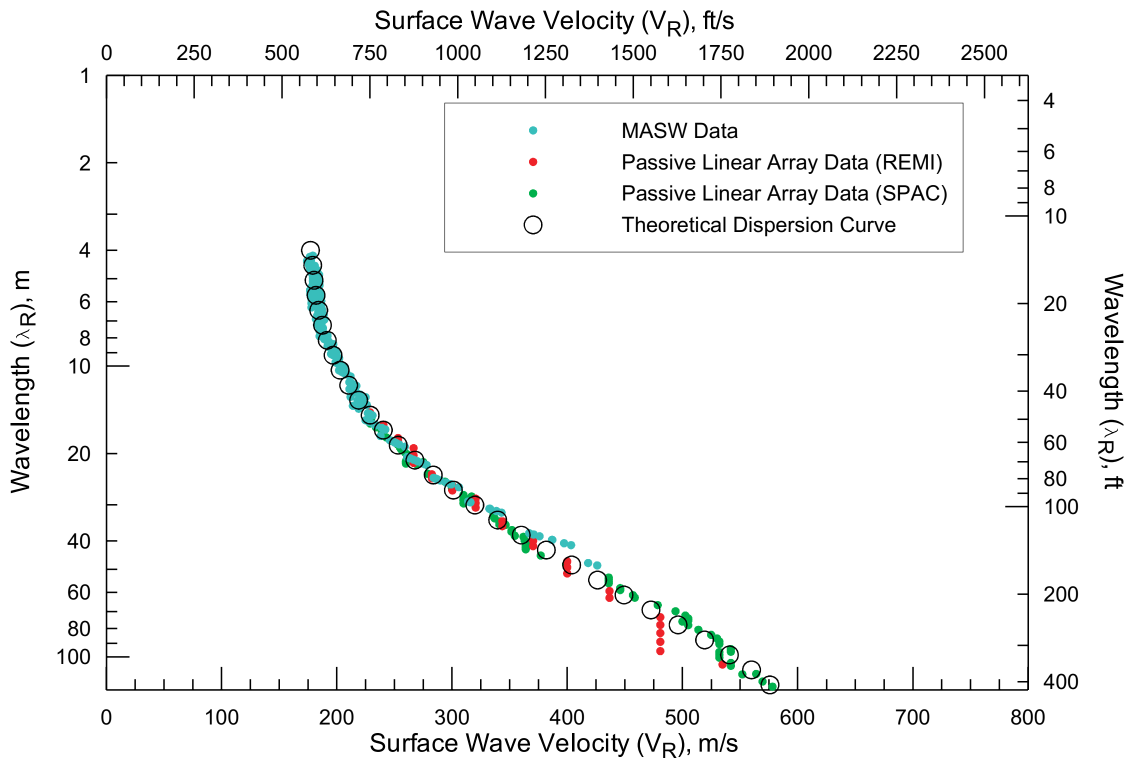

Comparison of Field Experimental Data and Theoretical Dispersion Curve from Active and Passive Surface Wave Array Z2-S6

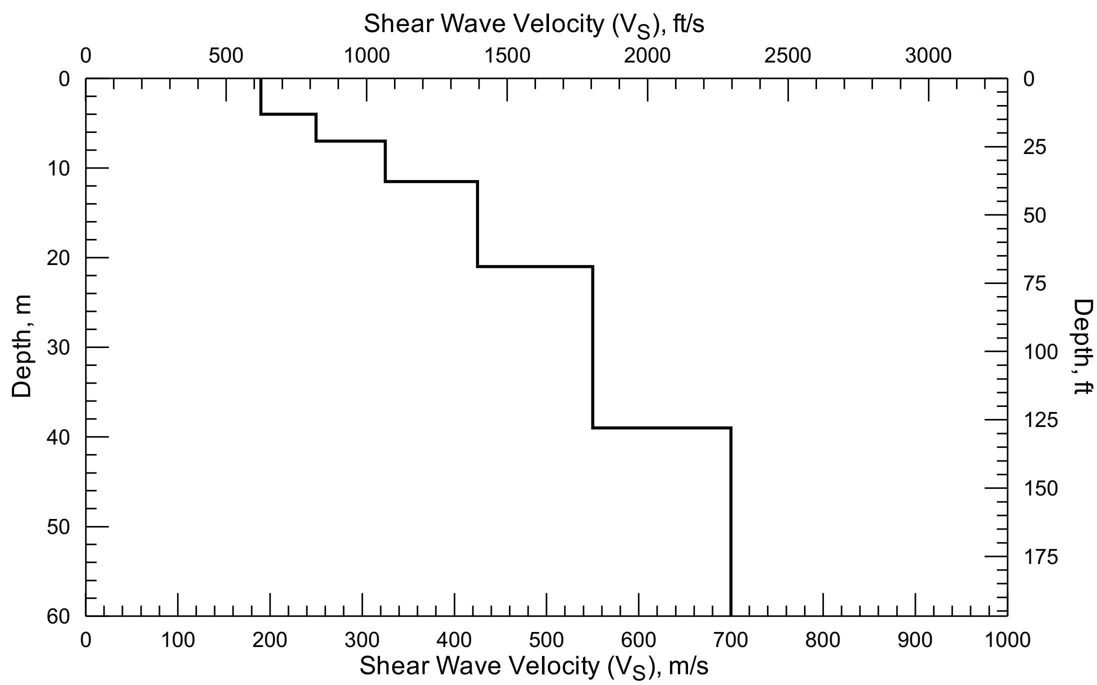

V_S Model from Active and Passive Surface Wave Array Z2-S6

GEOVision geophysical services

Project # 9001	FIGURE 28 VELOCITY MODEL FOR ACTIVE AND PASSIVE SURFACE WAVE ARRAY Z2-S6
Date: JUL 23, 2009	NEAR GRANADA ST AND HOLLAND AVE, LOS ANGELES, CALIFORNIA
Drawn By: A MARTIN	
Approved By: [signature]	PREPARED FOR CH2M HILL
File R:\...Project Files\2009\9001ch2mhill\report\figures\Figure28.cdr	

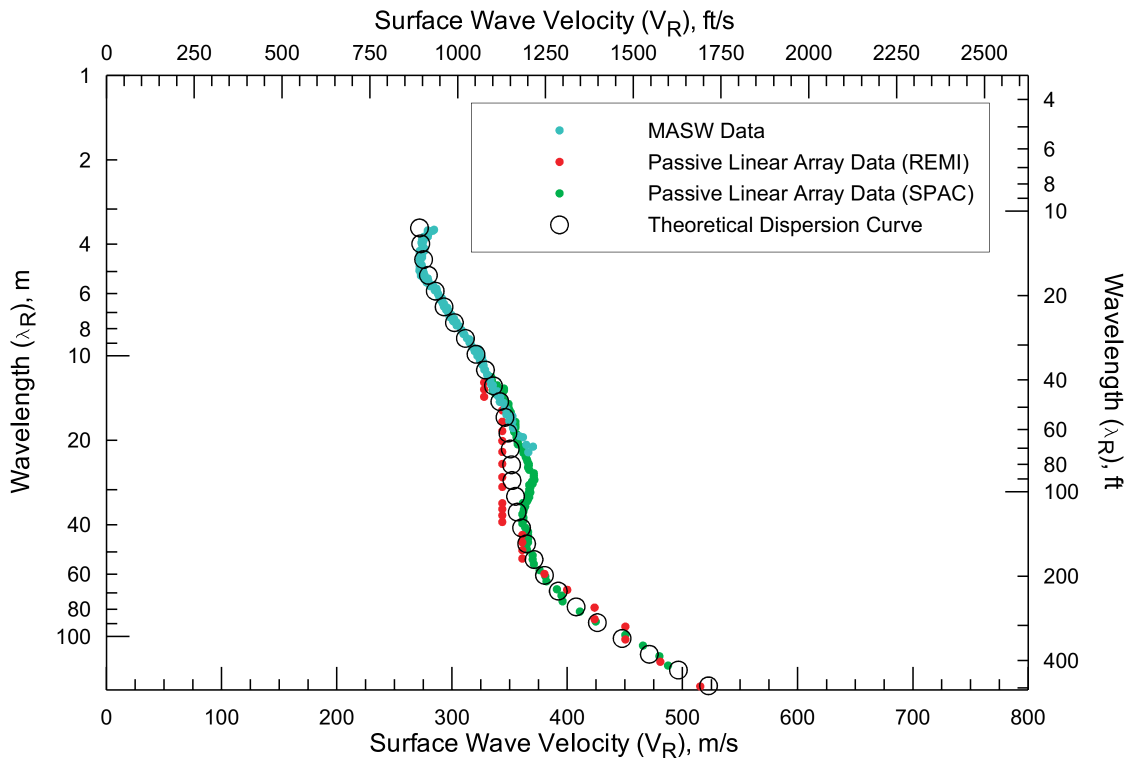

Comparison of Field Experimental Data and Theoretical Dispersion Curve from Active and Passive Surface Wave Array Z2-S7

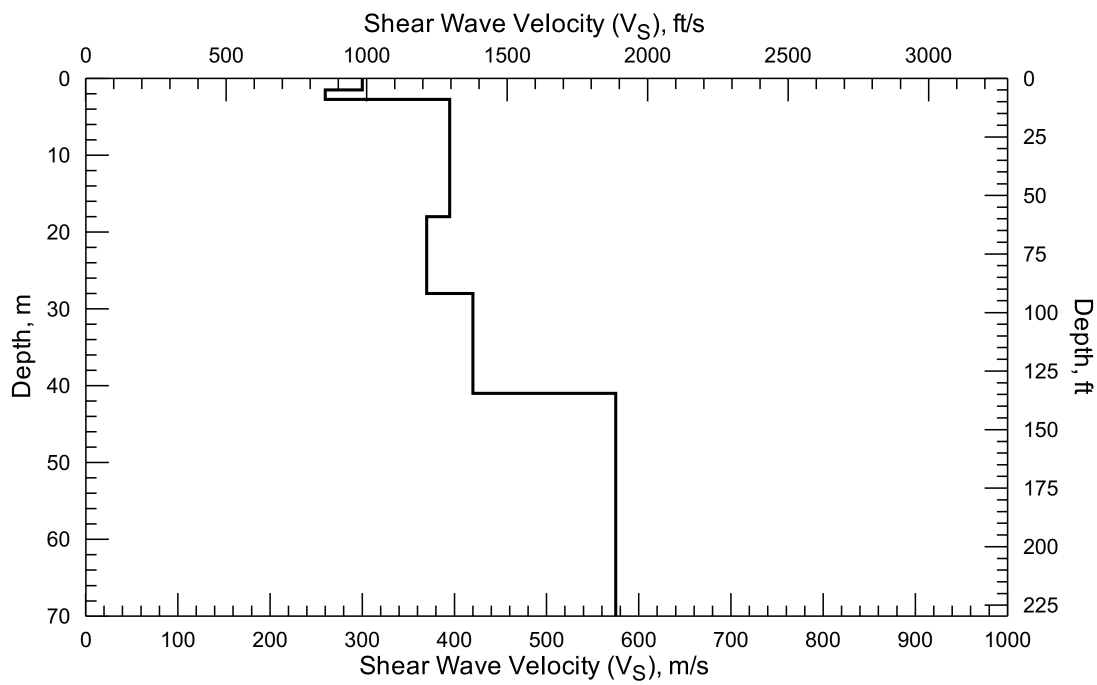

V_S Model from Active and Passive Surface Wave Array Z2-S7

GEOVision geophysical services	FIGURE 29 VELOCITY MODEL FOR ACTIVE AND PASSIVE SURFACE WAVE ARRAY Z2-S7
Project # 9001 Date: JUL 23, 2009 Drawn By: A MARTIN	FIGUEROA ST AND AVENUE 50, LOS ANGELES, CALIFORNIA
Approved By: [signature] File R:\...Project Files\2009\9001ch2mhill\report\figures\Figure29.cdr	PREPARED FOR CH2M HILL

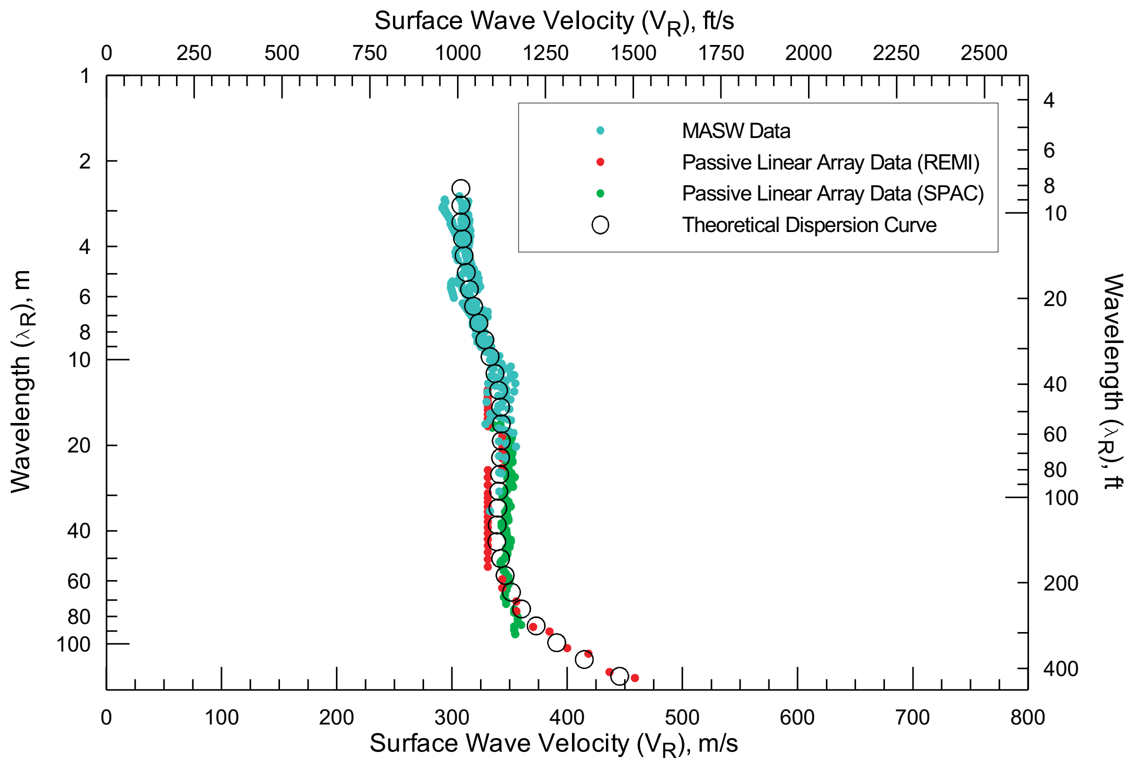

Comparison of Field Experimental Data and Theoretical Dispersion Curve from Active and Passive Surface Wave Array Z2-S8

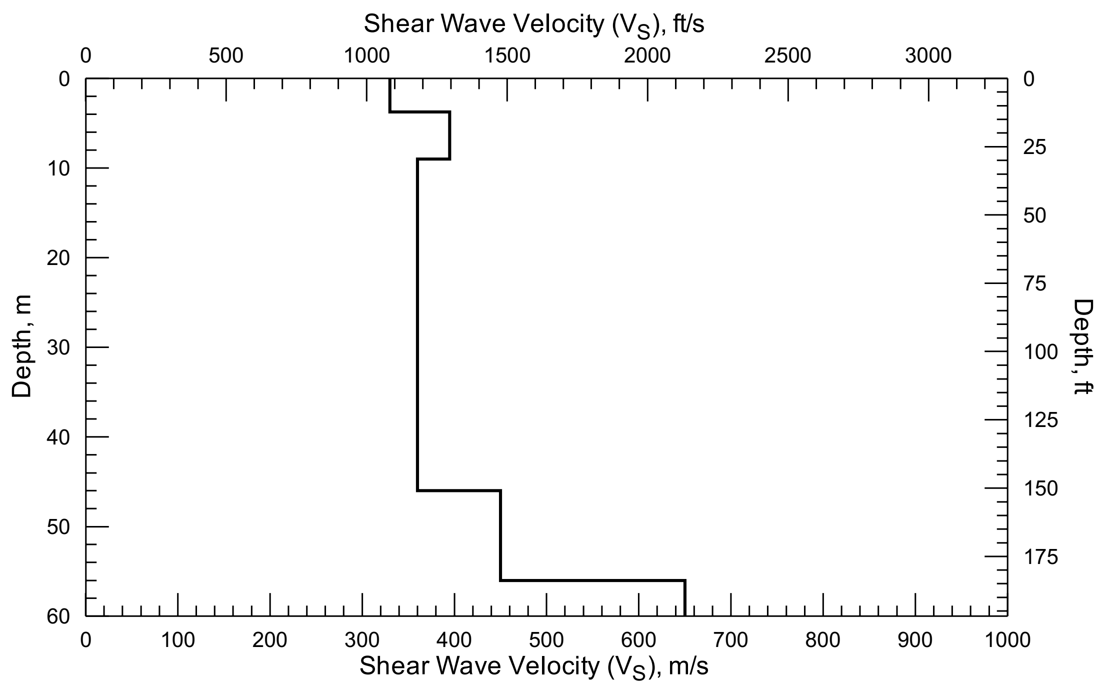

V_S Model from Active and Passive Surface Wave Array Z2-S8

GEOVision geophysical services

Project # 9001	FIGURE 30 VELOCITY MODEL FOR ACTIVE AND PASSIVE SURFACE WAVE ARRAY Z2-S8
Date: JUL 23, 2009	FIGUEROA ST AND AVENUE 54, LOS ANGELES, CALIFORNIA
Drawn By: A MARTIN	
Approved By: [signature]	PREPARED FOR CH2M HILL
File R:\...Project Files\2009\9001ch2mhill\report\figures\Figure30.cdr	

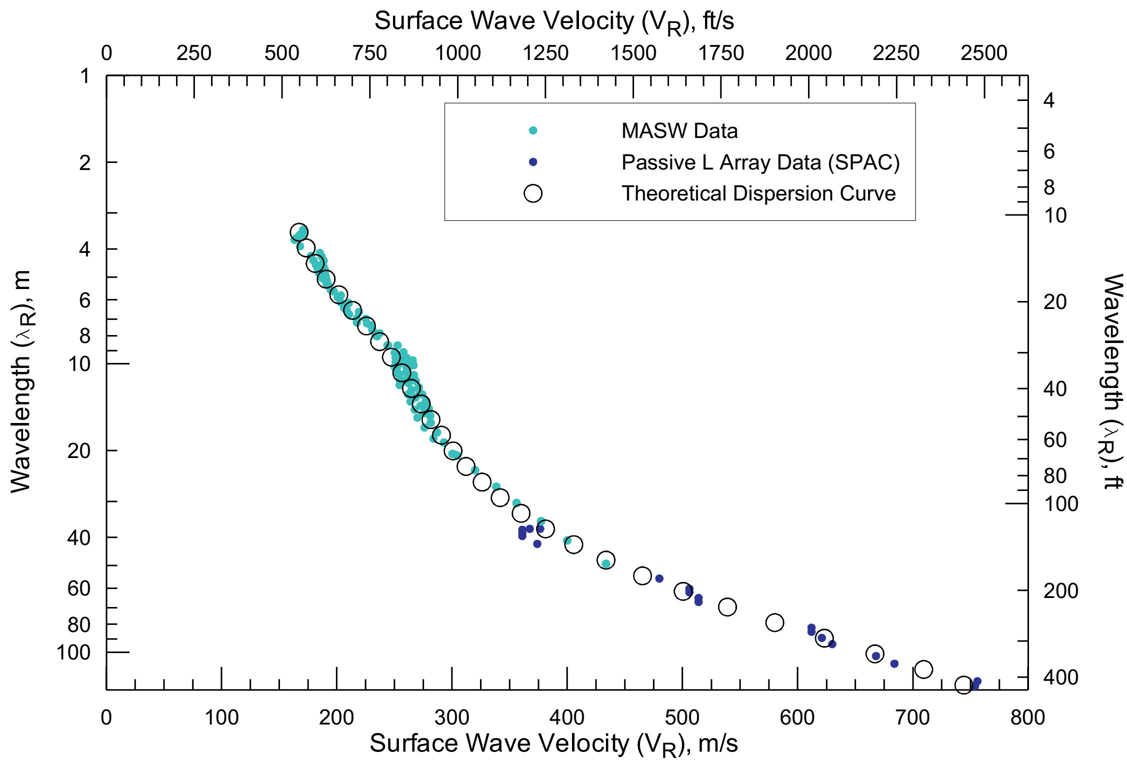

Comparison of Field Experimental Data and Theoretical Dispersion Curve from Active and Passive Surface Wave Array Z2-S9

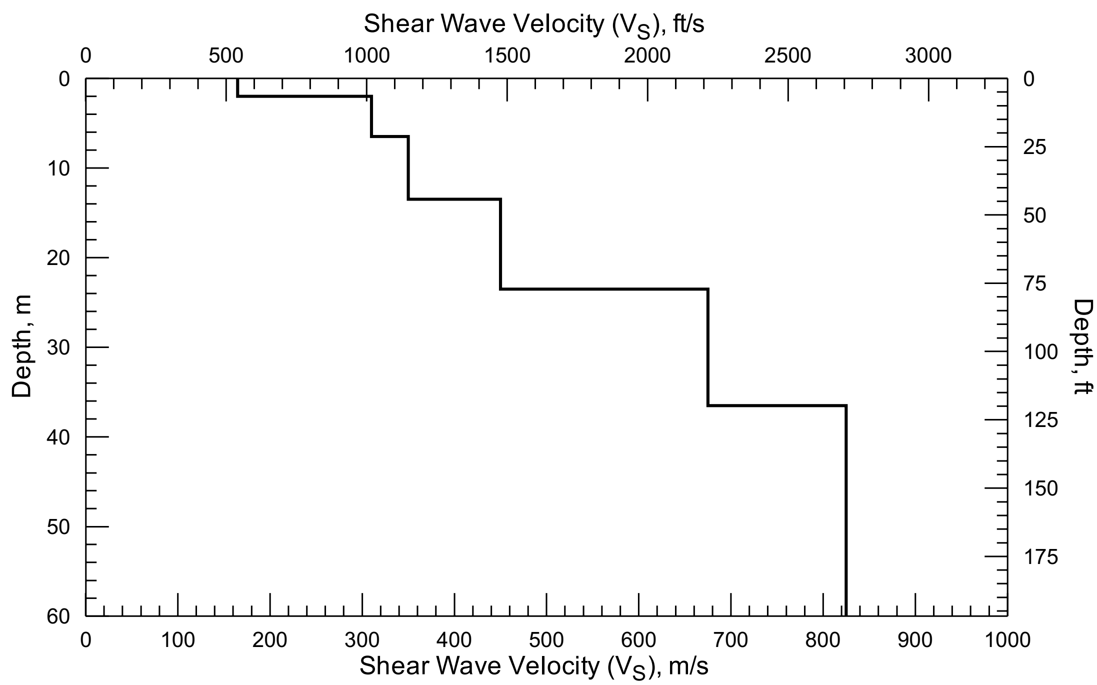

V_S Model from Active and Passive Surface Wave Array Z2-S9

GEOVision geophysical services

Project # 9001
Date: JUL 23, 2009
Drawn By: A MARTIN
Approved By: [signature]

File R:\...Project Files\2009\9001ch2mhill\report\figures\Figure31.cdr

FIGURE 31
VELOCITY MODEL FOR ACTIVE AND PASSIVE SURFACE WAVE ARRAY Z2-S9

REDFIELD AVE AND EBEY AVE, LOS ANGELES, CALIFORNIA

PREPARED FOR
CH2M HILL

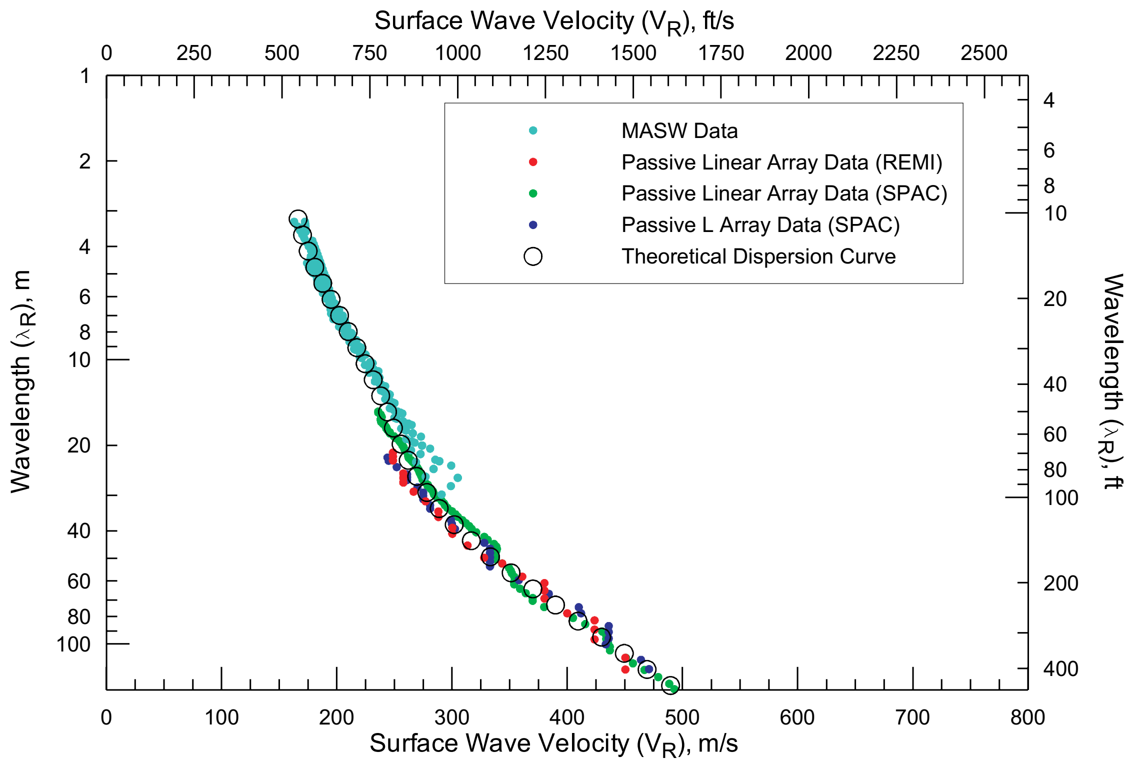

Comparison of Field Experimental Data and Theoretical Dispersion Curve from Active and Passive Surface Wave Array Z2-S10

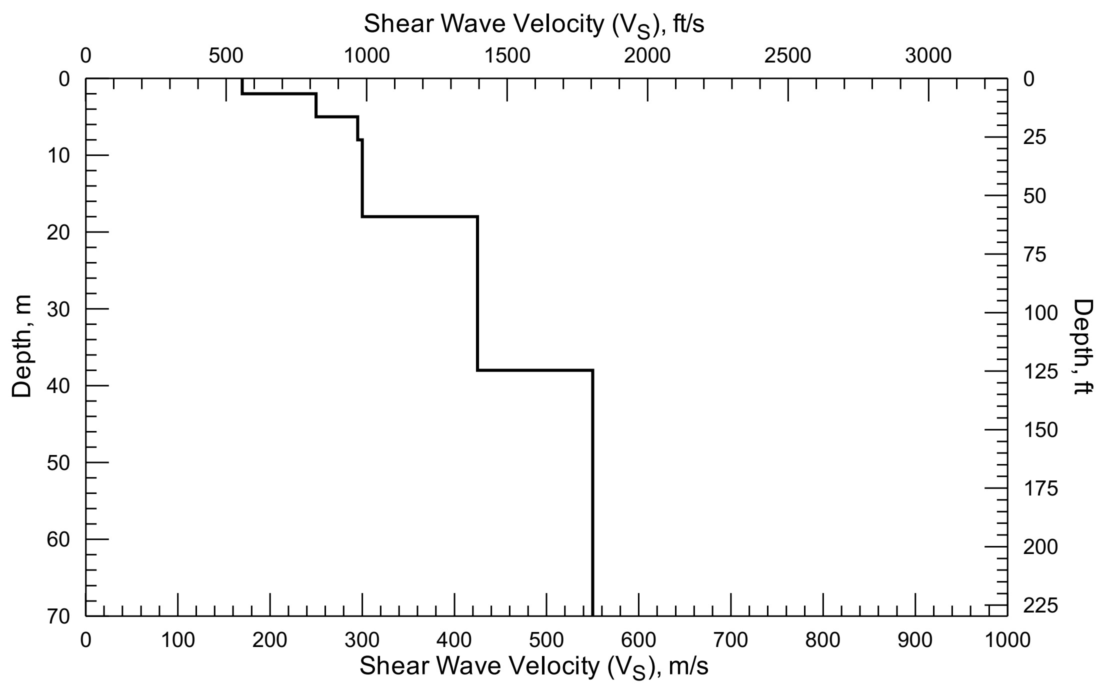

V_S Model from Active and Passive Surface Wave Array Z2-S10

GEOVision geophysical services	FIGURE 32 VELOCITY MODEL FOR ACTIVE AND PASSIVE SURFACE WAVE ARRAY Z2-S10
Project # 9001 Date: JUL 23, 2009	PUEBLO AVE AND RENOVO ST, LOS ANGELES, CALIFORNIA
Drawn By: A MARTIN Approved By: Antony J Martin	PREPARED FOR CH2M HILL

File R:\...Project Files\2009\9001ch2mhill\report\figures\Figure32.cdr

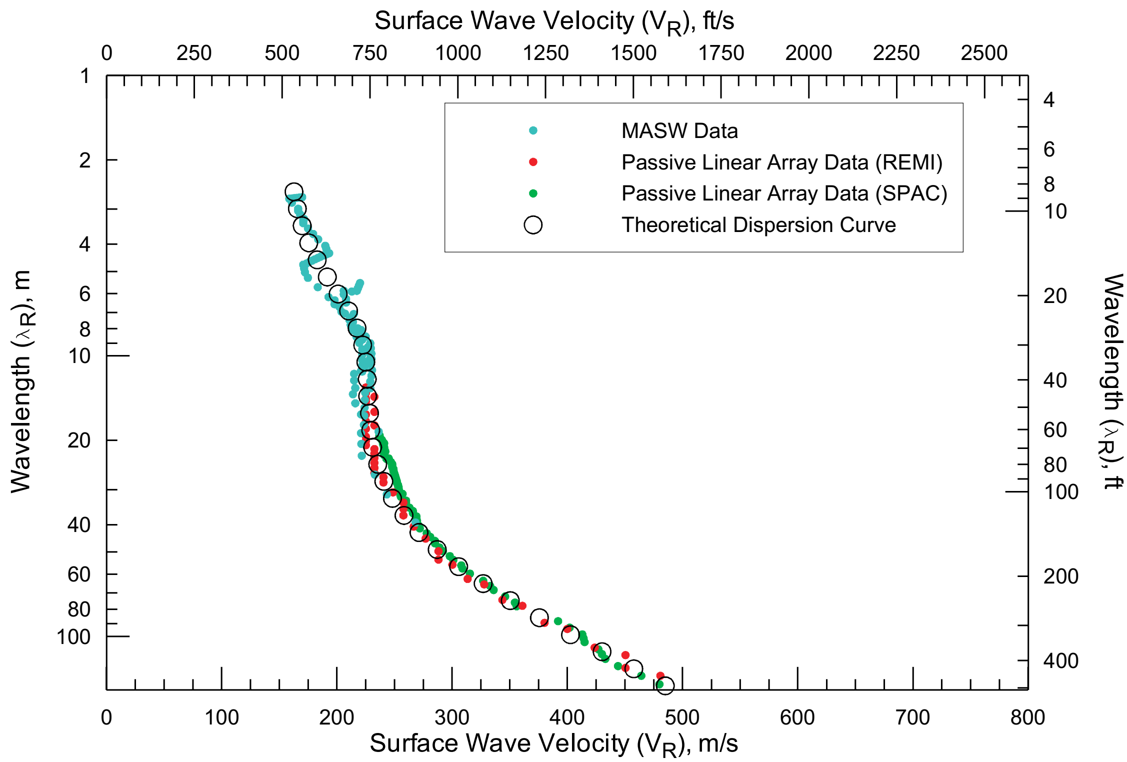

Comparison of Field Experimental Data and Theoretical Dispersion Curve from Active and Passive Surface Wave Array Z2-S11

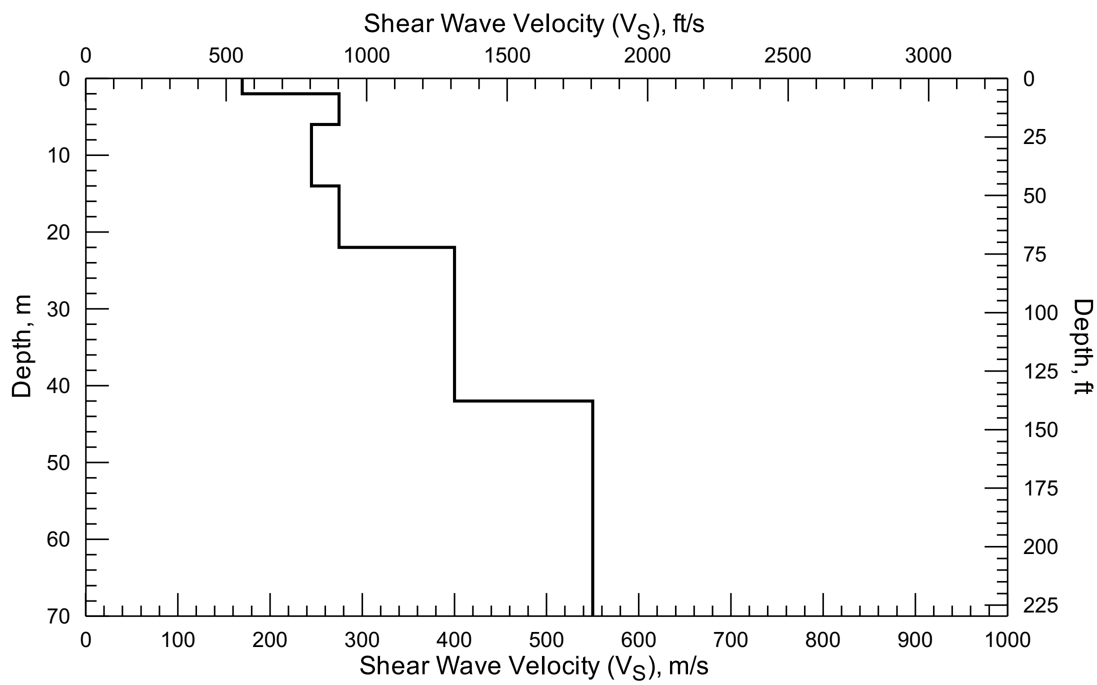

V_S Model from Active and Passive Surface Wave Array Z2-S11

GEOVision geophysical services	FIGURE 33 VELOCITY MODEL FOR ACTIVE AND PASSIVE SURFACE WAVE ARRAY Z2-S11
Project # 9001 Date: JUL 23, 2009 Drawn By: A MARTIN	PUEBLO AVE AND HUNTINGTON DR, LOS ANGELES, CALIFORNIA
Approved By: [signature] File R:\...Project Files\2009\9001ch2mhill\report\figures\Figure33.cdr	PREPARED FOR CH2M HILL

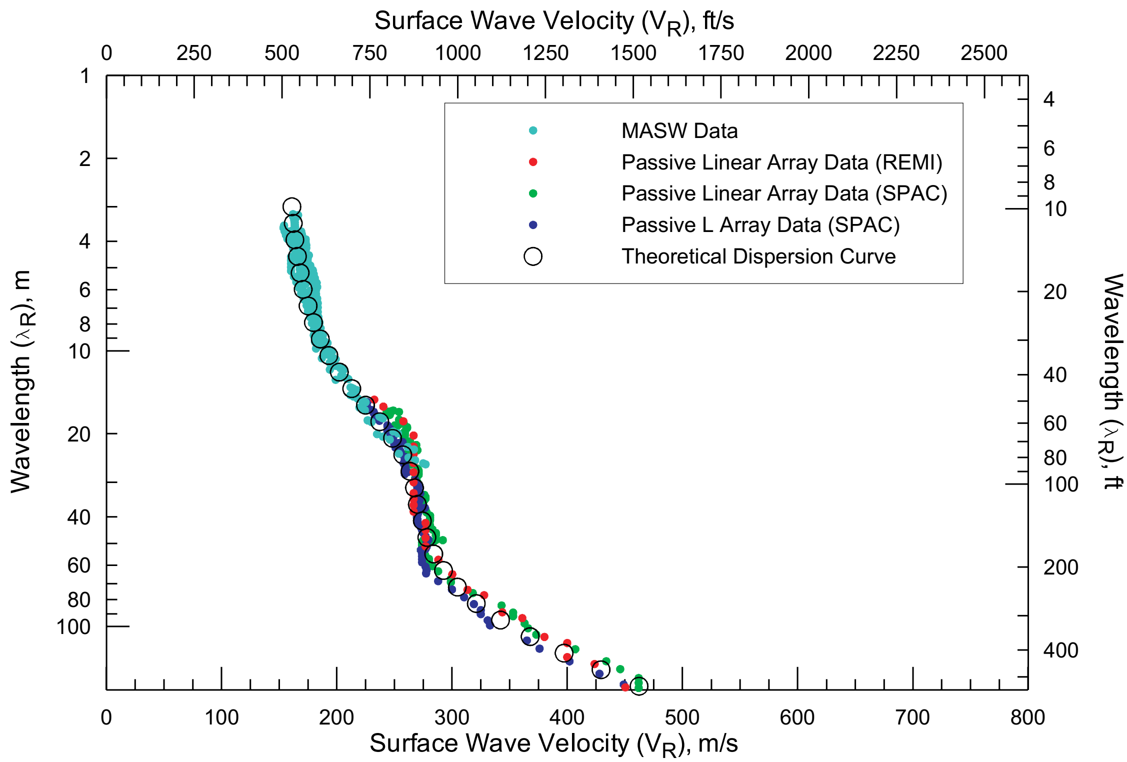

Comparison of Field Experimental Data and Theoretical Dispersion Curve from Active and Passive Surface Wave Array Z2-S12

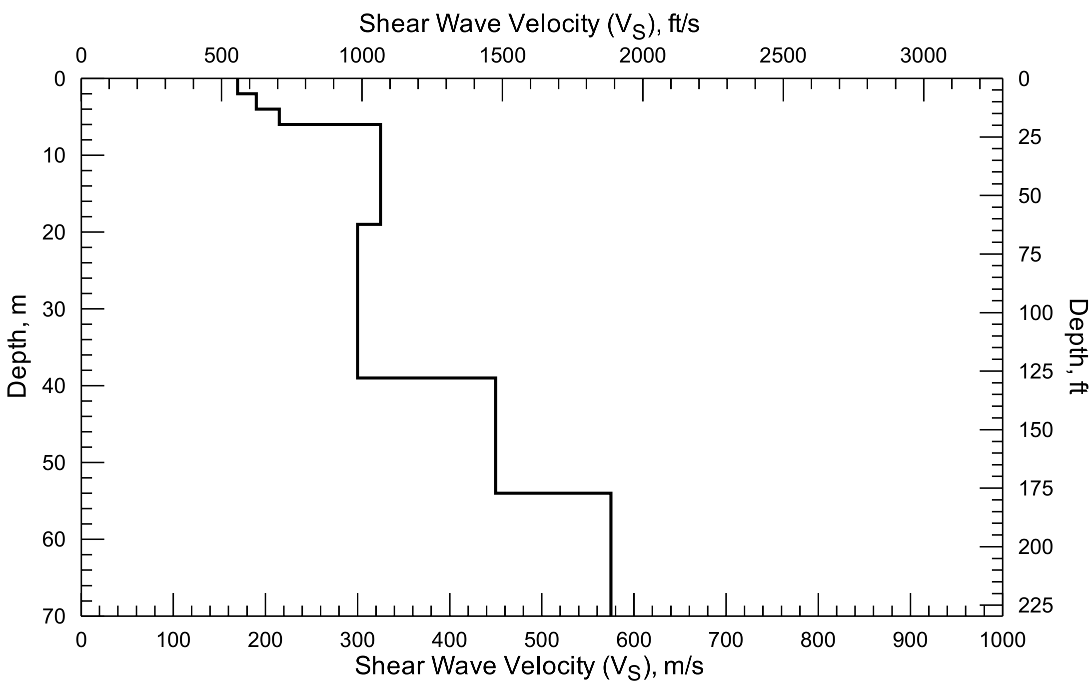

V_S Model from Active and Passive Surface Wave Array Z2-S12

GEOVision geophysical services	FIGURE 34 VELOCITY MODEL FOR ACTIVE AND PASSIVE SURFACE WAVE ARRAY Z2-S12
Project # 9001 Date: JUL 23, 2009 Drawn By: A MARTIN Approved By: [signature]	WARWICK AVE AND ALLAN ST, LOS ANGELES, CALIFORNIA
File R:\...Project Files\2009\9001ch2mhill\report\figures\Figure34.cdr	PREPARED FOR CH2M HILL

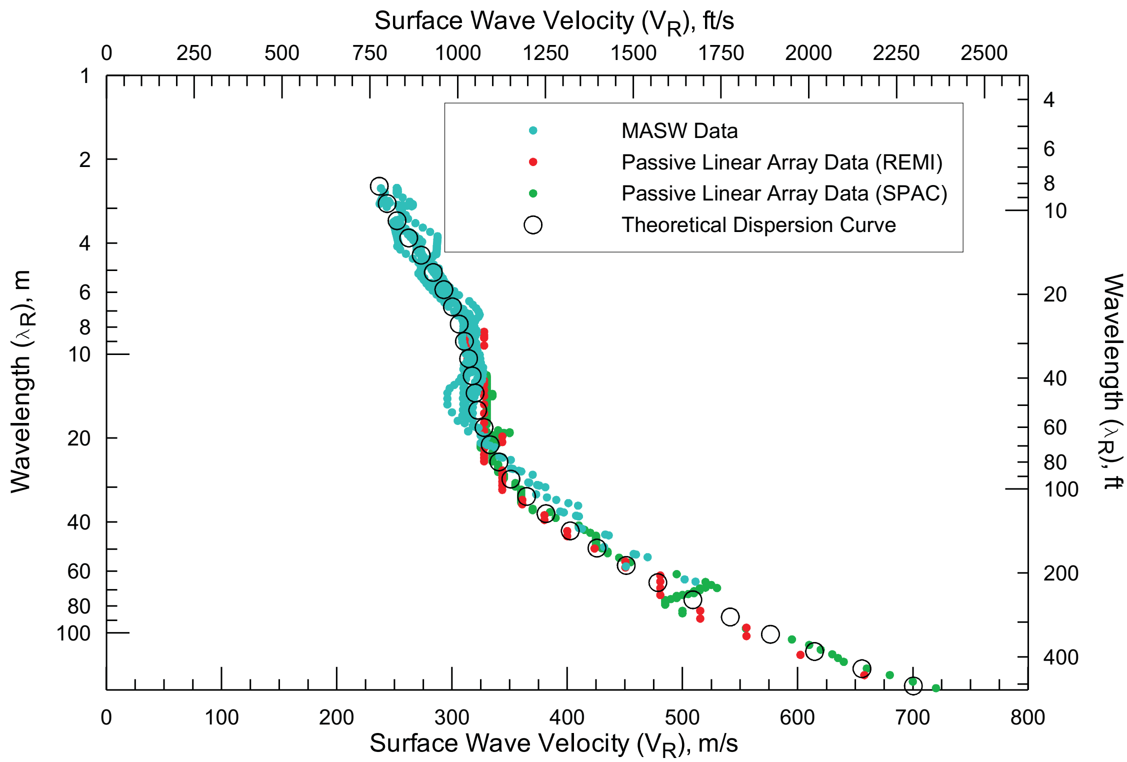

Comparison of Field Experimental Data and Theoretical Dispersion Curve from Active and Passive Surface Wave Array Z3-S1

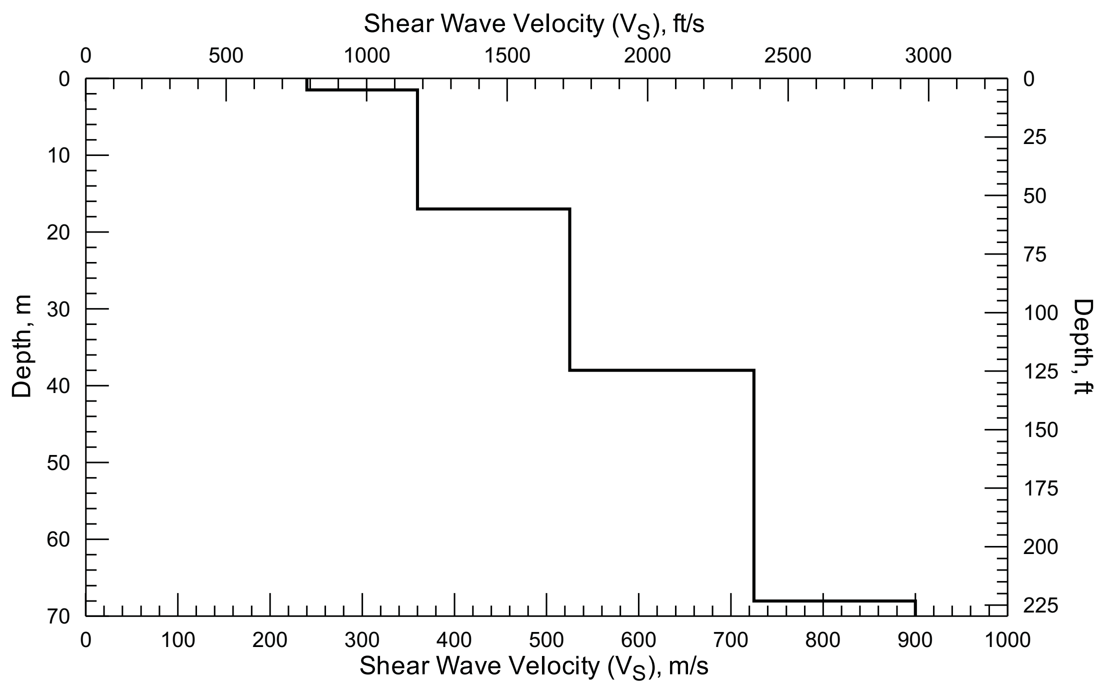

V_S Model from Active and Passive Surface Wave Array Z3-S1

GEOVision geophysical services

Project # 9001	FIGURE 35 VELOCITY MODEL FOR ACTIVE AND PASSIVE SURFACE WAVE ARRAY Z3-S1
Date: JUL 24, 2009	SAN MIGUEL RD AND SIERRA VIEW RD, PASADENA, CALIFORNIA
Drawn By: A MARTIN	
Approved By:	PREPARED FOR CH2M HILL
File R:\...Project Files\2009\9001ch2mhill\report\figures\Figure35.cdr	

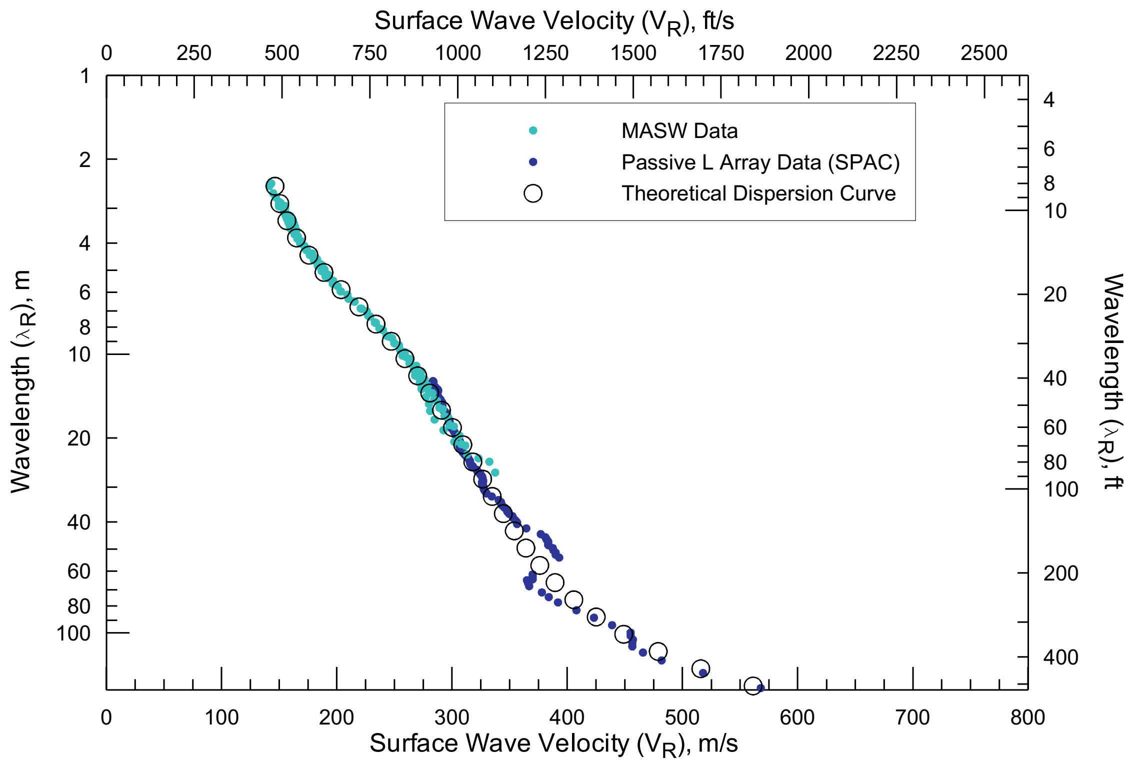

Comparison of Field Experimental Data and Theoretical Dispersion Curve from Active and Passive Surface Wave Array Z3-S2

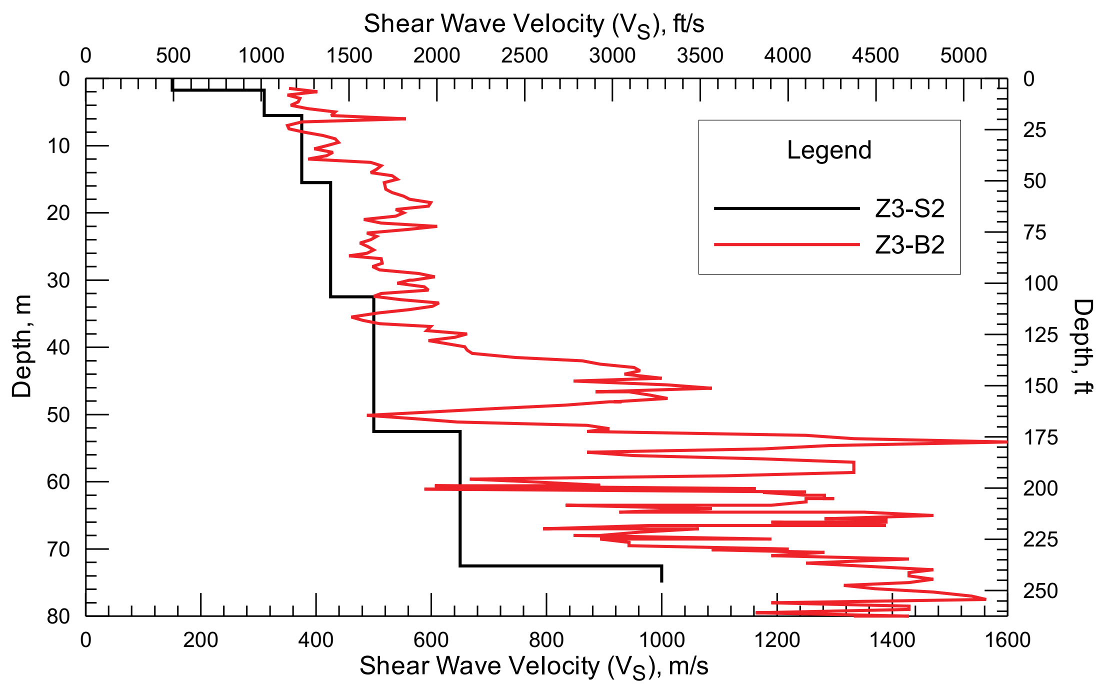

V_S Model from Active and Passive Surface Wave Array Z3-S2

GEOVision geophysical services	FIGURE 36 VELOCITY MODEL FOR ACTIVE AND PASSIVE SURFACE WAVE ARRAY Z3-S2
Project # 9001 Date: JUL 24, 2009 Drawn By: A MARTIN	PASADENA AVE AND PALMETTO DR, PASADENA, CALIFORNIA
Approved By: Antony J Martin File R:\...Project Files\2009\9001ch2mhill\report\figures\Figure36.cdr	PREPARED FOR CH2M HILL

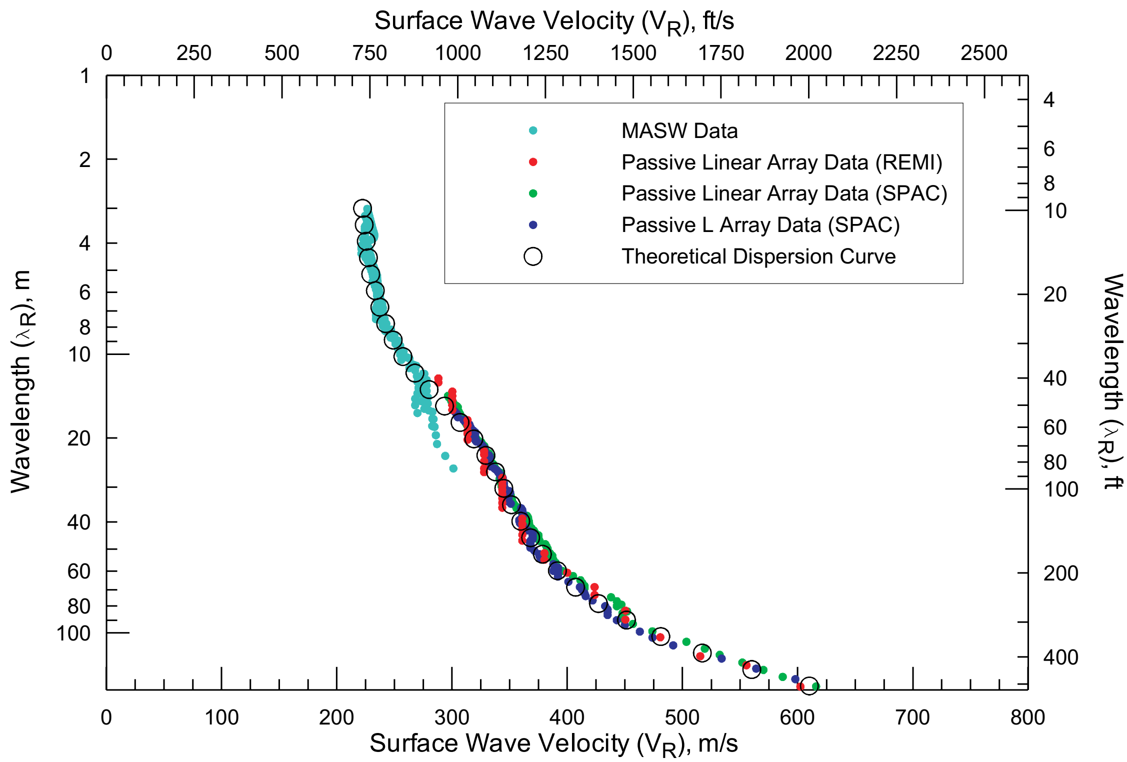

Comparison of Field Experimental Data and Theoretical Dispersion Curve from Active and Passive Surface Wave Array Z3-S3

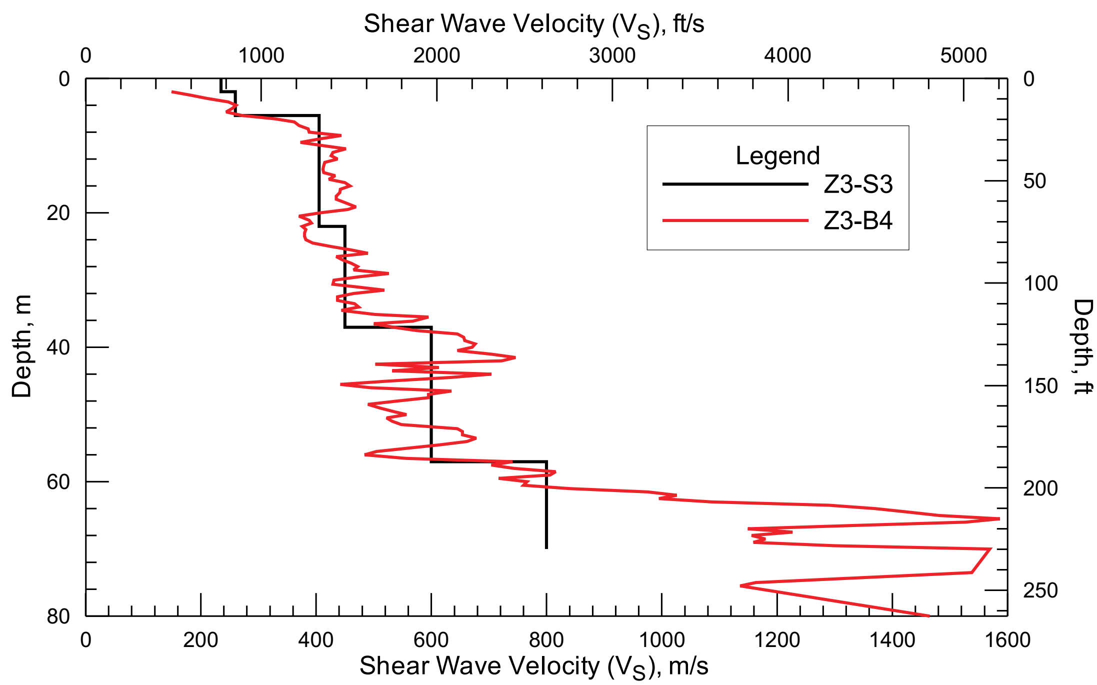

V_S Model from Active and Passive Surface Wave Array Z3-S3

GEOVision geophysical services

Project # 9001
Date: JUL 24, 2009
Drawn By: A MARTIN
Approved By: [signature]
File R:\...Project Files\2009\9001ch2mhill\report\figures\Figure37.cdr

FIGURE 37
VELOCITY MODEL FOR ACTIVE AND PASSIVE SURFACE WAVE ARRAY Z3-S3

RAYMOND AVE AND FILLMORE ST,
PASADENA, CALIFORNIA

PREPARED FOR
CH2M HILL

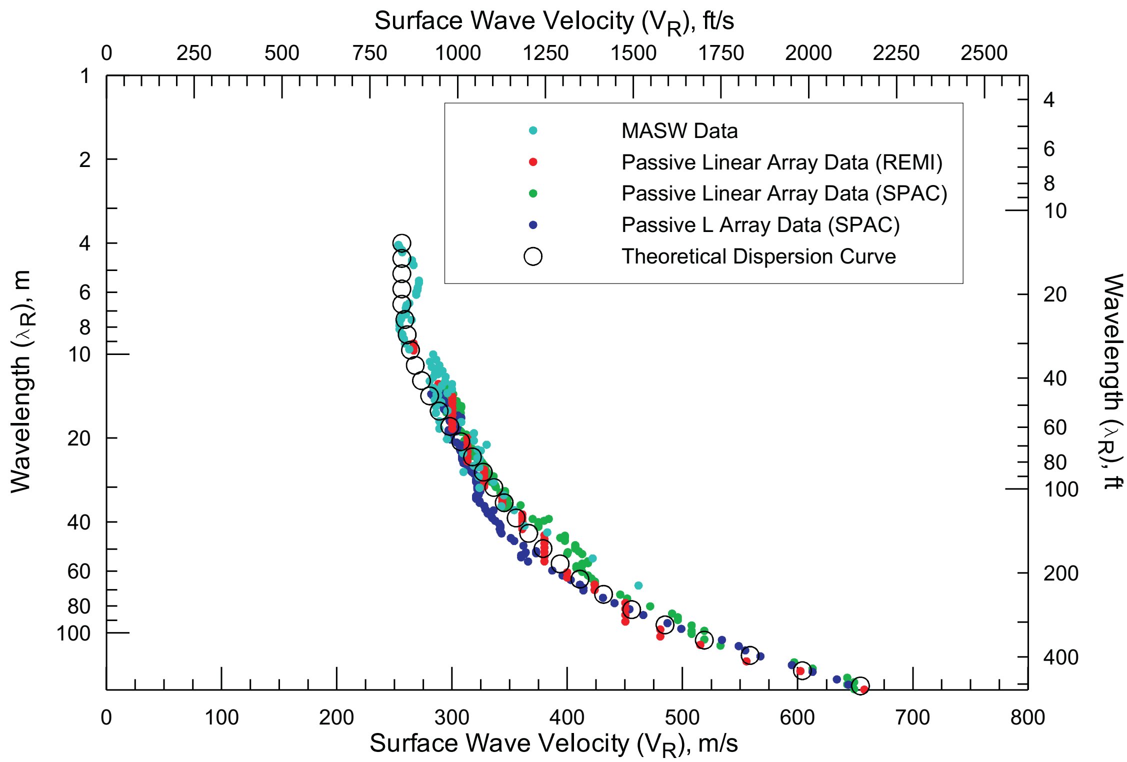

Comparison of Field Experimental Data and Theoretical Dispersion Curve from Active and Passive Surface Wave Array Z3-S4

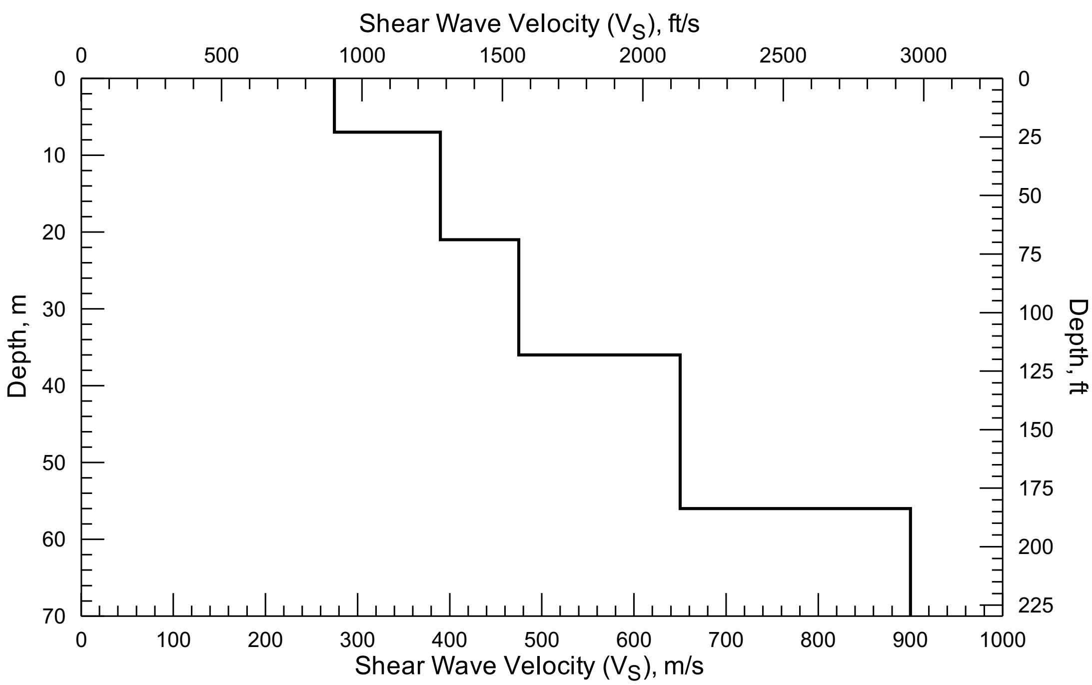

V_S Model from Active and Passive Surface Wave Array Z3-S4

GEOVision geophysical services	FIGURE 38 VELOCITY MODEL FOR ACTIVE AND PASSIVE SURFACE WAVE ARRAY Z3-S4
Project # 9001 Date: JUL 24, 2009 Drawn By: A MARTIN	RAYMOND AVE AND GLENARM ST, PASADENA, CALIFORNIA
Approved By: Antony J Martin File R:\...Project Files\2009\9001ch2mhill\report\figures\Figure38.cdr	PREPARED FOR CH2M HILL

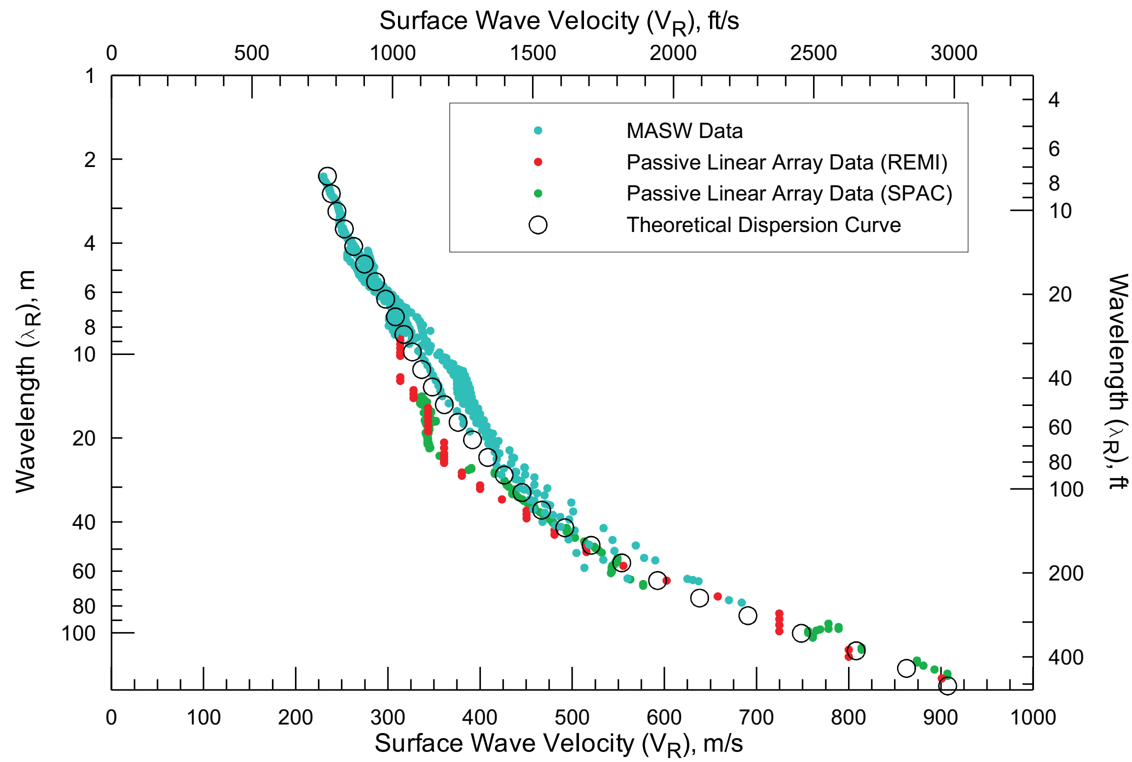

Comparison of Field Experimental Data and Theoretical Dispersion Curve from Active and Passive Surface Wave Array Z3-S5

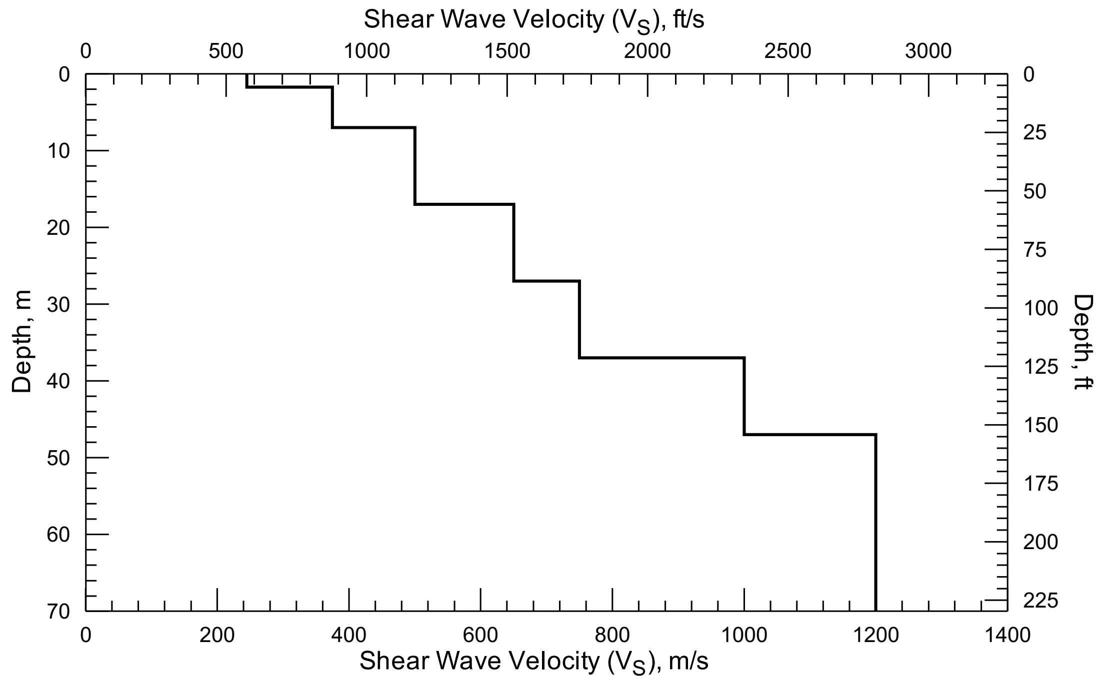

V_S Model from Active and Passive Surface Wave Array Z3-S5

GEOVision geophysical services	FIGURE 39 VELOCITY MODEL FOR ACTIVE AND PASSIVE SURFACE WAVE ARRAY Z3-S5
Project # 9001 Date: JUL 24, 2009 Drawn By: A MARTIN	PASADENA AVE AND ARLINGTON DR, PASADENA, CALIFORNIA
Approved By: Antony J Martin File R:\...Project Files\2009\9001ch2mhill\report\figures\Figure39.cdr	PREPARED FOR CH2M HILL

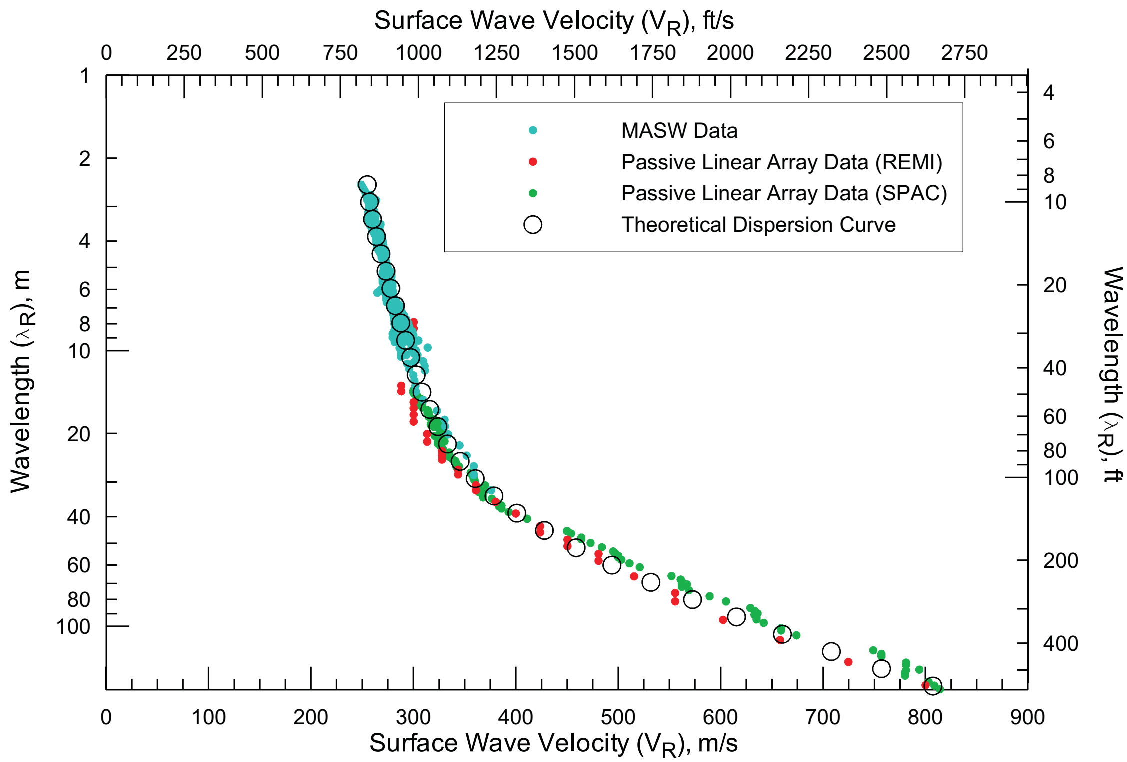

Comparison of Field Experimental Data and Theoretical Dispersion Curve from Active and Passive Surface Wave Array Z3-S6

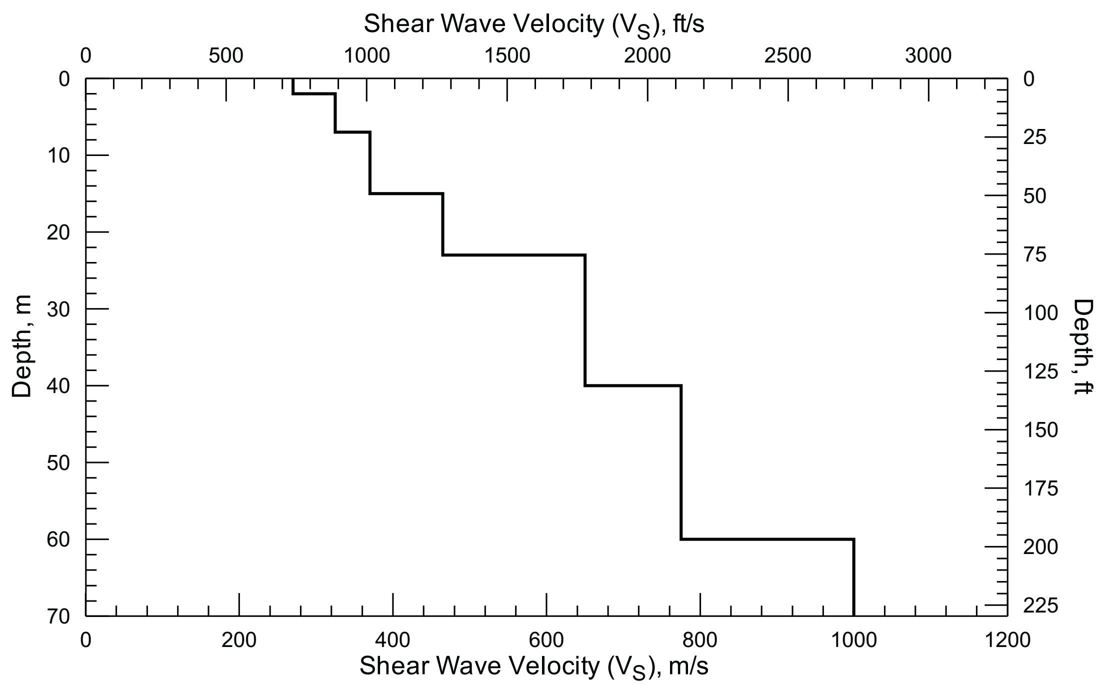

V_S Model from Active and Passive Surface Wave Array Z3-S6

GEOVision geophysical services

	FIGURE 40 VELOCITY MODEL FOR ACTIVE AND PASSIVE SURFACE WAVE ARRAY Z3-S6
Project # 9001	GRAND AVE AND MADELINE DR, PASADENA, CALIFORNIA
Date: JUL 24, 2009	
Drawn By: A MARTIN	
Approved By: [signature]	PREPARED FOR CH2M HILL
File R:\...Project Files\2009\9001ch2mhill\report\figures\Figure40.cdr	

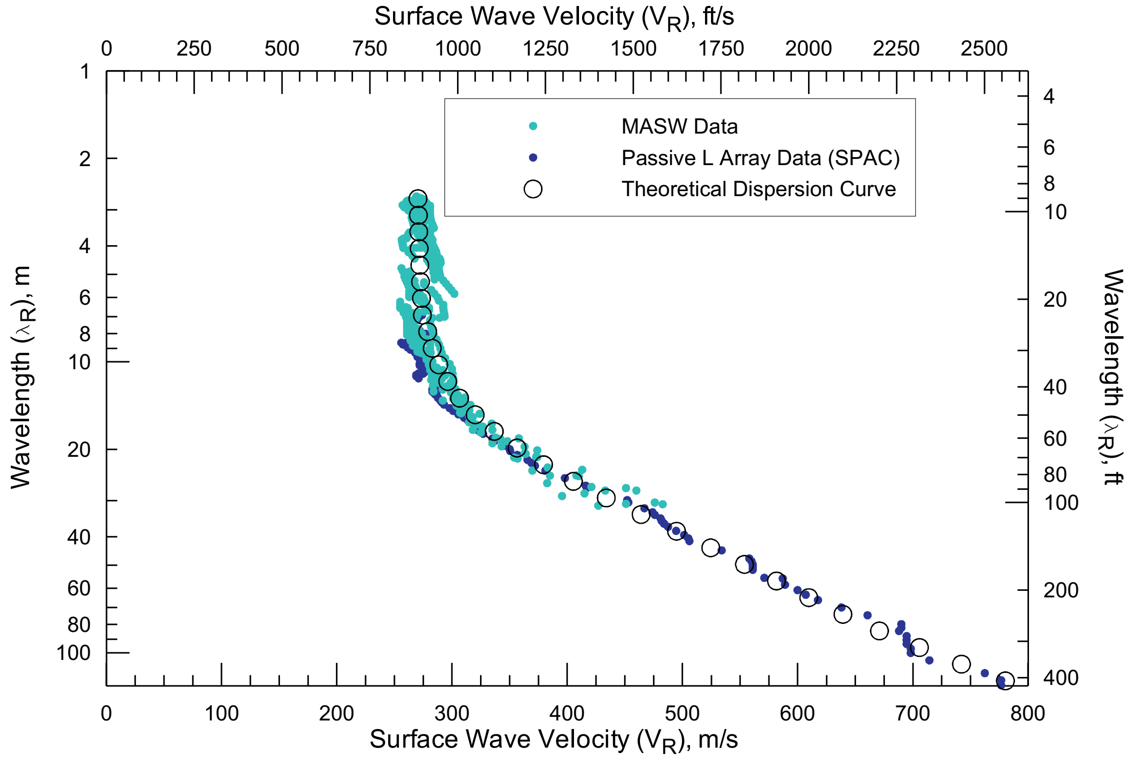

Comparison of Field Experimental Data and Theoretical Dispersion Curve from Active and Passive Surface Wave Array Z3-S7

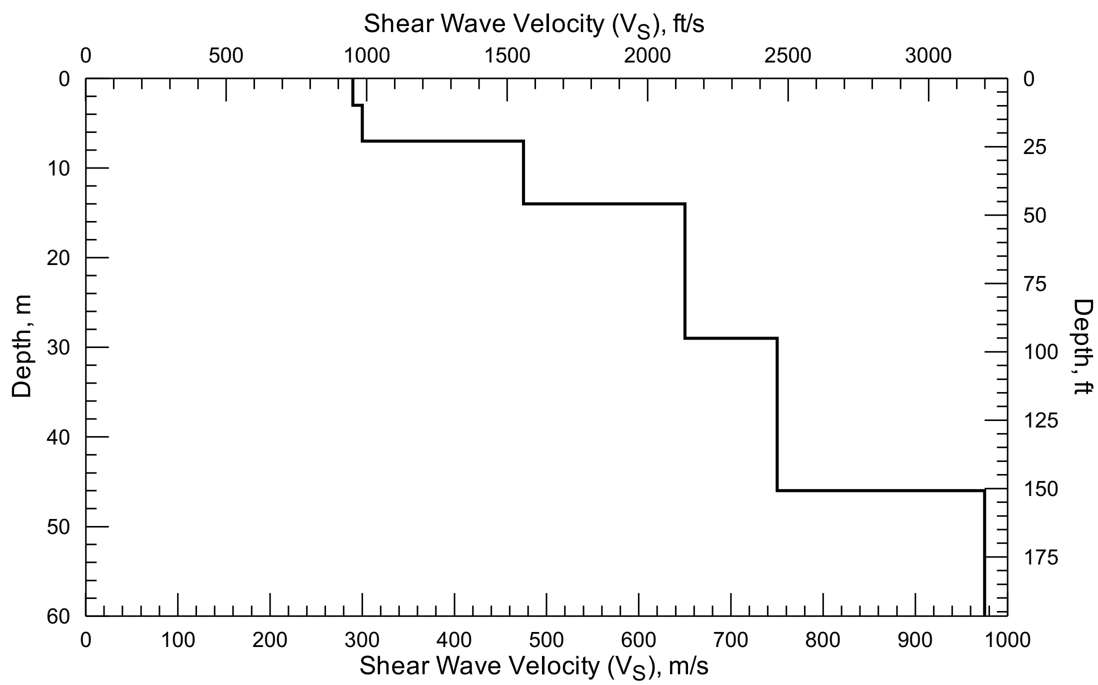

V_S Model from Active and Passive Surface Wave Array Z3-S7

GEOVision geophysical services

Project # 9001
Date: JUL 24, 2009
Drawn By: A MARTIN
Approved By:
File R:\...Project Files\2009\9001ch2mhill\report\figures\Figure41.cdr

FIGURE 41
VELOCITY MODEL FOR ACTIVE AND PASSIVE SURFACE WAVE ARRAY Z3-S7

GRAND AVE AND COLUMBIA ST, PASADENA, CALIFORNIA

PREPARED FOR CH2M HILL

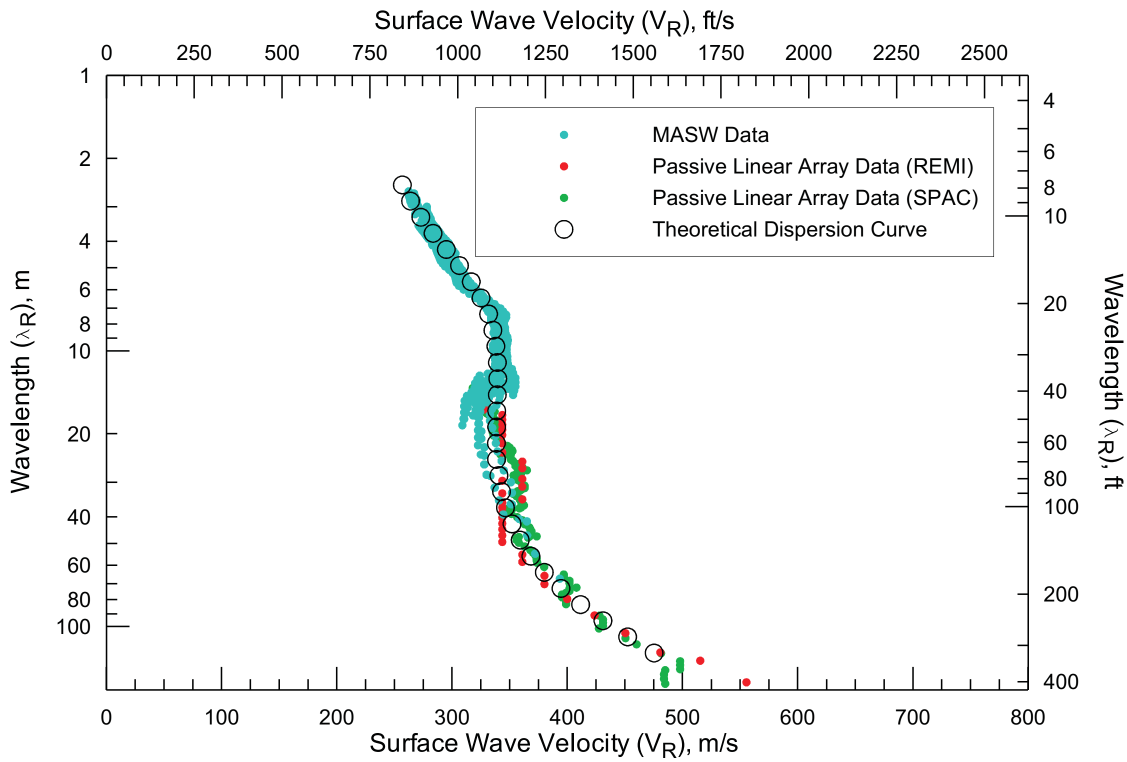

Comparison of Field Experimental Data and Theoretical Dispersion Curve from Active and Passive Surface Wave Array Z3-S8

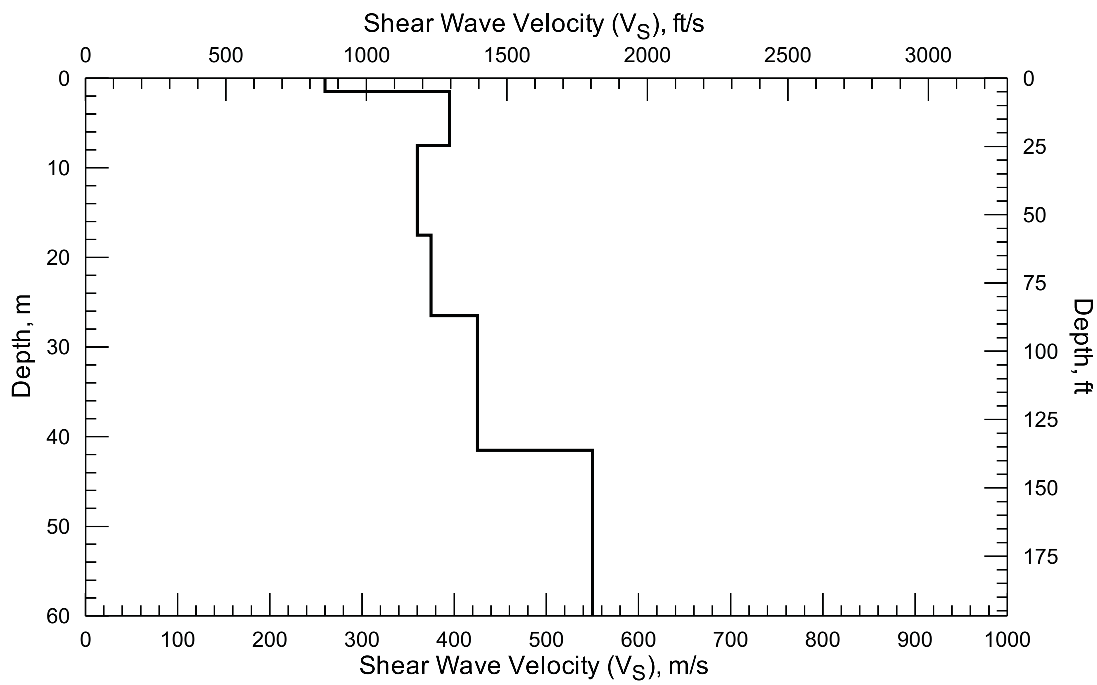

V_S Model from Active and Passive Surface Wave Array Z3-S8

GEOVision geophysical services	FIGURE 42 VELOCITY MODEL FOR ACTIVE AND PASSIVE SURFACE WAVE ARRAY Z3-S8
Project # 9001 Date: JUL 24, 2009 Drawn By: A MARTIN	N AVENUE 65 AND REPTON ST, LOS ANGELES, CALIFORNIA
Approved By: Antony J Martin File R:\...Project Files\2009\9001ch2mhill\report\figures\Figure42.cdr	PREPARED FOR CH2M HILL

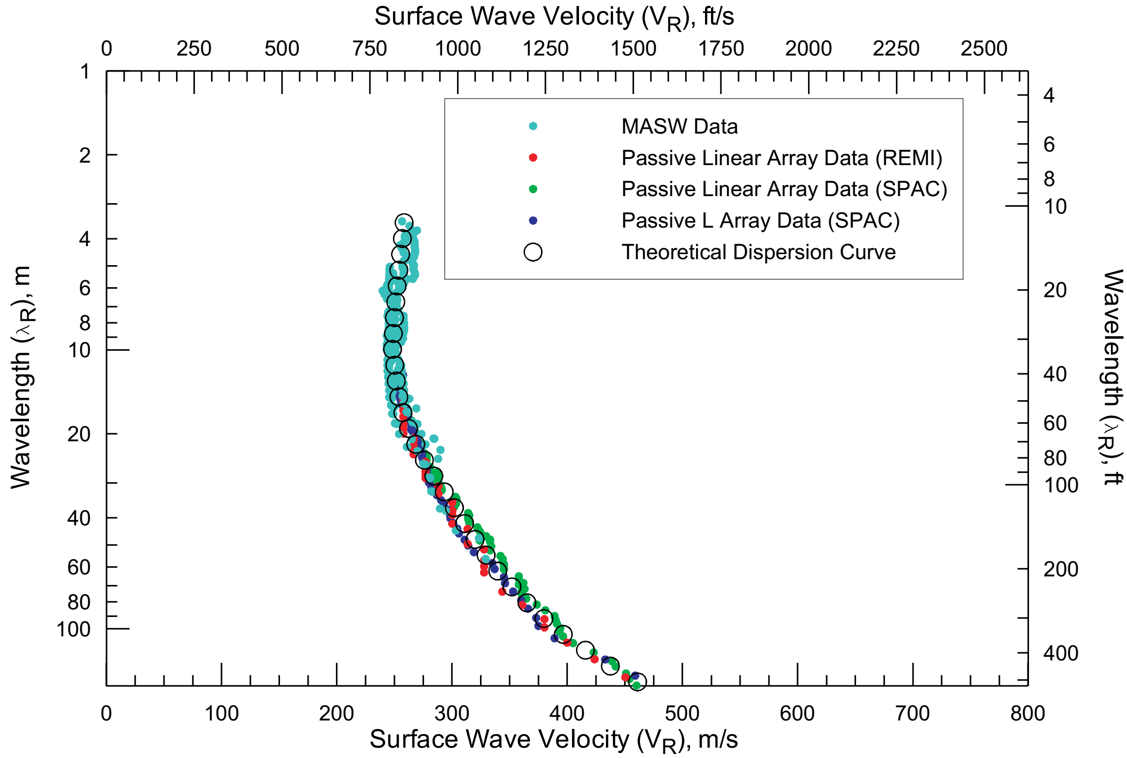

Comparison of Field Experimental Data and Theoretical Dispersion Curve from Active and Passive Surface Wave Array Z3-S9

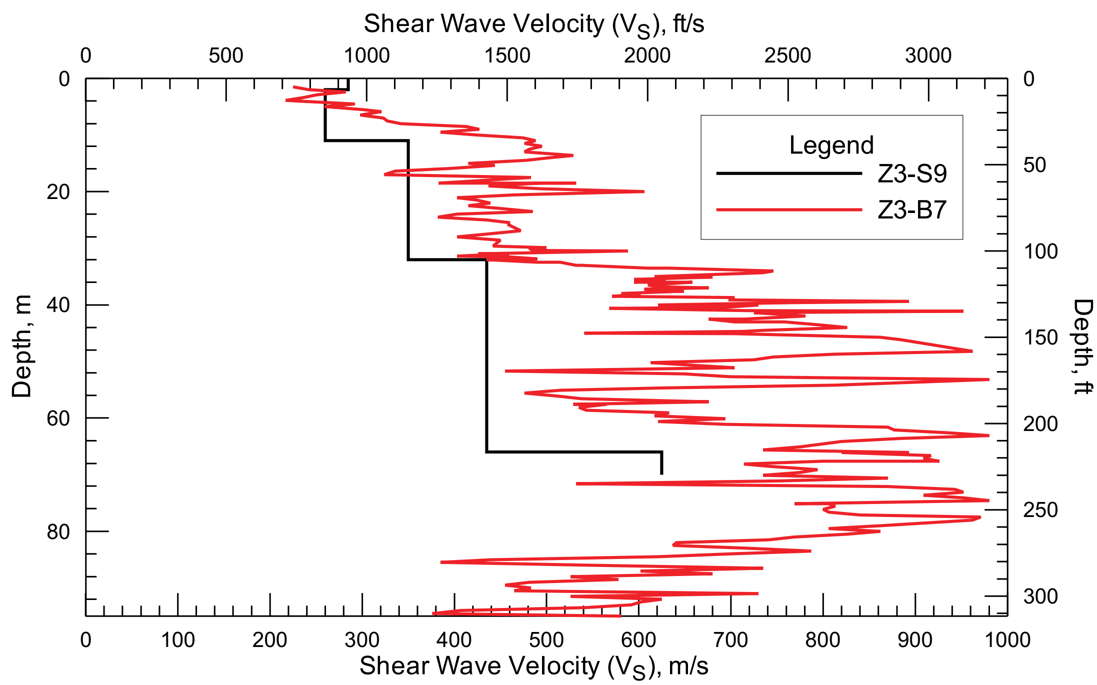

V_S Model from Active and Passive Surface Wave Array Z3-S9

GEOVision geophysical services	FIGURE 43 VELOCITY MODEL FOR ACTIVE AND PASSIVE SURFACE WAVE ARRAY Z3-S9
Project # 9001 Date: JUL 24, 2009 Drawn By: A MARTIN	SAN PASCUAL AVE AND HOUGH ST, LOS ANGELES, CALIFORNIA
Approved By: Antony J Martin File R:\...Project Files\2009\9001ch2mhill\report\figures\Figure43.cdr	PREPARED FOR CH2M HILL

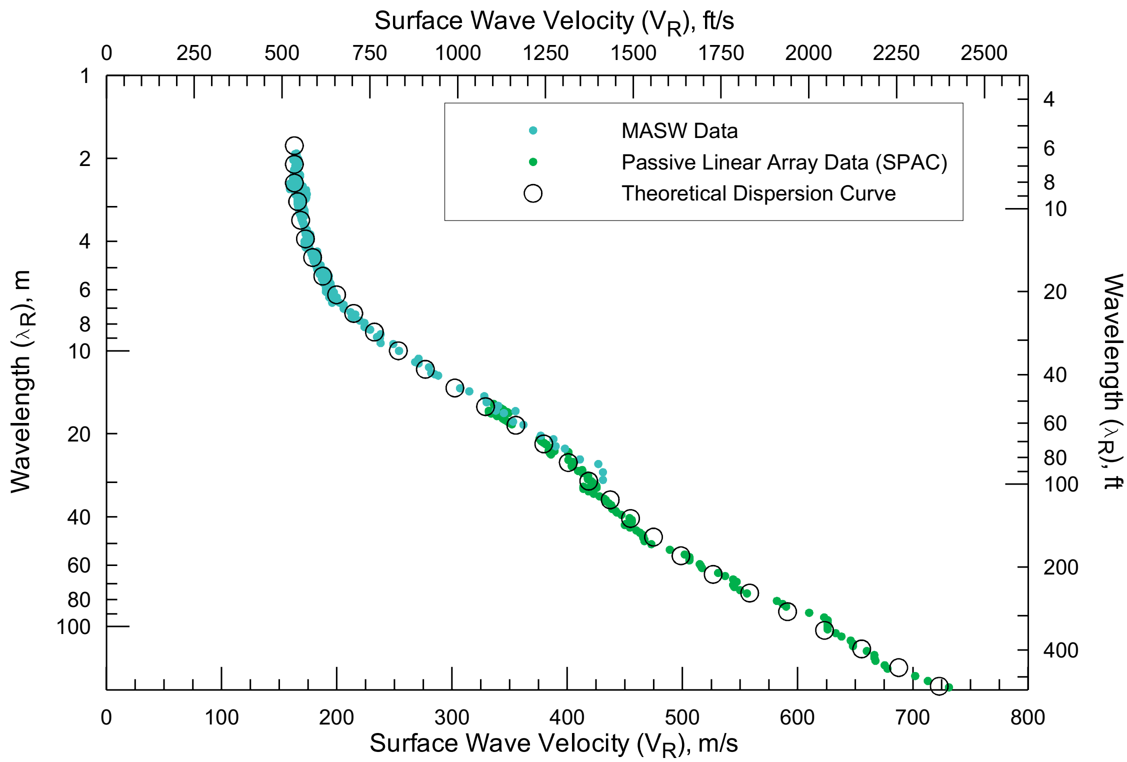

Comparison of Field Experimental Data and Theoretical Dispersion Curve from Active and Passive Surface Wave Array Z3-S10

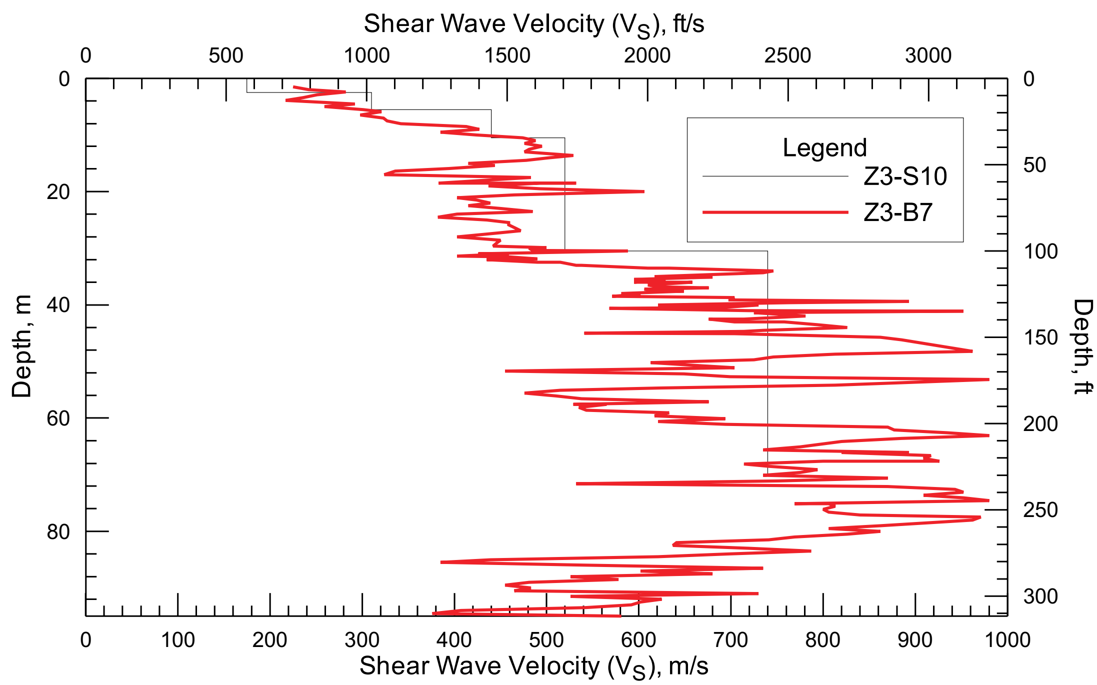

V_S Model from Active and Passive Surface Wave Array Z3-S10

GEOVision geophysical services	FIGURE 44 VELOCITY MODEL FOR ACTIVE AND PASSIVE SURFACE WAVE ARRAY Z3-S10
Project # 9001 Date: JUL 24, 2009 Drawn By: A MARTIN	SAN PASCUAL AVE, LOS ANGELES, CALIFORNIA
Approved By: Antony J Martin File R:\...Project Files\2009\9001ch2mhill\report\figures\Figure44.cdr	PREPARED FOR CH2M HILL

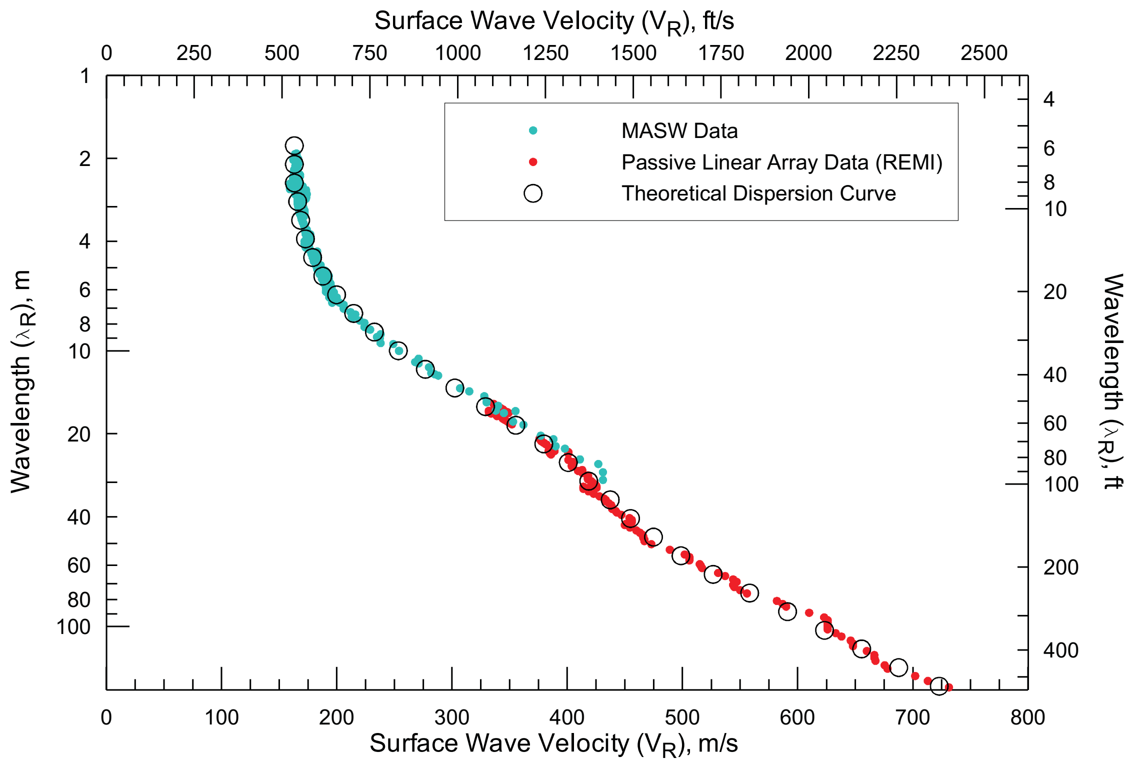

Comparison of Field Experimental Data and Theoretical Dispersion Curve from Active and Passive Surface Wave Array Z3-S11

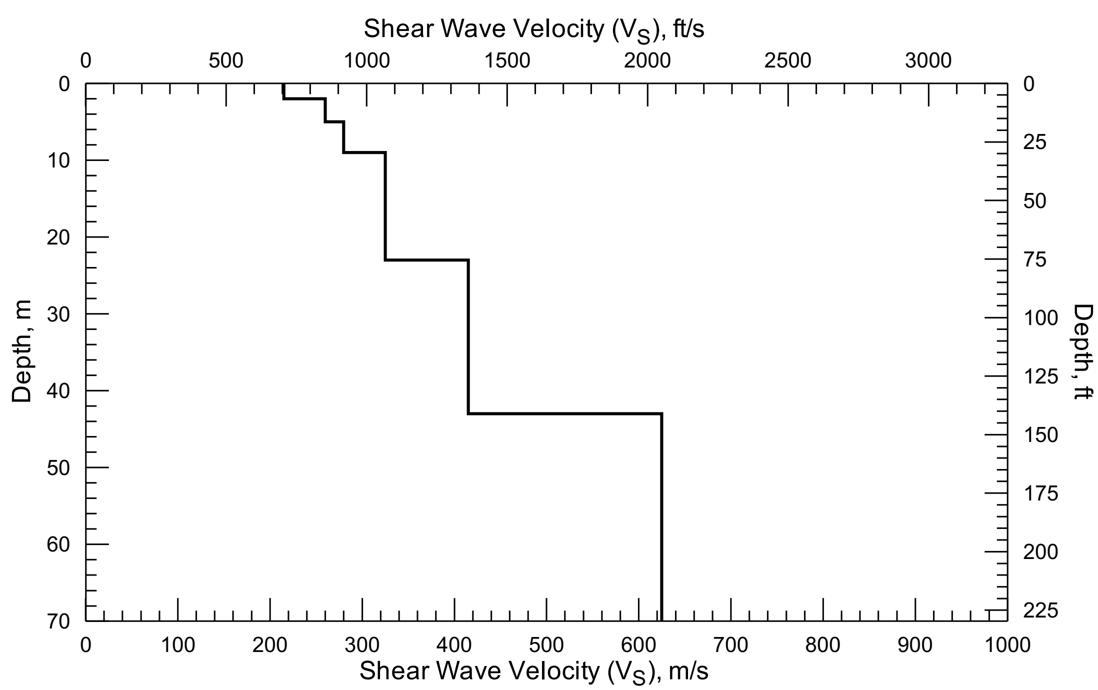

V_S Model from Active and Passive Surface Wave Array Z3-S11

GEOVision geophysical services	FIGURE 45 VELOCITY MODEL FOR ACTIVE AND PASSIVE SURFACE WAVE ARRAY Z3-S11
Project # 9001 Date: JUL 24, 2009	MERIDIAN AVE AND BUENA VISTA ST, SOUTH PASADENA, CALIFORNIA
Drawn By: A MARTIN Approved By: *Antony J Martin* File R:\...Project Files\2009\9001ch2mhill\report\figures\Figure45.cdr	PREPARED FOR CH2M HILL

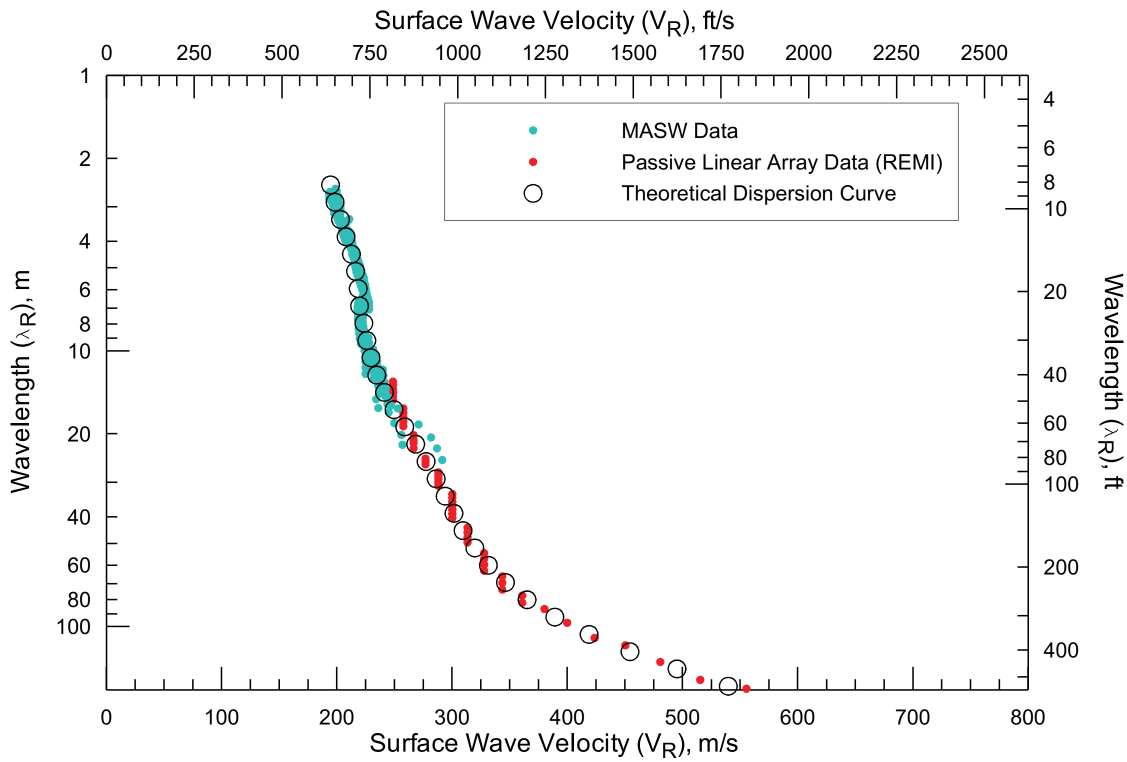

Comparison of Field Experimental Data and Theoretical Dispersion Curve from Active and Passive Surface Wave Array Z3-S12

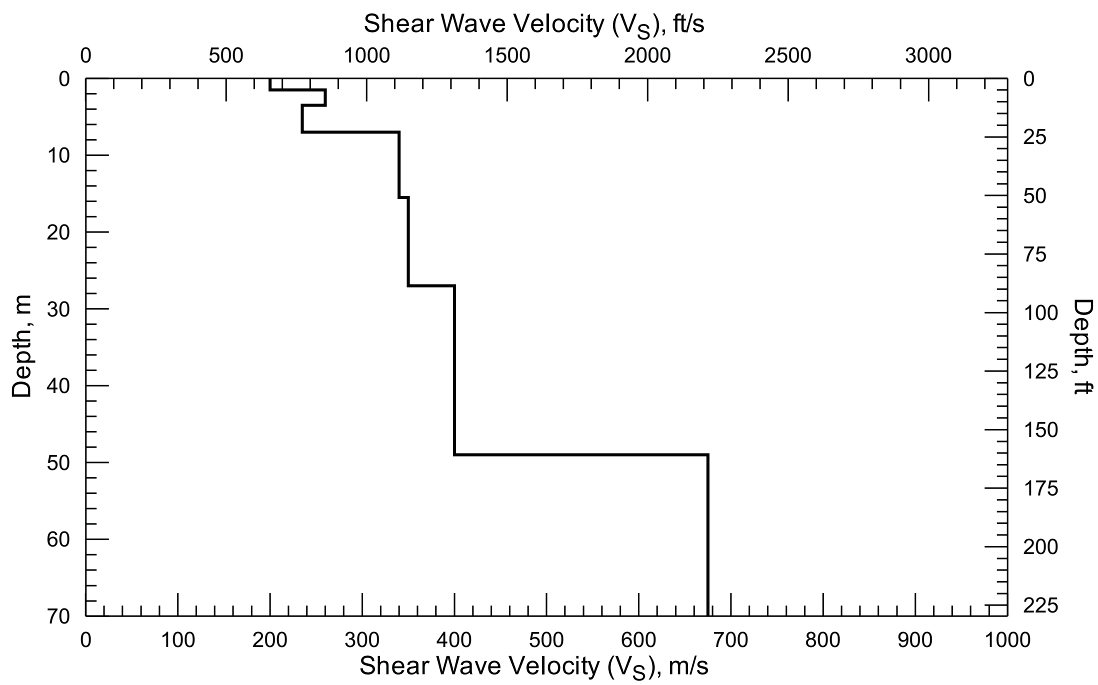

V_S Model from Active and Passive Surface Wave Array Z3-S12

GEOVision geophysical services	FIGURE 46 VELOCITY MODEL FOR ACTIVE AND PASSIVE SURFACE WAVE ARRAY Z3-S12
Project # 9001 Date: JUL 24, 2009 Drawn By: A MARTIN Approved By: Antony J Martin	BRENT AVE AND HOPE ST, SOUTH PASADENA, CALIFORNIA
File R:\...Project Files\2009\9001ch2mhill\report\figures\Figure46.cdr	PREPARED FOR CH2M HILL

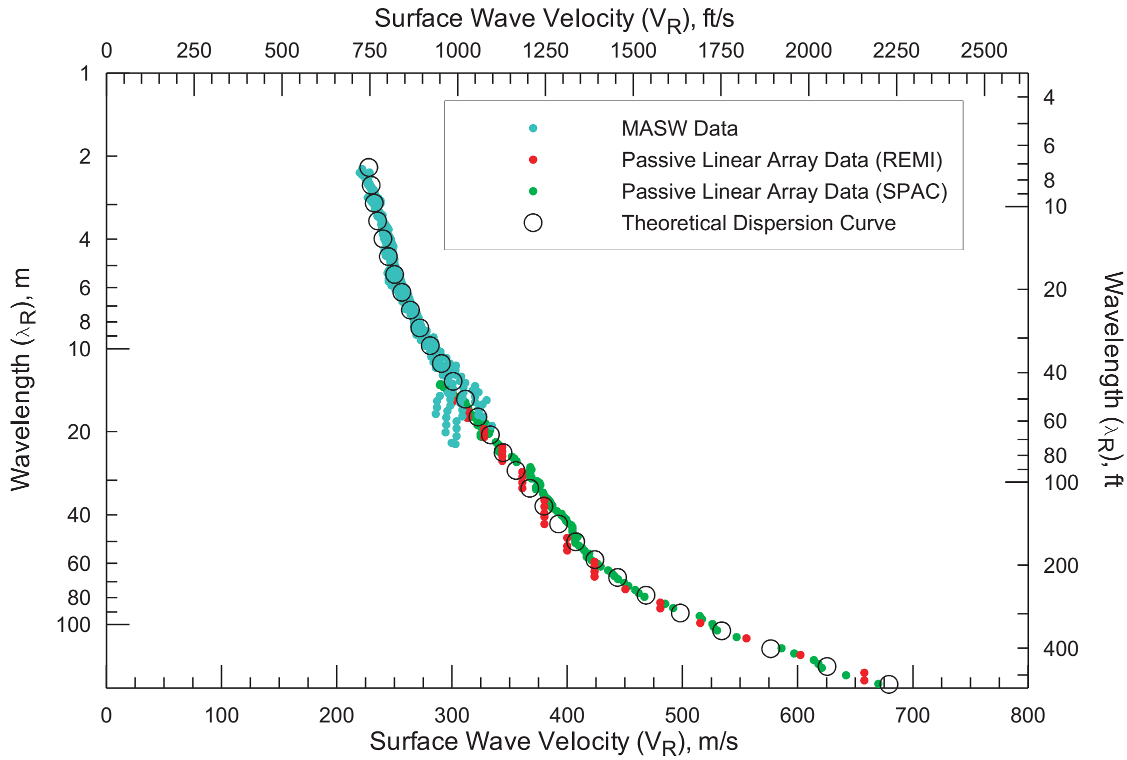

Comparison of Field Experimental Data and Theoretical Dispersion Curve from Active and Passive Surface Wave Array Z3-S13

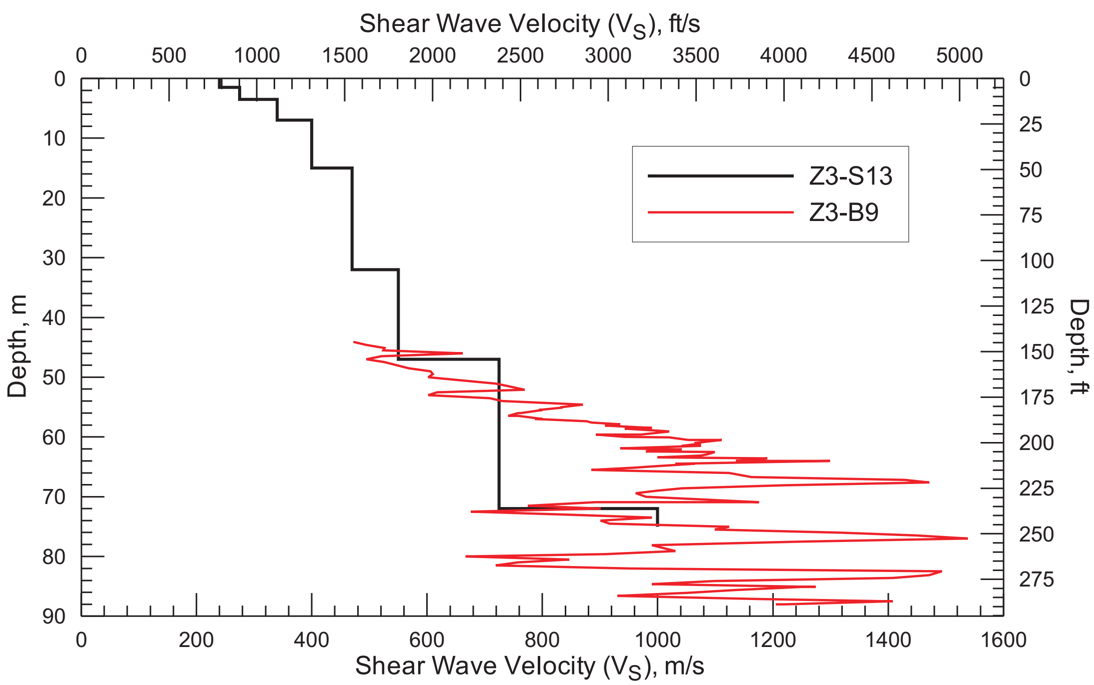

V_S Model from Active and Passive Surface Wave Array Z3-S13

GEOVision geophysical services	FIGURE 47 VELOCITY MODEL FOR ACTIVE AND PASSIVE SURFACE WAVE ARRAY Z3-S13
Project # 9001 Date: JUL 27, 2009 Drawn By: A MARTIN	PASADENA AVE AND MISSION ST, SOUTH PASADENA, CALIFORNIA
Approved By: [signature] File R:\...Project Files\2009\9001ch2mhill\report\figures\Figure47.cdr	PREPARED FOR CH2M HILL

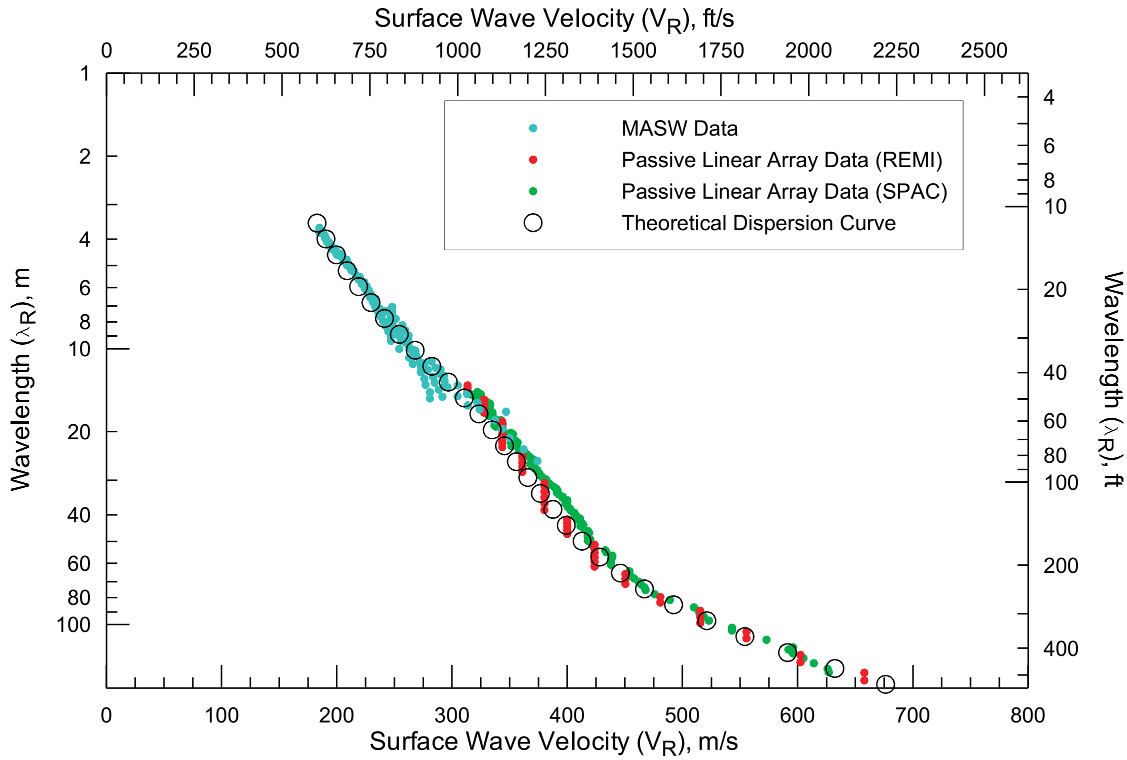

Comparison of Field Experimental Data and Theoretical Dispersion Curve from Active and Passive Surface Wave Array Z3-S14

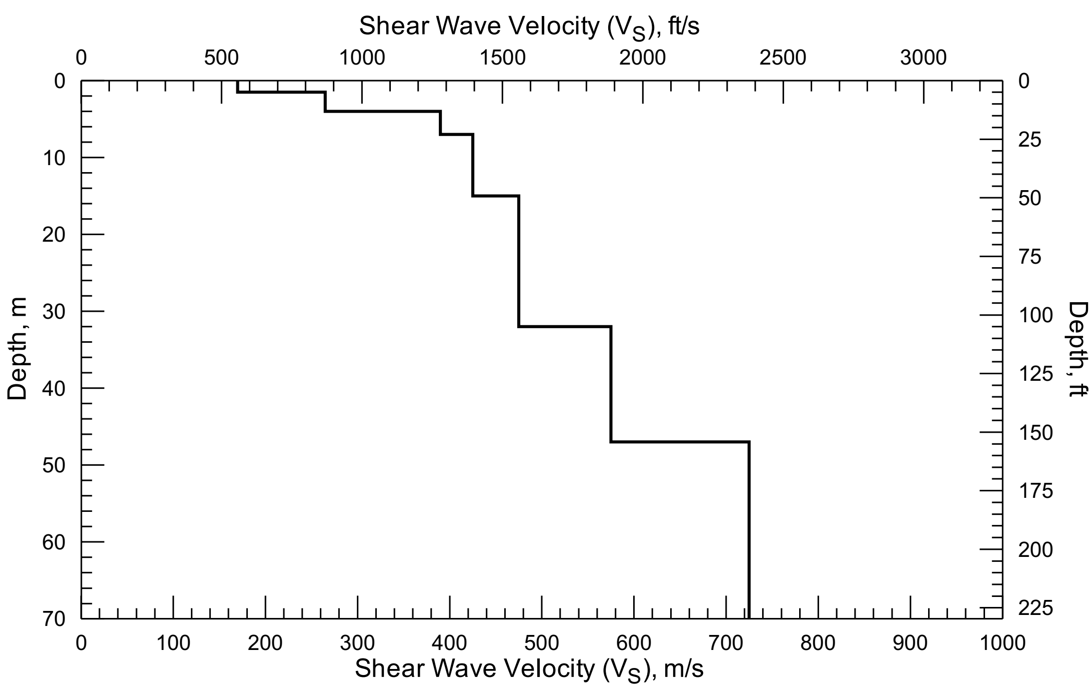

V_S Model from Active and Passive Surface Wave Array Z3-S14

GEOVision geophysical services

FIGURE 48
VELOCITY MODEL FOR ACTIVE AND PASSIVE SURFACE WAVE ARRAY Z3-S14

Project # 9001
Date: JUL 27, 2009
Drawn By: A MARTIN
Approved By: [signature]
File R:\...Project Files\2009\9001ch2mhill\report\figures\Figure48.cdr

PASADENA AVE AND HAWTHORNE ST, SOUTH PASADENA, CALIFORNIA

PREPARED FOR
CH2M HILL

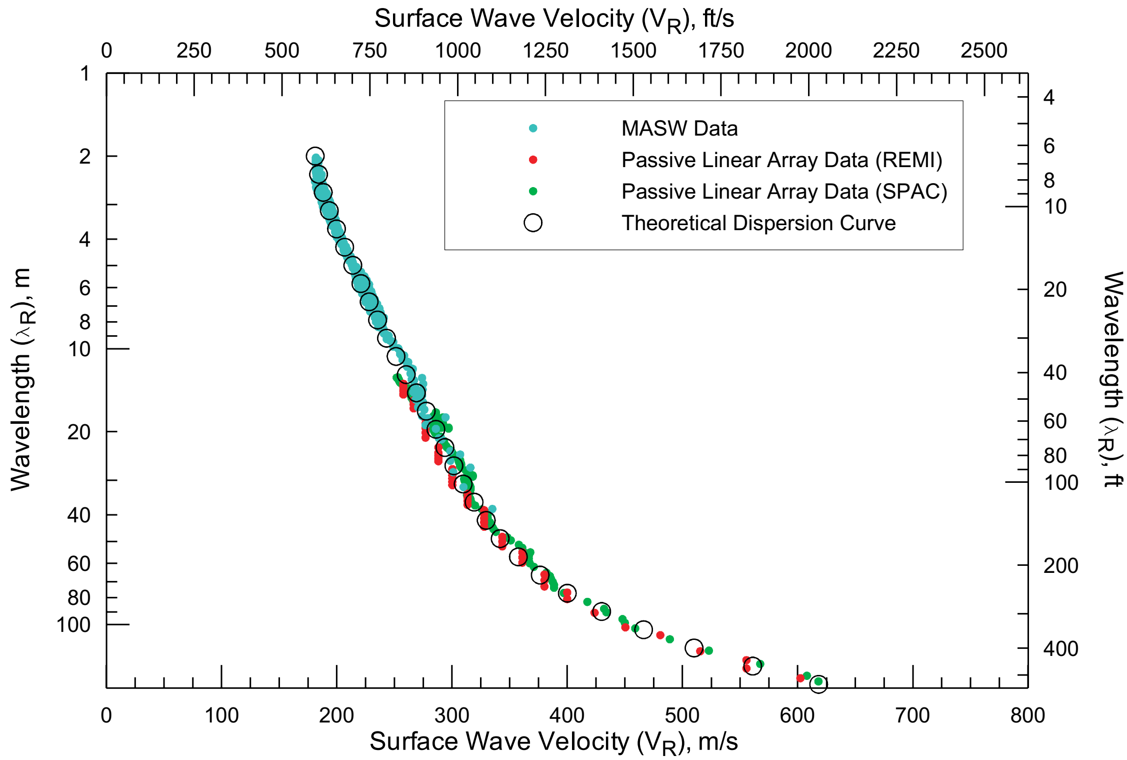

Comparison of Field Experimental Data and Theoretical Dispersion Curve from Active and Passive Surface Wave Array Z3-S15

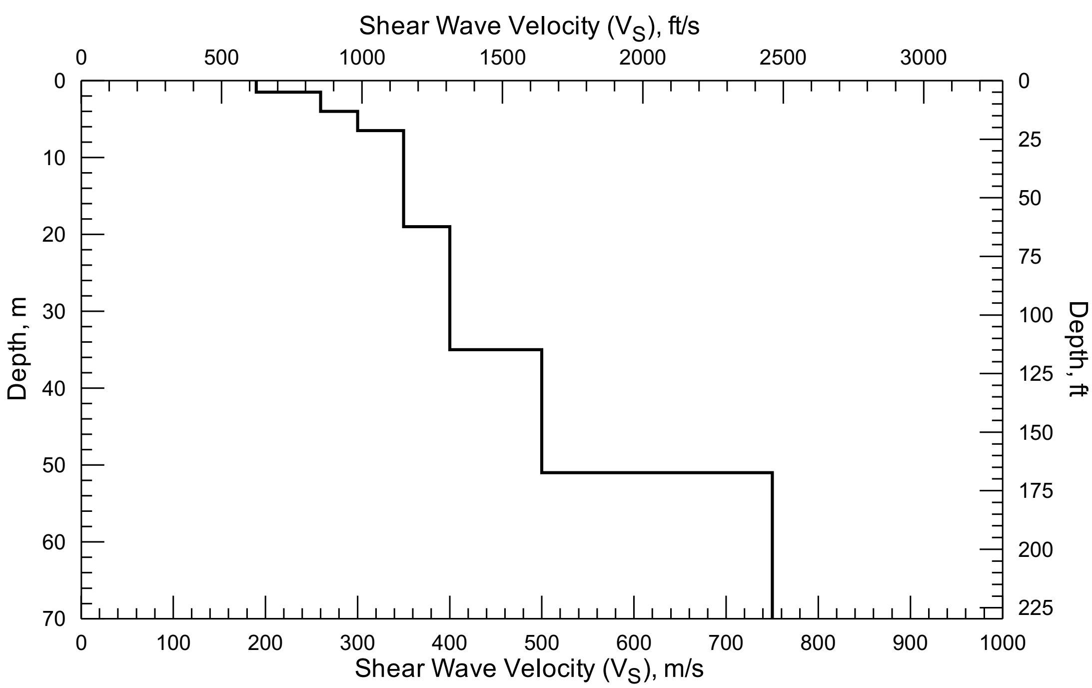

V_S Model from Active and Passive Surface Wave Array Z3-S15

GEOVision geophysical services	FIGURE 49 VELOCITY MODEL FOR ACTIVE AND PASSIVE SURFACE WAVE ARRAY Z3-S15
Project # 9001 Date: JUL 27, 2009 Drawn By: A MARTIN Approved By: [signature]	MONTEREY RD AND MERIDIAN AVE, SOUTH PASADENA, CALIFORNIA
File R:\...Project Files\2009\9001ch2mhill\report\figures\Figure49.cdr	PREPARED FOR CH2M HILL

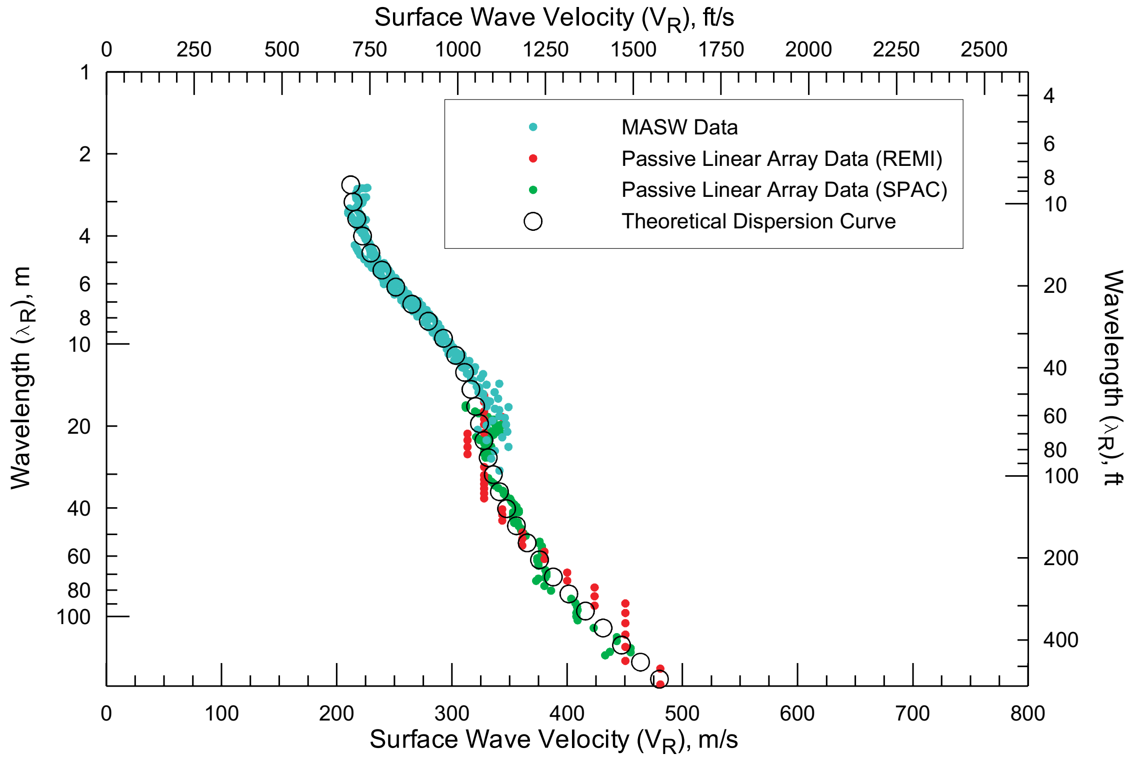

Comparison of Field Experimental Data and Theoretical Dispersion Curve from Active and Passive Surface Wave Array Z3-S16

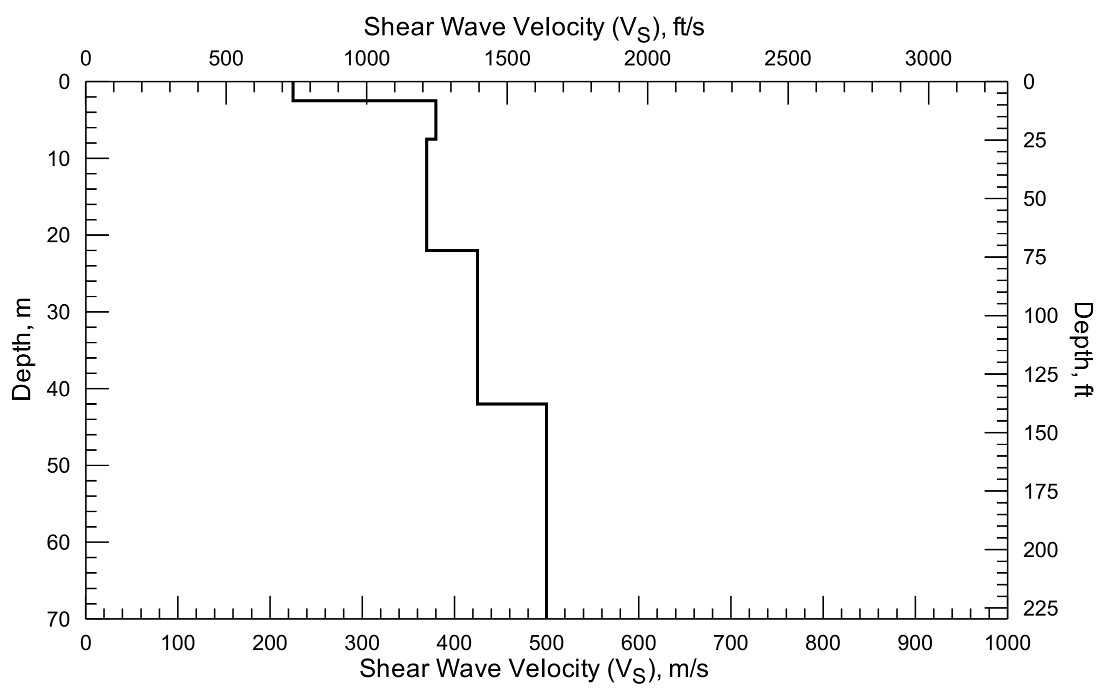

V_S Model from Active and Passive Surface Wave Array Z3-S16

GEOVision geophysical services	FIGURE 50 VELOCITY MODEL FOR ACTIVE AND PASSIVE SURFACE WAVE ARRAY Z3-S16
Project # 9001	MARENGO AVE AND SPRUCE ST, SOUTH PASADENA, CALIFORNIA
Date: JUL 27, 2009	
Drawn By: A MARTIN	
Approved By:	PREPARED FOR CH2M HILL
File R:\...Project Files\2009\9001ch2mhill\report\figures\Figure50.cdr	

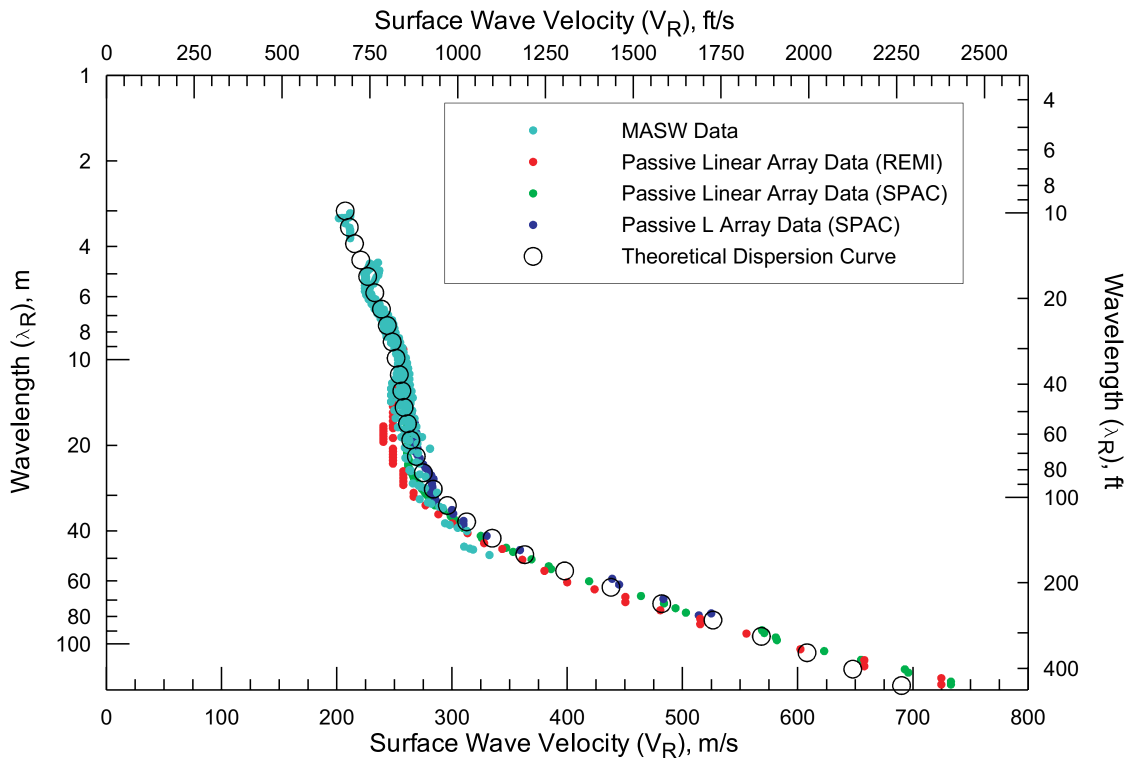

Comparison of Field Experimental Data and Theoretical Dispersion Curve from Active and Passive Surface Wave Array Z3-S17

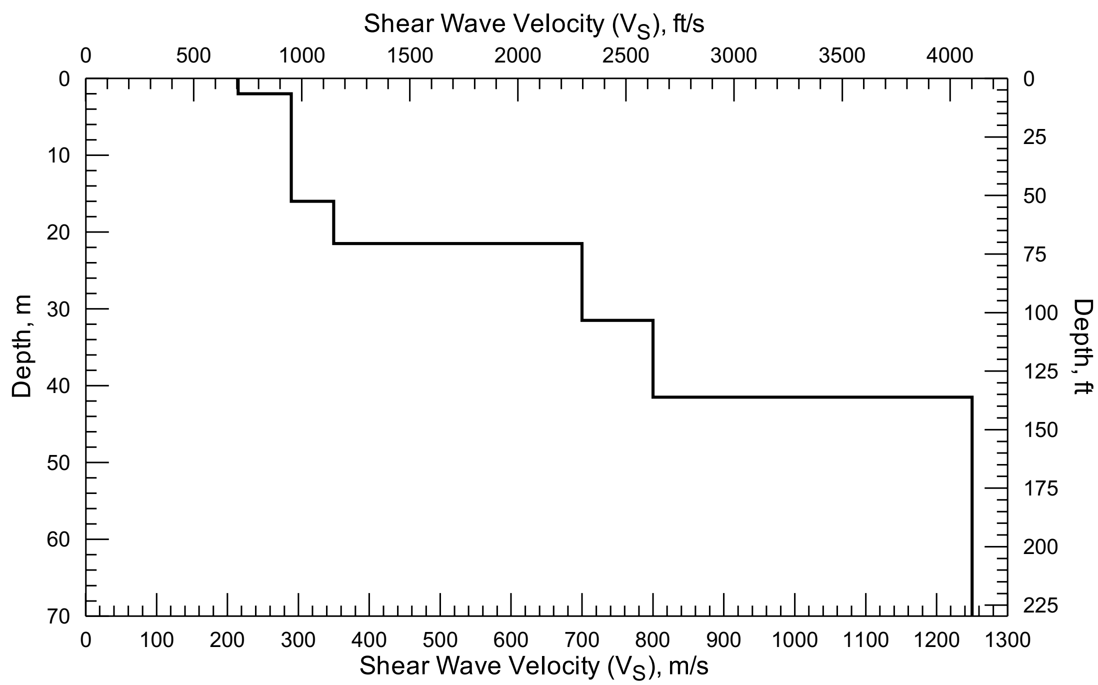

V_S Model from Active and Passive Surface Wave Array Z3-S17

GEOVision geophysical services	FIGURE 51 VELOCITY MODEL FOR ACTIVE AND PASSIVE SURFACE WAVE ARRAY Z3-S17
Project # 9001 Date: JUL 27, 2009	VIA DEL REY AND LOS ALISOS ST, SOUTH PASADENA, CALIFORNIA
Drawn By: A MARTIN Approved By: *[signature]* File R:\...Project Files\2009\9001ch2mhill\report\figures\Figure51.cdr	PREPARED FOR CH2M HILL

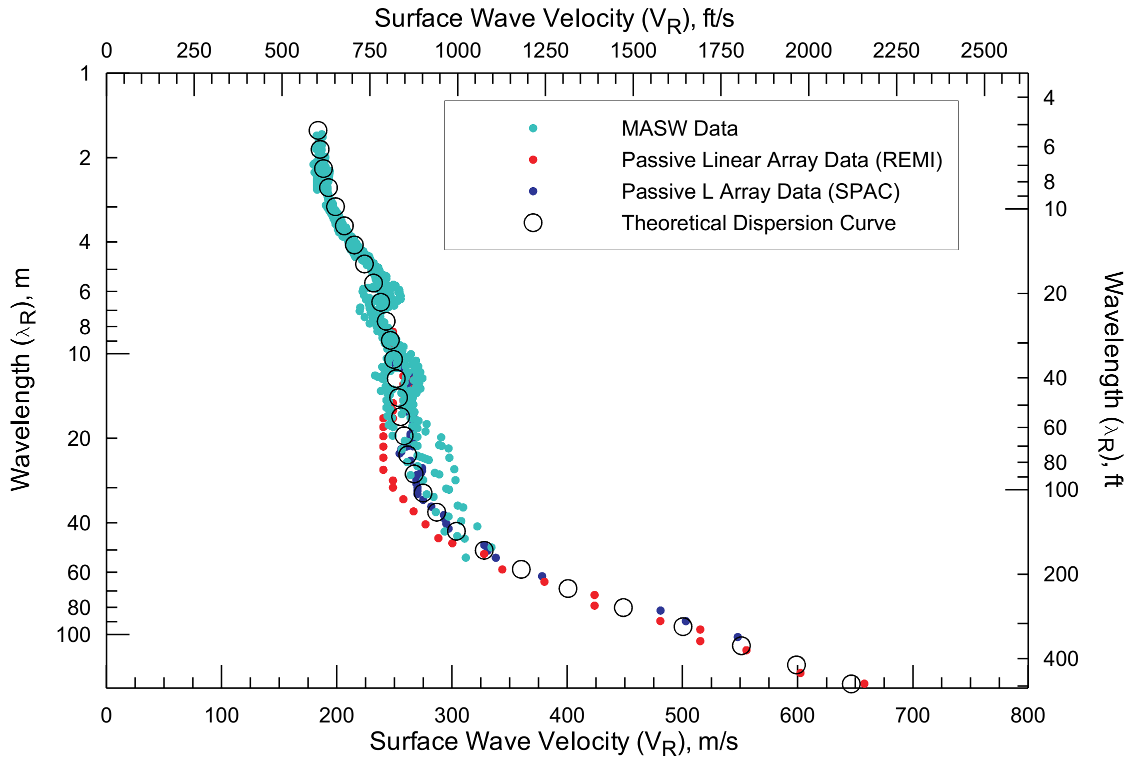

Comparison of Field Experimental Data and Theoretical Dispersion Curve from Active and Passive Surface Wave Array Z3-S18

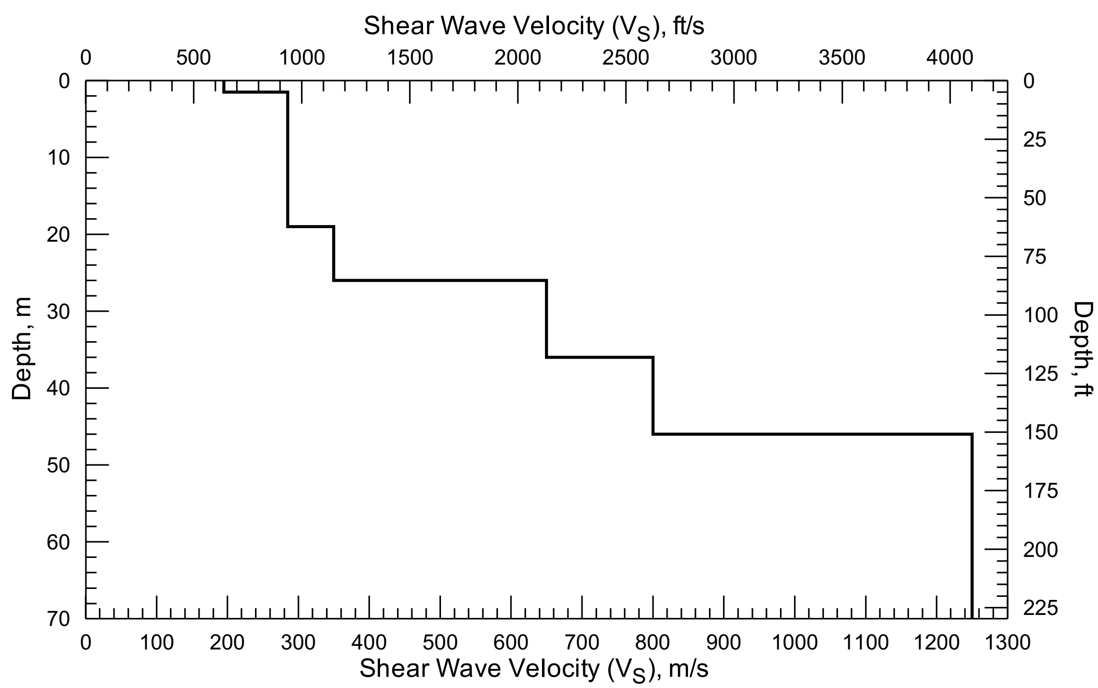

V_S Model from Active and Passive Surface Wave Array Z3-S18

GEOVision geophysical services	FIGURE 52 VELOCITY MODEL FOR ACTIVE AND PASSIVE SURFACE WAVE ARRAY Z3-S18
Project # 9001 Date: JUL 27, 2009 Drawn By: A MARTIN Approved By: [signature]	VIA DEL REY AND LA TERRAZA ST, SOUTH PASADENA, CALIFORNIA
File R:\...Project Files\2009\9001ch2mhill\report\figures\Figure52.cdr	PREPARED FOR CH2M HILL

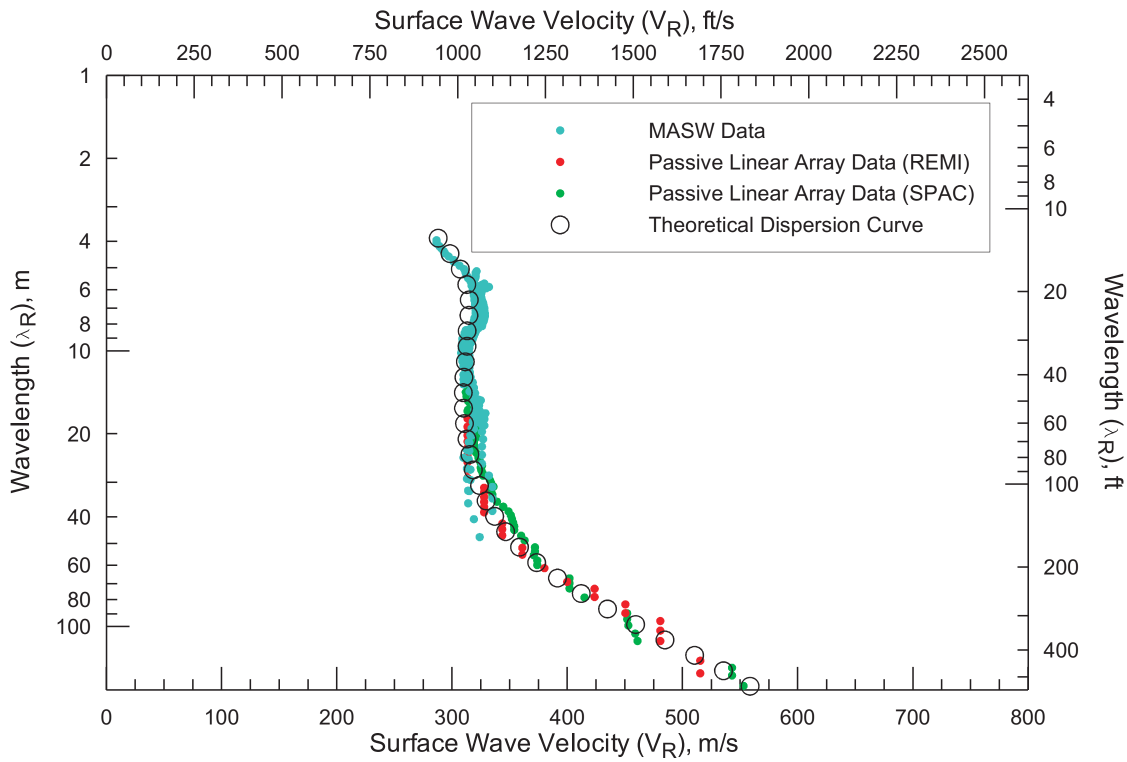

Comparison of Field Experimental Data and Theoretical Dispersion Curve from Active and Passive Surface Wave Array Z3-S19

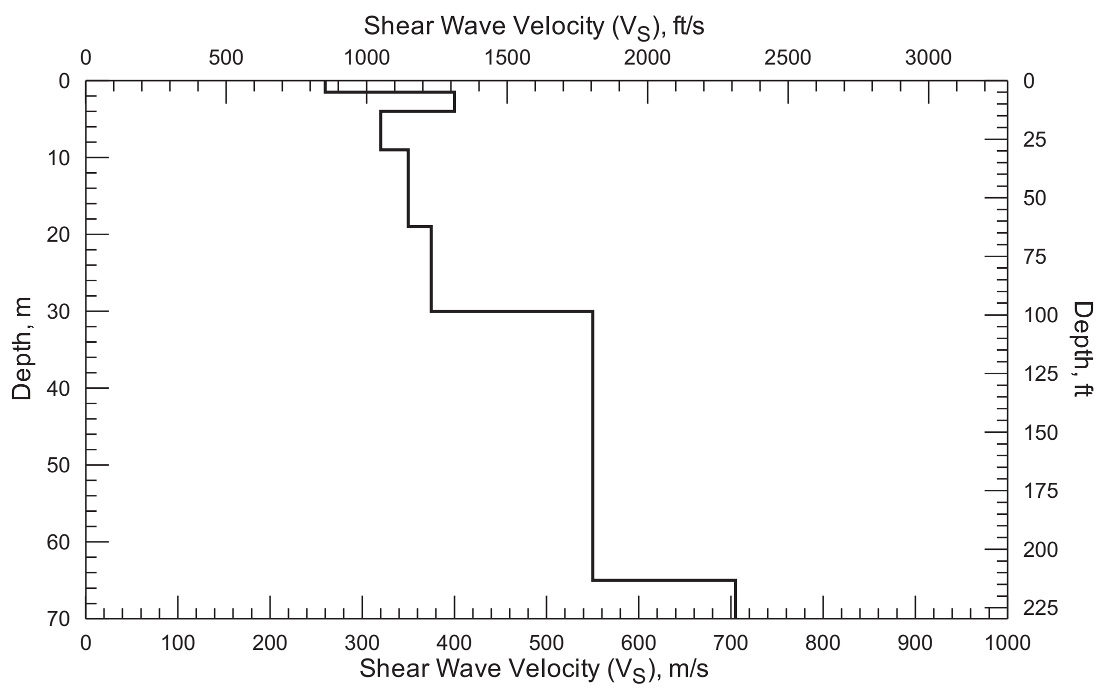

V_S Model from Active and Passive Surface Wave Array Z3-S19

GEOVision geophysical services	FIGURE 53 VELOCITY MODEL FOR ACTIVE AND PASSIVE SURFACE WAVE ARRAY Z3-S19
Project # 9001 Date: JUL 27, 2009	BERKSHIRE AVE AND KENDALL AVE, LOS ANGELES, CALIFORNIA
Drawn By: A MARTIN Approved By:	PREPARED FOR CH2M HILL

File R:\...Project Files\2009\9001ch2mhill\report\figures\Figure53.cdr

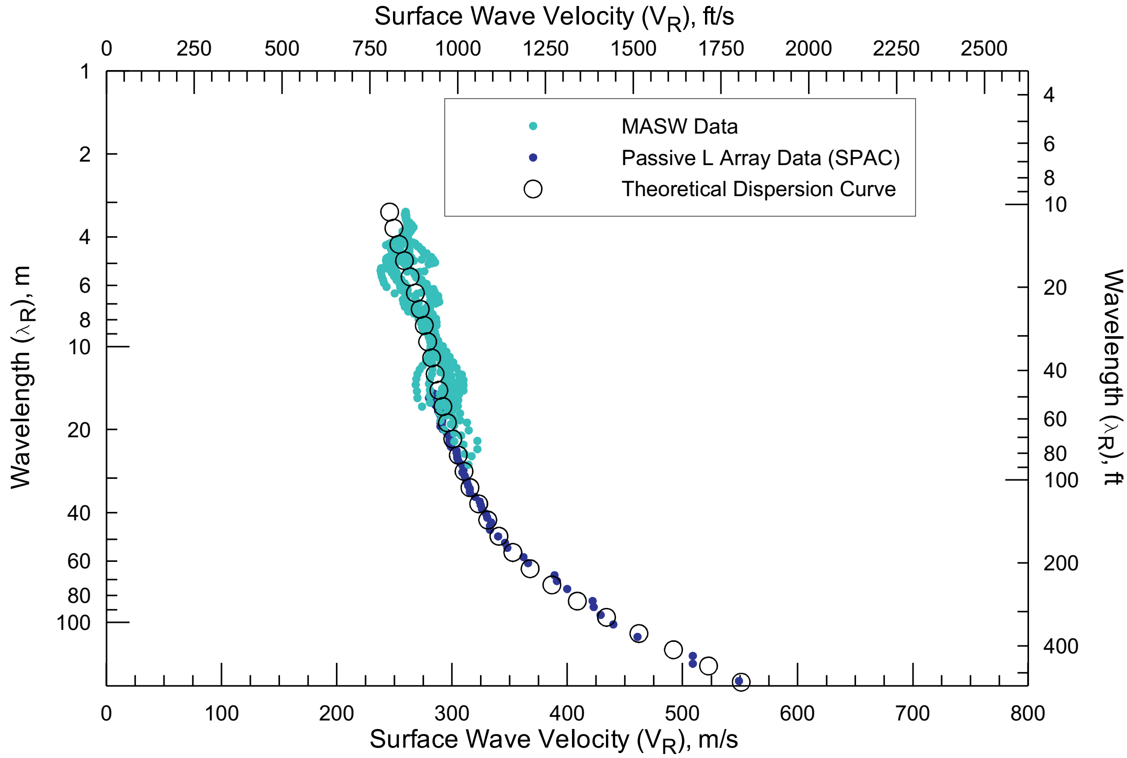

Comparison of Field Experimental Data and Theoretical Dispersion Curve from Active and Passive Surface Wave Array Z3-S20

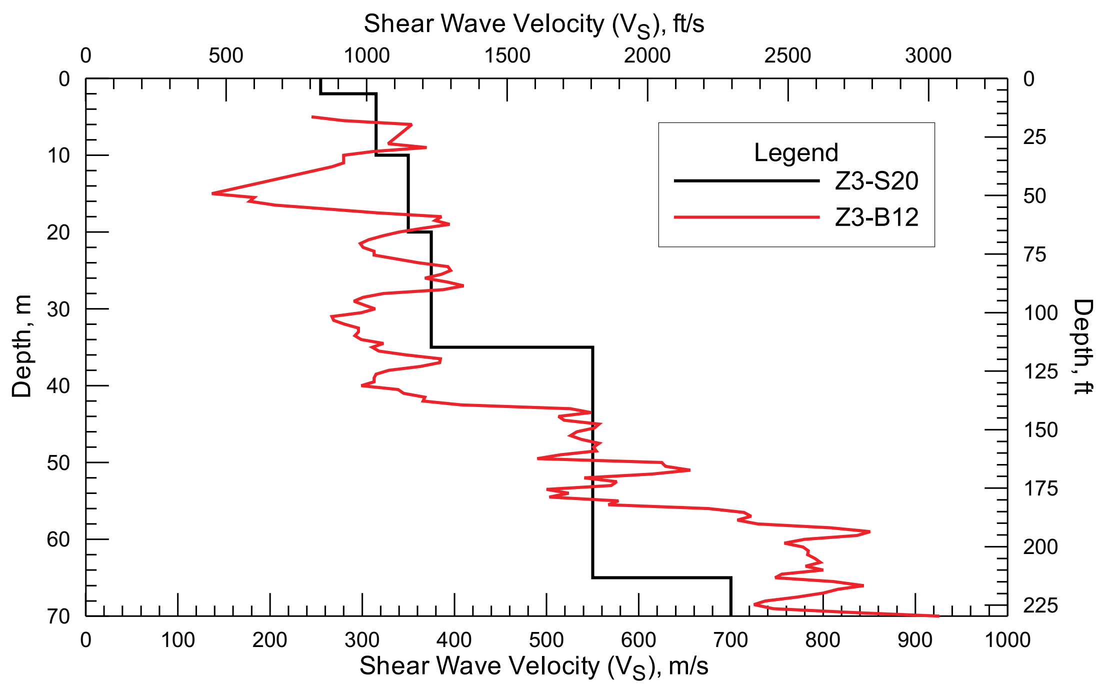

V_S Model from Active and Passive Surface Wave Array Z3-S20

GEOVision geophysical services	FIGURE 54 VELOCITY MODEL FOR ACTIVE AND PASSIVE SURFACE WAVE ARRAY Z3-S20
Project # 9001 Date: JUL 27, 2009 Drawn By: A MARTIN Approved By: [signature]	WESTMONT DR AND KEATS ST, ALHAMBRA, CALIFORNIA
File R:\...Project Files\2009\9001ch2mhill\report\figures\Figure54.cdr	PREPARED FOR CH2M HILL

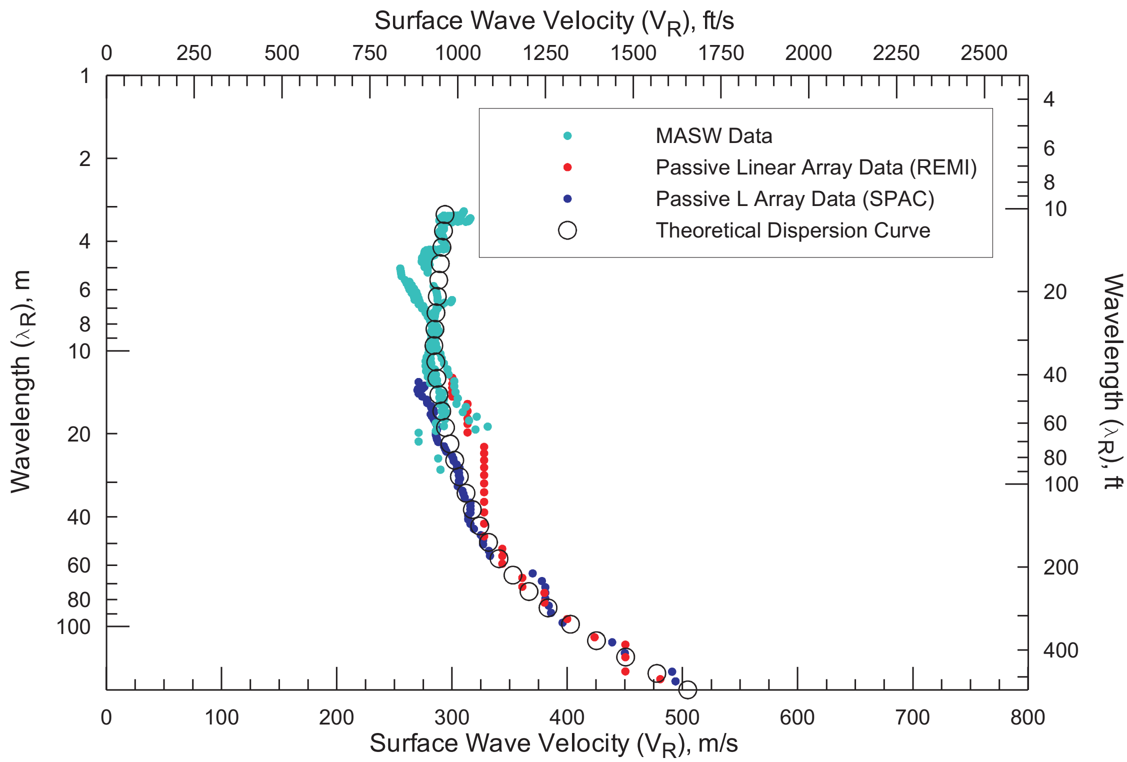

Comparison of Field Experimental Data and Theoretical Dispersion Curve from Active and Passive Surface Wave Array Z3-S21

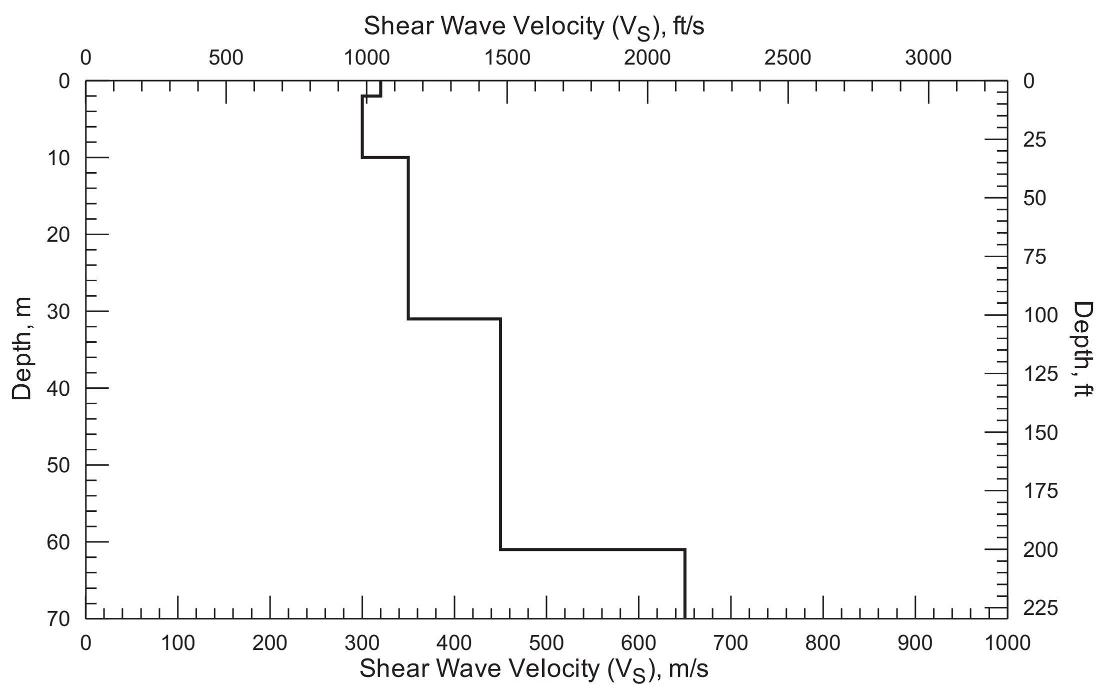

V_S Model from Active and Passive Surface Wave Array Z3-S21

GEOVision geophysical services	FIGURE 55 VELOCITY MODEL FOR ACTIVE AND PASSIVE SURFACE WAVE ARRAY Z3-S21
Project # 9001 Date: JUL 27, 2009 Drawn By: A MARTIN Approved By: Antony J Martin	WINCHESTER AVE AND NORWICH AVE, ALHAMBRA, CALIFORNIA
File R:\...Project Files\2009\9001ch2mhill\report\figures\Figure55.cdr	PREPARED FOR CH2M HILL

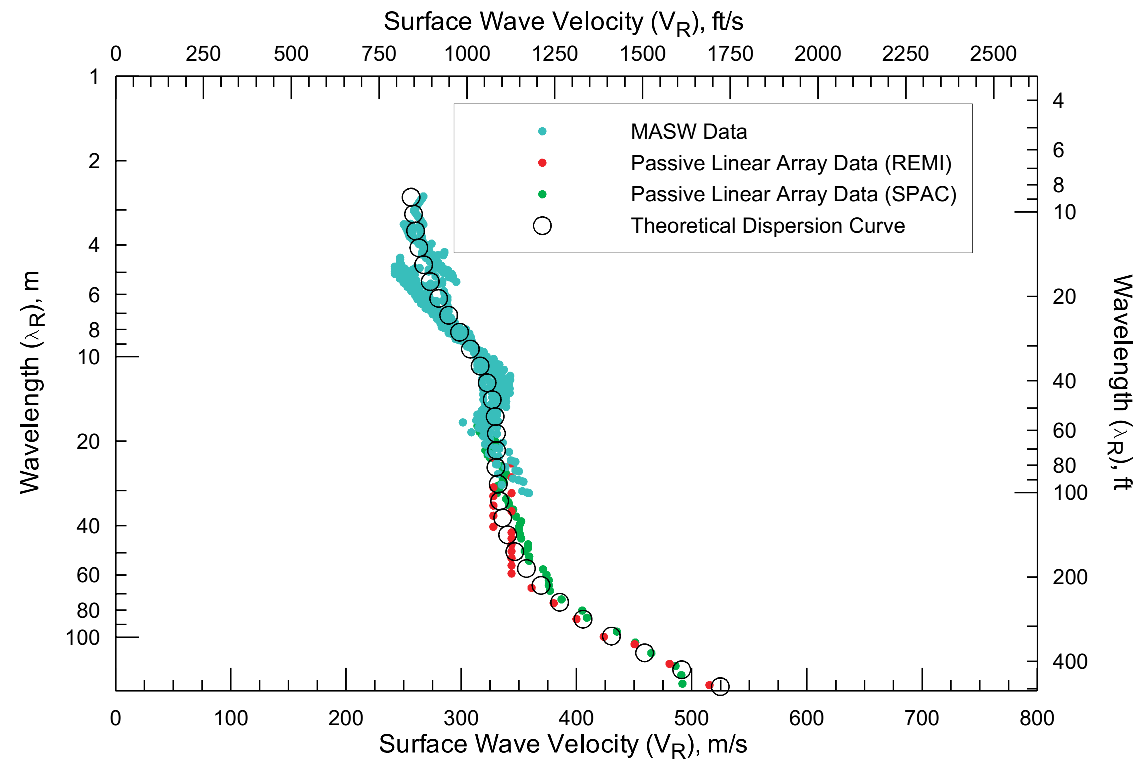

Comparison of Field Experimental Data and Theoretical Dispersion Curve from Active and Passive Surface Wave Array Z3-S22

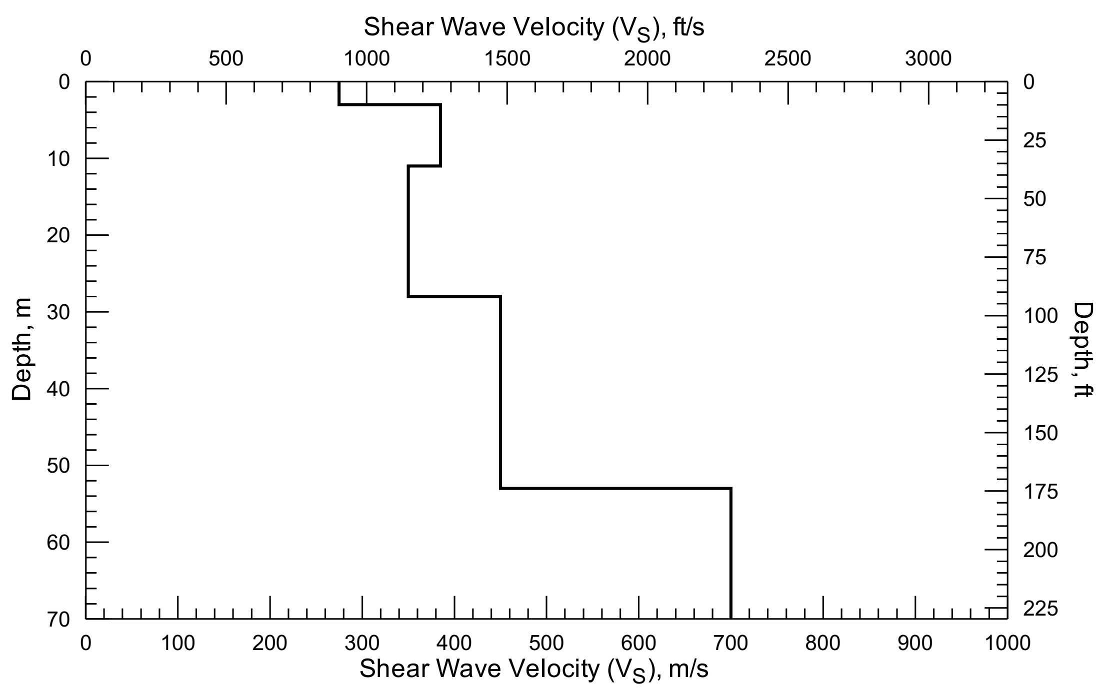

V_S Model from Active and Passive Surface Wave Array Z3-S22

GEOVision geophysical services

Project # 9001	FIGURE 56 VELOCITY MODEL FOR ACTIVE AND PASSIVE SURFACE WAVE ARRAY Z3-S22
Date: JUL 27, 2009	WINCHESTER AVE AND CONCORD AVE, ALHAMBRA, CALIFORNIA
Drawn By: A MARTIN	
Approved By: [signature]	PREPARED FOR CH2M HILL
File R:\...Project Files\2009\9001ch2mhill\report\figures\Figure56.cdr	

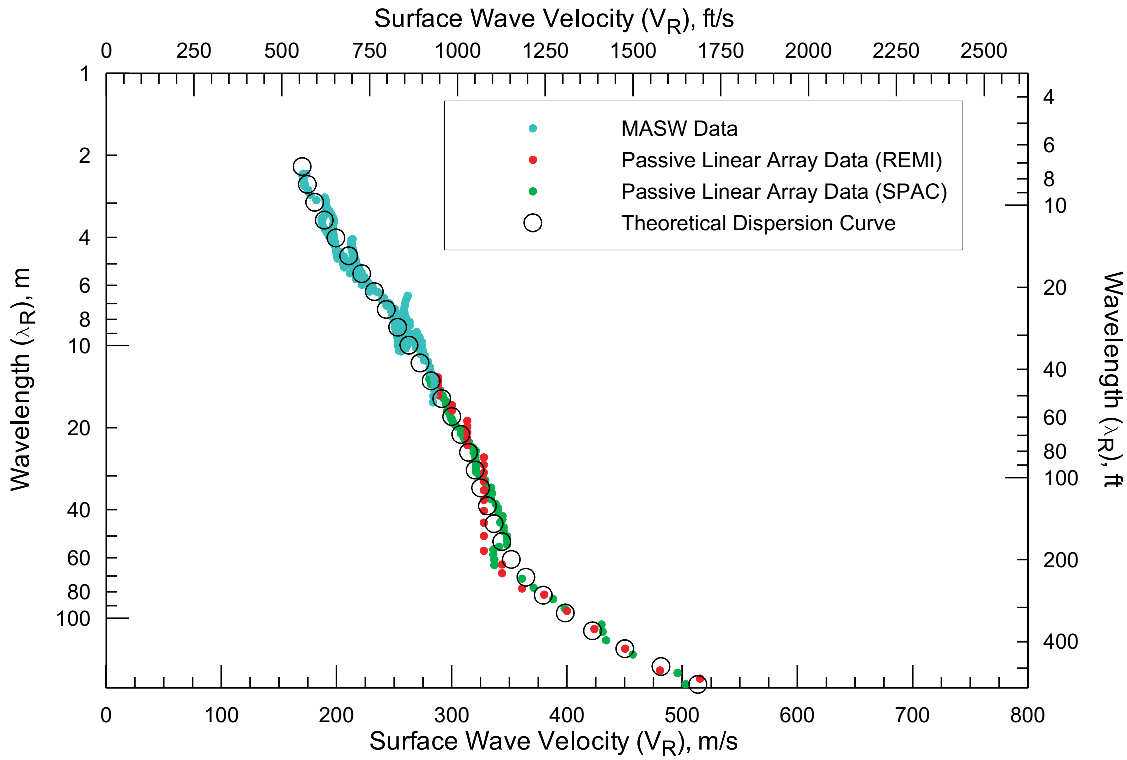

Comparison of Field Experimental Data and Theoretical Dispersion Curve from Active and Passive Surface Wave Array Z3-S23

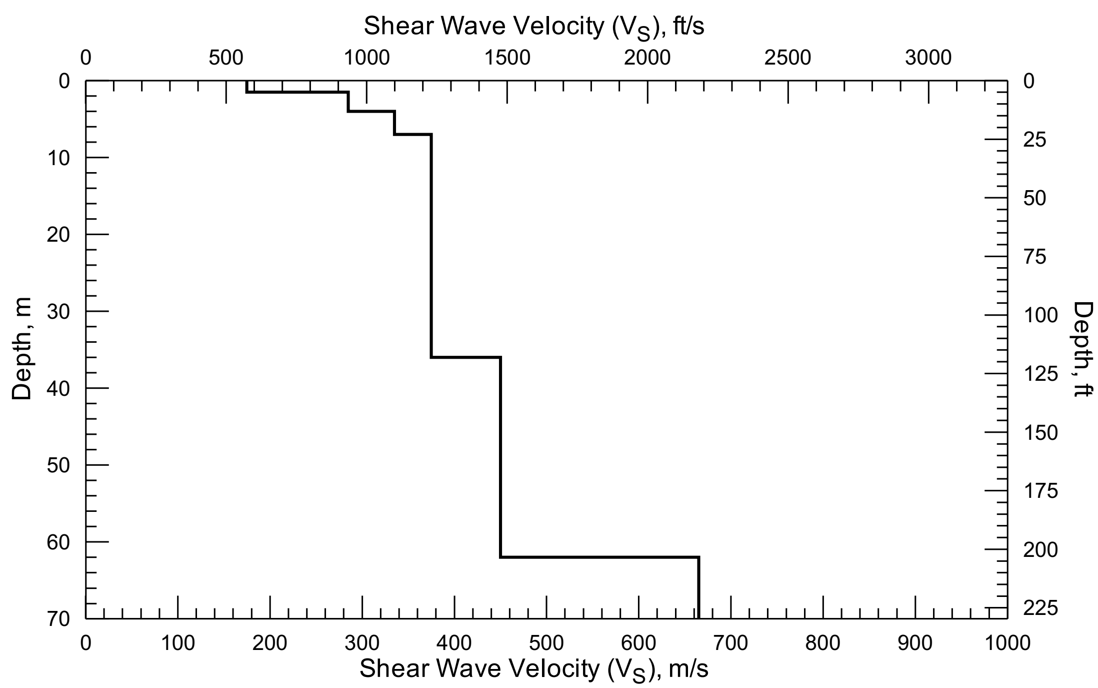

V_S Model from Active and Passive Surface Wave Array Z3-S23

GEOVision geophysical services	FIGURE 57 VELOCITY MODEL FOR ACTIVE AND PASSIVE SURFACE WAVE ARRAY Z3-S23
Project # 9001	WESTMONT DR AND VALLEY BLVD, ALHAMBRA, CALIFORNIA
Date: JUL 27, 2009	
Drawn By: A MARTIN	
Approved By: Antony J Martin	PREPARED FOR CH2M HILL
File R:\...Project Files\2009\9001ch2mhill\report\figures\Figure57.cdr	

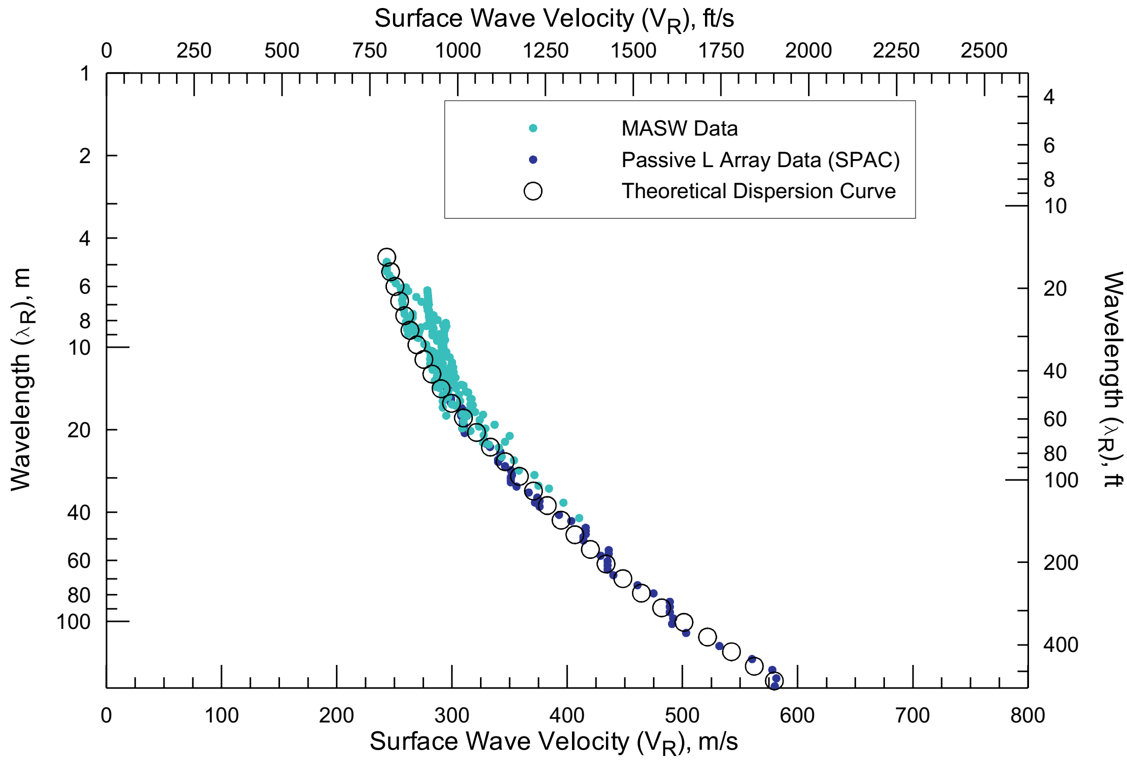

Comparison of Field Experimental Data and Theoretical Dispersion Curve from Active and Passive Surface Wave Array Z3-S24

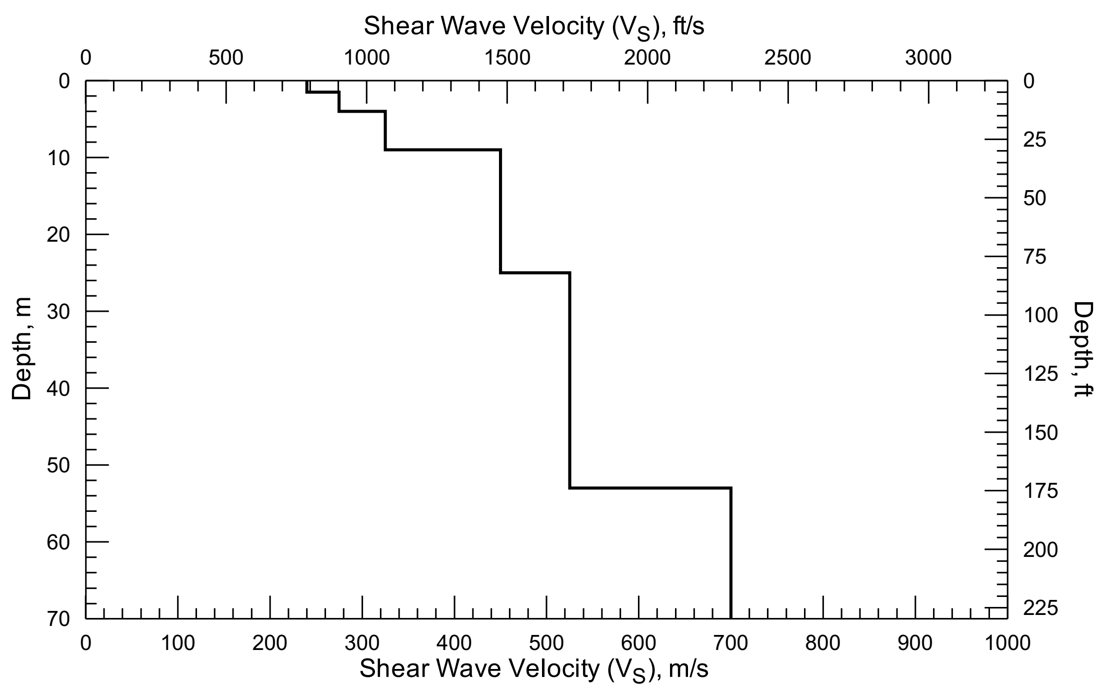

V_S Model from Active and Passive Surface Wave Array Z3-S24

GEOVision geophysical services

Project # 9001
Date: JUL 27, 2009
Drawn By: A MARTIN
Approved By: [signature]
File R:\...Project Files\2009\9001ch2mhill\report\figures\Figure58.cdr

FIGURE 58
VELOCITY MODEL FOR ACTIVE AND PASSIVE SURFACE WAVE ARRAY Z3-S24

WESTMONT DR AND GLENAVEN AVE, ALHAMBRA, CALIFORNIA

PREPARED FOR
CH2M HILL

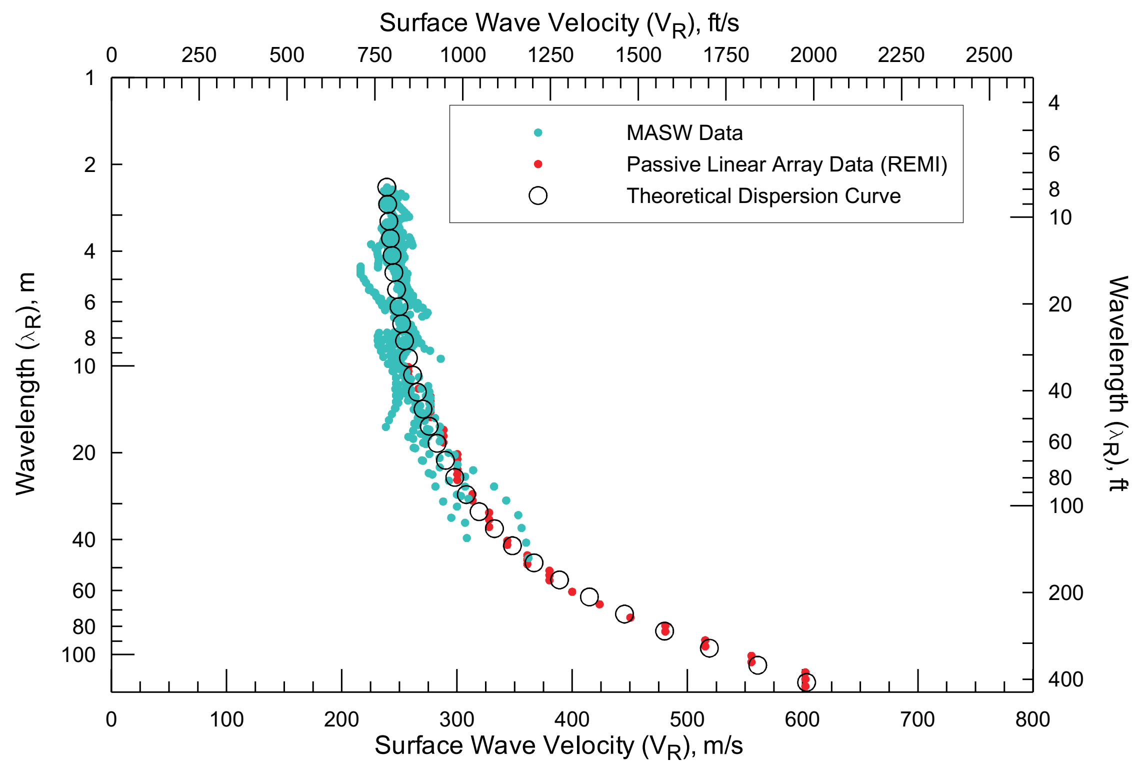

Comparison of Field Experimental Data and Theoretical Dispersion Curve from Active and Passive Surface Wave Array Z4-S1

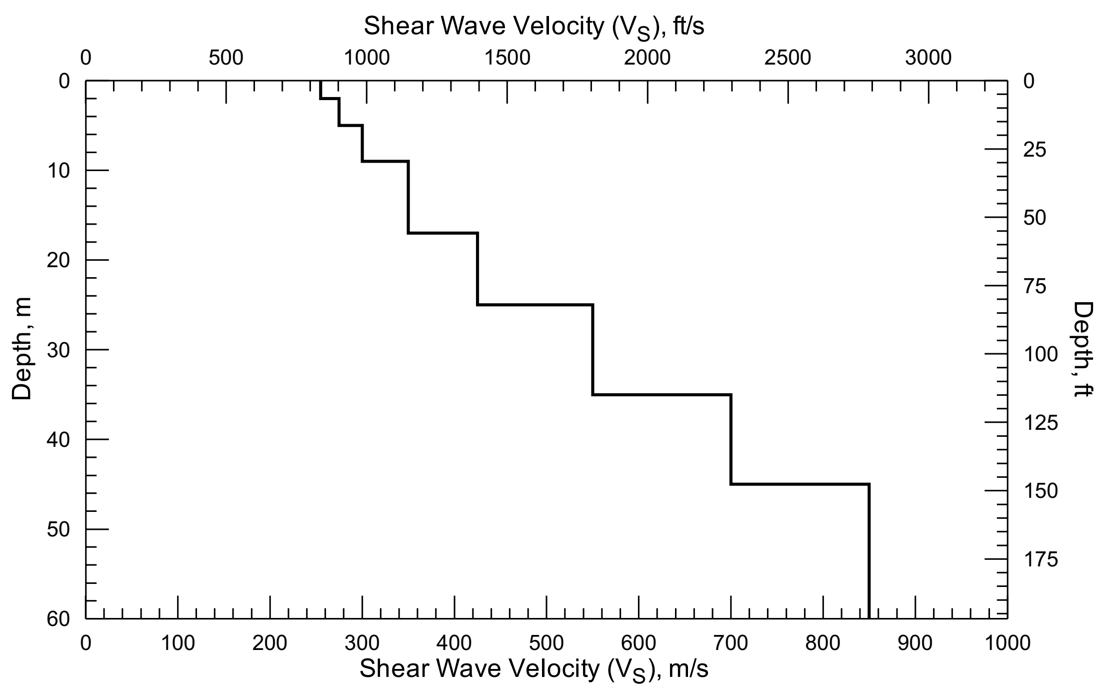

V_S Model from Active and Passive Surface Wave Array Z4-S1

GEOVision geophysical services

Project # 9001
Date: JUL 29, 2009
Drawn By: A MARTIN
Approved By: Antony J Martin
File R:\...Project Files\2009\9001ch2mhill\report\figures\Figure59.cdr

FIGURE 59
VELOCITY MODEL FOR ACTIVE AND PASSIVE SURFACE WAVE ARRAY Z4-S1

ONEIDA ST AND S VINEDO AVE, PASADENA, CALIFORNIA

PREPARED FOR
CH2M HILL

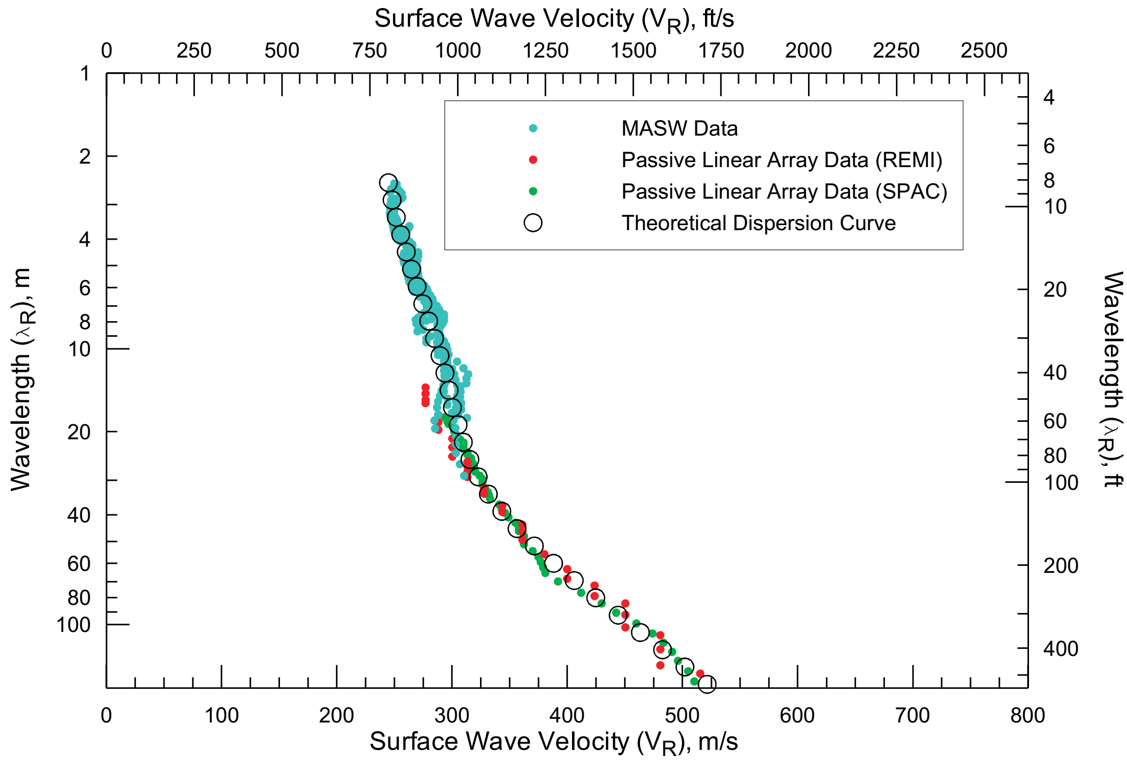

Comparison of Field Experimental Data and Theoretical Dispersion Curve from Active and Passive Surface Wave Array Z4-S2

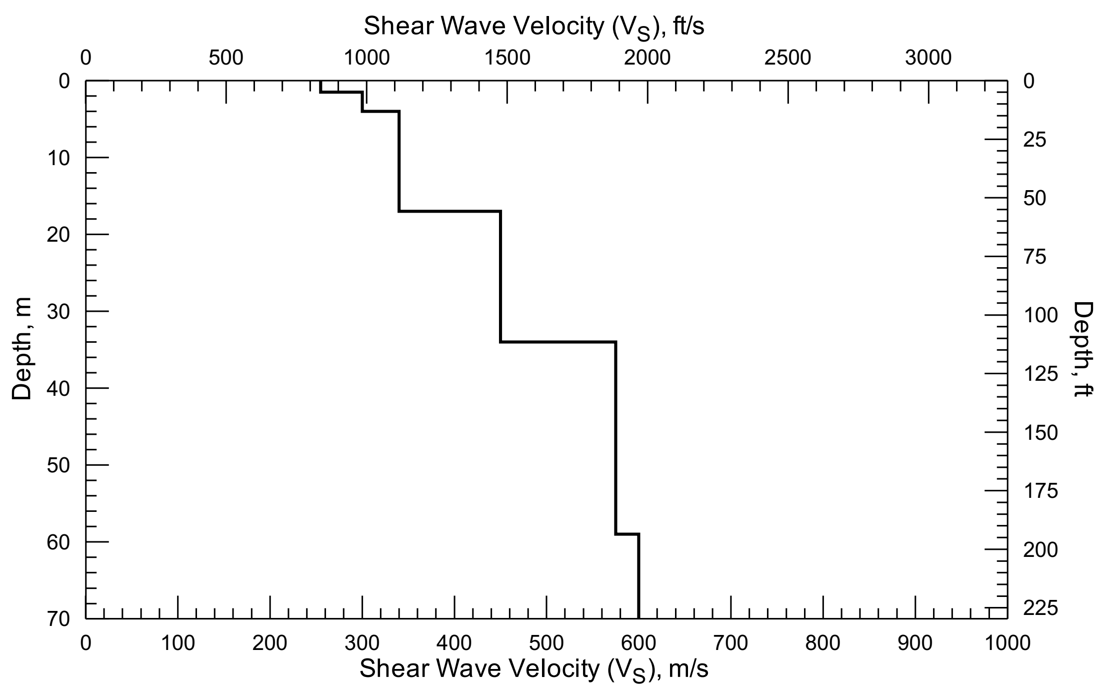

V_S Model from Active and Passive Surface Wave Array Z4-S2

GEOVision geophysical services	FIGURE 60 VELOCITY MODEL FOR ACTIVE AND PASSIVE SURFACE WAVE ARRAY Z4-S2
Project # 9001 Date: JUL 29, 2009 Drawn By: A MARTIN Approved By:	OXFORD RD NEAR ORLANDO RD, SAN MARINO, CALIFORNIA
File R:\...Project Files\2009\9001ch2mhill\report\figures\Figure60.cdr	PREPARED FOR CH2M HILL

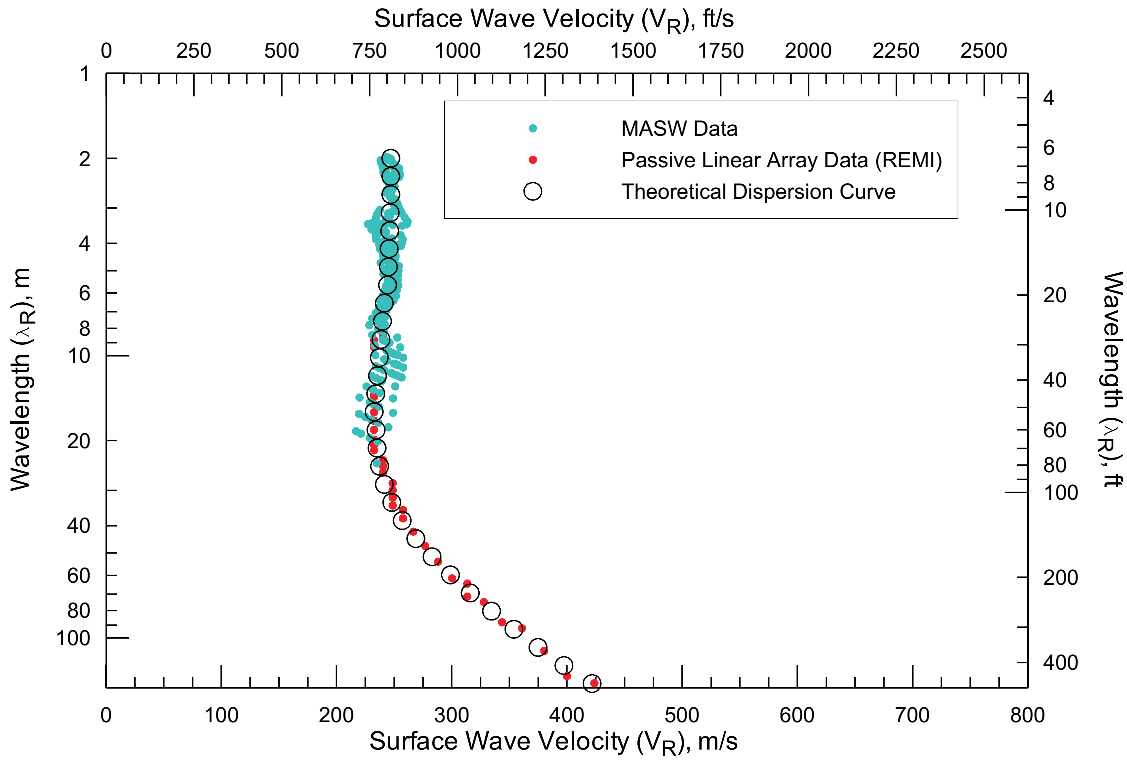

Comparison of Field Experimental Data and Theoretical Dispersion Curve from Active and Passive Surface Wave Array Z4-S3

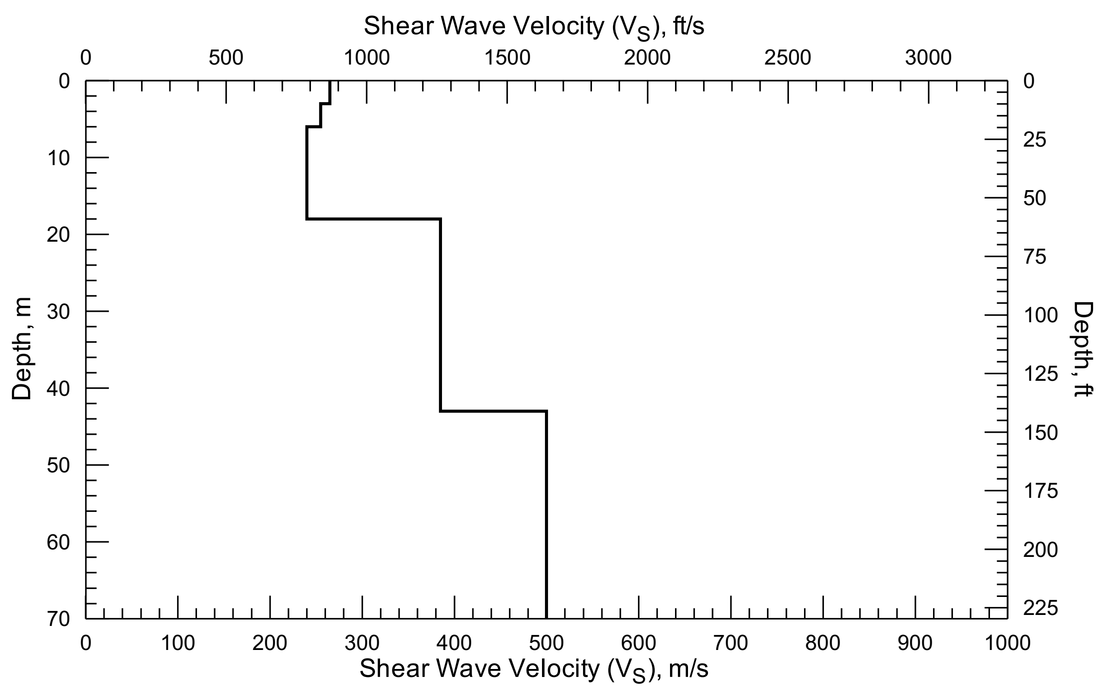

V_S Model from Active and Passive Surface Wave Array Z4-S3

GEOVision geophysical services	FIGURE 61 VELOCITY MODEL FOR ACTIVE AND PASSIVE SURFACE WAVE ARRAY Z4-S3
Project # 9001 Date: JUL 29, 2009 Drawn By: A MARTIN Approved By: Antony J Martin	OXFORD RD NEAR STRATFORD RD, SAN MARINO, CALIFORNIA
File R:\...Project Files\2009\9001ch2mhill\report\figures\Figure61.cdr	PREPARED FOR CH2M HILL

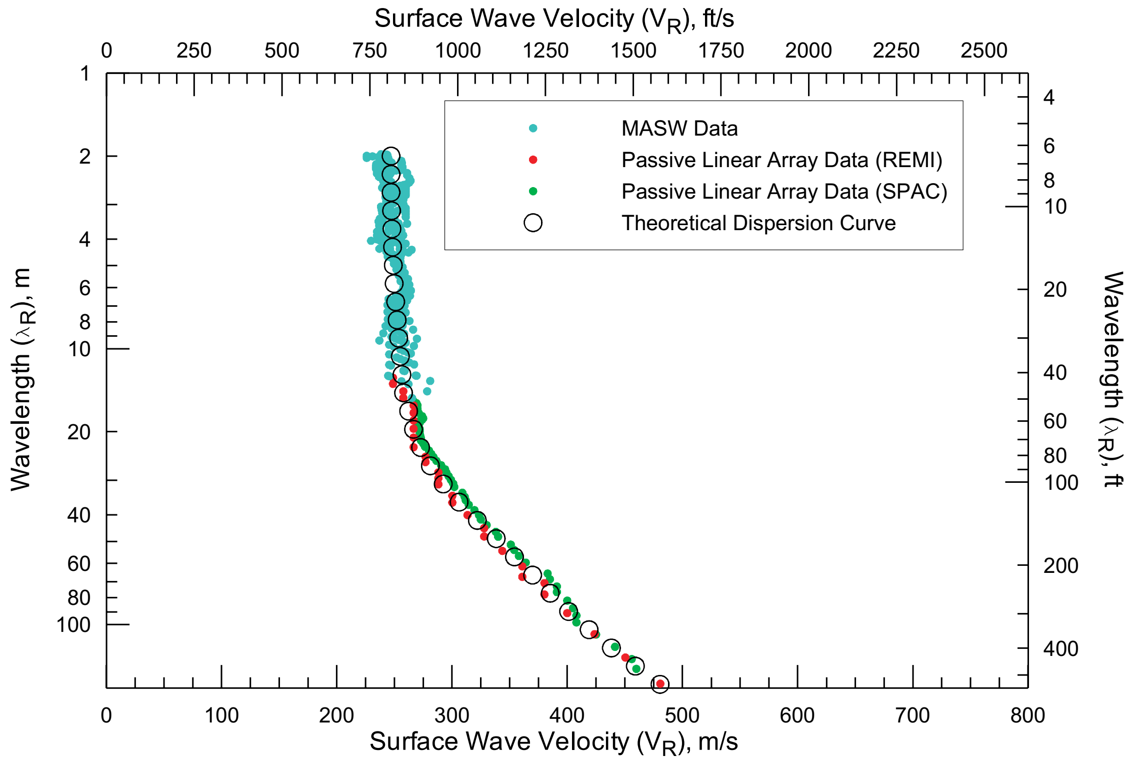

Comparison of Field Experimental Data and Theoretical Dispersion Curve from Active and Passive Surface Wave Array Z4-S4

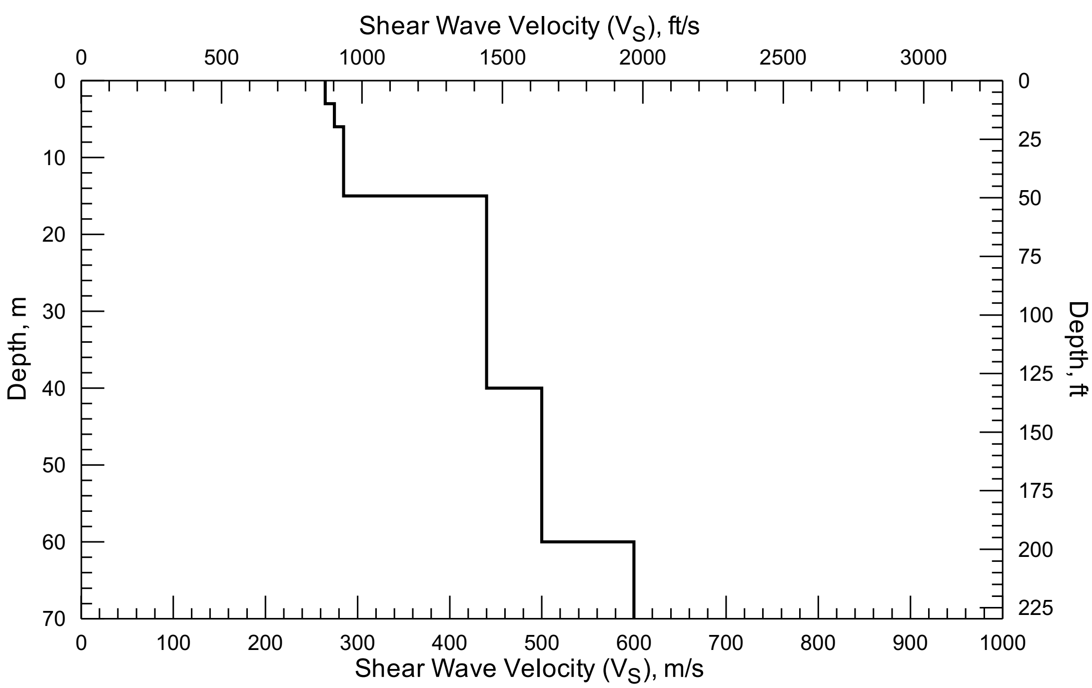

V_S Model from Active and Passive Surface Wave Array Z4-S4

GEOVision geophysical services

Project # 9001	FIGURE 62 VELOCITY MODEL FOR ACTIVE AND PASSIVE SURFACE WAVE ARRAY Z4-S4
Date: JUL 29, 2009	OXFORD RD NEAR EUSTON RD, SAN MARINO, CALIFORNIA
Drawn By: A MARTIN	
Approved By:	PREPARED FOR CH2M HILL

File R:\...Project Files\2009\9001ch2mhill\report\figures\Figure62.cdr

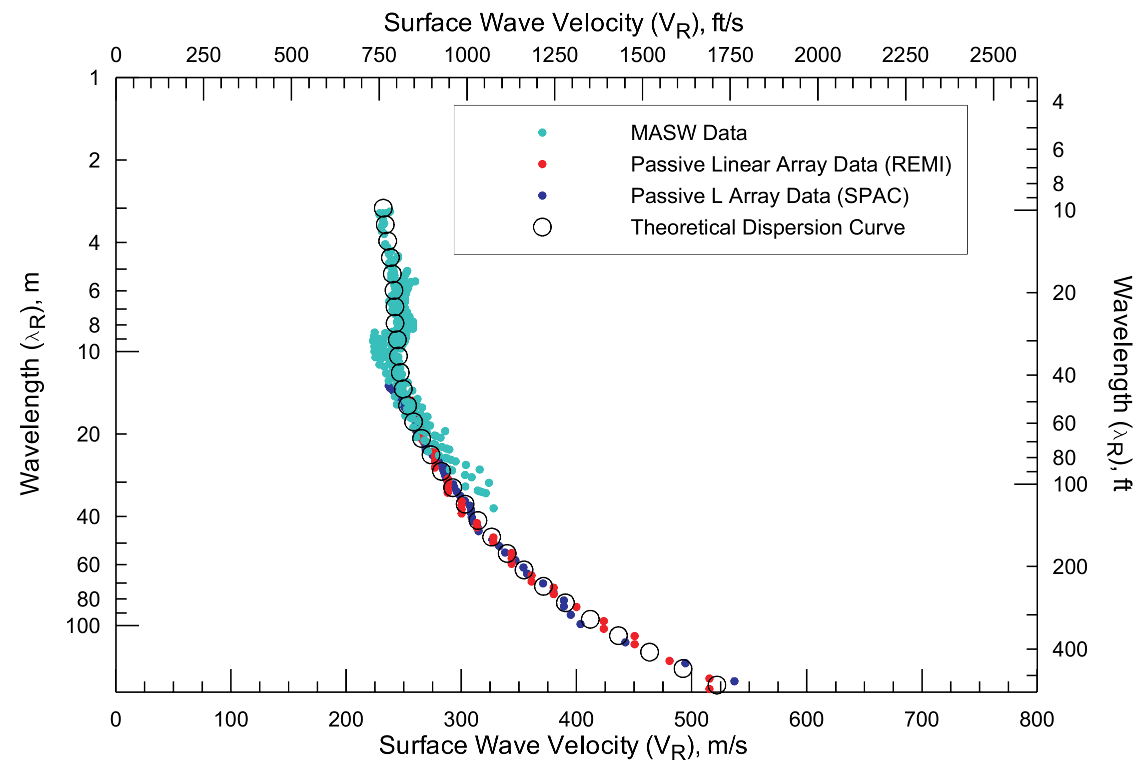

Comparison of Field Experimental Data and Theoretical Dispersion Curve from Active and Passive Surface Wave Array Z4-S5

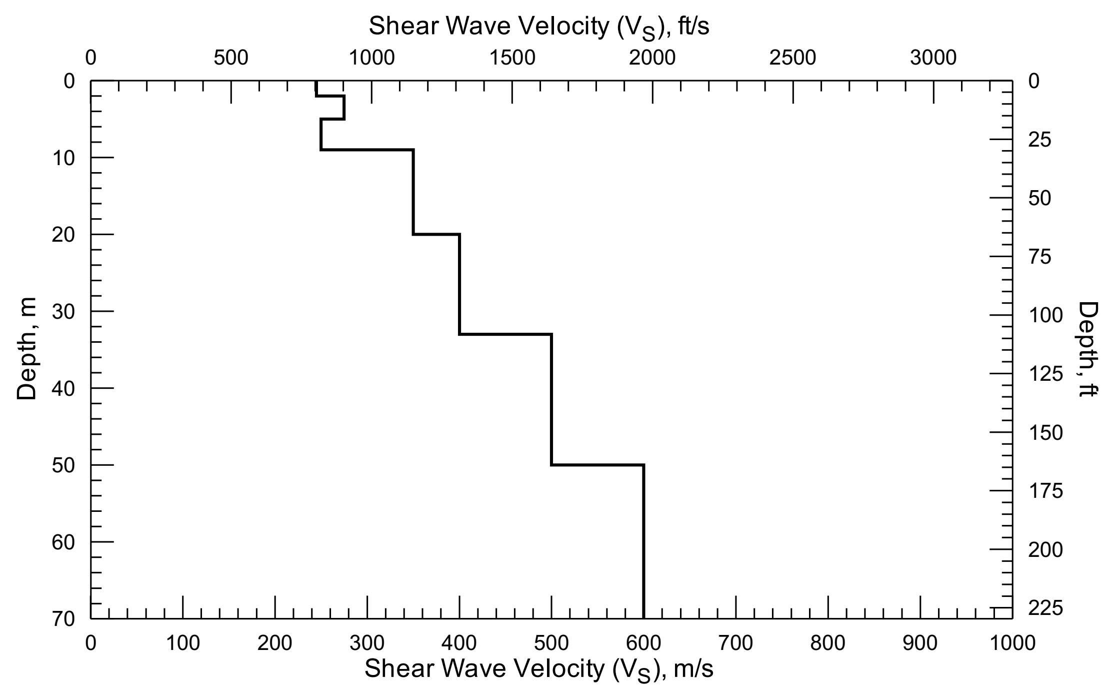

V_S Model from Active and Passive Surface Wave Array Z4-S5

GEOVision geophysical services

Project # 9001
Date: JUL 29, 2009
Drawn By: A MARTIN
Approved By: [signature]
File R:\...Project Files\2009\9001ch2mhill\report\figures\Figure63.cdr

FIGURE 63
VELOCITY MODEL FOR ACTIVE AND PASSIVE SURFACE WAVE ARRAY Z4-S5

MONTEREY RD AND VIRGIIA RD, SAN MARINO, CALIFORNIA

PREPARED FOR
CH2M HILL

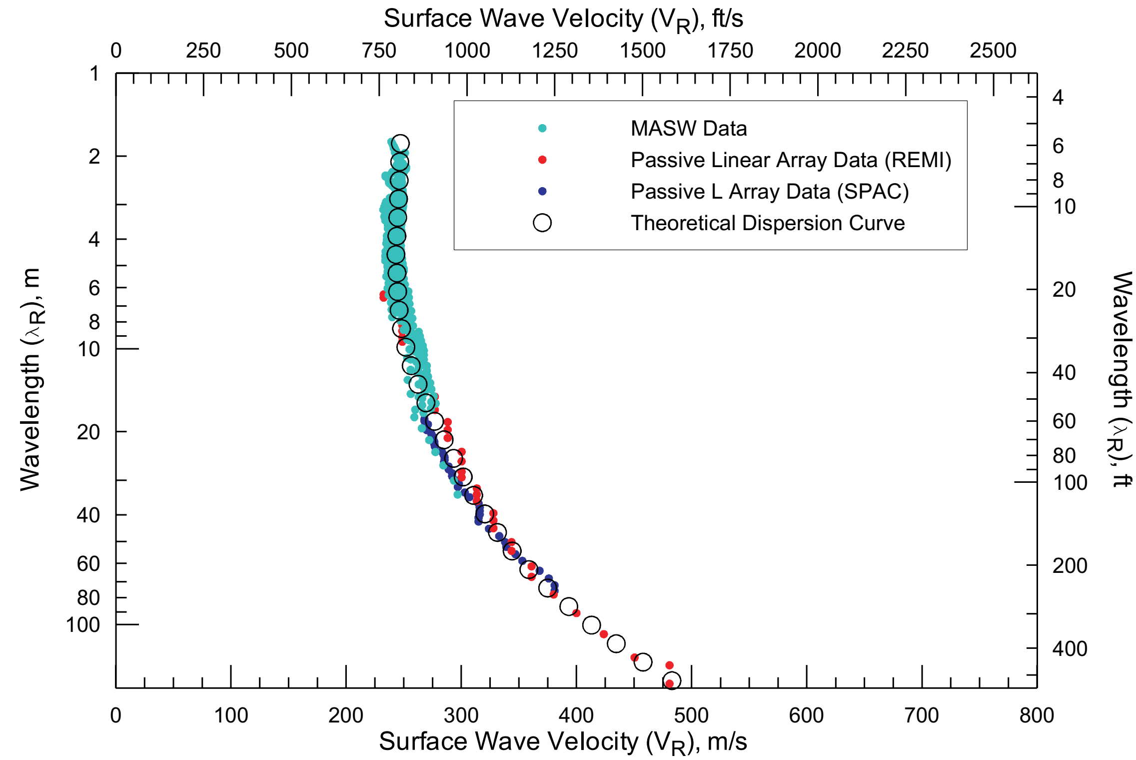

Comparison of Field Experimental Data and Theoretical Dispersion Curve from Active and Passive Surface Wave Array Z4-S6

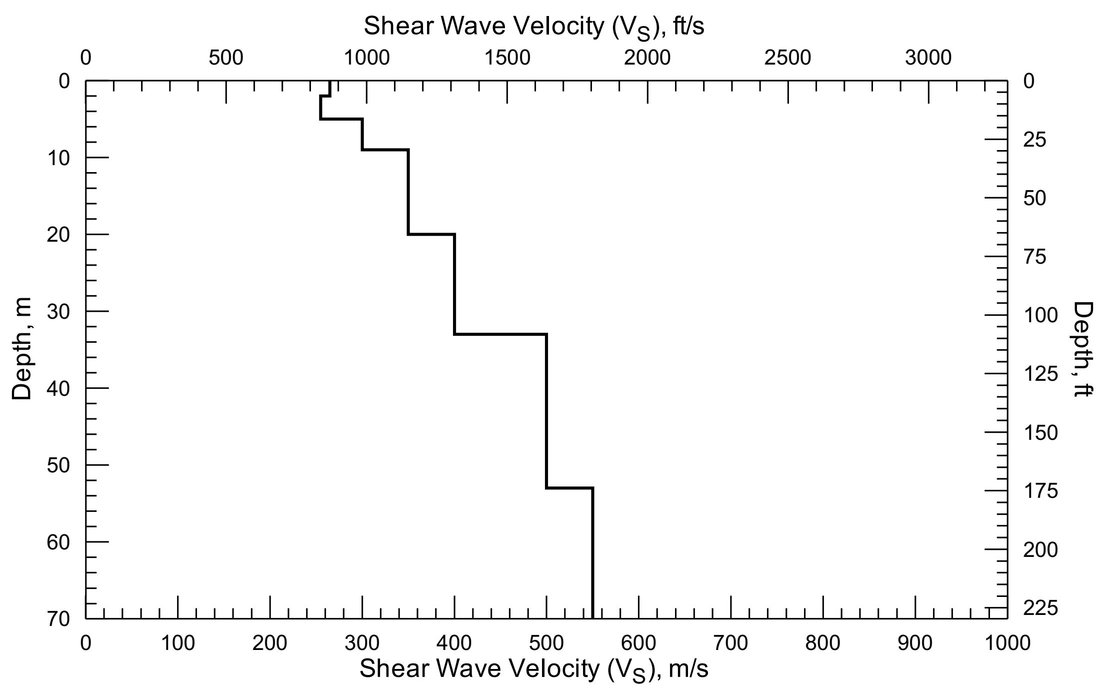

V_S Model from Active and Passive Surface Wave Array Z4-S6

GEOVision geophysical services

Project # 9001	FIGURE 64 VELOCITY MODEL FOR ACTIVE AND PASSIVE SURFACE WAVE ARRAY Z4-S6
Date: JUL 29, 2009	HUNTINGTON DR AND GRANADA AVE, SAN MARINO, CALIFORNIA
Drawn By: A MARTIN	
Approved By: Antony J Martin	PREPARED FOR CH2M HILL
File R:\...Project Files\2009\9001ch2mhill\report\figures\Figure64.cdr	

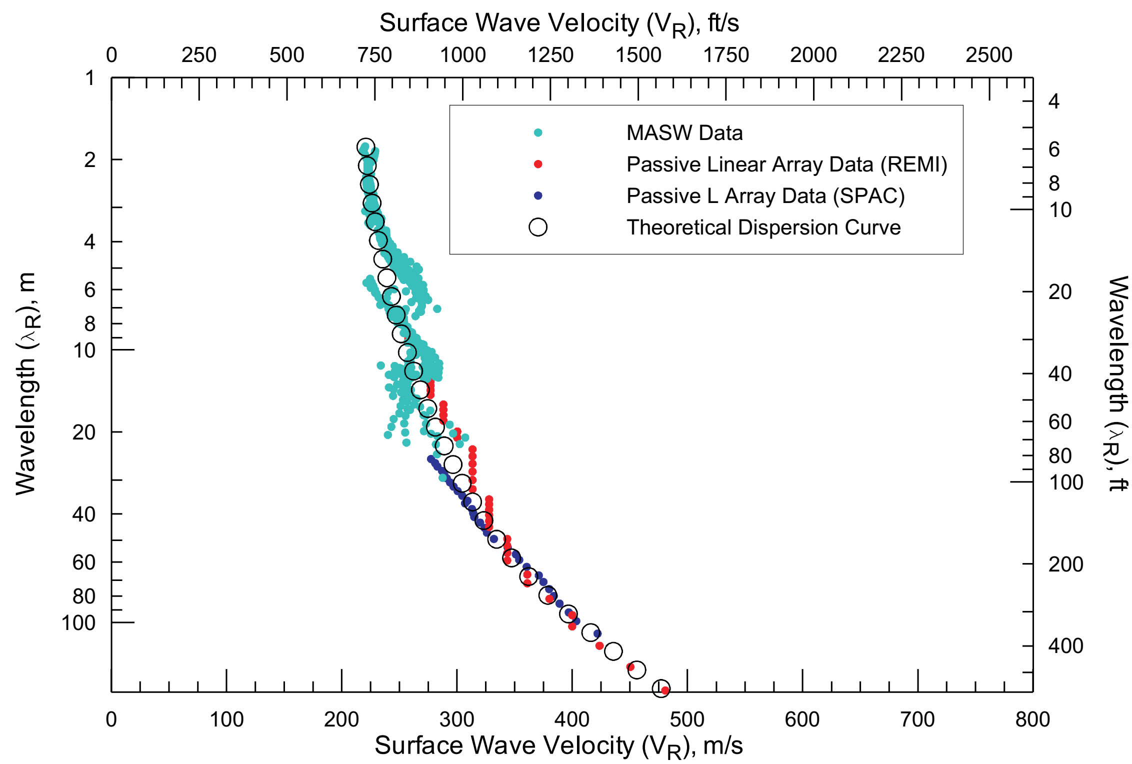

Comparison of Field Experimental Data and Theoretical Dispersion Curve from Active and Passive Surface Wave Array Z4-S7

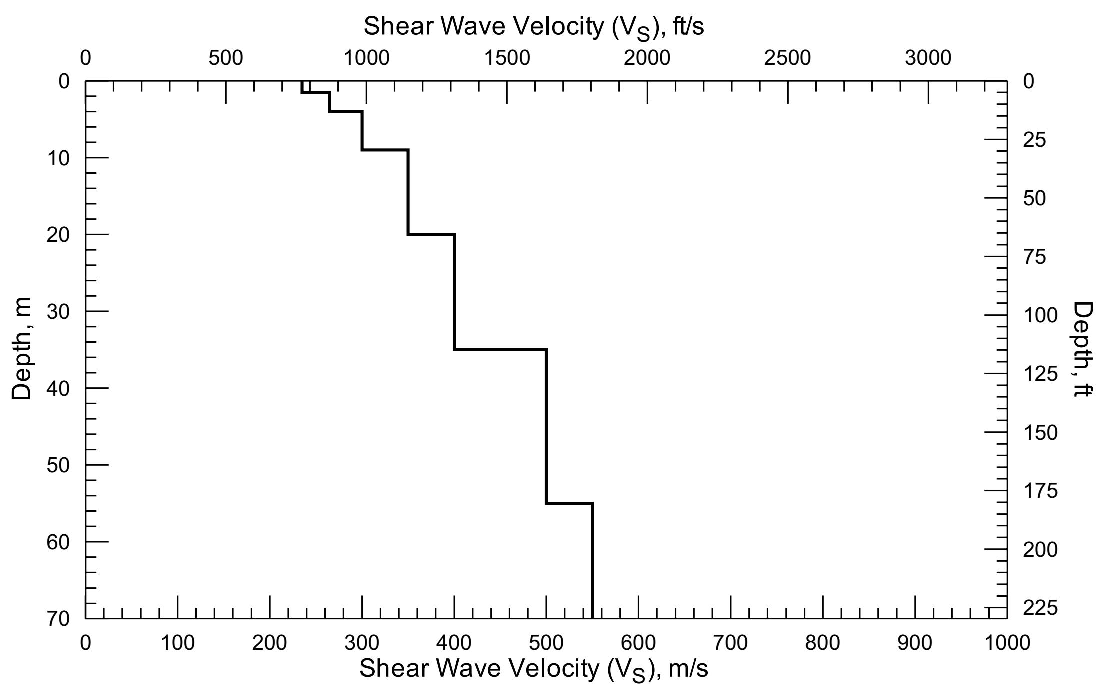

V_S Model from Active and Passive Surface Wave Array Z4-S7

GEOVision geophysical services

Project # 9001	FIGURE 65 VELOCITY MODEL FOR ACTIVE AND PASSIVE SURFACE WAVE ARRAY Z4-S7
Date: JUL 29, 2009	HUNTINGTON DR AND STORY PL, SAN MARINO, CALIFORNIA
Drawn By: A MARTIN	
Approved By: Antony J Martin	PREPARED FOR CH2M HILL
File R:\...Project Files\2009\9001ch2mhill\report\figures\Figure65.cdr	

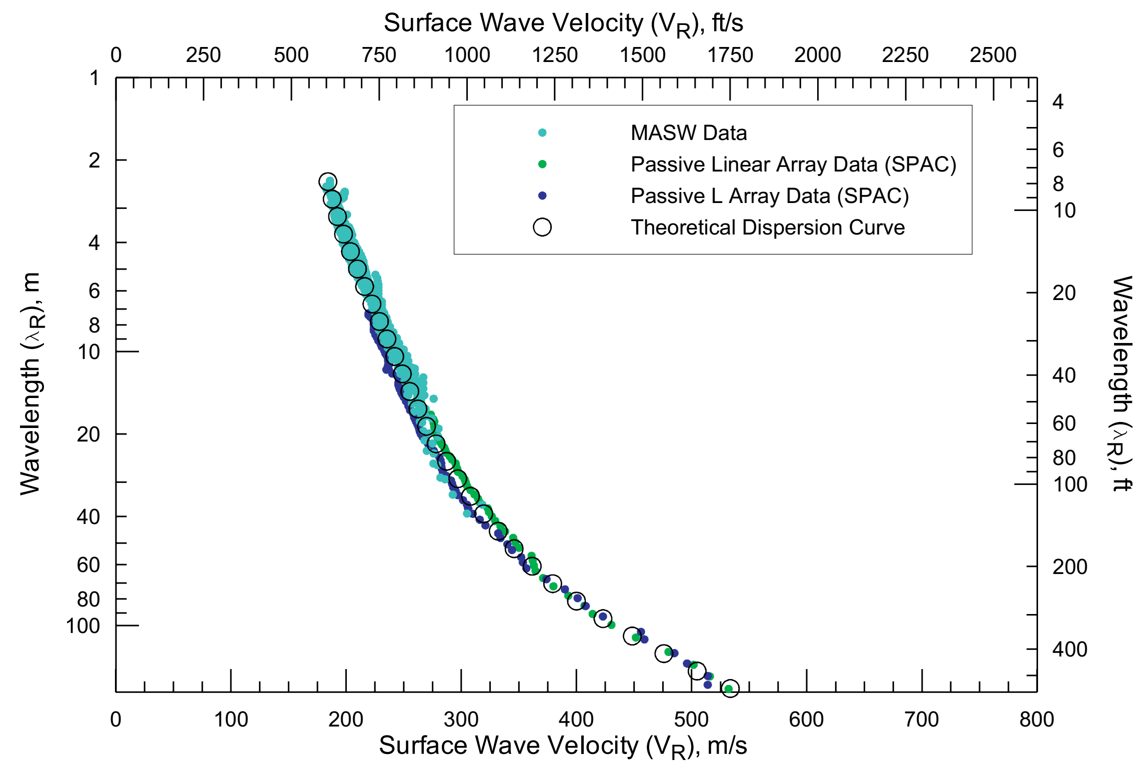

Comparison of Field Experimental Data and Theoretical Dispersion Curve from Active and Passive Surface Wave Array Z4-S8

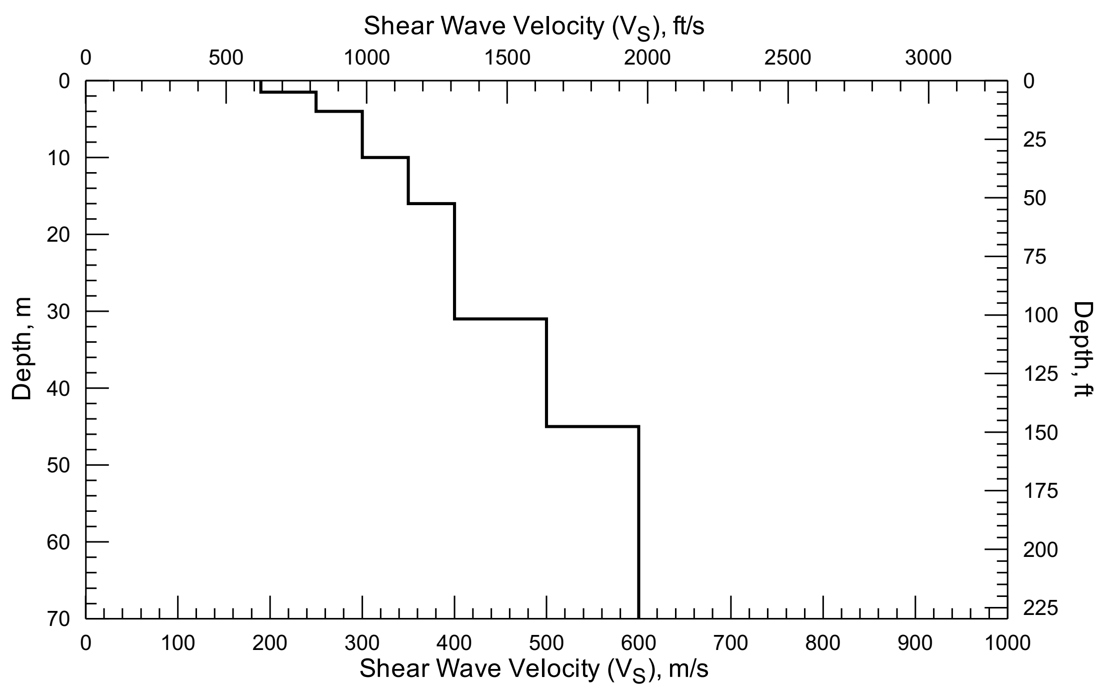

V_S Model from Active and Passive Surface Wave Array Z4-S8

GEOVision geophysical services	FIGURE 66 VELOCITY MODEL FOR ACTIVE AND PASSIVE SURFACE WAVE ARRAY Z4-S8
Project # 9001 Date: JUL 29, 2009 Drawn By: A MARTIN	GARFIELD AVE AND MCLEAN ST, ALHAMBRA, CALIFORNIA
Approved By: [signature] File R:\...Project Files\2009\9001ch2mhill\report\figures\Figure66.cdr	PREPARED FOR CH2M HILL

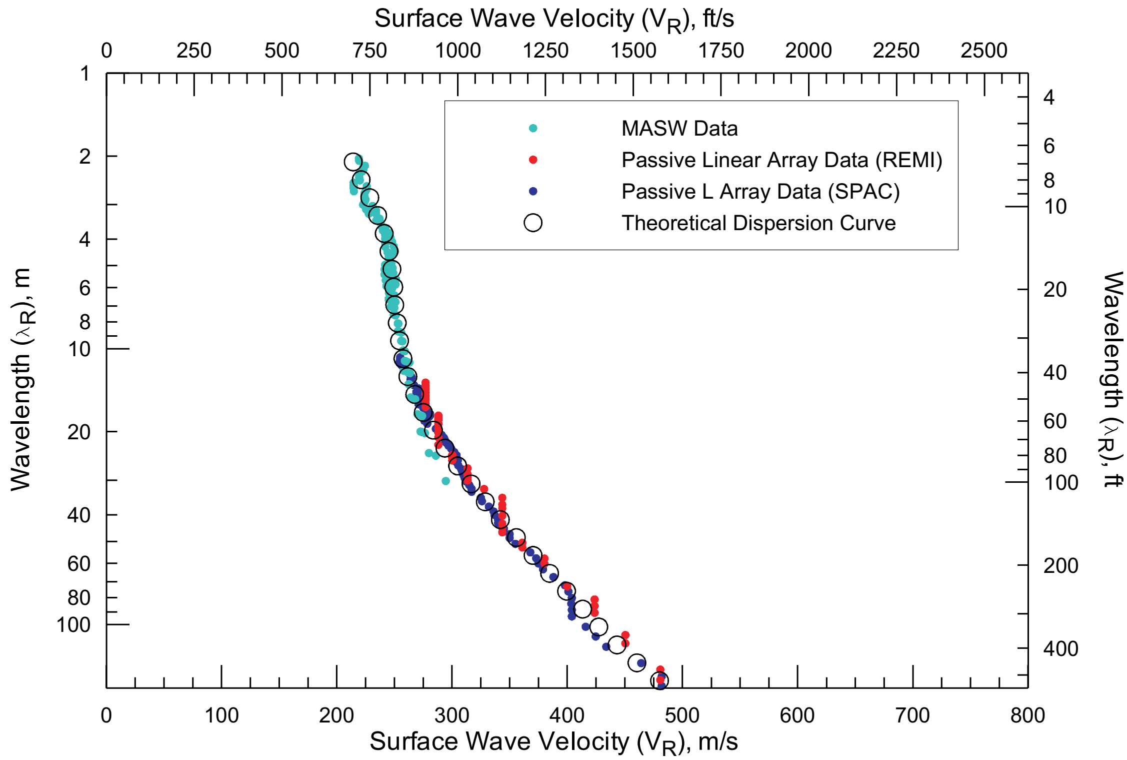

Comparison of Field Experimental Data and Theoretical Dispersion Curve from Active and Passive Surface Wave Array Z4-S9

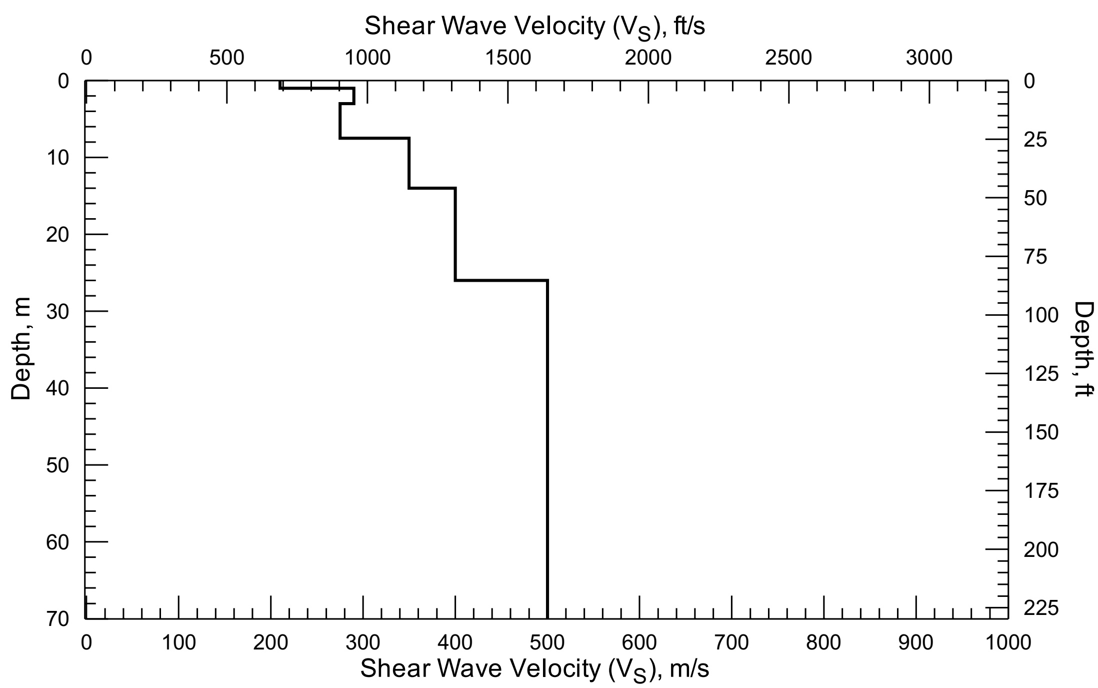

V_S Model from Active and Passive Surface Wave Array Z4-S9

GEOVision geophysical services	FIGURE 67 VELOCITY MODEL FOR ACTIVE AND PASSIVE SURFACE WAVE ARRAY Z4-S9
Project # 9001 Date: JUL 29, 2009 Drawn By: A MARTIN	BUSHNELL AVE AND LARCH ST, ALHAMBRA, CALIFORNIA
Approved By: [signature] File R:\...Project Files\2009\9001ch2mhill\report\figures\Figure67.cdr	PREPARED FOR CH2M HILL

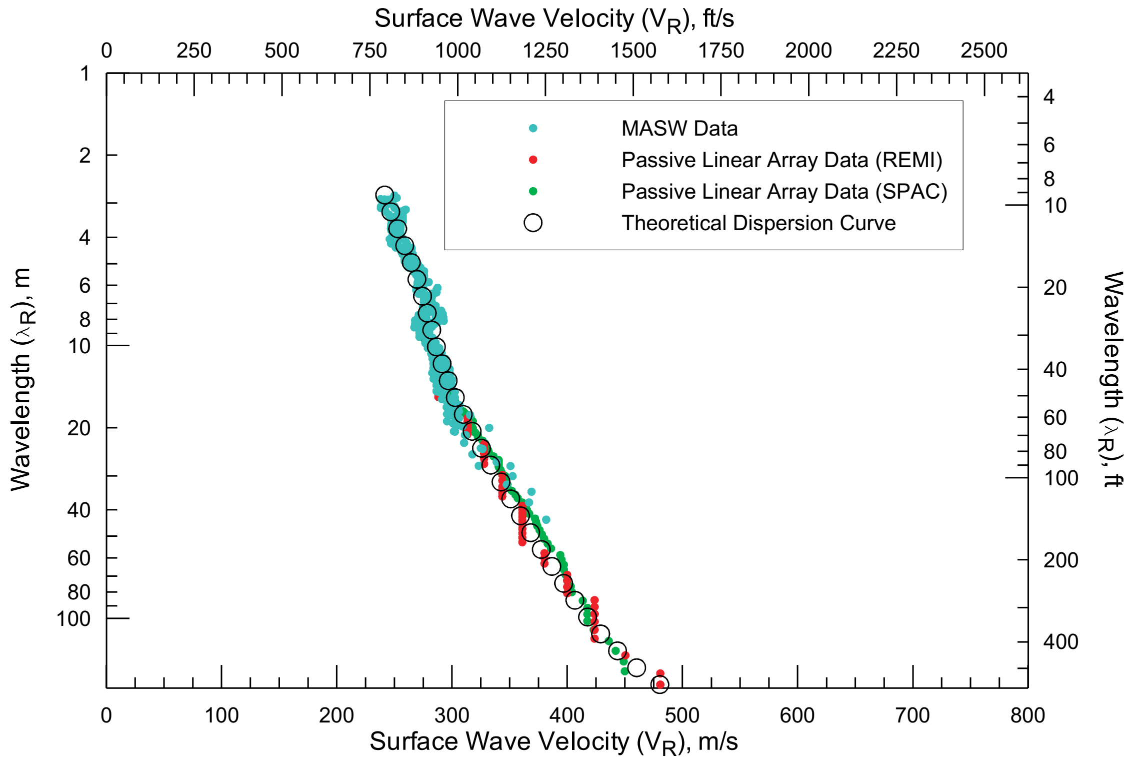

Comparison of Field Experimental Data and Theoretical Dispersion Curve from Active and Passive Surface Wave Array Z4-S10

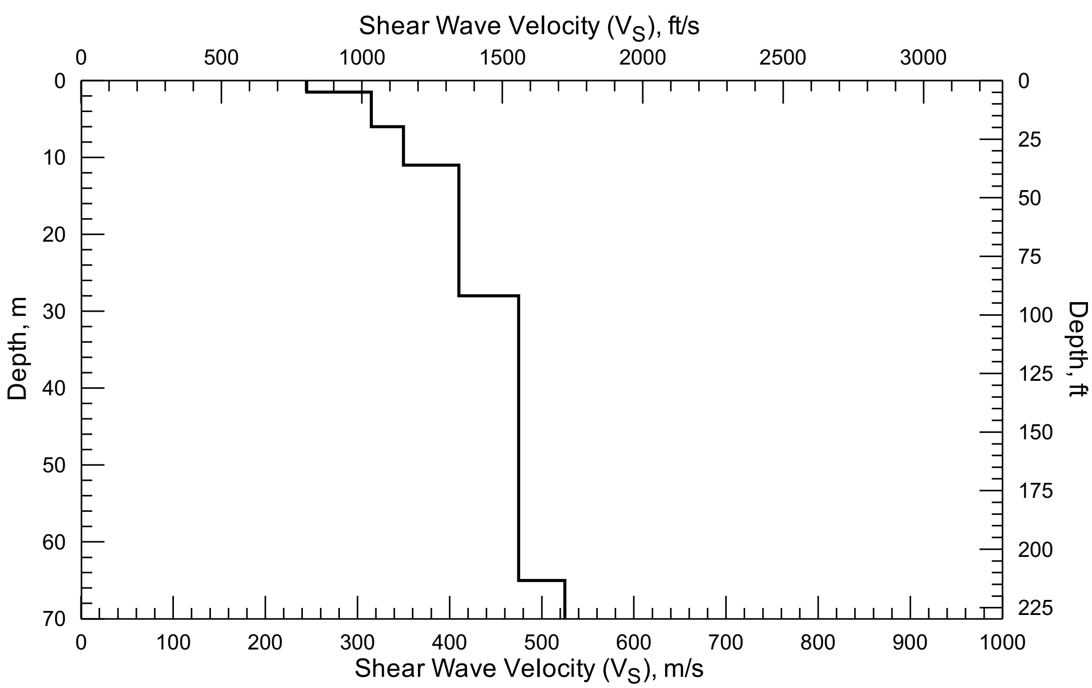

V_S Model from Active and Passive Surface Wave Array Z4-S10

GEOVision geophysical services	FIGURE 68 VELOCITY MODEL FOR ACTIVE AND PASSIVE SURFACE WAVE ARRAY Z4-S10
Project # 9001 Date: JUL 29, 2009 Drawn By: A MARTIN	COMMONWEALTH AVE AND DATE AVE, ALHAMBRA, CALIFORNIA
Approved By: Antony J Martin File R:\...Project Files\2009\9001ch2mhill\report\figures\Figure68.cdr	PREPARED FOR CH2M HILL

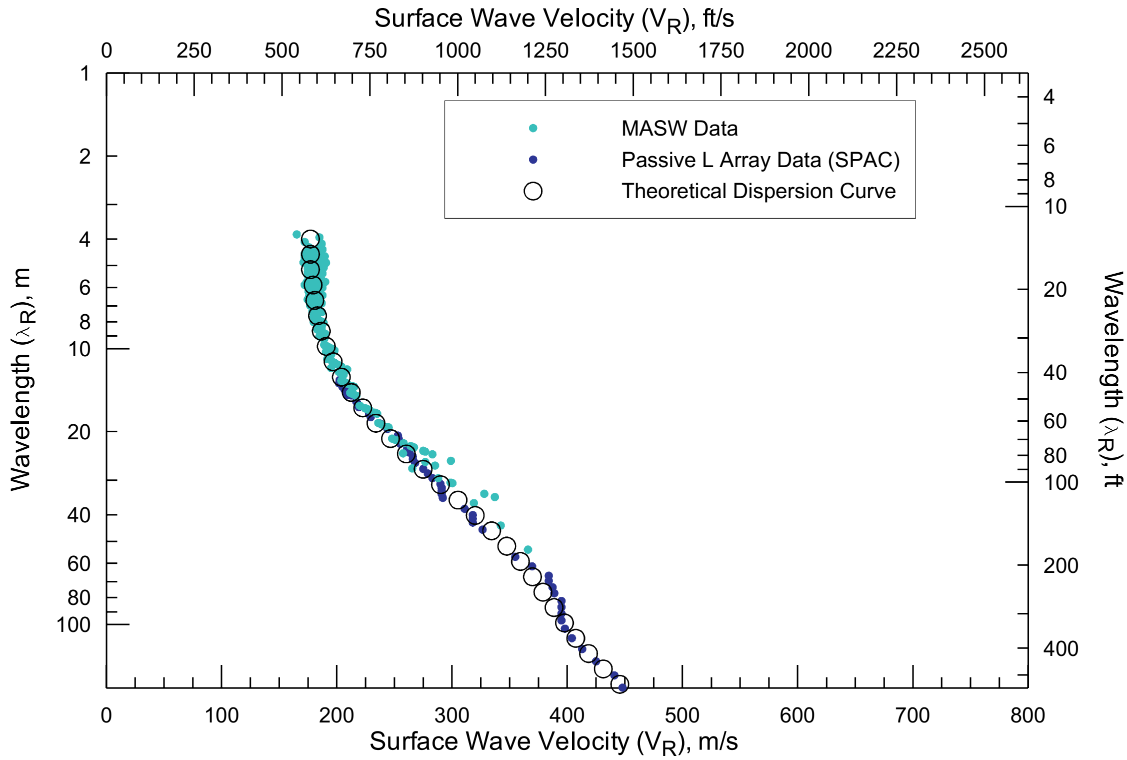

Comparison of Field Experimental Data and Theoretical Dispersion Curve from Active and Passive Surface Wave Array Z5-S1

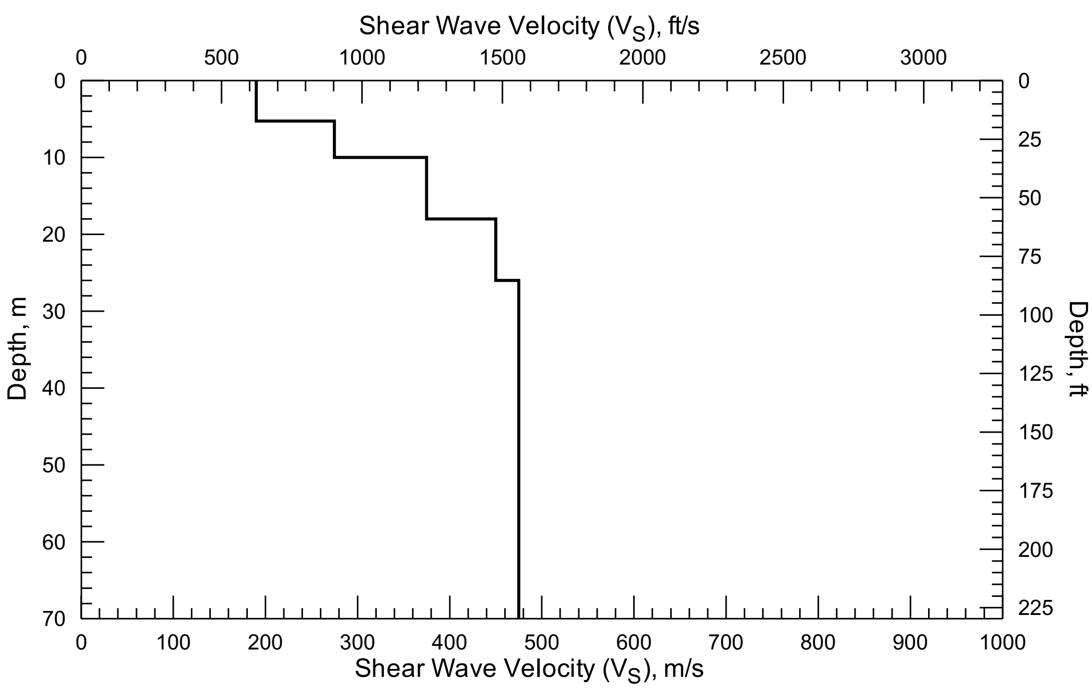

V_S Model from Active and Passive Surface Wave Array Z5-S1

GEOVision geophysical services	FIGURE 69 VELOCITY MODEL FOR ACTIVE AND PASSIVE SURFACE WAVE ARRAY Z5-S1
Project # 9001 Date: JUL 29, 2009 Drawn By: A MARTIN	RIO HONDO PKWY AND HAMMILL RD, EL MONTE, CALIFORNIA
Approved By:	PREPARED FOR CH2M HILL

File R:\...Project Files\2009\9001ch2mhill\report\figures\Figure69.cdr

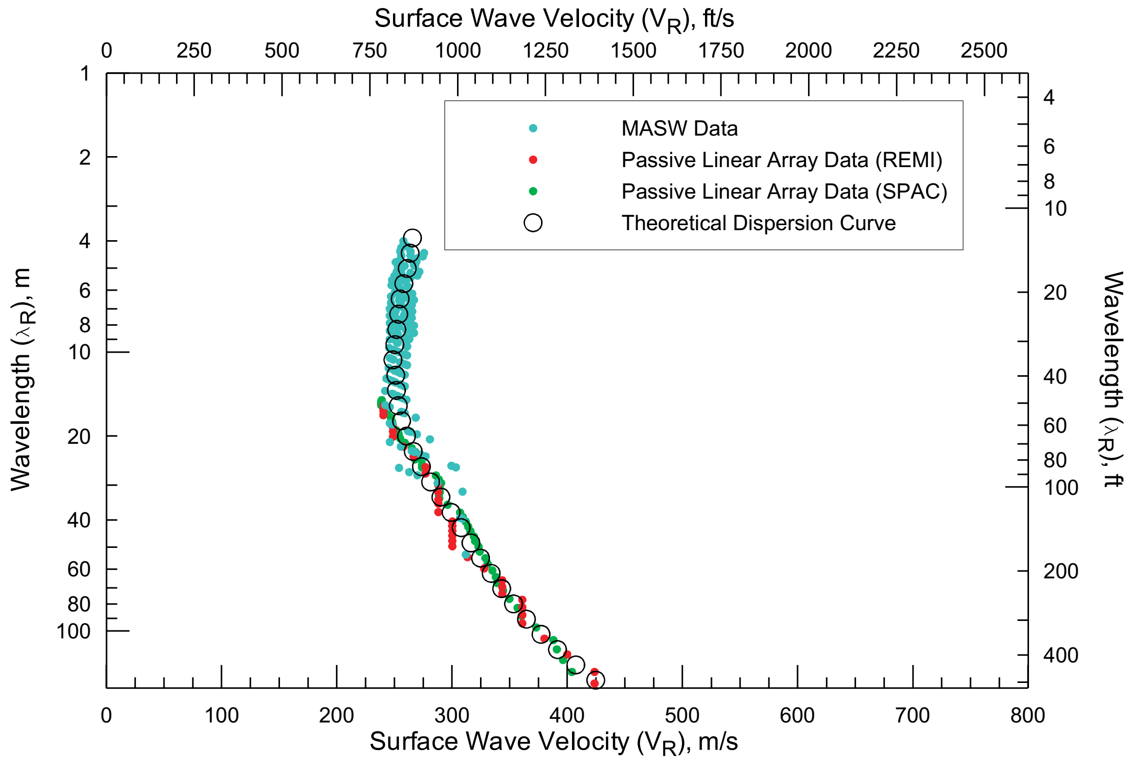

Comparison of Field Experimental Data and Theoretical Dispersion Curve from Active and Passive Surface Wave Array Z5-S2

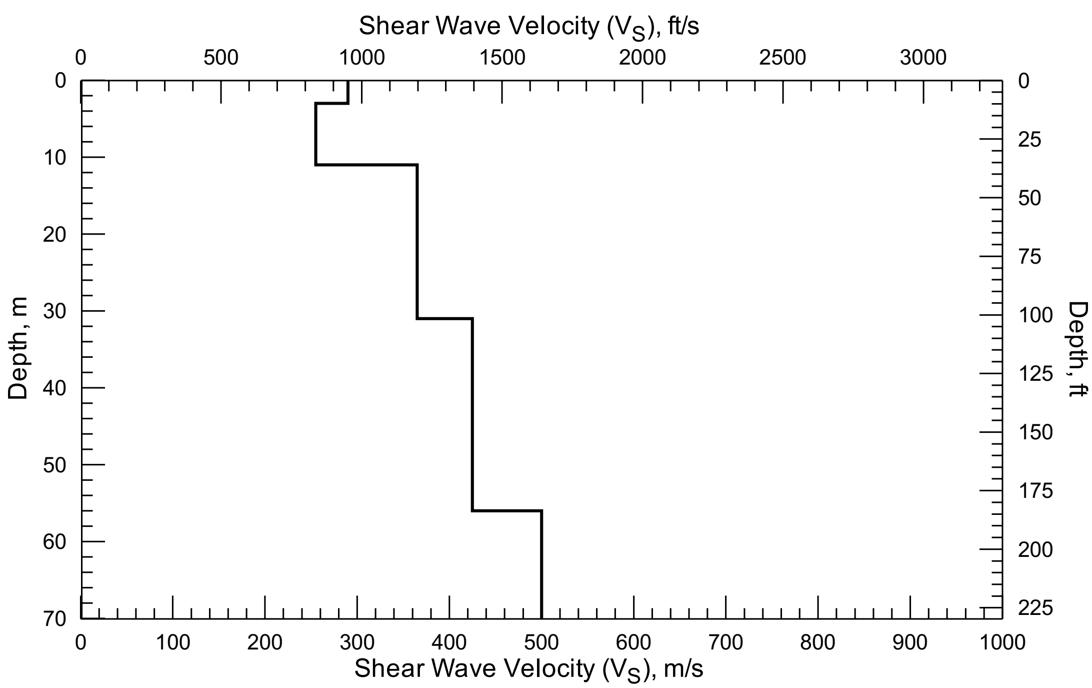

V_S Model from Active and Passive Surface Wave Array Z5-S2

GEOVision geophysical services	FIGURE 70 VELOCITY MODEL FOR ACTIVE AND PASSIVE SURFACE WAVE ARRAY Z5-S2
Project # 9001 Date: JUL 29, 2009 Drawn By: A MARTIN Approved By: [signature]	GRAND AVE AND FARAGO AVE, TEMPLE CITY, CALIFORNIA
File R:\...Project Files\2009\9001ch2mhill\report\figures\Figure70.cdr	PREPARED FOR CH2M HILL

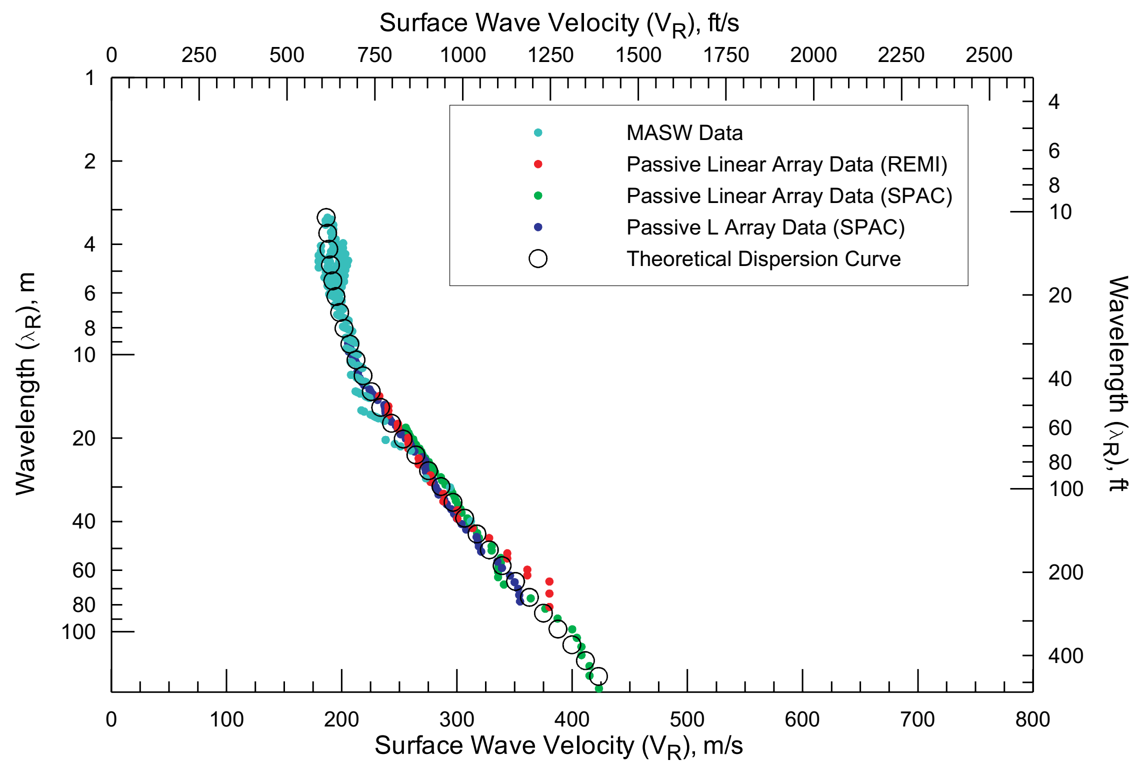

Comparison of Field Experimental Data and Theoretical Dispersion Curve from Active and Passive Surface Wave Array Z5-S3

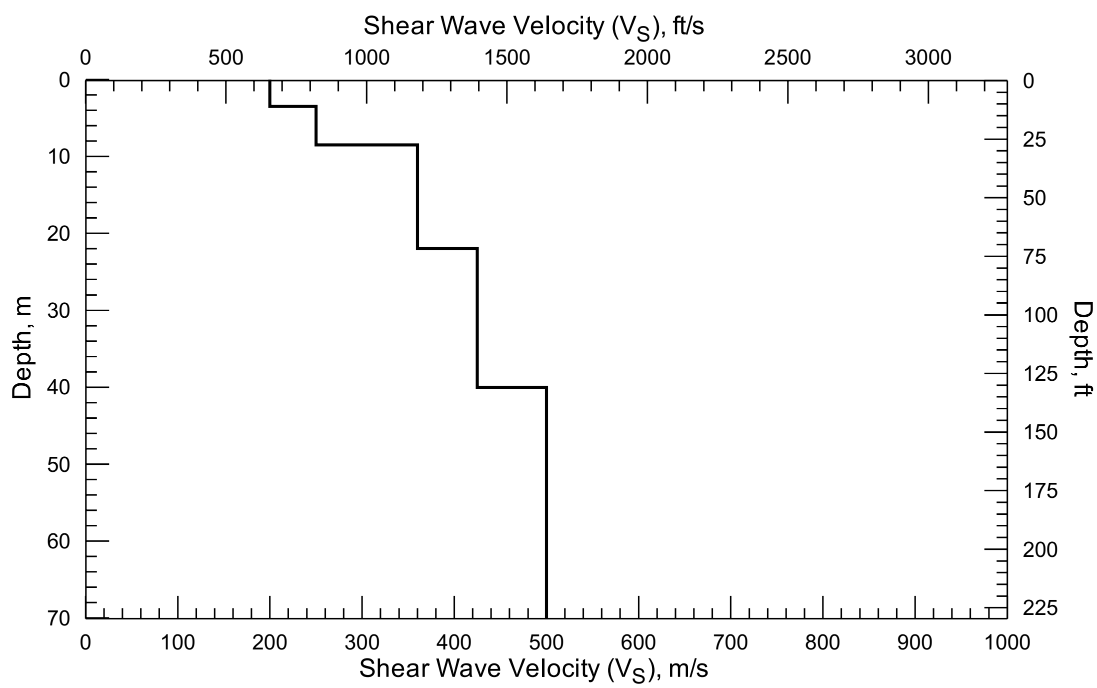

V_S Model from Active and Passive Surface Wave Array Z5-S3

GEOVision geophysical services	FIGURE 71 VELOCITY MODEL FOR ACTIVE AND PASSIVE SURFACE WAVE ARRAY Z5-S3
Project # 9001 Date: JUL 29, 2009 Drawn By: A MARTIN	LA ROSA DR AND RYLAND AVE, TEMPLE CITY, CALIFORNIA
Approved By: [signature] File R:\...Project Files\2009\9001ch2mhill\report\figures\Figure71.cdr	PREPARED FOR CH2M HILL

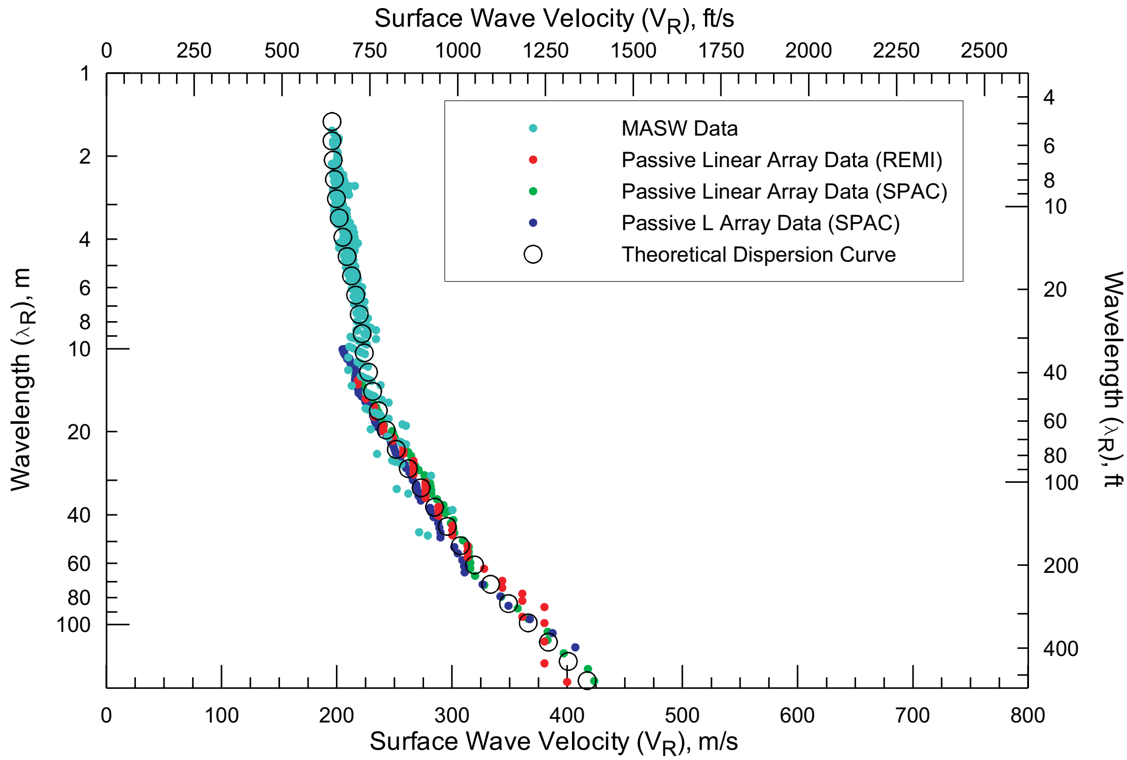

Comparison of Field Experimental Data and Theoretical Dispersion Curve from Active and Passive Surface Wave Array Z5-S4

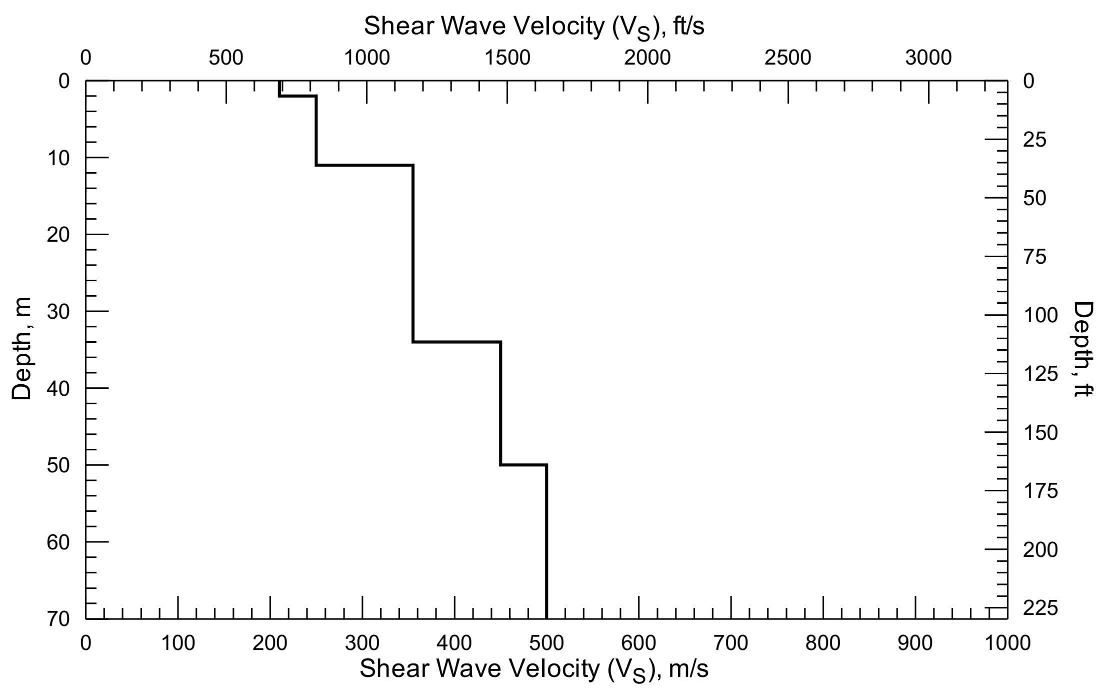

V_S Model from Active and Passive Surface Wave Array Z5-S4

GEOVision geophysical services	FIGURE 72 VELOCITY MODEL FOR ACTIVE AND PASSIVE SURFACE WAVE ARRAY Z5-S4
Project # 9001 Date: JUL 29, 2009 Drawn By: A MARTIN Approved By: [signature]	CLOVERLY AVE AND BLACKLEY ST, TEMPLE CITY, CALIFORNIA
File R:\...Project Files\2009\9001ch2mhill\report\figures\Figure72.cdr	PREPARED FOR CH2M HILL

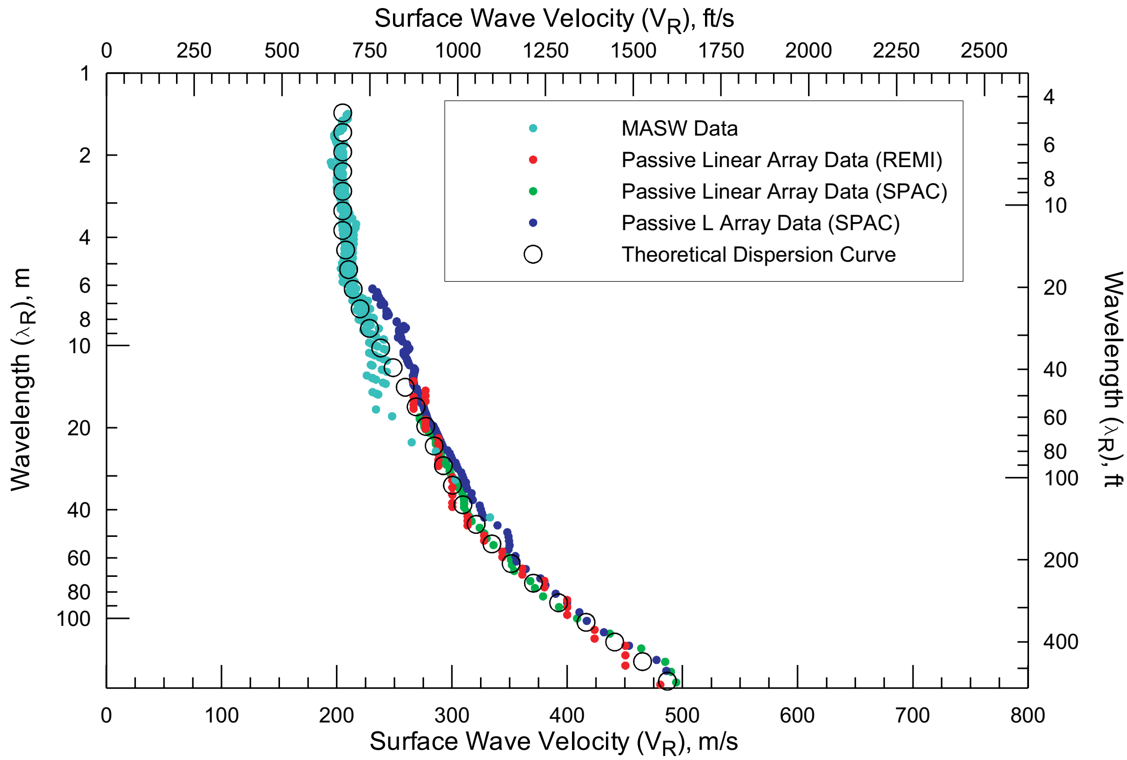

Comparison of Field Experimental Data and Theoretical Dispersion Curve from Active and Passive Surface Wave Array Z5-S6

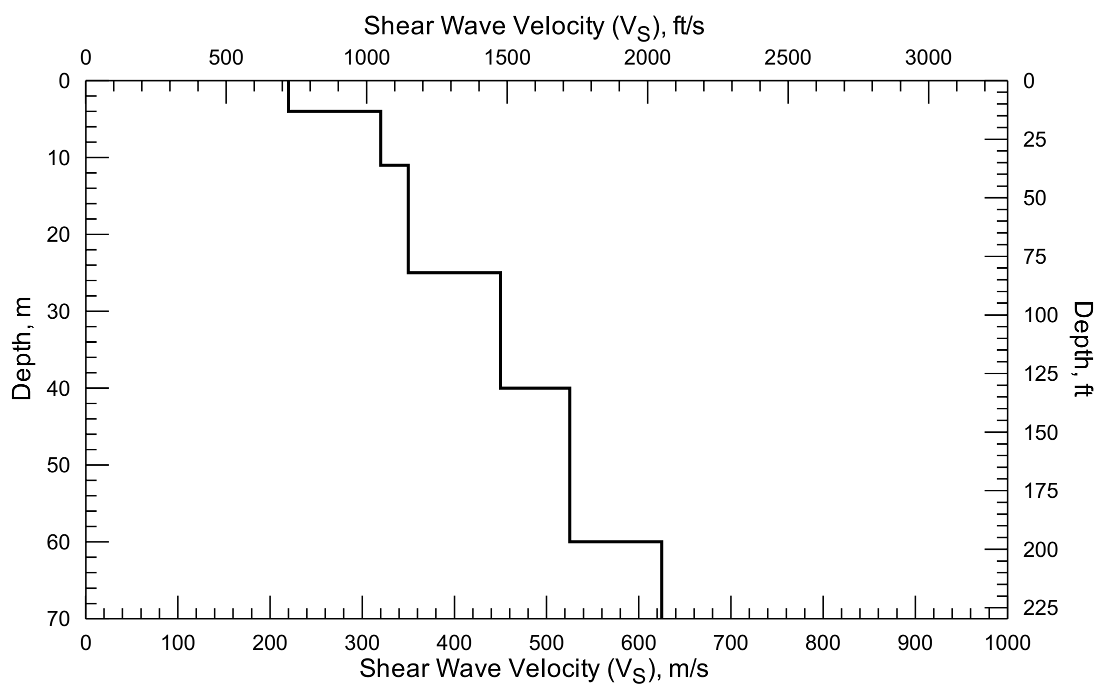

V_S Model from Active and Passive Surface Wave Array Z5-S6

GEOVision geophysical services

FIGURE 73
VELOCITY MODEL FOR ACTIVE AND PASSIVE SURFACE WAVE ARRAY Z5-S6

Project # 9001
Date: JUL 29, 2009
Drawn By: A MARTIN
Approved By: [signature]

GLADYS AVE AND FAIRVIEW AVE, SAN GABRIEL, CALIFORNIA

PREPARED FOR
CH2M HILL

File R:\...Project Files\2009\9001ch2mhill\report\figures\Figure73.cdr

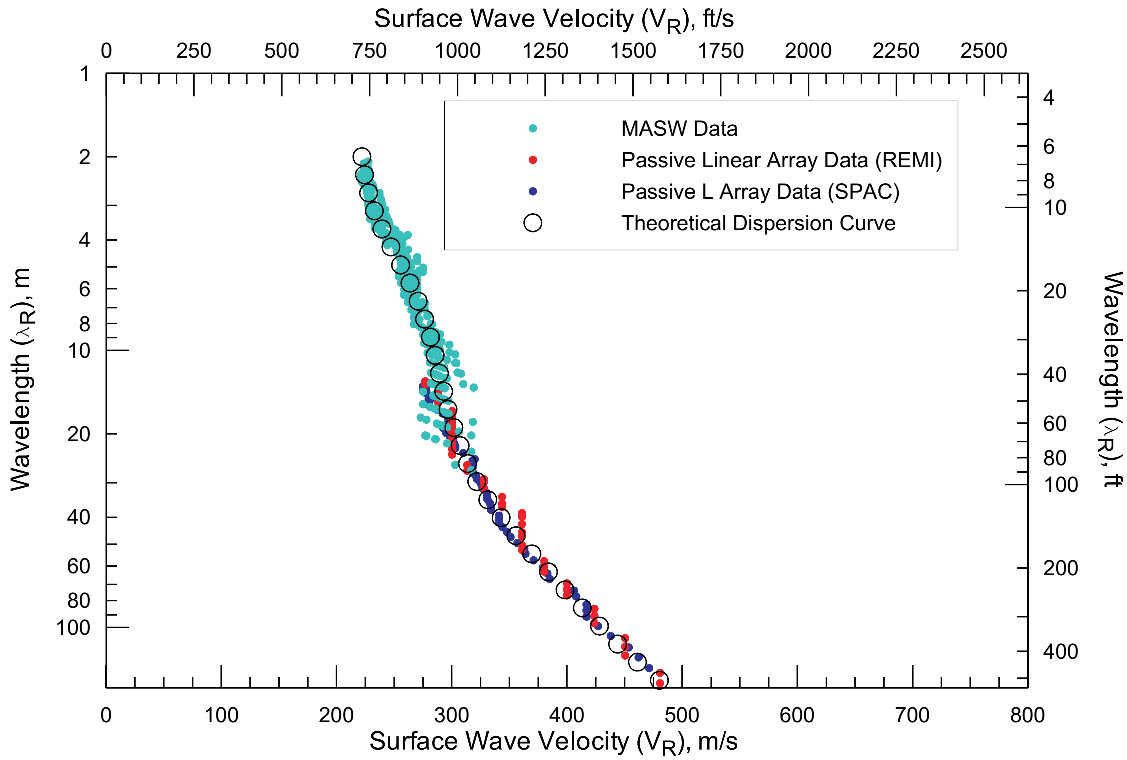

Comparison of Field Experimental Data and Theoretical Dispersion Curve from Active and Passive Surface Wave Array Z5-S7

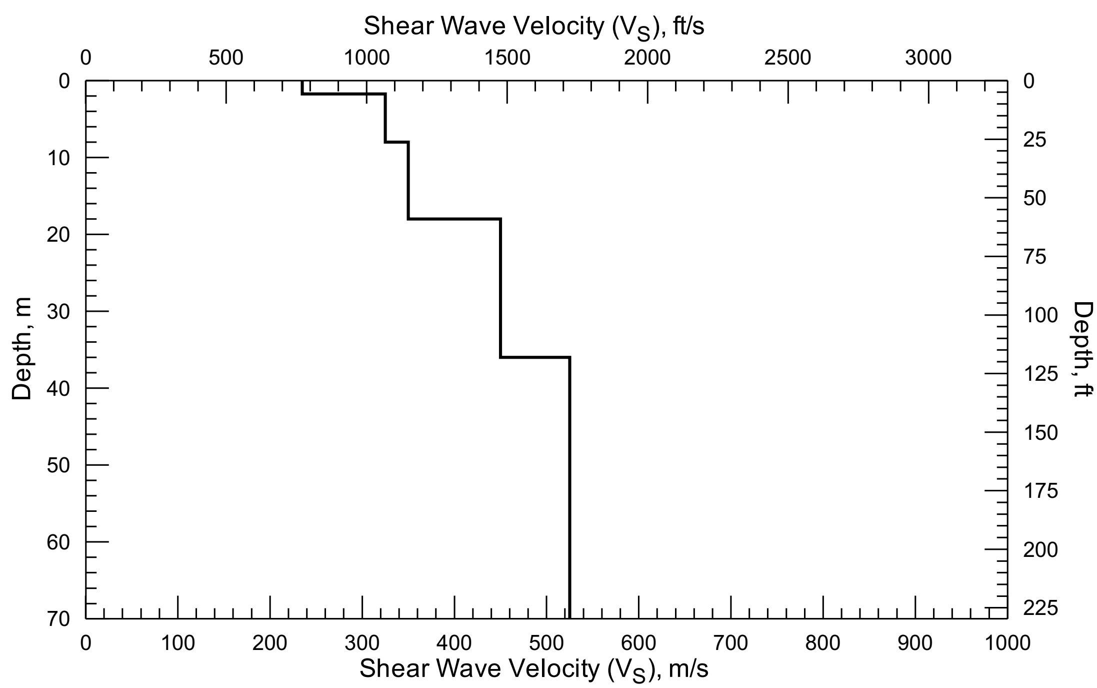

V_S Model from Active and Passive Surface Wave Array Z5-S7

GEOVision geophysical services	FIGURE 74 VELOCITY MODEL FOR ACTIVE AND PASSIVE SURFACE WAVE ARRAY Z5-S7
Project # 9001 Date: JUL 29, 2009	ABBOT AVE AND HAZELL WAY SAN GABRIEL, CALIFORNIA
Drawn By: A MARTIN Approved By: *Antony J Martin* File R:\...Project Files\2009\9001ch2mhill\report\figures\Figure74.cdr	PREPARED FOR CH2M HILL

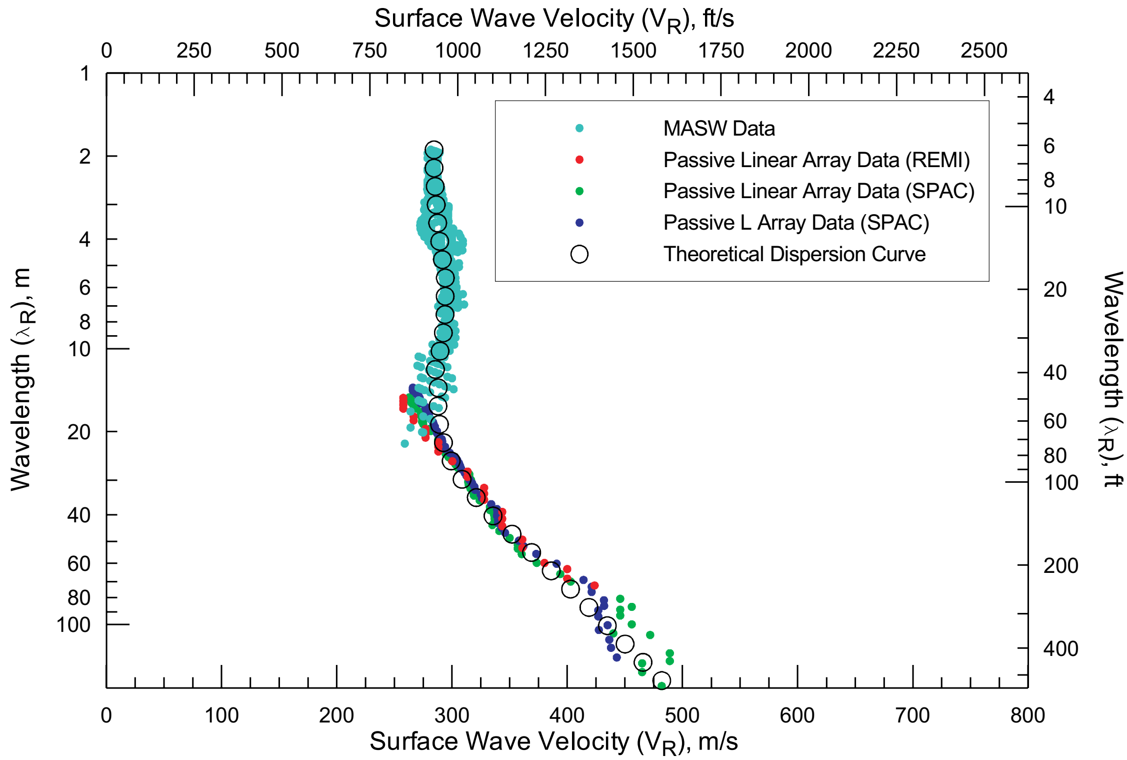

Comparison of Field Experimental Data and Theoretical Dispersion Curve from Active and Passive Surface Wave Array Z5-S8

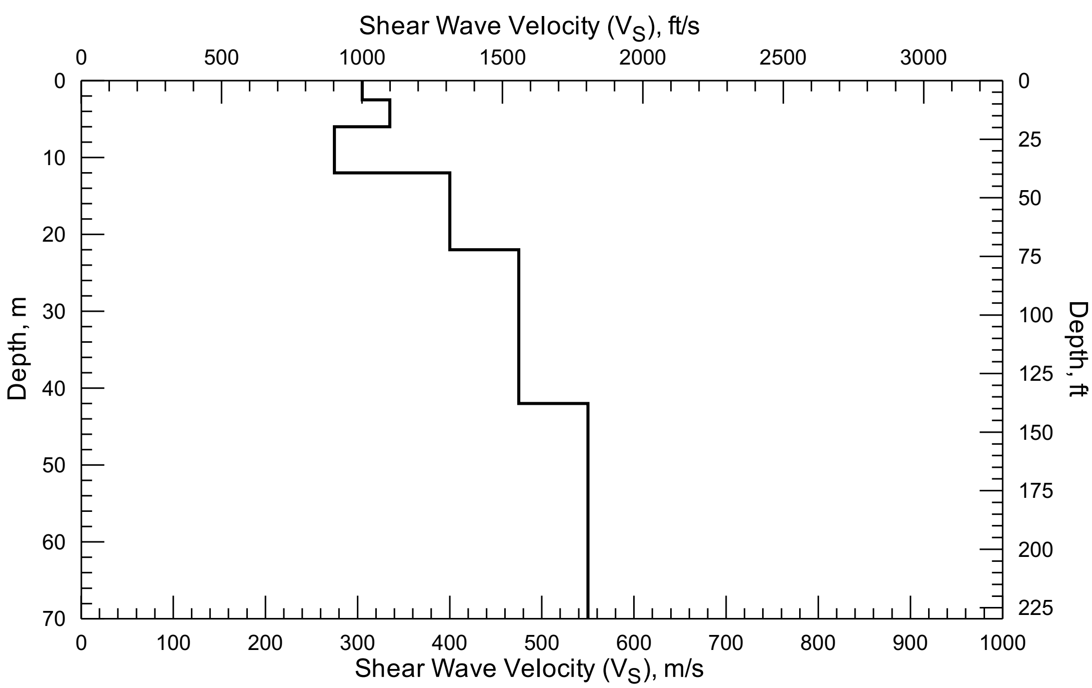

V_S Model from Active and Passive Surface Wave Array Z5-S8

GEOVision geophysical services

Project # 9001
Date: JUL 29, 2009
Drawn By: A MARTIN
Approved By:
File R:\...Project Files\2009\9001ch2mhill\report\figures\Figure75.cdr

FIGURE 75
VELOCITY MODEL FOR ACTIVE AND PASSIVE SURFACE WAVE ARRAY Z5-S8

SHORB ST AND VEGA ST, ALHAMBRA, CALIFORNIA

PREPARED FOR
CH2M HILL

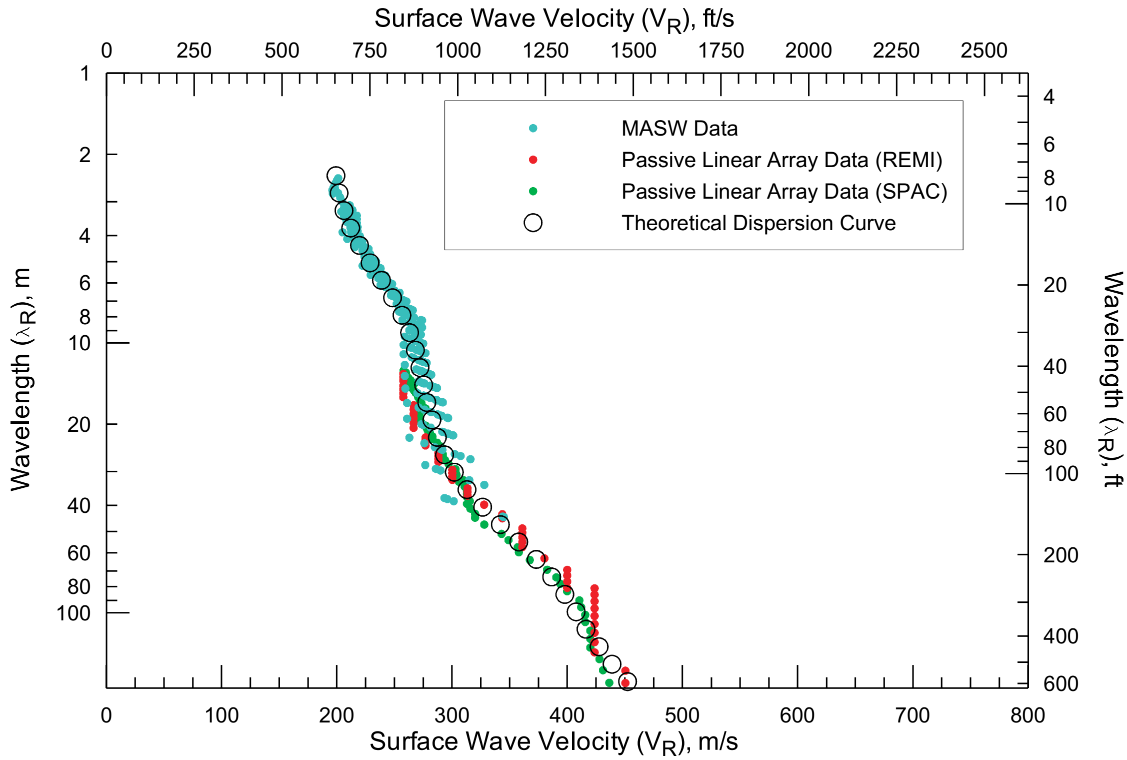

Comparison of Field Experimental Data and Theoretical Dispersion Curve from Active and Passive Surface Wave Array Z5-S9

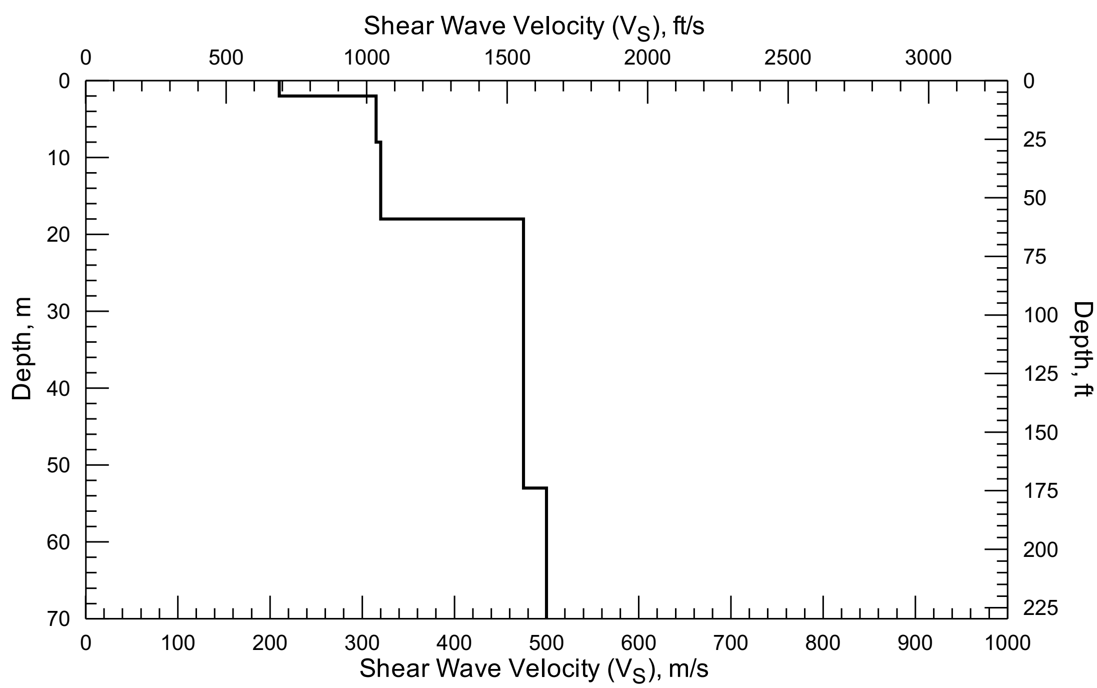

V_S Model from Active and Passive Surface Wave Array Z5-S9

GEOVision geophysical services	FIGURE 76 VELOCITY MODEL FOR ACTIVE AND PASSIVE SURFACE WAVE ARRAY Z5-S9
Project # 9001 Date: JUL 29, 2009	SHORB ST AND HIDALGO AVE, ALHAMBRA, CALIFORNIA
Drawn By: A MARTIN Approved By:	PREPARED FOR CH2M HILL
File R:\...Project Files\2009\9001ch2mhill\report\figures\Figure76.cdr	

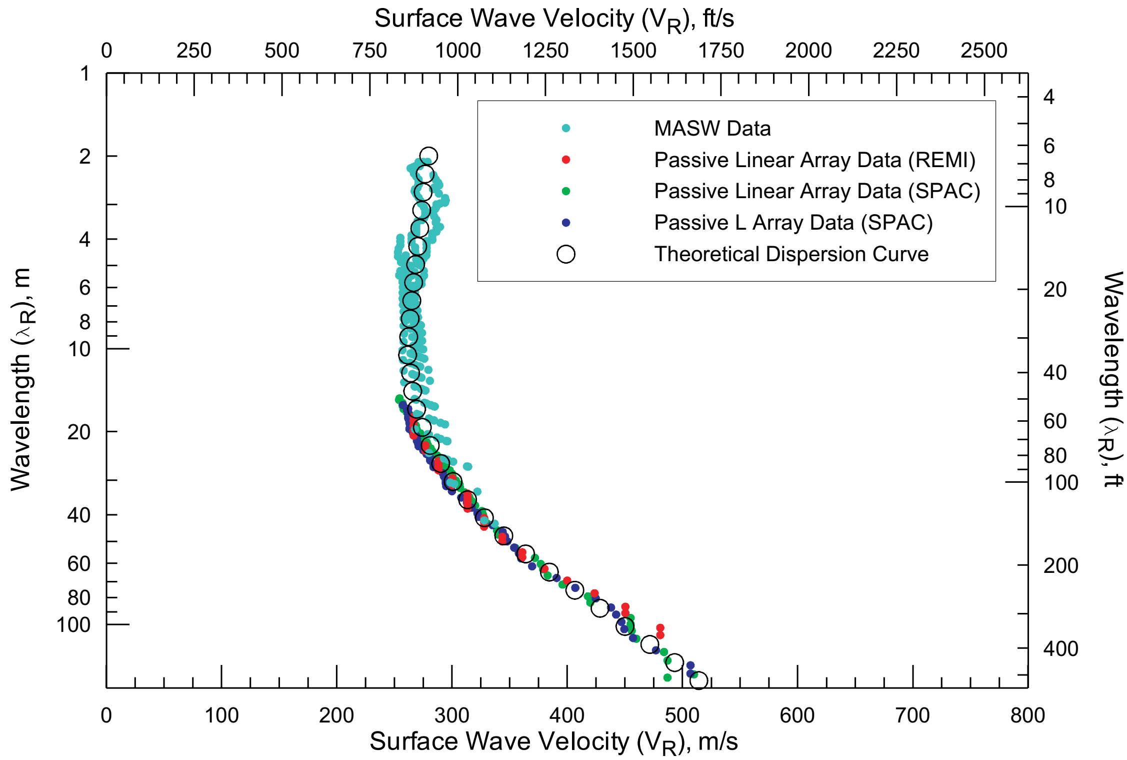

Comparison of Field Experimental Data and Theoretical Dispersion Curve from Active and Passive Surface Wave Array Z5-S10

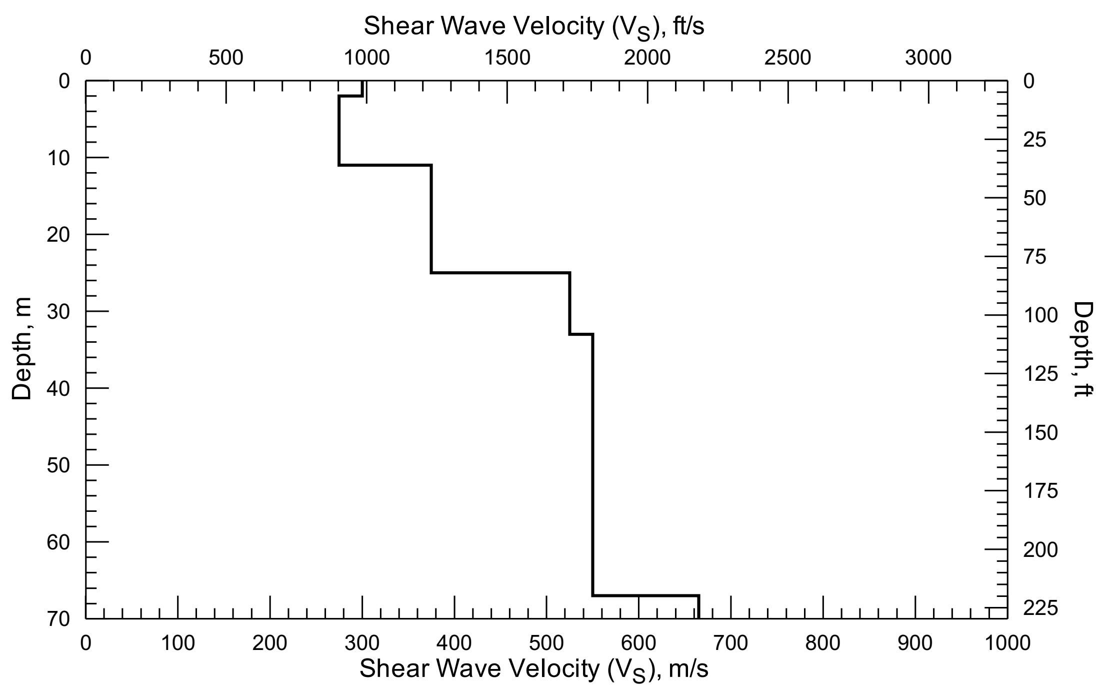

V_S Model from Active and Passive Surface Wave Array Z5-S10

GEOVision geophysical services	FIGURE 77 VELOCITY MODEL FOR ACTIVE AND PASSIVE SURFACE WAVE ARRAY Z5-S10
Project # 9001 Date: JUL 29, 2009 Drawn By: A MARTIN Approved By:	S 2ND ST AND W ADAMS AVE, ALHAMBRA, CALIFORNIA
File R:\...Project Files\2009\9001ch2mhill\report\figures\Figure77.cdr	PREPARED FOR CH2M HILL

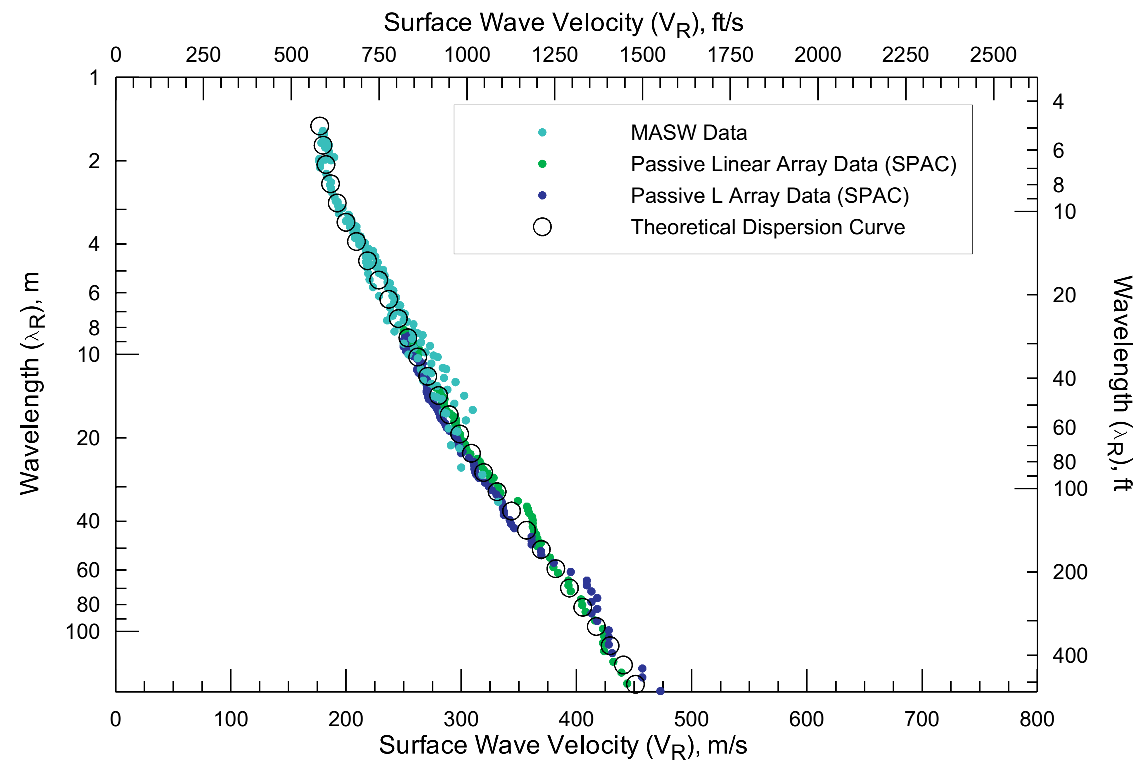

Comparison of Field Experimental Data and Theoretical Dispersion Curve from Active and Passive Surface Wave Array Z5-S11

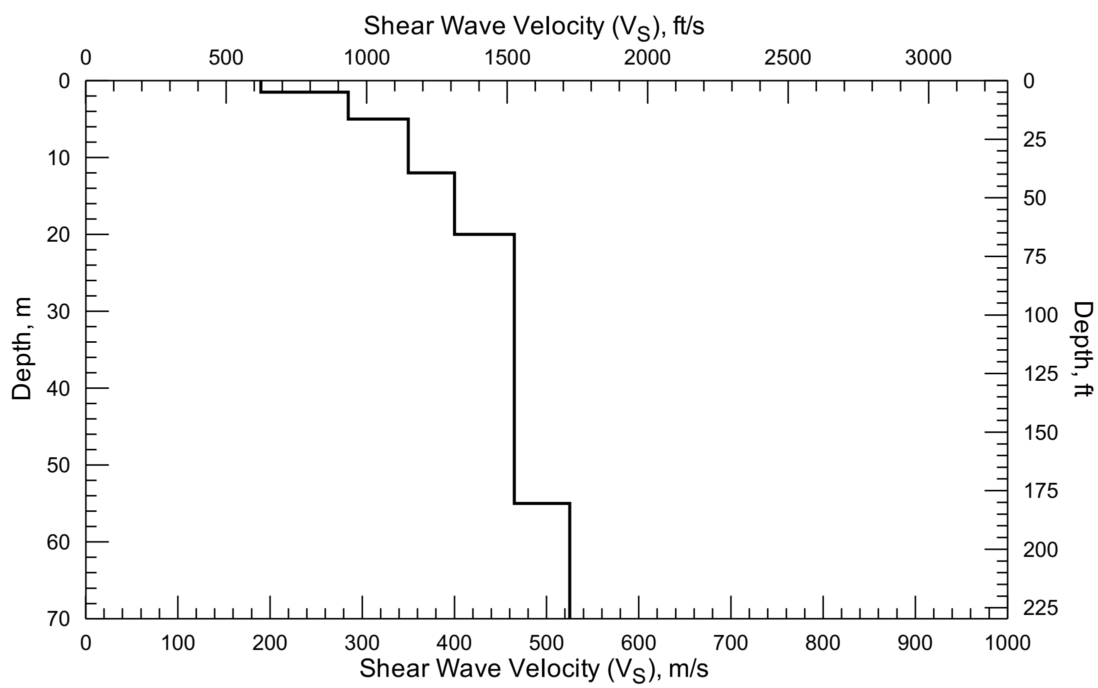

V_S Model from Active and Passive Surface Wave Array Z5-S11

GEOVision geophysical services	FIGURE 78 VELOCITY MODEL FOR ACTIVE AND PASSIVE SURFACE WAVE ARRAY Z5-S11
Project # 9001 Date: JUL 29, 2009 Drawn By: A MARTIN Approved By:	SHORB ST AND BENITO AVE, ALHAMBRA, CALIFORNIA
File R:\...Project Files\2009\9001ch2mhill\report\figures\Figure78.cdr	PREPARED FOR CH2M HILL

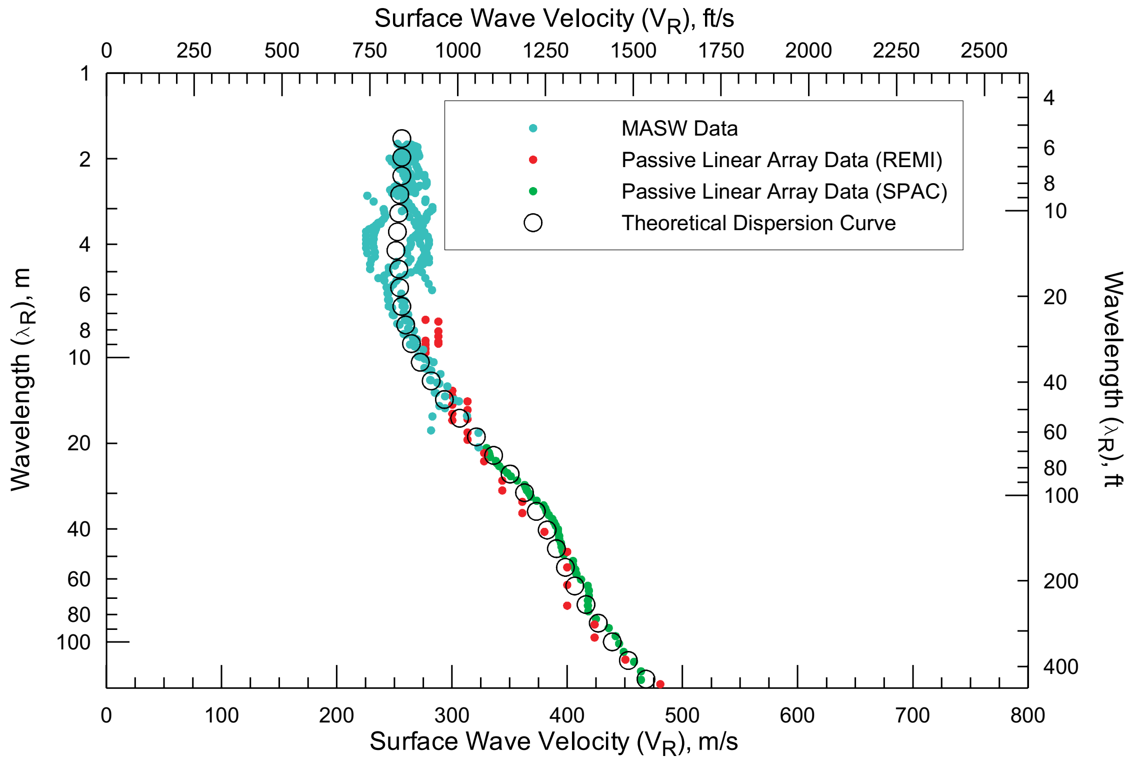

Comparison of Field Experimental Data and Theoretical Dispersion Curve from Active and Passive Surface Wave Array Z5-S12

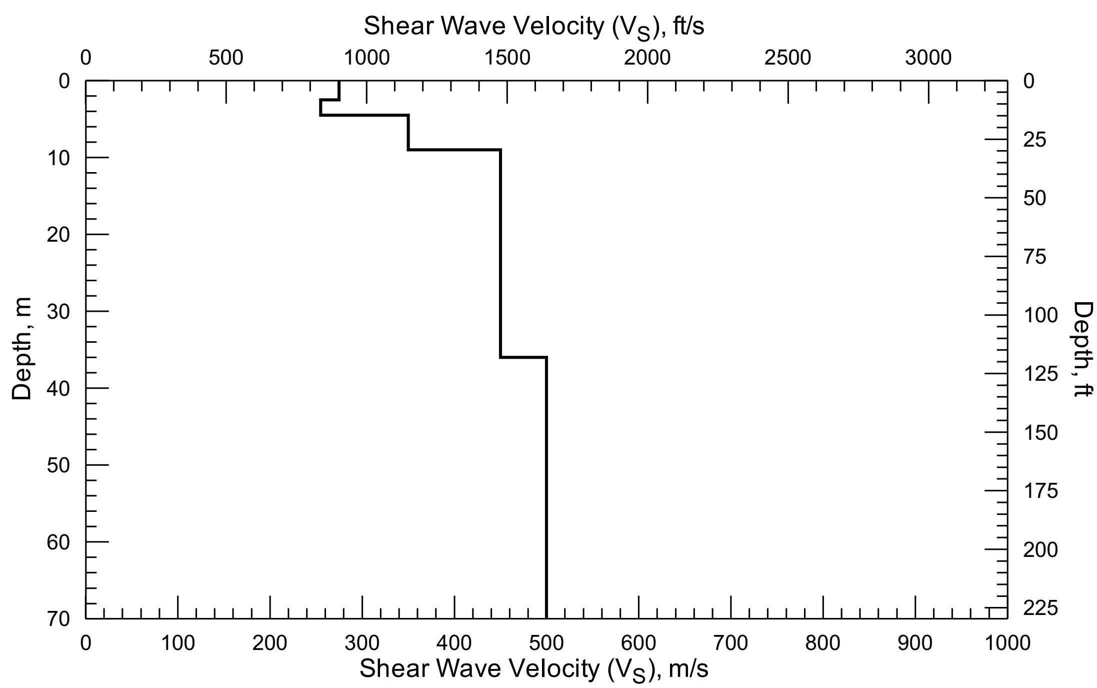

V_S Model from Active and Passive Surface Wave Array Z5-S12

GEOVision geophysical services

Project # 9001
Date: JUL 29, 2009
Drawn By: A MARTIN
Approved By: Antony J Martin

File R:\...Project Files\2009\9001ch2mhill\report\figures\Figure79.cdr

FIGURE 79
VELOCITY MODEL FOR ACTIVE AND PASSIVE SURFACE WAVE ARRAY Z5-S12

NORWOOD PL AND EDGEWOOD DR, ALHAMBRA, CALIFORNIA

PREPARED FOR
CH2M HILL

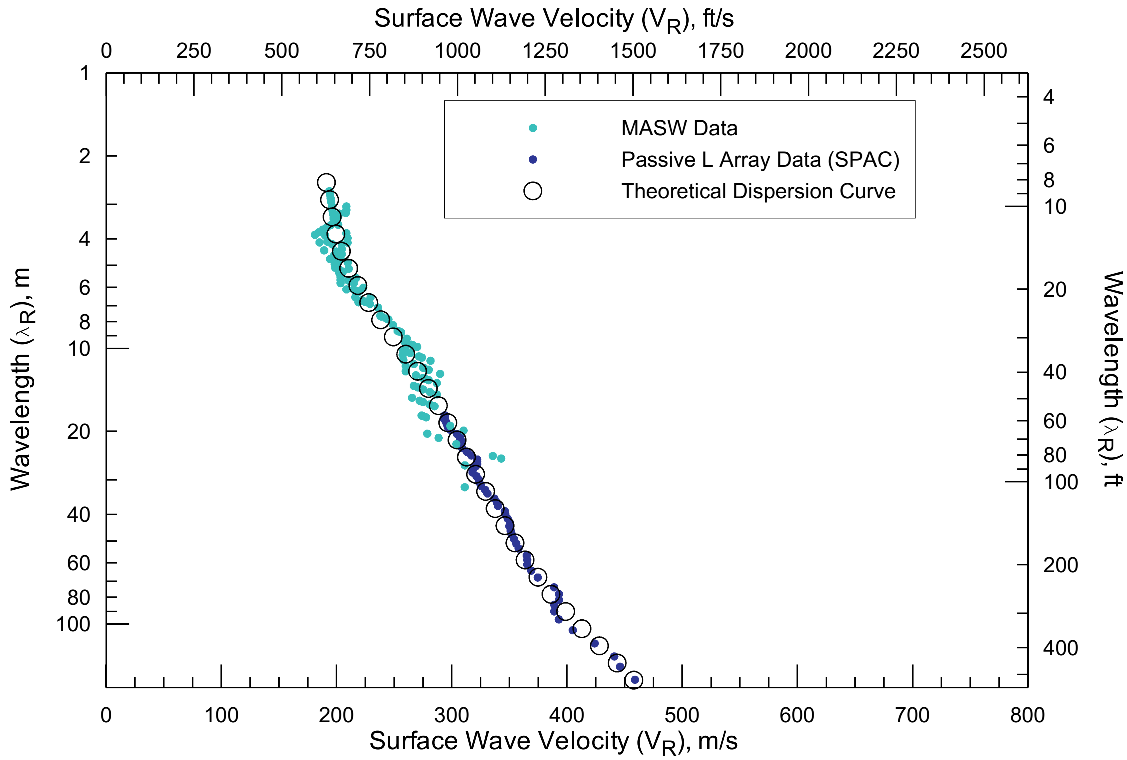

Comparison of Field Experimental Data and Theoretical Dispersion Curve from Active and Passive Surface Wave Array Z5-S13

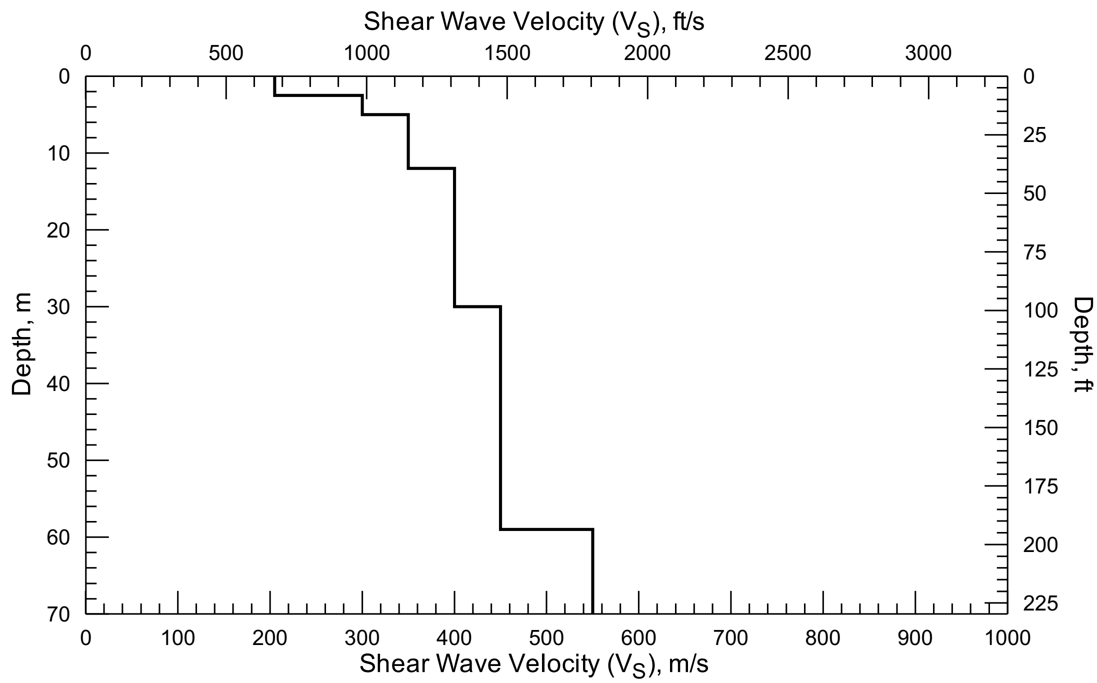

V_S Model from Active and Passive Surface Wave Array Z5-S13

GEOVision geophysical services	FIGURE 80 VELOCITY MODEL FOR ACTIVE AND PASSIVE SURFACE WAVE ARRAY Z5-S13
Project # 9001 Date: JUL 29, 2009	ROSS AVE AND EDGEWOOD DR, ALHAMBRA, CALIFORNIA
Drawn By: A MARTIN Approved By: Antony J Martin	PREPARED FOR CH2M HILL
File R:\...Project Files\2009\9001ch2mhill\report\figures\Figure80.cdr	